

Identification and Development of Photocatalysts for Building Molecular Complexity

Dissertation

Zur Erlangung des Doktorgrades der Naturwissenschaften

(Dr. rer. nat.)

an der Fakultät für Chemie und Pharmazie

der Universität Regensburg



vorgelegt von

Alessa Blanka Rolka

aus Soest

2023

The experimental work has been carried out between January 2019 and June 2021 under the supervision of Prof. Dr. Burkhard König at the University of Regensburg, Institute of Organic Chemistry and between August 2021 and July 2022 under the supervision of Prof. Dr. Burkhard König and Prof. Dr. F. Dean Toste at the University of California, Berkeley (USA).

Date of submission: 15.02.2023

Date of colloquium: 03.04.2023

Board of examiners:

Prof. Dr. Arno Pfitzner (chair)

Prof. Dr. Burkhard König (1st referee)

Prof. Dr. F. Dean Toste (2nd referee)

Prof. Dr. Patrick Nürnberger (examiner)

„We are the only species that lives in zoos of our own design.“

Christopher Ryan

TABLE OF CONTENTS

1	BIFUNCTIONAL ORGANIC PHOTOCATALYSTS FOR ENANTIOSELECTIVE VISIBLE-LIGHT MEDIATED PHOTOCATALYSIS	1
1.1	Introduction.....	3
1.2	Bifunctional lactam-photocatalyst	4
1.3	Bifunctional photocatalysts for aerobic oxidation reactions	6
1.4	Bifunctional urea-photocatalysts	8
1.5	Bifunctional photoaminocatalysts	9
1.6	Bifunctional chiral phosphoric acid (CPA) photocatalysts.....	10
1.7	Conclusion	16
1.8	References.....	17
2	DEAROMATIC CYCLOADDITIONS UTILIZING AN ORGANIC PHOTSENSITIZER: AN ALTERNATIVE TO IRIIDIUM CATALYSIS	25
2.1	Introduction.....	27
2.2	Results and discussion.....	29
2.3	Conclusion	35
2.4	Experimental part	36
2.4.1	General information	36
2.4.2	Properties of 2CzPN	37
2.4.3	Optimization- and Solubility Studies	39
2.4.4	Experimental Procedures	44
2.4.5	Previous Works and Mechanisms.....	75
2.4.6	NMR-Spectra	76
2.4.7	X-Ray Structures and Data.....	77
2.5	References.....	81

3	PHOTOCATALYTIC C–H TRIFLUOROMETHYLTHIOLATION BY THE DECATUNGSTATE ANION	89
3.1	Introduction.....	91
3.2	Results and discussion.....	93
3.3	Conclusion	97
3.4	Experimental part	98
3.4.1	General information.....	98
3.4.2	General procedure for trifluoromethylthiolation	99
3.4.3	Optimization of the reaction conditions and detailed procedures.....	100
3.4.4	Experimental Procedures	103
3.4.5	NMR-Spectra	131
3.4.6	X-Ray Structures and Data	132
3.5	References.....	133
4	HYBRID CATALYSTS FOR ENANTIOSELECTIVE PHOTO-PHOSPHORIC ACID CATALYSIS	139
4.1	Introduction.....	141
4.2	Synthesis and challenges	145
4.3	Proof-of-concept reactions	151
4.4	Conclusion and outlook	154
4.5	Experimental part	155
4.5.1	General information.....	155
4.5.2	UV-VIS and Emission Spectra	156
4.5.3	Overview of Synthesis	157
4.5.4	Synthesis of Literature Reported Compounds	159
4.5.5	Synthesis of Novel Compounds.....	166
4.5.6	Proof-of-Concept Photoreactions	176
4.5.7	NMR-Spectra	181
4.6	References.....	200
5	SUMMARY	209

6	ZUSAMMENFASSUNG.....	213
7	APPENDIX.....	219
	7.1 Abbreviations	219
	7.2 Curriculum Vitae	224
8	DANKSAGUNG	229

CHAPTER 1

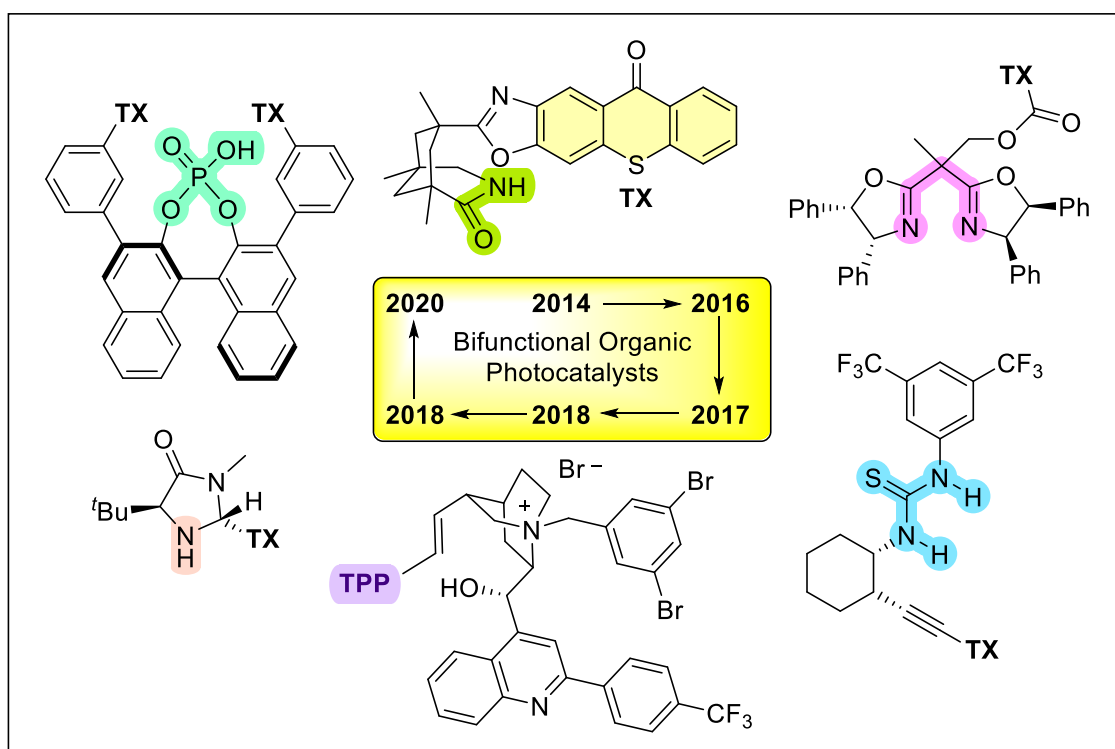
1 Bifunctional Organic Photocatalysts for Enantioselective Visible-Light Mediated Photocatalysis

At the date of submission of this thesis, a version of this chapter has been submitted for publication and is under review.

A. B. Rolka wrote the manuscript. B. König supervised the project.

Abstract

This chapter aims to highlight the developments in the field of visible-light mediated enantioselective photocatalysis utilizing bifunctional organic photocatalysts by giving an overview of the existing hybrid structures and the reactions they have been employed in. Further, an emphasis is put on the comparison to dual catalytic versions featuring two discrete catalysts, when applicable. Organic bifunctional structures in this context are defined as the combination of organic photocatalyst moieties that can be activated by visible light with chiral catalysts, responsible for enantioselective induction, in one sole catalyst.



1.1 Introduction

The field of photocatalysis has seen the accomplishment of many important transformations that pose a challenge to achieve under alternative conditions. Creative strategies utilizing light in combination with a well-chosen photocatalyst have not only been established as mild alternatives for harsher synthetic conditions but have also led to the development of novel reaction routes. Many reviews over the last years have covered the success story of photocatalysis,¹ however, intensive research in the field is still ongoing. In particular, enantioselective versions of photocatalytic protocols still pose a significant challenge due to the generation of transient and highly reactive photo-excited intermediates.² Successful implementation of chirality has often been achieved by the utilization of dual catalytic strategies³ in which an achiral photocatalyst is separate from an additional, asymmetry-inducing chiral catalyst. However, it has also been shown that chiral motifs can be combined with a photocatalyst into a single structure, leading to a bifunctional catalyst that fulfills both roles.⁴ These bifunctional structures are the focus of this chapter.

The scope of this chapter will be limited to include only bifunctional organic photocatalysts used for enantioselective photocatalysis operating by visible light excitation. Bifunctional organic photocatalysts requiring activation by light outside of the visible range as well as bifunctional metal-based photocatalysts^{4,5} will not be covered in this chapter, neither will dual catalytic systems that are linked non-covalently.⁶

Further, as the mechanisms of operation for both dual catalytic and bifunctional catalytic systems, along with the relevant transition states explaining the stereochemical outcome, have been well covered in recent reviews,⁴ less focus here will be put on those topics. Instead, the emphasis will be placed on summarizing the existing work and recent developments and giving a perspective of their role within enantioselective photocatalysis by comparing the results of bifunctional catalytic systems to outcomes achieved with dual catalytic systems, when applicable.

1.2 Bifunctional lactam-photocatalyst

In 2014, the Bach group introduced the first example of a bifunctional chiral photocatalyst (**1**) that can efficiently absorb light in the visible region by merging a thioxanthone photocatalyst with a chiral derivative of Kemp's acid that serves as a hydrogen bonding motif (Figure 1-1A).⁷

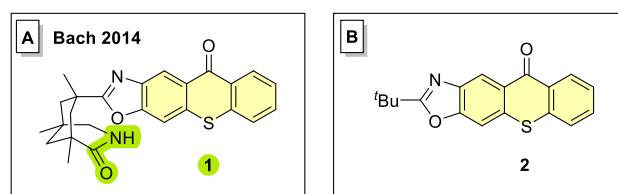
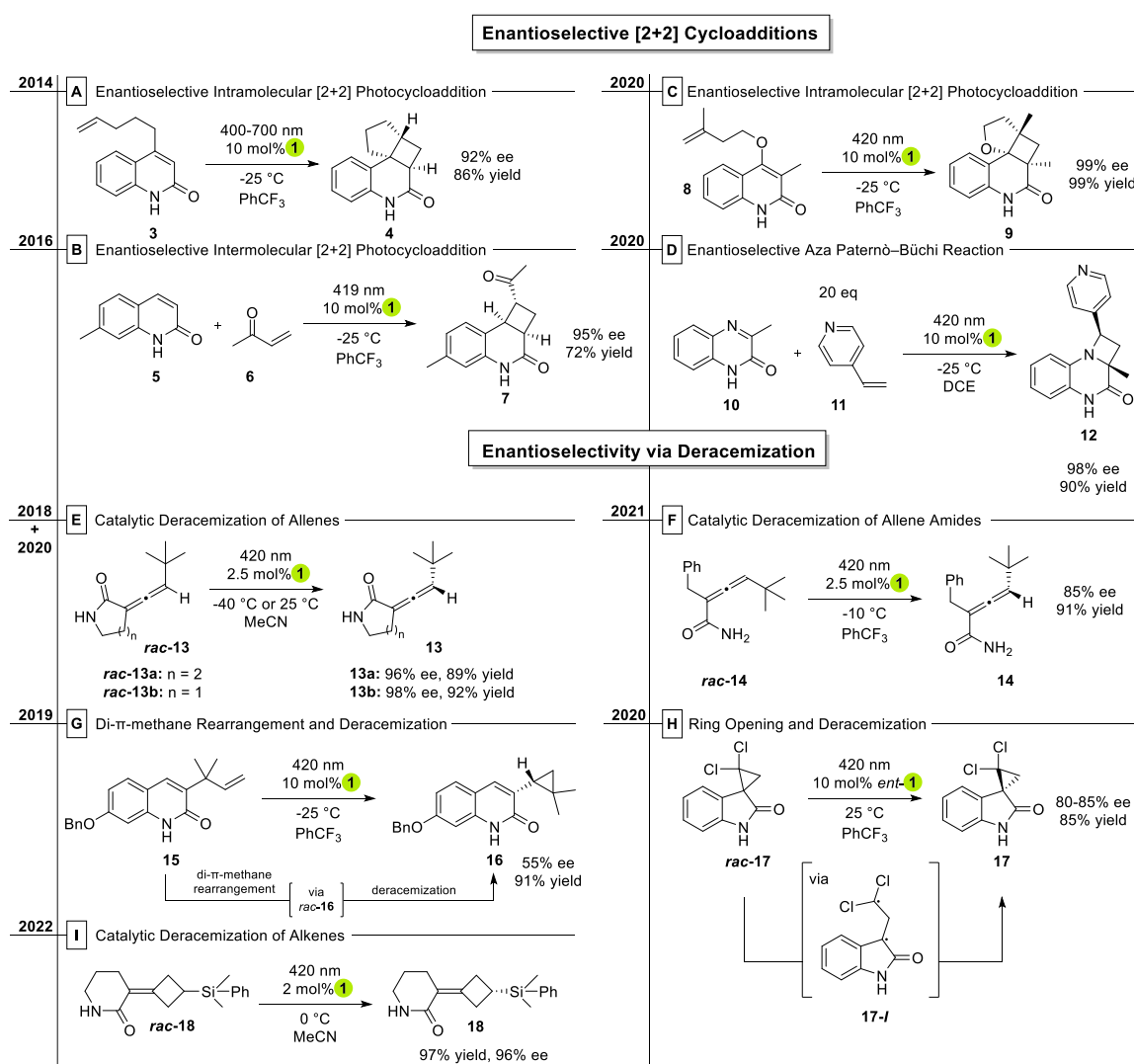


Figure 1-1: Structure of chiral, bifunctional thioxanthone-lactam photocatalyst **1** and an achiral version (**2**).

Since then, the utility of this catalyst has been demonstrated in a diverse range of transformations by the Bach group, the most recent one in 2022. Prior to this catalyst, bifunctional catalysts based on benzophenone or xanthone motifs had been successfully utilized for enantioselective catalysis, but required UV-light activation and were prone to decomposition by unwanted hydrogen atom abstraction.⁸ In their seminal publication in 2014, **1** was shown to effectively catalyze the intramolecular enantioselective [2+2] cycloaddition of quinolones **3** (Scheme 1-1A).⁷ High levels of enantiomeric excess (ee) between 87-96% were achieved with simultaneously high yields of 79-97% on eight different substrates. In 2016, the Bach group extended this methodology to include a more challenging intermolecular version of the transformation featuring 2(1*H*)-quinolones **5** and electron-deficient olefins **6** (Scheme 1-1B).⁹ Once again, high ee's of up to 95% (80-95%) were achieved with moderate to good yields (44-94%) for 14 quinolones as well as one isoquinolone. The scope of enantioselective [2+2] photocycloadditions was furthermore extended in 2020, first to include the intramolecular reaction utilizing 3-alkylquinolones **8** with 4-*O*-tethered alkenes (14 examples) and allenes (6 examples) (Scheme 1-1C, 72-99% yield and excellent ee's of 81-99%),¹⁰ and later to an intermolecular Aza Paternò-Büchi reaction of quinoxalinones **10** (Scheme 1-1D, 14 examples with yields between 50-99% and 86-98% ee).¹¹

In 2018 the group impressively introduced the ability of **1** to catalyze the deracemization of chiral allenes, allowing for the conversion of racemic allenes **13a** into enantiomerically enriched material with excellent ee's of 89-97% in 17 examples (Scheme 1-1E, $n = 2$, yields between 52%-quant.).^{12a} Two years later, the methodology was extended to include trisubstituted allenes with a 3-(1'-alkenylidene)-pyrrolidin-2-one motif **13b** (Scheme 1-1E, $n = 1$, 13 examples with yields between

60-96% and again excellent ee's of 86-98%), as well as one tetrasubstituted allene (85% yield, 45% ee) and one seven-membered 3-(1'-alkenylidene)-azepan-2-one (87% yield, 62% ee).^{12b} Subsequent reactions of the enantioenriched chiral allenes in a Diels-Alder or bromination reaction showcased the ability to convert the axial chirality of the allenes to point chirality. Further, in 2021, enantioenriched acyclic allene amides **14** were also impressively shown to be accessible by photochemical deracemization from *rac*-**14** in 19 examples with high ee's ranging from 73% to 93% (Scheme 1-1F, yields between 74%-quant.).¹³



Scheme 1-1: Visible-light-mediated reactions catalyzed by bifunctional thioxanthone **1**.

In addition to chiral allenes, the ability of **1** to induce deracemizations was further applied to a variety of reactions yielding chiral products. In 2019, this process was key for the enantioselective synthesis of cyclopropane **16** that proceeded via an initial di- π -methane rearrangement of 3-allyl-

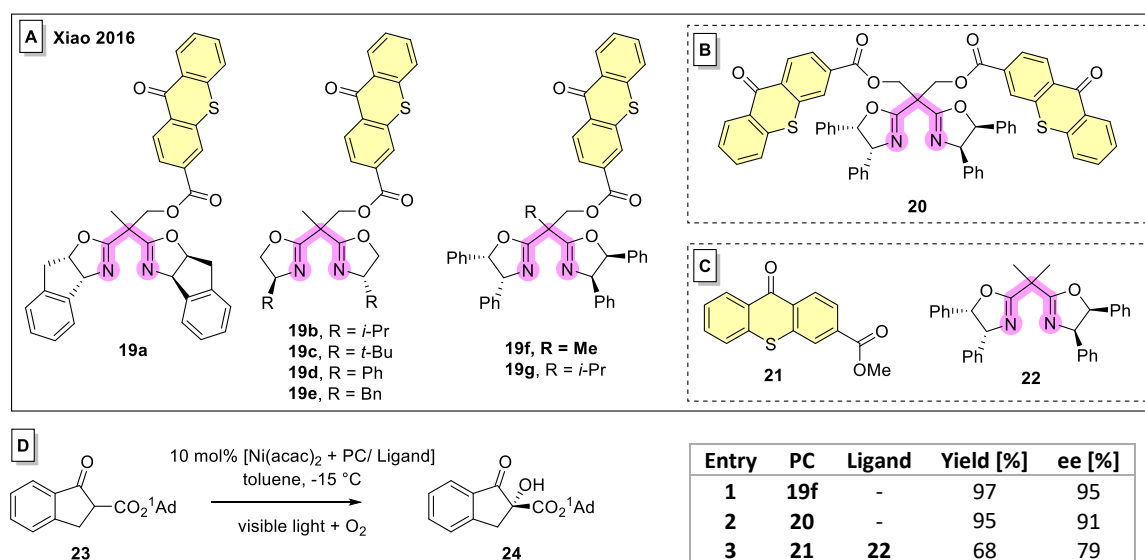
substituted quinolones **15** (Scheme 1-1G) to yield racemic **16** that was followed by a deracemization to give chiral **16** (nine examples with yields between 88-96% yield and moderate ee's of 32-55%).¹⁴ Additionally, in 2020 they further published the deracemization of eight differently substituted chiral spirocyclopropyl oxindoles **17** with *ent*-**1** (Scheme 1-1H), with the reaction assumed to be operating via a reversible ring opening (**17-I**) (65%-97% yield, 50-85% ee) and subsequent recyclization that results in a net enantioenrichment.¹⁵ Most recently in 2022, the Bach group applied the thioxanthone **1**-catalyzed deracemization to alkenes **18**, furnishing chiral tetrasubstituted olefins in excellent enantioselectivities (Scheme 1-1I, 16 examples with yields between 51%-quant. and with high ee's of 81%-96%).¹⁶

All of these reactions (Scheme 1-1) are assumed to be operating by a triplet energy transfer mechanism, with thioxanthone being the photosensitizer.¹⁷ Its triplet energy of 263 kJ/mol^{12a} is comparable to that of the parent thioxanthone **TX** (265 kJ/mol,^{17d} for structure see Scheme 1-5C), indicating that in theory it should be capable of catalyzing triplet-sensitization reactions achievable with the achiral **TX** catalyst. The ability of bifunctional catalyst **1** featuring a lactam binding site to promote enantioselective deracemization reactions can be at least partially rationalized on the basis of the strong distance dependency of triplet energy transfer in solution. This dependence allows minimal differences in association constants and proximity between the two enantiomeric substrates and the sensitizer - which form diastereomeric complexes upon binding - to affect the relative rates of energy transfer to the individual enantiomers and thus influence the enantioselective control of a photochemical process. Control experiments utilizing achiral thioxanthone **2** lacking a binding site (Figure 1-1B) in the racemization of allene *ent*-**13a** (Scheme 1-1E) supported this distance dependent hypothesis due to a much lower quantum yield than the inversion from *ent*-**13a** to **13a** catalyzed by **1** ($\phi \approx 0.1$ vs. $\phi 0.52 \pm 0.03$).^{12a}

1.3 Bifunctional photocatalysts for aerobic oxidation reactions

Up until the end of 2016, the lactam-based chiral thioxanthone **1** was the only bifunctional thioxanthone catalyst utilized in enantioselective photocatalysis. However, the Xiao group introduced a novel class of bifunctional catalysts to the field in 2016 by linking chiral bisoxazoline ligands to thioxanthone (**19**, Scheme 1-2A).¹⁸ Their performance as chiral catalysts together with Ni(acac)₂ as a Lewis acid was evaluated for the enantioselective aerobic oxidation of β -ketoesters with impressive results, yielding **24** with an excellent enantioselectivity of 95% (Scheme 1-2D, entry 1) with catalyst **19f**. Interestingly, the thioxanthone catalyst **20** featuring two thioxanthone

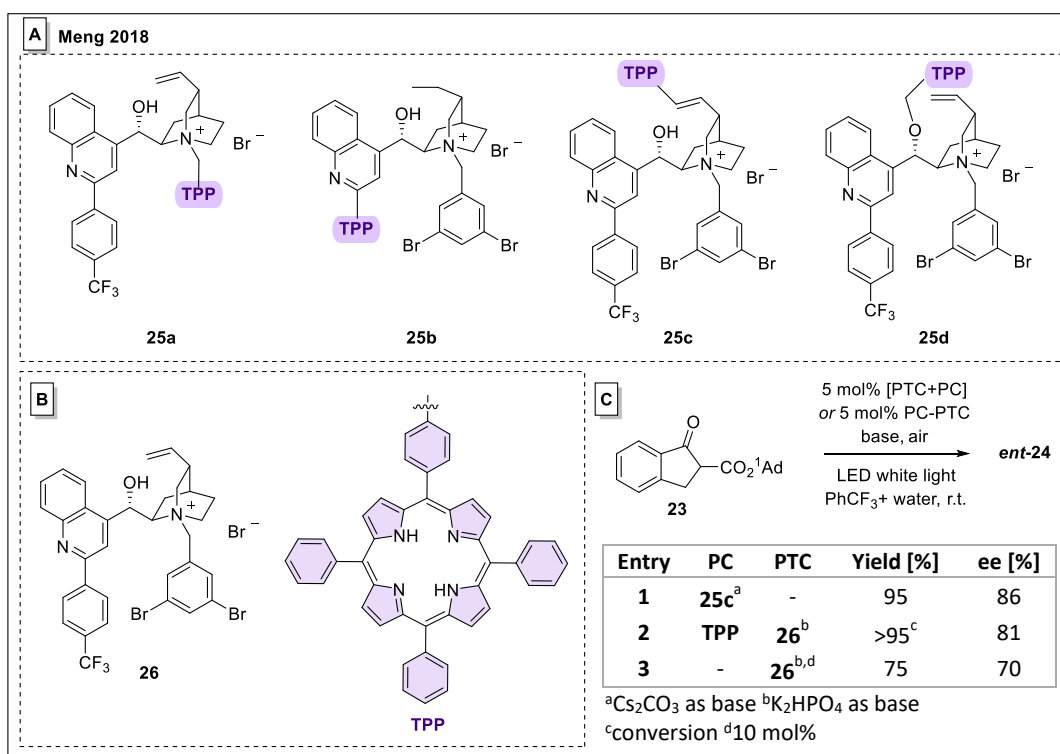
moieties (Scheme 1-2B) showed a reduced enantioselectivity of 91% (Scheme 1-2D, entry 2). Moreover, a control experiment utilizing a dual catalytic system closest to the bifunctional catalyst (Scheme 1-2C, 10 mol% of sensitizer **21** and 10 mol% of separate ligand **22**) under otherwise identical reaction conditions gave **24** with significantly decreased yield (68%) and ee (79%), demonstrating the benefit of the bifunctional catalyst. In total, 22 substrates were enantioselectively oxidized in overall good yields (78-98%) and with high ee's (75-95%). However, in a more recent publication, control experiments utilizing a modified dual catalytic system consisting of thioxanthone **TX** as a photocatalyst and **22** as a chiral ligand under slightly altered reaction conditions (10 W 525 nm-green light, MTBE as solvent) gave **24** in 88% yield with a high level of enantioinduction (94% ee). Furthermore, by switching from thioxanthone **TX** to tetraphenylporphyrin (**TPP**) as sensitizer, the catalyst loading could be decreased to only 0.5 mol% while simultaneously increasing the yield to 99% with an excellent enantioselectivity of 95% ee.¹⁹



Scheme 1-2: Enantioselective aerobic oxidation of β -ketoesters utilizing thioxanthone-based catalysts **19**.

A different approach to accessing chiral **24** utilizing a novel bifunctional catalyst consisting of a phase-transfer catalyst (**PTC**) and **TPP** as an organic sensitizer was published in 2018 by the Meng group (**25**, Scheme 1-3A).²⁰ Comparably high yield (95%) and still high – but lower compared to the performance with **19f** – enantioselectivity (86%) was reported with **25c** as the bifunctional catalyst (Scheme 1-3C, entry 1). In this case, the utilization of **TPP** as a sensitizer and **26** as a separate **PTC** that is not linked to the photocatalyst (Scheme 1-3B) gave similar yield with only slightly diminished ee (Scheme 1-3C, entry 2).²¹ Even without the use of **TPP**, moderate yield (75%)

and ee (70%) were achieved by the same group in 2019, with sensitization likely occurring through the formation of a chiral enolate complex between the β -ketoester and the PTC under basic conditions (Scheme 1-3C, entry 3).^{22,23}



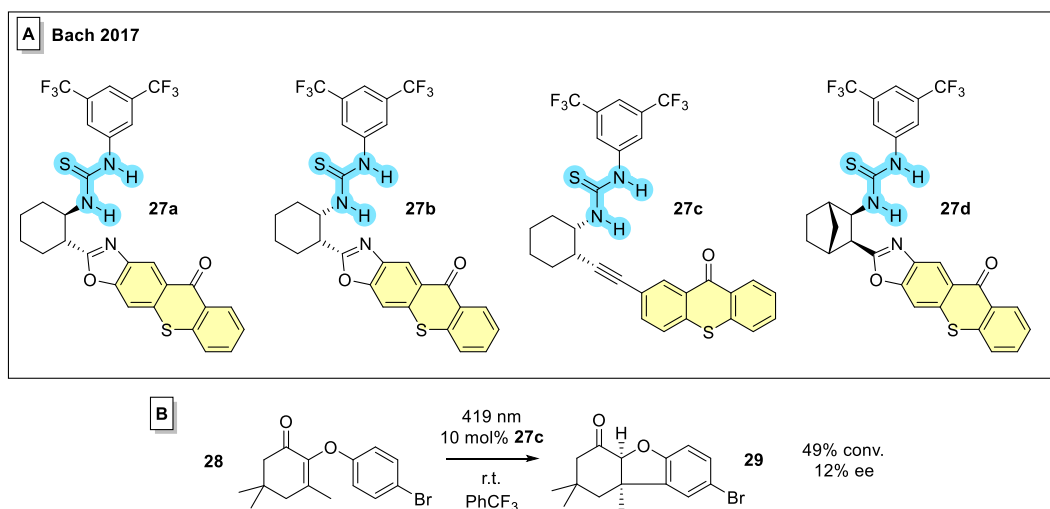
Scheme 1-3: Enantioselective aerobic oxidation of β -ketoesters utilizing TPP-based catalysts.

In 2019 Coeffard et al. reported on the synthesis of a bifunctional photocatalyst consisting of a chiral quinine organocatalyst linked to an iodo-BODIPY photosensitizer.²⁴ They employed it in stereoselective α -oxygenation reactions, achieving up to 40% enantiomeric excess. Due to boron being part of the photocatalytic unit and falling into the category of metalloids, it is not considered purely organic in the context of this review and is therefore not shown.

1.4 Bifunctional urea-photocatalysts

The development of bifunctional catalysts picked up speed after 2016 and the pool of existing bifunctional catalysts was extended further in 2017 by the Bach group.²⁵ They reported the synthesis of four thioxanthone-urea hybrid catalysts **27** (Scheme 1-4A); however, in a preliminary unoptimized test reaction (Scheme 1-4B) with **27c**, only low ee (12%) and moderate conversion

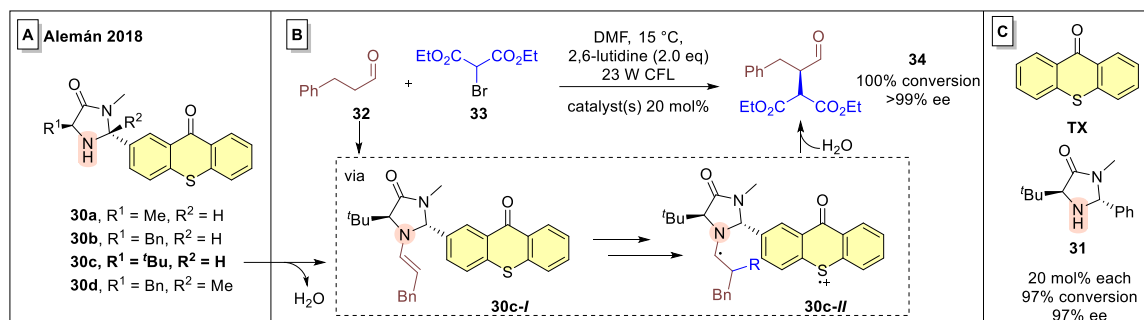
(49%) was achieved. To the best of our knowledge, no further follow-up reactions have been reported involving these catalysts.



Scheme 1-4: Chiral urea-thioxanthone hybrid photocatalysts and cyclization of 2-aryloxycyclohex-2-enone **28**.

1.5 Bifunctional photoaminocatalysts

In 2018, the group of Alemán introduced bifunctional photoaminocatalysts **30**, that creatively combine a chiral imidazolidinone with thioxanthone (Scheme 1-5A).²⁶ This work built upon the seminal work of MacMillan from 2008, demonstrating how merging photoredox catalysis with organocatalysis can serve as a powerful tool for the asymmetric alkylation of aldehydes. In the original MacMillan system, 0.5 mol% of Ru(bpy)₃Cl₂ as a photoredox catalyst coupled with 20 mol% of an imidazolidinone organocatalyst gave rise to excellent ee of the alkylation product (up to 99%).²⁷ Other alternative dual catalytic approaches have since been reported, including purely organic-based systems.^{28,29} However, catalysts **30a-30d** represent the first example of bifunctional photoaminocatalysts for enantioselective α -alkylation of aldehydes **32** (Scheme 1-5B). Within this catalyst class, **30c** was found to give the best results in the studied test reaction of **32** with **33**. The utility of **30c** was highlighted by achieving overall high enantioselectivities and yields (12 examples, yields of 55-99%, ee's between 84-99%). Furthermore, this bifunctional system performed slightly better than a control dual catalytic system using parent thioxanthone **TX** and structurally related imidazolidinone catalyst **31** (Scheme 1-5C), although the difference may lie within experimental error.



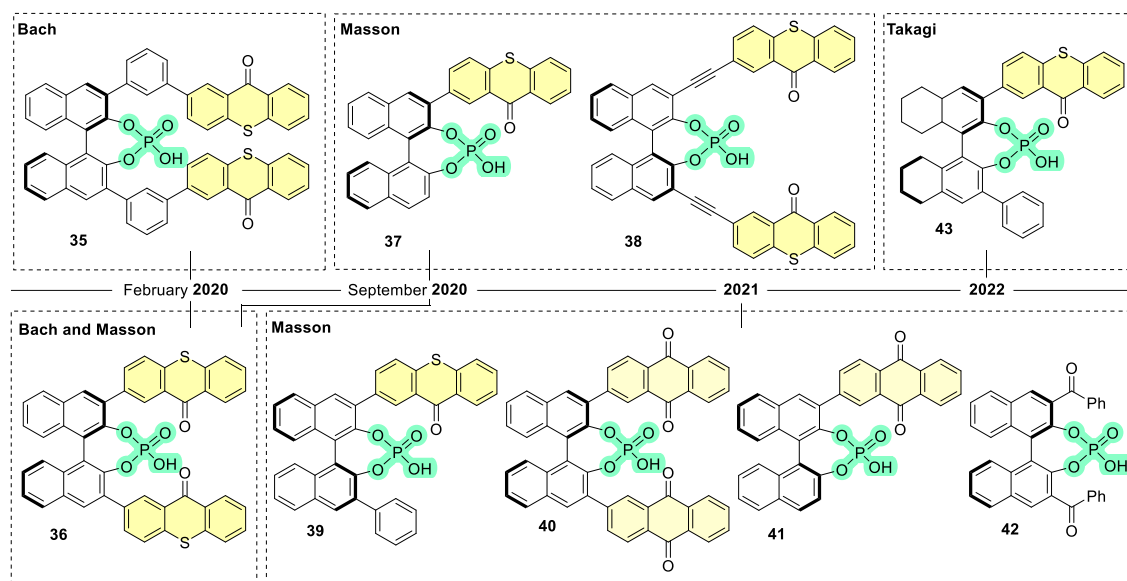
Scheme 1-5: Chiral bifunctional photoaminocatalysts **30** for the asymmetric alkylation of aldehydes.

The group conducted extensive mechanistic experiments and among other things found that the overall quantum yield of the α -alkylation of hydrocinnamaldehyde **32** with diethyl bromomalonate **33** was lower for the bifunctional catalyst **30c** than for the dual catalytic system (**TX** + **31**) ($\phi = 2.4$ vs. $\phi = 4.4$). Based on the mechanism originally proposed by the MacMillan group, the catalytic cycle with bifunctional catalyst **30c** was assumed to proceed via enamine intermediate **30c-I**, formed through condensation of **30c** with aldehyde **32**. After visible light excitation, the attached thioxanthone moiety reduces diethyl bromomalonate **33** to the corresponding debrominated alkyl radical, while getting oxidized to the radical cation. Subsequent addition of the alkyl radical to the enamine double bond results in α -amino radical intermediate **30c-II**, which is oxidized either via a chain-propagation process that occurs through reduction of the alkyl bromide or by a termination event via reduction of the previously generated thioxanthone radical cation. This intramolecular redox process was believed to be a contributing factor for the lower quantum yield observed for the bifunctional catalyst.

1.6 Bifunctional chiral phosphoric acid (CPA) photocatalysts

Starting with the first bifunctional C₂-symmetric chiral phosphoric acid photocatalysts (**CPA-PA**) published by the Bach group in 2020³⁰ (Scheme 1-6, **35** and **36**), the combination of carbonyl-based photosensitizers with chiral phosphoric acid backbones has been reported by multiple groups. The Masson group independently reported the synthesis of **36** in the same year as the Bach group in addition to a monosubstituted C₁-symmetric derivative (**37**) and alkyne coupled catalyst **38**.³¹ The same group later built on this concept and extended the scope of bifunctional chiral photocatalysts to include an additional C₁-symmetric thioxanthone **39**, anthraquinones (**40** and **41**), aryl ketones (**42**) and a non-visible light absorbing benzophenone coupled (*S*)-BINOL-

derived phosphoric acid (not shown).³² In 2022, Takagi and Tanimoto published a derivative of **39** with a modified chiral phosphoric acid back bone (**43**).³³



Scheme 1-6: Overview of visible-light absorbing bifunctional chiral phosphoric acid photocatalysts.

The reactions that these catalysts have been utilized in are manifold (Scheme 1-7). The Bach group employed **35** in an intermolecular cycloaddition of cyclopentene **45** with β -carboxyl-substituted cyclic enones **44** (Scheme 1-7A).³⁰ After benzylation, the enantioenriched cycloaddition products **47** were obtained in moderate to good ee's (44-86%) on a relatively small substrate scope (6 examples). Enantioinduction was proposed to be the result of a lowered triplet energy of the substrate upon hydrogen bonding between the carboxylic acid of the substrate **44** and the chiral phosphoric acid moiety of **35**. Interestingly, the measured triplet energy for **35** was lower than the reported triplet energy for the parent thioxanthone (**TX** = 265 kJ/mol,^{17d} **35**: 235 kJ/mol). Moreover, **36** did not achieve any enantioinduction.

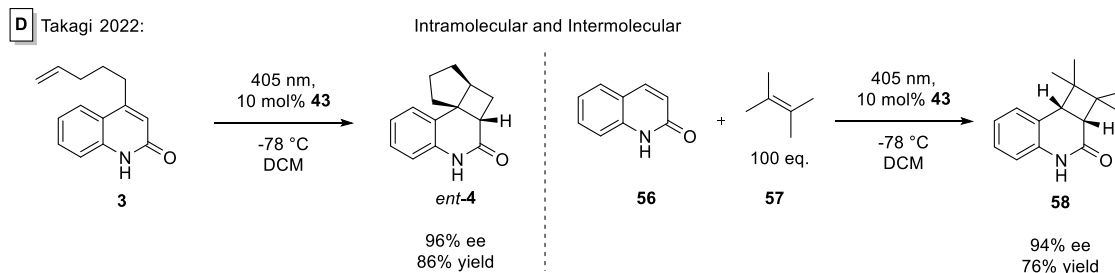
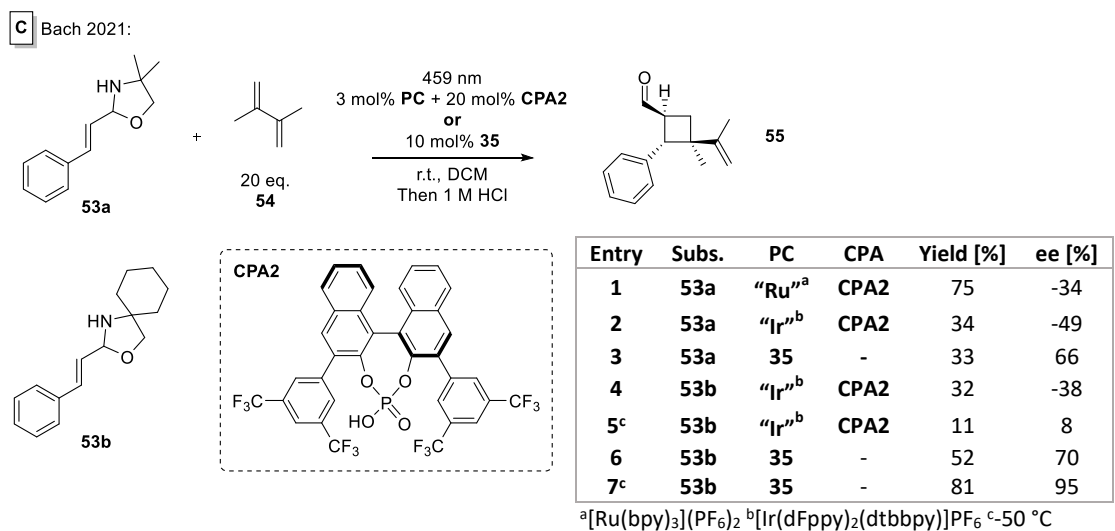
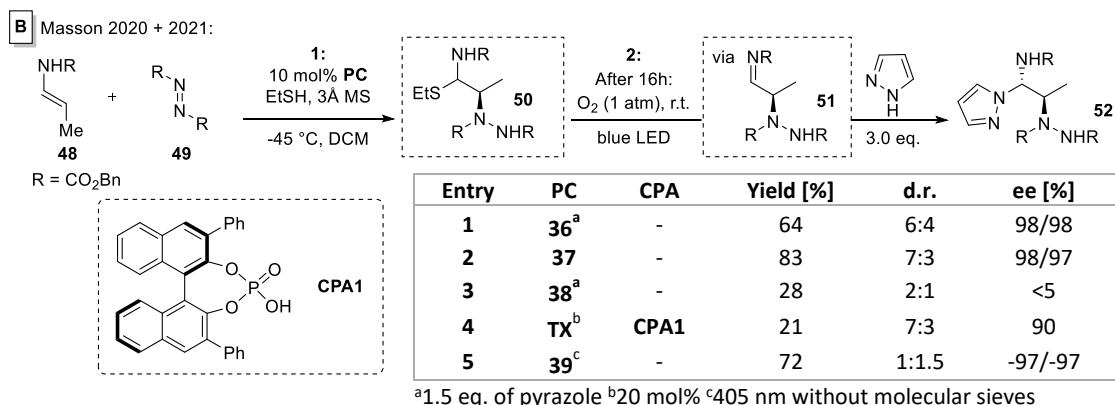
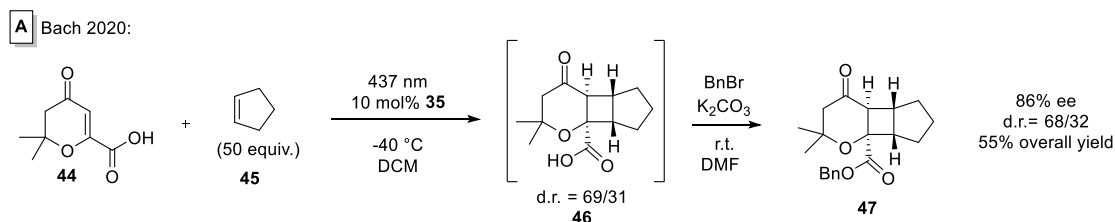
In contrast, the Masson group achieved an excellent ee (98%, 64% yield, d.r. 6:4) with **36** in the synthesis of 1,2-diamines **52** via an electrophilic amination.^{31,34} (Scheme 1-7B). However, unlike in Bach's work, the enantioselectivity in this sequence is induced by the attached chiral phosphoric acid in non-photochemical steps via hydrogen bonding, whereas the role of the attached photocatalyst is the photocatalytic generation of reactive imine intermediate **51** than can subsequently react with the nucleophile pyrazole. Switching catalysts from **36** to **37** achieved an equally high ee, but with an improved d.r. of 7:3 along with an increased yield of 72%, possibly as

a result of decreased intramolecular bleaching due to the removal of the second thioxanthone moiety. This yield was found to be further improved to 83% (Scheme 1-7B, entry 2) after doubling the equivalents of pyrazole (from 1.5 eq. to 3.0 eq.). In contrast, no significant enantioselectivity was observed with **38** (<5%) (Scheme 1-7B, entry 3). The comparison to a dual catalytic system with thioxanthone **TX** and phosphoric acid **CPA1** under the optimized reaction conditions resulted in the same diastereoselective ratio of 7:3 with a slightly lower ee (90%) and a significantly decreased yield of 21% (Scheme 1-7B, entry 4), validating the benefit of bifunctional catalyst **37**. In 2021, the Masson group tested their new generation of bifunctional photo-phosphoric acid catalysts discussed earlier (**39-42**) under the optimized reaction conditions for the electrophilic β -amination of enecarbamates **48**. However, only **39** (Scheme 1-7B, entry 5) achieved significant enantioinduction with visible light.³²

In the same year (2021), the Bach group published further results utilizing their chiral phosphoric acid **35** in intermolecular [2+2] cycloadditions (Scheme 1-7C).³⁵ Impressive enantioselectivity was achieved (84-98% ee) with moderate to high yields (54-96%) in 19 examples. NMR studies suggest that the reaction proceeds via the formation of an iminium ion upon protonation of **53** that remains bound to the bifunctional chiral acid counterion in a hydrogen-bond assisted ion pair, allowing for enantiofacial differentiation. The attached thioxanthone moieties can then sensitize the iminium ion in an energy-transfer mechanism. Control experiments revealed that both the photocatalyst and the chiral phosphoric acid were required for a successful reaction. Dual catalytic systems consisting of chiral phosphoric acid **CPA2** and a separate ruthenium ("Ru" = [Ru(bpy)₃](PF₆)₂) or iridium ("Ir" = [Ir(dFppy)₂(dtbbpy)]PF₆) photocatalyst were also investigated (Scheme 1-7C, entries 1-2 and 4-5). However, under all tested conditions, the enantioselectivity did not exceed 49% (-49% ee, Scheme 1-7C, entry 2). This is in contrast to the reaction utilizing bifunctional catalyst **35** which could be optimized to furnish **55** in an excellent enantioselectivity of 95% with a good yield of 81% (Scheme 1-7C, entry 7), highlighting the superiority of the bifunctional system in this reaction.

As described earlier (see Scheme 1-1A and 1-1B), the Bach group achieved the visible-light mediated [2+2] photocycloaddition of quinolones **3**, first in an intramolecular fashion and then in an intermolecular way utilizing chiral hydrogen bonding catalyst **1** (Figure 1-1A). In 2022, Takagi and Tanimoto showed that C₁-symmetric chiral phosphoric acid **43** is also able to achieve high enantioselectivities in these transformations (Scheme 1-7D), presumably due to hydrogen bonding between quinolone **3** and the phosphoric acid of **43** as well as π - π interactions of thioxanthone with quinolone. The effectiveness of the bifunctional photocatalyst was

demonstrated on four examples for the intramolecular reaction of **3** with yields ranging from 86%-95% and excellent ee's of 91-97%, and on five intermolecular examples with **56** and 100 equivalents of 2,3-dimethyl 2-butene **57** (yields: 24-99%, ee's: 73-98%).³³



Scheme 1-7: Enantioselective reactions catalyzed by chiral photo-phosphoric acid catalysts.

Lastly, the newest addition to this family of bifunctional catalysts is represented by **4CzIPN**- and **2CzPN**-derived phosphoric acid photocatalyst hybrids **59** and **60** (Figure 1-2) published recently by the König and Toste groups.³⁶

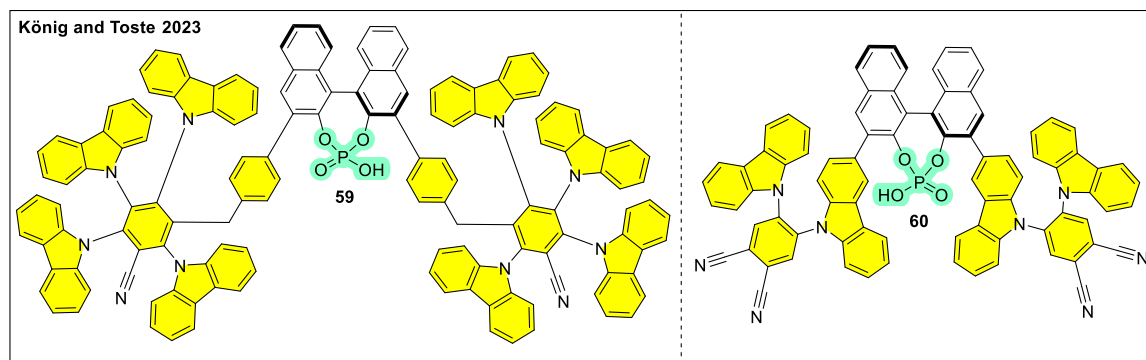
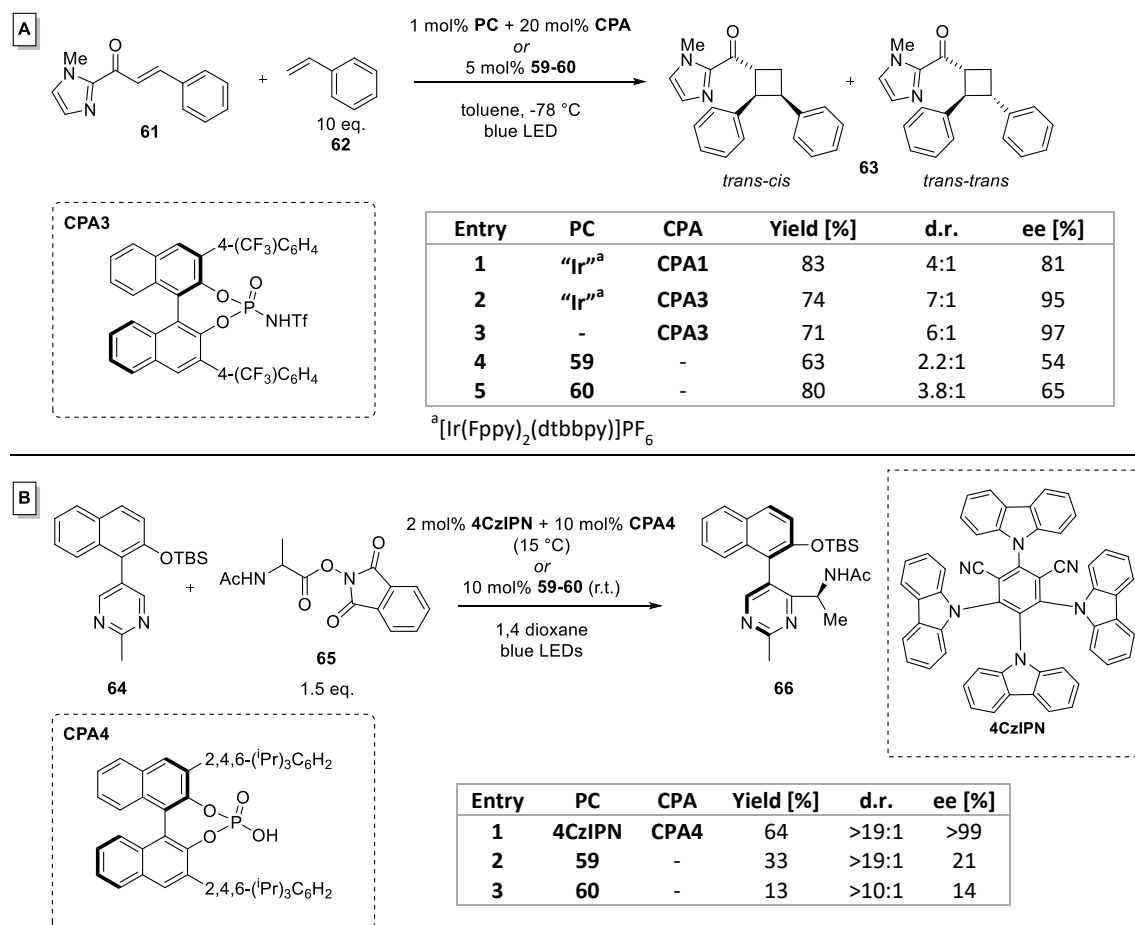


Figure 1-2: Structures of chiral cyanoarene-based chiral phosphoric acid catalysts **59** and **60**.

In preliminary experiments, their potential to act as both chiral energy transfer and photoredox catalysts has been established in the [2+2] cycloaddition of **61** originally published by Yoon³⁷ (Scheme 1-8A) and in a photoredox catalyzed Minisci reaction based on the work of Xiao^{38,39} (Scheme 1-8B). In these proof-of-concept reactions, the cyano-based bifunctional catalysts gave lower enantioselective results than the previously reported dual catalytic systems. However, the reactions were not optimized for the novel catalysts and research into their use is still ongoing.



Scheme 1-8: Enantioselective reactions catalyzed by chiral cyanoarene-based photo-phosphoric acid catalysts.

1.7 Conclusion

Since the introduction of thioxanthone-based photocatalyst **1** in 2014, the development of bifunctional organic photocatalysts has gained attention and a multitude of hybrid catalysts have been reported. The majority of these catalysts rely on thioxanthone as the photocatalytic moiety, but **TPP** and donor-acceptor cyanoarene-based photocatalysts have also been successfully linked to chiral motifs. In many cases where a comparison of the bifunctional catalyst to dual catalytic systems is available, a significant improvement of either yield or enantioselectivity (or both) has been observed when utilizing the sole bifunctional catalytic system. These comparisons also present the opportunity to investigate the operating mechanism better and draw insightful conclusions. However, there have also been reactions where no or no major benefit of the bifunctional system was visible. Additionally, some of the reported structures require increased synthetic effort compared to a dual catalytic counterpart and careful selection and development of new reactions, tailored to the bifunctional catalyst, might be necessary to unfold the full potential of these catalyst scaffolds. Overall, this field of photocatalysis remains underdeveloped, but has shown great potential and the establishment of new bifunctional catalysts presents an exciting avenue of photocatalysis.

1.8 References

- [1] For selected reviews on photocatalysis see: (a) Bellotti, P.; Huang, H.-M.; Faber, T.; Glorius, F. Photocatalytic Late-Stage C–H Functionalization. *Chem. Rev.* **2023**, DOI: 10.1021/acs.chemrev.2c00478. (b) Chan, A. Y.; Perry, I. B.; Bissonnette, N. B.; Buksh, B. F.; Edwards, G. A.; Frye, L. I.; Garry, O. L.; Lavagnino, M. N.; Li, B. X.; Liang, Y.; Mao, E.; Millet, A.; Oakley, J. V.; Reed, N. L.; Sakai, H. A.; Seath, C. P.; MacMillan, D. W. C. Metallaphotoredox: The Merger of Photoredox and Transition Metal Catalysis. *Chem. Rev.* **2022**, *122*, 1485-1542. (c) Hojo, R.; Polgar, A. M.; Hudson, Z. M. Thermally Activated Delayed Fluorescence Sensitizers As Organic and Green Alternatives in Energy-Transfer Photocatalysis. *ACS Sustainable Chem. Eng.* **2022**, *10*, 9665-9678. (d) Rigotti, T.; Alemán, J. Visible light photocatalysis – from racemic to asymmetric activation strategies. *Chem. Commun.* **2020**, *56*, 11169-11190. (e) Marzo, L.; Pagire, S. K.; Reiser, O.; König, B. Visible-Light Photocatalysis: Does It Make a Difference in Organic Synthesis? *Angew. Chem. Int. Ed.* **2018**, *57*, 10034-10072. (f) Twilton, J.; Le, C.; Zhang, P.; Shaw, M. H.; Evans, R. W.; MacMillan, D. W. C. The Merger of Transition Metal and Photocatalysis. *Nat. Rev. Chem.* **2017**, *1*, No. 0052. (g) Romero, N. A.; Nicewicz, D. A. Organic Photoredox Catalysis. *Chem. Rev.* **2016**, *116*, 10075-10166. (h) Prier, C. K.; Rankic, D. A.; MacMillan, D. W. C. Visible Light Photoredox Catalysis with Transition Metal Complexes: Applications in Organic Synthesis. *Chem. Rev.* **2013**, *113*, 5322-5363.
- [2] For selected reviews on enantioselective photocatalysis see: (a) Großkopf, J.; Kratz, T.; Rigotti, T.; Bach, T. Enantioselective Photochemical Reactions Enabled by Triplet Energy Transfer. *Chem. Rev.* **2022**, *122*, 1626-1653. (b) Verma, R.; Jindal, P.; Prasad, J.; Kothari, S. L.; Lamba, N. P.; Dandia, A.; Khangarot, R. K.; Chauhan, M. S. Recent Trends in Photocatalytic Enantioselective Reactions. *Top. Curr. Chem. (Z)* **2022**, *380*, 48. (c) Hoffmann, N. Enantioselective synthesis of heterocyclic compounds using photochemical reactions. *Photochem Photobiol Sci.* **2021**, *20*, 1657-1674. (d) Prentice, C.; Morrisson, J.; Smith, A. D.; Zysman-Colman, E. Recent developments in enantioselective photocatalysis. *Beilstein J. Org. Chem.* **2020**, *16*, 2363-2441. (e) Saha, D. Catalytic Enantioselective Radical Transformations Enabled by Visible Light. *Chem. Asian J.* **2020**, *15*, 2129-215. (f) Jiang, C.; Chen, W.; Zheng, W.-H.; Lu, H. Advances in asymmetric visible-light photocatalysis, 2015–2019. *Org. Biomol. Chem.* **2019**, *17*, 8673-8689. (g) Silvi, M.; Melchiorre, P. Enhancing the potential of enantioselective organocatalysis with light. *Nature* **2018**, *554*, 41-49. (h) Zou, Y.-Q.; F. M.; Bach, T. Iminium and enamine catalysis in enantioselective photochemical

- reactions. *Chem. Soc. Rev.* **2018**, *47*, 278-290. (i) Brenninger, C.; Jolliffe, J. D.; Bach, T. Chromophore Activation of α,β -Unsaturated Carbonyl Compounds and Its Application to Enantioselective Photochemical Reactions. *Angew. Chem. Int. Ed.* **2018**, *57*, 14338-14349. (j) Brimioulle, R.; Lenhart, D.; Maturi, M. M.; Bach, T. Enantioselective Catalysis of Photochemical Reactions. *Angew. Chem. Int. Ed.* **2015**, *54*, 3872-3890. (k) Meggers, E. Asymmetric catalysis activated by visible light. *Chem. Commun.* **2015**, *51*, 3290-3301.
- [3] For selected recent reviews specifically on dual catalytic strategies see: (a) Roy, S.; Paul, H.; Chatterjee, I. Light-Mediated Aminocatalysis: The Dual-Catalytic Ability Enabling New Enantioselective Route. *Eur. J. Org. Chem.* **2022**, e202200446. (b) Guo, F.; Wang, H.; Ye, X.; Tan, C.-H. Advanced Synthesis Using Photocatalysis Involved Dual Catalytic System. *Eur. J. Org. Chem.* **2022**, e202200326. (c) Yao, W.; Bazan-Bergamino, E. A.; Ngai, M.-Y. Asymmetric Photocatalysis Enabled by Chiral Organocatalysts. *ChemCatChem.* **2022**, *14*, e202101292.
- [4] (a) Mondal, S.; Dumur, F.; Gimes, D.; Sibi, M. P.; Bertrand, M. P.; Nechab, M. Enantioselective Radical Reactions Using Chiral Catalysts. *Chem. Rev.* **2022**, *122*, 5842-5976. (b) Genzink, M. J.; Kidd, J. B.; Swords, W. B.; Yoon, T. P. Chiral Photocatalyst Structures in Asymmetric Photochemical Synthesis. *Chem. Rev.* **2022**, *122*, 1654-1716.
- [5] For a review covering enantioselective photocatalysis with chiral at metal catalysts see: Huang, X.; Meggers, E. Asymmetric Photocatalysis with Bis-Cyclometalated Rhodium Complexes. *Acc. Chem. Res.* **2019**, *52*, 833-847.
- [6] For a recent review on ion-pairing catalysis see: Schirmer, T. E.; König, B. Ion-Pairing Catalysis in Stereoselective, Light-Induced Transformations. *J. Am. Chem. Soc.* **2022**, *144*, 19207-19218.
- [7] Alonso, R.; Bach, T. A Chiral Thioxanthone as an Organocatalyst for Enantioselective [2+2] Photocycloaddition Reactions Induced by Visible Light. *Angew. Chem. Int. Ed.* **2014**, *53*, 4368-4371.
- [8] For a review see: (a) Burg, F.; Bach, T. Lactam Hydrogen Bonds as Control Elements in Enantioselective Transition-Metal-Catalyzed and Photochemical Reactions. *J. Org. Chem.* **2019**, *84*, 8815-8836. For selected publications see: (b) Maturi, M. M.; Bach, T. Enantioselective Catalysis of the Intermolecular [2+2] Photocycloaddition between 2-Pyridones and Acetylenedicarboxylates. *Angew. Chem. Int. Ed.* **2014**, *53*, 7661-7664. (c) Müller, C.; Bauer, A.; Maturi, M. M.; Cuquerella, M. C.; Miranda, M. A.; Bach, T. Enantioselective Intramolecular [2+2]-Photocycloaddition Reactions of 4-Substituted

- Quinolones Catalyzed by a Chiral Sensitizer with a Hydrogen-Bonding Motif. *J. Am. Chem. Soc.* **2011**, *133*, 16689-16697. (d) Müller, C.; Bauer, A.; Bach, T. Light-Driven Enantioselective Organocatalysis. *Angew. Chem. Int. Ed.* **2009**, *48*, 6640-6642. (e) Bauer, A.; Westkämper, F.; Grimme, S.; Bach, T. Catalytic enantioselective reactions driven by photoinduced electron transfer. *Nature* **2005**, *436*, 1139-1140. (f) Cauble, D. F.; Lynch, V.; Krische, M. J. Studies on the Enantioselective Catalysis of Photochemically Promoted Transformations: "Sensitizing Receptors" as Chiral Catalysts. *J. Org. Chem.* **2003**, *68*, 15-21.
- [9] Tröster, A.; Alonso, R.; Bauer, A.; Bach, T. Enantioselective Intermolecular [2+2] Photocycloaddition Reactions of 2(1*H*)-Quinolones Induced by Visible Light Irradiation. *J. Am. Chem. Soc.* **2016**, *138*, 7808-7811.
- [10] Li, X.; Christian, J.; Bach, T. Visible-Light-Mediated Enantioselective Photoreactions of 3-Alkylquinolones with 4-*O*-Tethered Alkenes and Allenes. *Org. Lett.* **2020**, *22*, 3618-3622.
- [11] Li, X.; Großkopf, J.; Jandl, C.; Bach, T. Enantioselective, Visible Light Mediated Aza Paternò-Büchi Reactions of Quinoxalinones. *Angew. Chem.* **2021**, *133*, 2716-2720.
- [12] (a) Hölzl-Hobmeier, A.; Bauer, A.; Silva, A. V.; Huber, S. M.; Bannwarth, C.; Bach, T. Catalytic deracemization of chiral allenes by sensitized excitation with visible light. *Nature* **2018**, *564*, 240-243. (b) Plaza, M.; Jandl, C.; Bach, T. Photochemical Deracemization of Allenes and Subsequent Chirality Transfer. *Angew. Chem. Int. Ed.* **2020**, *59*, 12785-12788.
- [13] Plaza, M.; Großkopf, J.; Breitenlechner, S.; Bannwarth, C.; Bach, T. Photochemical Deracemization of Primary Allene Amides by Triplet Energy Transfer: A Combined Synthetic and Theoretical Study. *J. Am. Chem. Soc.* **2021**, *143*, 11209-11217.
- [14] Tröster, A.; Bauer, A.; Jandl, C.; Bach, T. Enantioselective Visible-Light-Mediated Formation of 3-Cyclopropylquinolones by Triplet-Sensitized Deracemization. *Angew. Chem.* **2019**, *131*, 3576-3579.
- [15] Li, X.; Kutta, R. J.; Jandl, C.; Bauer, A.; Nürnberger, P.; Bach, T. Photochemically Induced Ring Opening of Spirocyclopropyl Oxindoles: Evidence for a Triplet 1,3 Diradical Intermediate and Deracemization by a Chiral Sensitizer. *Angew. Chem. Int. Ed.* **2020**, *59*, 21640-21647.
- [16] Kratz, T.; Steinbach, P.; Breitenlechner, S.; Storch, G.; Bannwarth, C.; Bach, T. Photochemical Deracemization of Chiral Alkenes via Triplet Energy Transfer. *J. Am. Chem. Soc.* **2022**, *144*, 10133-10138.

- [17] For a review on thioxanthone as photocatalyst see: (a) Nikitas, N. F.; Gkizis, P. L.; Kokotos, C. G. Thioxanthone: a powerful photocatalyst for organic reactions. *Org. Biomol. Chem.* **2021**, *19*, 5237-5253. For additional papers investigating the mechanism see: (b) Zhou, T.-P.; Zhong, F.; Wu, Y.; Liao, R.-Z. Regioselectivity and stereoselectivity of intramolecular [2+2] photocycloaddition catalyzed by chiral thioxanthone: a quantum chemical study. *Org. Biomol. Chem.* **2021**, *19*, 1532-1540. (c) Yang, Y.; Wen, Y.; Dang, Z.; Yu, H. Mechanistic Investigation of Visible-Light-Induced Intermolecular [2+2] Photocycloaddition Catalyzed with Chiral Thioxanthone. *J. Phys. Chem. A* **2017**, *121*, 4552-4559. For triplet energy values see: (d) S. L. Murov, I. Carmichael, G. L. Hug, *Handbook of Photochemistry*, 2nd ed., Dekker, New York, **1993**, p. 80, 91.
- [18] Ding, W.; L.-Q.; Zhou, Q.-Q.; Wei, Y.; Chen, J.-R.; Xiao, W.-J. Bifunctional Photocatalysts for Enantioselective Aerobic Oxidation of β -Ketoesters. *J. Am. Chem. Soc.* **2017**, *139*, 63-66.
- [19] Yin, H.; Wang, C.-J.; Zhao, Y.-G.; He, Z.-Y.; Chu, M.-M.; Wang, Y.-F.; Xu, D.-Q. Asymmetric bis(oxazoline)-Ni(II) catalyzed α -hydroxylation of cyclic β -keto esters under visible light. *Org. Biomol. Chem.* **2021**, *19*, 6588-6592.
- [20] Tang, X.-F.; Feng, S.-H.; Wang, Y.-K.; Yang, F.; Zheng, Z.-H.; Zhao, J.-N.; Wu, Y.-F.; Yin, H.; Liu, G.-Z.; Meng, Q.-W. Bifunctional Metal-Free Photo-Organocatalysts for Enantioselective Aerobic Oxidation of β -Dicarbonyl Compounds. *Tetrahedron* **2018**, *74*, 3624-3633.
- [21] With K_2HPO_4 as base, the ee with catalyst **25c** was also decreased to 80%.
- [22] Scheme 1-3, Table entry 3 taken from: Tang, X.-F.; Zhao, J.-N.; Wu, Y.-F.; Feng, S.-H.; Yang, F.; Yu, Z.-Y.; Meng, Q.-W. Visible-Light-Driven Enantioselective Aerobic Oxidation of β -Dicarbonyl Compounds Catalyzed by Cinchona-Derived Phase Transfer Catalysts in Batch and Semi-Flow. *Adv. Synth. Catal.* **2019**, *361*, 5245-5252.
- [23] For other work utilizing **TPP** and **PTC** in this reaction see: (a) Tang, X.-F.; Zhao, J.-N.; Wu, Y.-F.; Zheng, Z.-H.; Feng, S.-H.; Yu, Z.-Y.; Liu, G.-Z.; Meng, Q.-W. Enantioselective photooxygenation of β -dicarbonyl compounds in batch and flow photomicroreactors. *Org. Biomol. Chem.* **2019**, *17*, 7938-7942. (b) Wang, Y.; Yin, H.; Tang, X.; Wu, Y.; Meng, Q.; Gao, Z. A Series of Cinchona-Derived *N*-Oxide Phase-Transfer Catalysts: Application to the Photo-Organocatalytic Enantioselective α -Hydroxylation of β -Dicarbonyl Compounds *J. Org. Chem.* **2016**, *81*, 7042-7050. (c) Wang, Y.; Zheng, Z.; Lian, M.; Yin, H.; Zhao, J.; Meng, Q.; Gao, Z. Photo-organocatalytic enantioselective α -hydroxylation of β -keto esters and

- β -keto amides with oxygen under phase transfer catalysis. *Green Chem.* **2016**, *18*, 5493-5499.
- [24] Fischer, J.; Mele, L.; Serier-Brault, H.; Nun, P.; Coeffard, V. Controlling Photooxygenation with a Bifunctional Quinine-BODIPY Catalyst: Towards Asymmetric Hydroxylation of β -Dicarbonyl Compounds. *Eur. J. Org. Chem.* **2019**, *2019*, 6352-6358.
- [25] Mayr, F.; Mohr, L.-M.; Rodriguez, E.; Bach, T. Synthesis of Chiral Thiourea-Thioxanthone Hybrids. *Synthesis*, **2017**, *49*, 5238-5250.
- [26] Rigotti, T.; Casado-Sánchez, A.; Cabrera, S.; Pérez-Ruiz, R.; Liras, M.; de la Peña O'Shea, V. A.; Alemán, J. A Bifunctional Photoaminocatalyst for the Alkylation of Aldehydes: Design, Analysis, and Mechanistic Studies. *ACS Catal.* **2018**, *8*, 5928-5940.
- [27] Nicewicz, D. A.; MacMillan, D. W. C. Merging Photoredox Catalysis with Organocatalysis: The Direct Asymmetric Alkylation of Aldehydes. *Science* **2008**, *322*, 77-80.
- [28] For another dual catalytic metal-based system see: Gualandi, A.; Marchini, M.; Mengozzi, L.; Natali, M.; Lucarini, M.; Ceroni, P.; Cozzi, P. G. Organocatalytic Enantioselective Alkylation of Aldehydes with $[\text{Fe}(\text{bpy})_3]\text{Br}_2$ Catalyst and Visible Light. *ACS Catal.* **2015**, *5*, 5927-5931.
- [29] For purely organic systems see: (a) Fidaly, K.; Ceballos, C.; Falguières, A.; Sylla-Iyarreta Veitia, M.; Guy, A.; Ferroud, C. Visible light photoredox organocatalysis: a fully transition metal-free direct asymmetric α -alkylation of aldehydes. *Green Chem.* **2012**, *14*, 1293-1297. (b) Neumann, M.; Földner, S.; König, B.; Zeitler, K. Metal-free, cooperative asymmetric organophotoredox catalysis with visible light. *Angew. Chem. Int. Ed.* **2011**, *50*, 951-954.
- [30] Pecho, F.; Zou, Y.-Q.; Gramüller, J.; Mori, T.; Huber, S. M.; Bauer, A.; Gschwind, R. M.; Bach, T. A Thioxanthone Sensitizer with a Chiral Phosphoric Acid Binding Site: Properties and Applications in Visible Light-Mediated Cycloadditions. *Chem. Eur. J.* **2020**, *26*, 5190-5194.
- [31] Lyu, J.; Claraz, A.; Vitale, M. R.; Allain, C.; Masson, G. Preparation of Chiral Photosensitive Organocatalysts and Their Application for the Enantioselective Synthesis of 1,2-Diamines. *J. Org. Chem.* **2020**, *85*, 12843-12855.
- [32] Lyu, J.; Leone, M.; Claraz, A.; Allain, C.; Neuville, L.; Masson, G. Syntheses of new chiral chimeric photoorganocatalysts. *RSC Adv.* **2021**, *11*, 36663-36669.
- [33] Takagi, R.; Tanimoto, T. Enantioselective [2+2] photocycloaddition of quinolone using a C_1 -symmetric chiral phosphoric acid as a visible-light photocatalyst. *Org. Biomol. Chem.* **2022**, *20*, 3940-3947.

- [34] For previous work of the group see: (a) Levitre, G.; Audubert, C.; Dumoulin, A.; Goual, N.; Retailleau, P.; Moreau, X.; Masson, G. Combining Organocatalysis and Photoredox Catalysis: An Asymmetric Synthesis of chiral β -amino α -Substituted Tryptamines. *ChemCatChem* **2019**, *11*, 5723-5727. (b) Dumoulin, A.; Bernadat, G.; Masson, G. Enantioselective Three-Component Amination of Enecarbamates Enables the Synthesis of Structurally Complex Small Molecules. *J. Org. Chem.* **2017**, *82*, 1775-1789. (c) Dumoulin, A.; Lalli, C.; Retailleau, P.; Masson, G. Catalytic, highly enantioselective, direct amination of enecarbamates. *Chem. Commun.* **2015**, *51*, 5383-5386.
- [35] Pecho, F.; Sempere, Y.; Gramüller, J.; Hörmann, F. M.; Gschwind, R. M.; Bach, T. Enantioselective [2+2] Photocycloaddition via Iminium Ions: Catalysis by a Sensitizing Chiral Brønsted Acid. *J. Am. Chem. Soc.* **2021**, *143*, 9350-9354.
- [36] Rolka, A. B.; Toste, F. D.; König, B. Hybrid Catalysts for Enantioselective Photo-Phosphoric Acid Catalysis. **2023**, DOI: 10.26434/chemrxiv-2023-0v38p. (accessed 2023-02-07).
- [37] (a) For the chiral version see: Sherbrook, E. M.; Genzink, M. J.; Park, B.; Guzei, I. A.; Baik, M.-H.; Yoon, T. P. Chiral Brønsted acid-controlled intermolecular asymmetric [2+2] photocycloadditions. *Nat. Commun.* **2021**, *12*, 5735. (b) For the racemic version see: Sherbrook, E. M.; Jung, H.; Cho, D.; Baik, M.-H.; Yoon, T. P. Brønsted acid catalysis of photosensitized cycloadditions. *Chem. Sci.* **2020**, *11*, 856-861.
- [38] Liang, D.; Chen, J.-R.; Tan, L.-P.; He, Z.-W.; Xiao, W.-J. Catalytic Asymmetric Construction of Axially and Centrally Chiral Heterobiaryls by Minisci Reaction. *J. Am. Chem. Soc.* **2022**, *144*, 6040-6049.
- [39] For seminal work see: Proctor, R. S. J.; Davis, H. J.; Phipps, R. J. Catalytic enantioselective Minisci-type addition to heteroarenes. *Science* **2018**, *360*, 419-422.

CHAPTER 2

2 Dearomative Cycloadditions Utilizing an Organic Photosensitizer: An Alternative to Iridium Catalysis

This chapter has been published. Reprinted (adapted) with permission from:

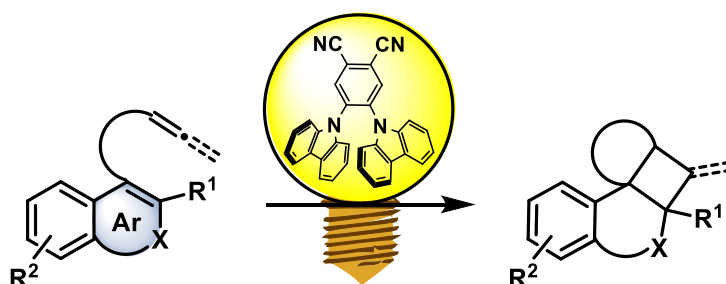
A. B. Rolka, B. König, *Org. Lett.* **2020**, *22*, 5035-5040.

Copyright 2020 American Chemical Society.

A. B. Rolka conceived the project, conducted all experiments and syntheses unless otherwise stated, and wrote the manuscript. A. Chatterjee synthesized the starting material for compound **5d**. X-ray crystallographic analysis was performed by the X-Ray structure analysis department of the University of Regensburg, particularly by B. Hischa. B. König supervised the project.

Abstract

A highly efficient, cheap, and organic alternative to the commonly used iridium photosensitizer ($\text{Ir}[\text{dF}(\text{CF}_3)\text{ppy}]_2(\text{dtbpy})\text{PF}_6$ (**[Ir-F]**) is presented for visible-light energy transfer catalysis. The organic dye **2CzPN** surpasses **[Ir-F]** in selectivity while at the same time being easily accessible in one step. The catalyst is recyclable and, due to its uncharged nature, soluble in nonpolar solvents such as toluene. Furthermore, the scope of molecular scaffolds that are compatible substrates for visible-light catalyzed dearomative cycloadditions is expanded.



- ✓ Cheap, organic photosensitizer
 - ✓ Visible light
 - ✓ Rapid increase in complexity
 - ✓ Access to polycyclic frameworks
 - ✗ Expensive iridium catalyst
 - ✗ Harsh UV light
-

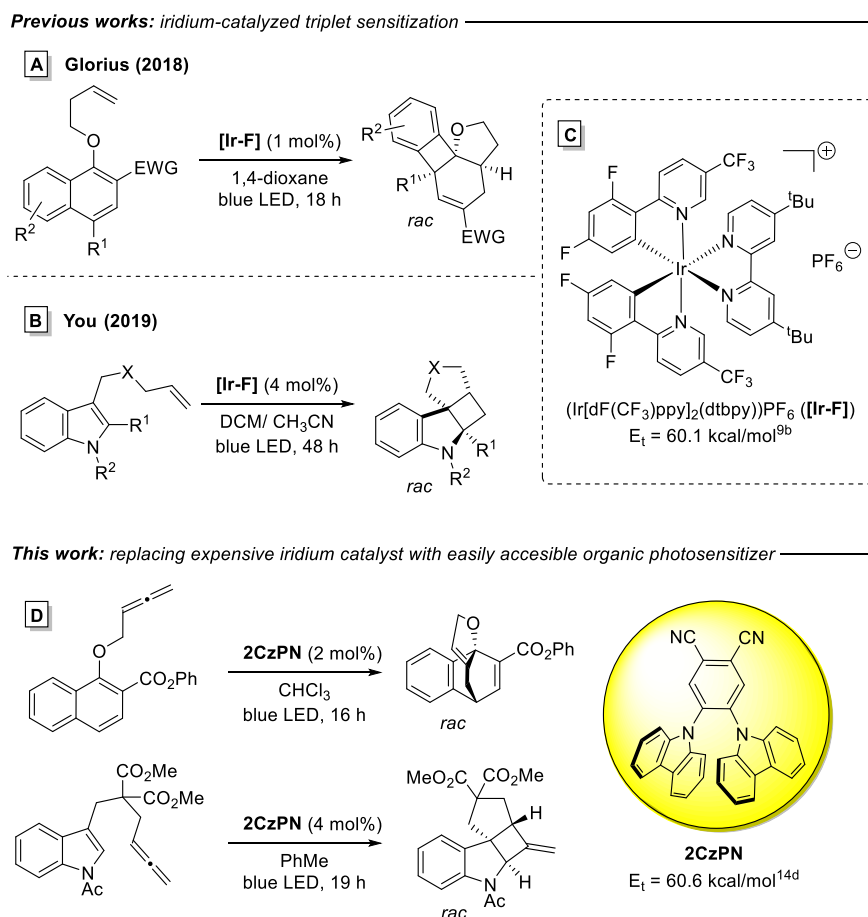
2.1 Introduction

Over the past few years, energy transfer catalysis has gained significant attention and has emerged as a powerful synthetic tool.¹ The reasons for this are manifold, but of particular significance is the methodology's ability to rapidly generate high levels of molecular complexity.^{1a,2} This is elegantly highlighted by the works of Glorius et al.³ and You et al.⁴ that demonstrate the generation of polycyclic cores by intramolecular dearomative cycloadditions of naphthol (Scheme 2-1A) and indole derivatives (Scheme 2-1B). The resulting molecular scaffolds often map onto natural product frameworks and are challenging to synthesize via other means.⁵ One alternative to accessing these structures is the direct excitation of substrates by UV light. However, this method often leads to unwanted side reactions and poor selectivity.⁶ By utilizing visible light and suitable photosensitizers to indirectly activate molecules, the need for UV light and/or other harsh reaction conditions can be avoided.

Key to the success of such a mild visible-light catalyzed process is the careful selection of a photosensitizer whose triplet energy upon excitation with visible light and intersystem crossing matches the targeted molecules. In the past, photocatalysts (**PCs**) with sufficiently high triplet energies for challenging dearomative processes of the type depicted in Scheme 2-1 have been largely limited to iridium-based systems utilizing $(\text{Ir}[\text{dF}(\text{CF}_3)\text{ppy}]_2(\text{dtbpy}))\text{PF}_6$ (**[Ir-F]**) (Scheme 2-1C) and its derivatives.^{3,4,7} This catalyst, which has also been shown to be effective in other catalytic energy transfer processes, benefits from a long-lived excited triplet state and a high triplet energy.^{1,8,9} Despite these desirable traits, iridium catalysis has several significant drawbacks that limit its widespread use. On the economic side, iridium has the distinction of being the rarest of the rare earth metals and has a correspondingly high price that can make the cost of the catalyst prohibitively expensive.¹⁰ Furthermore, the presence of transition metals in pharmaceuticals is highly regulated, and use of an iridium photocatalyst in late stage steps is undesirable in regards to industrial applications of these complexity generating processes.¹¹ Finally, the charged nature of the expensive catalyst complicates its recyclability^{8d,12} as well as limits the catalyst's solubility in many common nonpolar solvents.^{10a}

This work aims to address these problems by avoiding iridium and offers a highly effective, cheap, neutral, and organic alternative for the widely utilized **[Ir-F]** photosensitizer. Based upon OLED research¹³ and reports about the photochemical and photophysical properties of organic dyes, we were drawn to 1,2-bis(carbazol-9-yl)-4,5-dicyanobenzene (**2CzPN**) (Scheme 2-1D) as a promising

candidate for this task.¹⁴ Specifically, the high triplet energy of this system at 60.6 kcal/mol (corresponding to $T_1 = 2.63$ eV)^{14d} as well as the prior use of this catalyst for photochromism¹⁵ led us to explore its performance in the dearomatization reactions of aforementioned naphthol and indole derivatives.

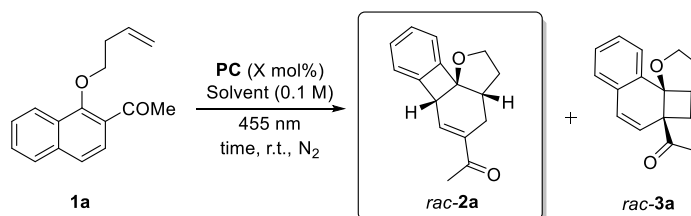


Scheme 2-1: Previously reported dearomatizations of naphthol-derivatives (**A**)³ and indole-derivatives (**B**)⁴ and structure of the organic alternative **2CzPN** (**D**) to (**[Ir-F]**) (**C**).

2.2 Results and discussion

The dearomative cycloaddition of naphthol **1a** was used as a model reaction to investigate the organic catalyst **2CzPN** (Table 2-1). To begin, **1a** and 5 mol% **2CzPN** were irradiated with 455 nm light in 1,4-dioxane at room temperature. Under these conditions, we were pleased to see full conversion of the starting material but with poor selectivity, as measured by the ratio of **2a:3a** (entry 1). This reaction proceeds via two sequential triplet energy excitation processes. First, excitation of **1a** results in a [2+2] cycloaddition to form **3a**, while subsequent excitation of **3a** followed by rearrangement furnishes **2a**. The ultimate ratio of **2a:3a** is influenced by the triplet energy of the catalyst and the rate of energy transfer. For the complete mechanism, see experimental part 2.4.5.1.

Table 2-1: Optimization studies for the organocatalytic dearomatization of naphthol **1a**^a



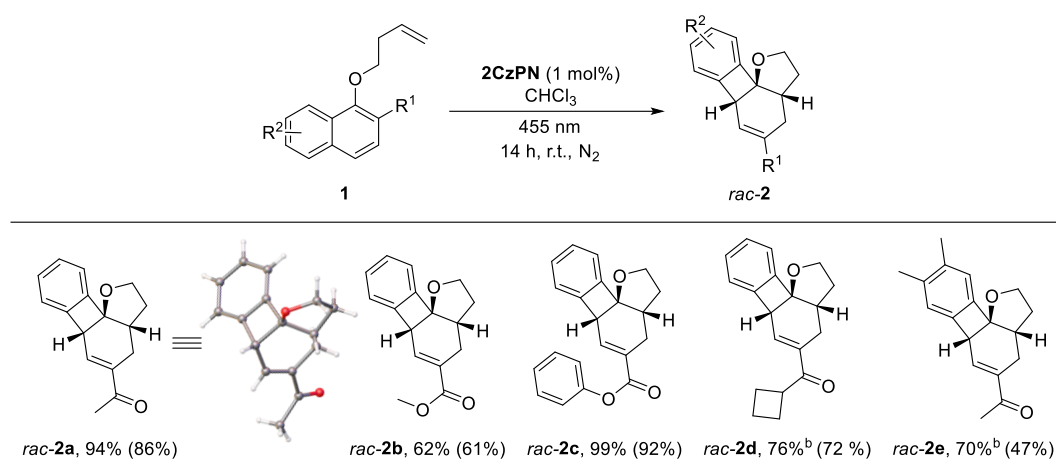
Entry	PC	X	Time	Solvent	Ratio 2a:3a ^b
1 ^c	2CzPN	5	17 h	1,4-dioxane	1.2:1
2 ^d	2CzPN	5	17 h	1,4-dioxane	1.2:1
3	2CzPN	5	17 h	PhMe	1.8:1
4	2CzPN	5	17 h	CHCl ₃	16:1
5	2CzPN	1	14 h	CHCl ₃	16 (94%) ^e :1
6	2CzPN	0.5	14 h	CHCl ₃	3:1
7	2CzPN	0.2	14 h	CHCl ₃	1:1.6
8 ^f	2CzPN	1	17 h	CHCl ₃	1:20
9	TX	5	17 h	CHCl ₃	N/A ^g
10	-	-	17 h	1,4-dioxane	N/A ^g

^aReactions were run at a 0.2 mmol scale. ^bDetermined by ¹H-crude NMR ratio. Entries with a ratio showed no other proton signals and full conversion with isolation of a mixture of **2a** and **3a** in near quantitative yield. ^c0.04 M ^d λ_{\max} = 405 nm light was used instead of λ_{\max} = 455 nm. ^e94% isolated yield confirms the use of the NMR ratio is a reliable indication of yield. ^f0.1 eq. of Sc(OTf)₃. ^gNot applicable. No conversion of starting material.

Lowering the wavelength from 455 to 405 nm did not influence selectivity (entry 2). After a brief screening of solvents, it was found that chloroform was ideal, leading to formation of **2a** with a high selectivity of 16:1 (entry 4). We were able to lower both the reaction time to 14 h and the catalyst loading to 1 mol% without impacting the reaction (entry 5). Further lowering the catalyst

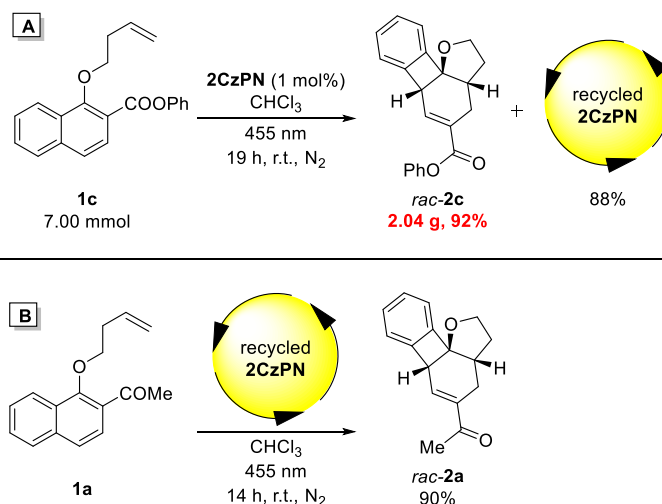
loading resulted in worse selectivity (entries 6 and 7). Through the addition of a Lewis acidic additive, the reaction could be directed toward the selective formation of **3a** (entry 8). However, this observed effect proved not to be general to other substrates. Therefore, 1 mol% **2CzPN** in chloroform irradiated at 455 nm for 14 h were chosen as the optimized conditions, giving **2a** in 94% isolated yield as a single diastereomer and with a **2a:3a** ratio of 16:1 (entry 5). In comparison, the optimized conditions of Glorius utilizing 1 mol% [**Ir-F**] (1,4-dioxane; 0.04 M; 18 h; 455 nm) achieved a ratio of 6:1 with a yield of 86%,³ showing that **2CzPN** is able to improve the selectivity of the reaction. Control experiments utilizing the organic photosensitizer thioxanthone (**TX**), which absorbs at lower wavelengths¹⁶ (entry 9), and irradiation without any catalyst (entry 10) resulted in no conversion, proving the necessity of **2CzPN**. With optimized conditions in hand, tailored to the organic dye **2CzPN**, the substrate scope was investigated to better compare **2CzPN** with [**Ir-F**]. To do so, five substrates were selected with different electronic and steric properties at the activating group R¹ as well as at the naphthyl ring R² (Table 2-2). For ease of comparison, the already reported yields with 1 mol% of the iridium catalyst [**Ir-F**] are included in brackets. Based upon these yields, it is evident that **2CzPN** is able to catalyze the dearomatization of naphthols in a highly efficient fashion that is comparable or superior to [**Ir-F**].

Table 2-2: Substrate scope of naphthols^a



^aYields are isolated yields. Yields in brackets are isolated yields of the originally reported reactions with 1 mol% [**Ir-F**].³ Reactions were run on a 0.2 mmol scale at 0.1 M. ^bTwo mol% **2CzPN**, 42 h.

Reactions with **2CzPN** readily scale and could be performed equally effectively in multiple gram quantities with only 1 mol% catalyst (Scheme 2-2A). We were also able to take advantage of **2CzPN**'s neutral charge to readily recycle the catalyst by means of column chromatography in 88% yield, and the recycled catalyst shows no change in activity upon reuse (Scheme 2-2B).



Scheme 2-2: Scale up of the reaction with recycling of catalyst (**A**) and subsequent reaction with recycled catalyst (**B**).

Motivated by the positive results, we explored the compatibility of **2CzPN** with the dearomatization of indole derivatives. This class of compounds represents a more challenging test due to their increased triplet energy. While the optimized conditions for naphthol dearomatization resulted in very poor conversion of **4a**, it was found that utilization of toluene as solvent allowed the reaction to proceed in high yields (experimental part 2.4.3.1). It is thought that the use of the less polar toluene solvent inhibits electron transfer from the indole substrate to the excited photocatalyst that preferentially occurs over triplet sensitization in polar solvents.

The ability to utilize nonpolar solvents with **2CzPN** highlights another advantage of this organic photosensitizer over the [Ir-F] system, which is only minimally soluble in toluene (100–1000 ppm)^{10a} and other nonpolar solvents due to its charged nature (Table 2-3). A comparison of the maximum solubility in a range of different solvents revealed a more than 100 times higher solubility of **2CzPN** in toluene. It is noteworthy that the organic catalyst retains high solubility in polar solvents.

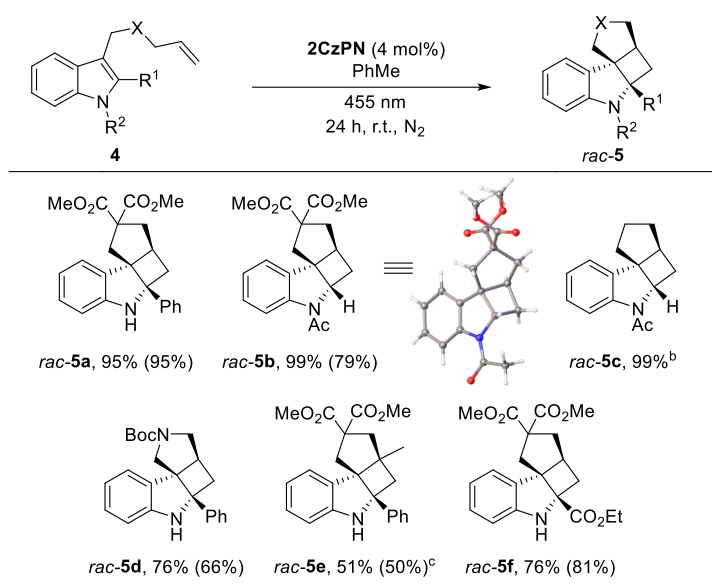
Table 2-3: Maximum solubilities of [Ir-F] and **2CzPN** in common organic solvents^a

Solvent	[Ir-F] ^b	2CzPN ^c
PhMe	7.0×10^{-5}	1.3×10^{-2}
1,4-dioxane ^c	2.2×10^{-4}	1.6×10^{-2}
DCM	5.6×10^{-3}	8.3×10^{-2}
Methyl <i>tert</i> -butyl ether	7.0×10^{-5}	9.2×10^{-4}
DMSO	1.6×10^{-1}	1.6×10^{-2}

^aMaximum solubility given as concentration (Molar). ^bAs reported by the group of Weaver.^{10a} ^cSee experimental part 2.4.3.4.

To demonstrate the efficiency of our conditions, a scope of indoles was investigated (Table 2-4).

Table 2-4: Substrate scope of indoles^a



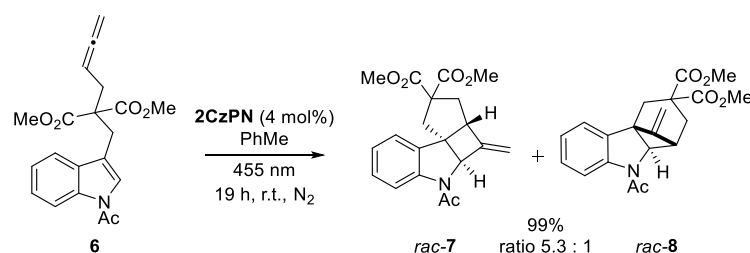
^aYields are isolated yields. Yields in brackets are isolated yields of the originally reported reactions with [Ir-F].⁴ Reactions run on a 0.05 mmol scale at 0.0125 M. ^bNineteen hours. ^cOriginally reported reaction with 8 mol% [Ir-F].

Just as with [Ir-F], substitution at the 2-position was well-tolerated (**5a**, **5d**, **5e**, and **5f**), as was the use of a more sterically hindered 1,1-disubstituted alkene (**5e**). The reaction proceeds utilizing substrates bearing the free indole N-H or an *N*-acetyl group, with the highest yields observed with the acetylated substrates (**5b**, **5c**). These nearly quantitative yields are thought to be attributed to the electron-withdrawing nature of the acetyl group, which lowers the triplet energy of the substrates while at the same time increasing their oxidation potential to limit redox events with the catalyst. Using an *N*-acetylated substrate, we were especially delighted to find that high levels of reactivity could be obtained without the bulky diester linker which facilitates ring closure via the Thorpe-Ingold-Effect (**5c**).¹⁷ Once again, for all substrates tested, the organic photosensitizer proved to be comparable or superior to [Ir-F] at equivalent catalyst loadings.⁴

Having established that the organic photocatalyst is an effective replacement for [Ir-F], we sought to test the organic photocatalyst on more challenging cases containing allene cycloaddition partners that have the potential to form highly strained methylcyclobutane products.¹⁸ This class of substrates is particularly intriguing due to the presence of an olefin in the product that can serve as a functional group handle for further structural elaboration. Whereas the direct UV excitation of aromatic rings followed by their trapping with allenes has been reported, little has been done within the field of visible-light triplet-sensitized chemistry.¹⁸ A rare example of triplet-sensitized

chemistry involving allenes is the work of Arai and Ohkuma, where 50 mol% of 3',4'-dimethoxyacetophenone sensitizer was required in the dearomative cycloaddition of indole derivatives.^{18d,e} However, in addition to the high catalyst loading, a high pressure mercury lamp was necessary (experimental part 2.4.5.2). Inspired by their work, we synthesized allene **6** to investigate whether **2CzPN** can overcome these significant limitations. Applying the same optimized conditions as for **4c**, we were pleased to see full conversion of **6** to the dearomatized products **7** and **8** in high yield and with a ratio of 5.3:1 (Table 2-5).

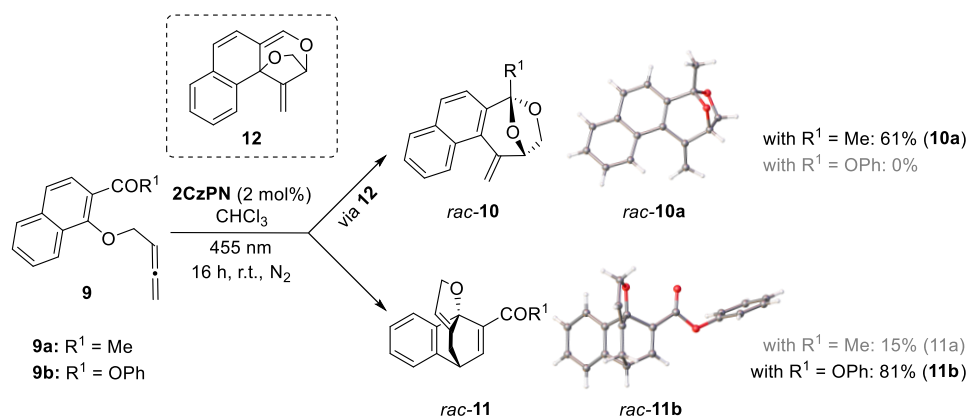
Table 2-5: Formation of methylenecyclobutane products from allene substituted indole **6**^a



^aIsolated yield. Reaction has previously not been reported with [Ir-F]. The reaction was run on a 0.05 mmol scale at 0.0125 M.

We next explored the previously unreported visible-light photochemistry of naphthol allene derivatives (Table 2-6). When treating naphthol ketone **9a** with slightly modified conditions described above for the dearomatization of naphthols, we were surprised to obtain the aromatic cyclic acetal **10a** as the main product in 61% yield.

Table 2-6: Dearomative cycloaddition of allene-substituted naphthol-derivatives^a



^aYields are isolated yields. Reaction has previously not been reported with [Ir-F]. Reactions were run on a 0.1 mmol scale at 0.05 M.

The product was confirmed by a single crystal X-ray analysis (experimental part 2.4.7.3) and supported by the literature-known UV-photochemistry of allenyl salicylaldehydes.^{18b,c} We believe that **10a** is formed via dearomatized intermediate **12** that upon 1,3-allylic transposition yields

product **10a**. As a minor side product under these conditions, dihydrofuran **11a** was also obtained via a 1,4-cycloaddition. By exchanging the acetyl group (**9a**) with a phenyl ester (**9b**), only the dearomatized product **11b** was observed in 81% yield.

2.3 Conclusion

In conclusion, we have shown **2CzPN** to be a highly effective and general triplet sensitizer that can serve as an effective replacement for the expensive [Ir-F] catalyst that has until now been the preferred sensitizer to activate substrates with high triplet energies via visible light. Through a series of direct comparisons, the organic catalyst consistently matched or outperformed the iridium catalyst in dearomative cycloadditions. The organic dye was furthermore applied in the previously not reported visible-light induced photocycloaddition of naphthol and indole allenes, giving rise to complex polycyclic frameworks. The catalyst itself is readily synthesized in gram quantities in one step from cheap and commercial starting materials and is bench-stable. Its uncharged nature allows for solubility in a broad range of polar and nonpolar solvents and for easy recovery and reuse of the catalyst via column chromatography. Finally, reactions performed with **2CzPN** have proven to be readily amenable to large, multigram scales. We believe that the presented work will facilitate a broader use of visible-light mediated triplet-sensitized reactions through the identification of a cheap organic replacement for the previously utilized iridium catalyst.

2.4 Experimental part

2.4.1 General information

All reagents were purchased from commercial suppliers (Sigma Aldrich, Alfa Aesar, Acros, Fluka, TCI or VWR) and used as received. Anhydrous solvents were obtained from Acros Organics in form of an AcroSeal bottle (“anhydrous”) or by drying over molecular sieves. Air sensitive reactions were performed in Schlenk vials or crimp capped vials under nitrogen (N₂) using plastic syringes and cannulas to transfer solvents or liquid reagents. Photoreactions were weighed in under air but degassed by three cycles of freeze pump thaw to ensure complete exclusion of air.

Analytical thin-layer chromatography (TLC) was performed using pre-coated ALUGRAM® Xtra SIL G/UV₂₅₄ sheets (Macherey-Nagel) and UV-light (254 nm or 365 nm) for visualization. Purification by flash column chromatography was performed on a Biotage® Isolera™ Spektra One using solvents of technical grade and silica gel 60 M (40-63 μm, 230-440 mesh, Merck) for intermediates and distilled solvents and pre-packed Biotage® SNAP Ultra columns for final product isolations.

All NMR spectra were measured at room temperature using either a Bruker Avance 300 (300 MHz for ¹H, 75 MHz for ¹³C) or Bruker Avance 400 (400 MHz for ¹H, 101 MHz for ¹³C). All chemical shifts are reported in δ-scale as parts per million [ppm] (multiplicity, coupling constant *J*, number of protons), relative to the solvent residual peaks as the internal standard. Coupling constants *J* are given in Hertz [Hz]. Abbreviations used for signal multiplicity: ¹H-NMR: b = broad, s = singlet, d = doublet, t = triplet, q = quartet, dd = doublet of doublets, ddd = doublet of doublet of doublets, dt = doublet of triplets, dq = doublet of quartets, qt = quartet of triplets, and m = multiplet;

HRMS (high resolution mass spectra) were measured at the Central Analytical Laboratory of the University of Regensburg. The device used is a Finnigan MAT 95, ThermoQuest Finnigan TSQ 7000, Finnigan MAT SSQ 710 A or an Agilent Q-TOF 6540 UHD instrument.

Infrared (IR) spectra were recorded neat on an Agilent Cary 630 FT-IR Spectrometer. Melting Points were measured in open capillary tubes using a Stanford Research System OptiMelt MPA 100 and are uncorrected. Centrifugation was carried out on an Eppendorf® Centrifuge 5702 RH. Photoreactions were performed using blue light OSRAM Oslon SSL 80 LDCQ7P-1U3U (blue, λ_{max} = 455 nm, I_{max} = 0.7 A, 1.12 W) as irradiation source. For irradiation with 405 nm Edison EDEV-SLC1-03 (λ_{max} = 405 nm, I_{max} = 700 mA, 400 mW) was used. Reactions were performed in crimp capped vials at 25 °C, controlled by a thermostat metal cooling block.

2.4.2 Properties of 2CzPN

2.4.2.1 UV-VIS and Emission Spectra

UV-Vis absorption spectroscopy was performed at 25 °C on a Varian Cary 100 Spectrometer with a 10 mm quartz cuvette.

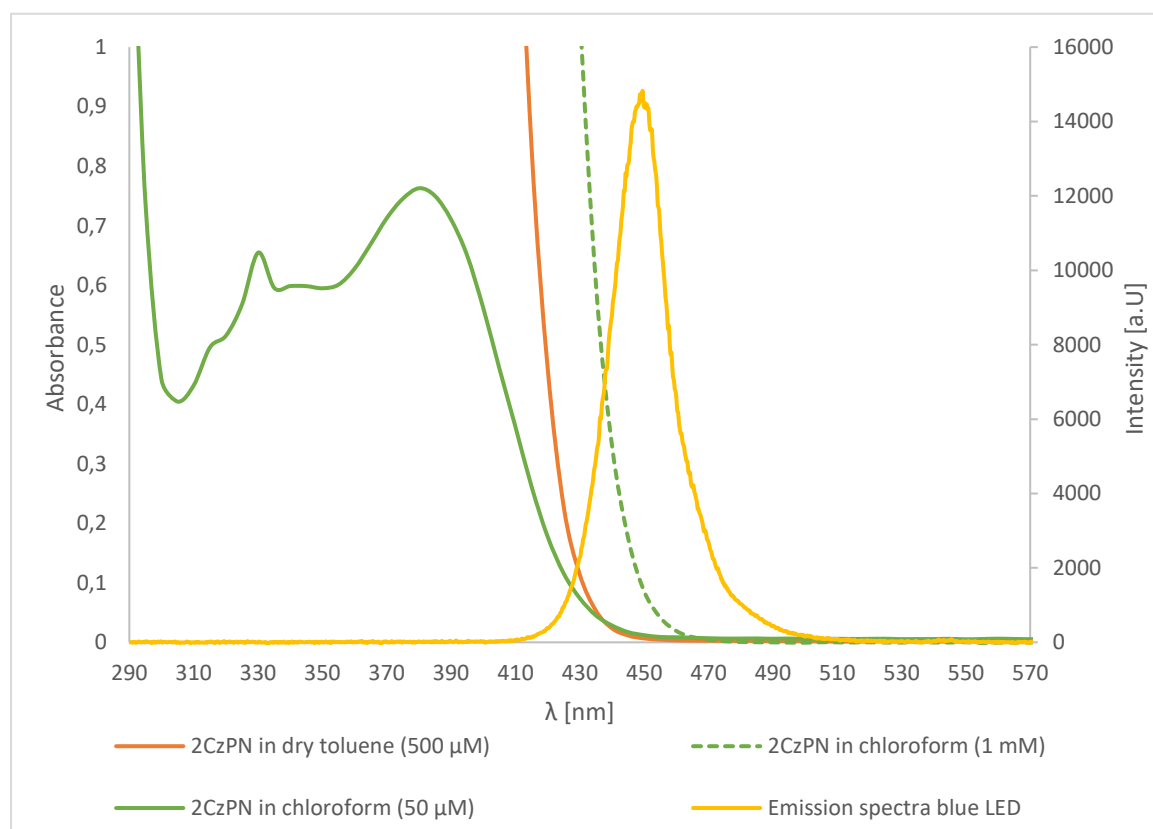


Figure S2-1: Emission spectra of used blue 455 nm LED and absorbance spectra of **2CzPN** in different concentrations and solvents. Control experiments using a 405 nm LED light source did not increase selectivity in the dearomatization of naphthol **1a**, therefore 455 nm was used as preferred light source.

2.4.2.2 Summarized Properties of 2CzPN from Literature

Triplet Energy of 2CzPN:^{14d}

2.63 eV corresponding to 60.6 kcal/mol;

Photoluminescence (PL) characteristics of 2CzPN in toluene under nitrogen:¹³

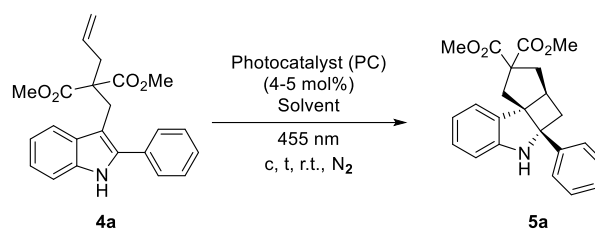
Emission λ_{em} (nm) = 473; PLQY (%) = 46.5; lifetime τ_p (ns) = 28.5; lifetime τ_d (μ s) = 166;

Redox potentials in volts of 2CzPN vs. saturated calomel electrode (SCE) in MeCN at room temperature:^{19,14b}

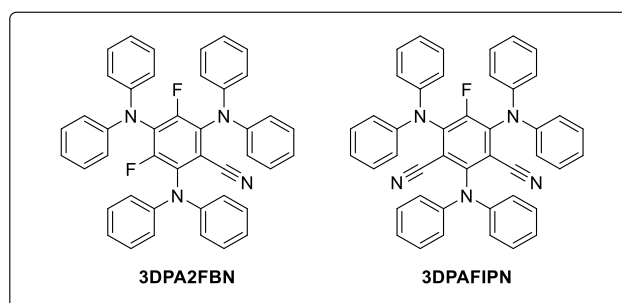
$E_{1/2}(P^+/*P) = -1.30$; $E_{1/2>(*P/P^-) = +1.32$; $E_{1/2}(P^+/P) = +1.47$; $E_{1/2}(P/P^-) = -1.45$;

2.4.3 Optimization- and Solubility Studies

2.4.3.1 Optimization Table for the Dearomatization of Indole-derivatives

Table S2-1: Optimization studies for the organocatalytic dearomatization of indole **4a**.

Entry	PC	PC loading	Time t	Concentration c	Ratio 4a:5a ^b	Solvent
1	2CzPN	5 mol%	48 h	0.1 M	20:1	DCM/MeCN (3:1)
2	2CzPN	5 mol%	48 h	0.1 M	20:1	Chloroform
3	2CzPN	5 mol%	48 h	0.1 M	3:1	Chloroform ^c
4	2CzPN	5 mol%	48 h	0.1 M	13:1	MeCN ^c
5	3DPA2FBN	5 mol%	48 h	0.1 M	1.5:1	MeCN ^c
6	3DPAFIPN	5 mol%	48 h	0.1 M	3:1	MeCN ^c
7	2CzPN	5 mol%	48 h	0.1 M	1:3	Toluene ^c
8	2CzPN	5 mol%	48 h	0.0125 M	1:20	Toluene ^c
9	2CzPN	4 mol%	24 h	0.0125 M	1:20 (95 %) ^d	Toluene ^c



^aReactions were performed with 0.2 mmol of **4a** at 0.1 M and 0.05 mmol of **4a** at 0.0125 M. ^bDetermined by ¹H-crude NMR ratio. Entries with a ratio showed no other proton signals. ^cAnhydrous solvent was used. ^d95% isolated yield confirms the use of the NMR ratio is a reliable indication of yield.

2.4.3.2 Control Experiments

All reactions were performed once in absence of catalyst and once in absence of irradiation source. Product formation was never observed in any of the investigated substrates (allene-substituted substrates, naphthol-derivatives and indole-derivatives).

2.4.3.3 Recycling of the Catalyst

General Information:

In each performed photoreaction, products were purified by column chromatography, which also allows for recycling of the catalyst through very minor adjustments of the solvent system. The details are explained below. After completion of the reaction, the crude mixture was concentrated in vacuo and submitted to flash column chromatography, starting with 100% DCM as solvent (blue gradient Figure S2-2 to S2-5). Under these conditions, the catalyst comes off the column as a clearly separated peak. Once the catalyst is off the column (which can also be visually observed due to the yellow band), the column is flushed with 100% petroleum ether (PE) or pentane followed by the appropriate EtOAc/PE solvent system (yellow gradient Figure S2-2-5) to isolate the products. Lastly, the column is flushed with 100% EtOAc to flush off the degradation product of the catalyst, which occurred in cases with long reaction time (42 h, Figure S2-2 vs. Figure S2-3). The degradation of the catalyst could also be visually observed, by change of the solution color from pale yellow to orange. In the large-scale synthesis of **2c**, **2CzPN** was recycled in 88% yield and reused without further purification in the synthesis of **2a**, resulting in excellent isolated yields (90%). Although the ¹H-NMR of the recycled catalyst showed small impurities, they did not have an impact on the catalyst's performance. If needed, analytically pure **2CzPN** can be obtained by recrystallizing the compound from acetone/hexane.

2.4.3.3.1 Naphthol-derivatives

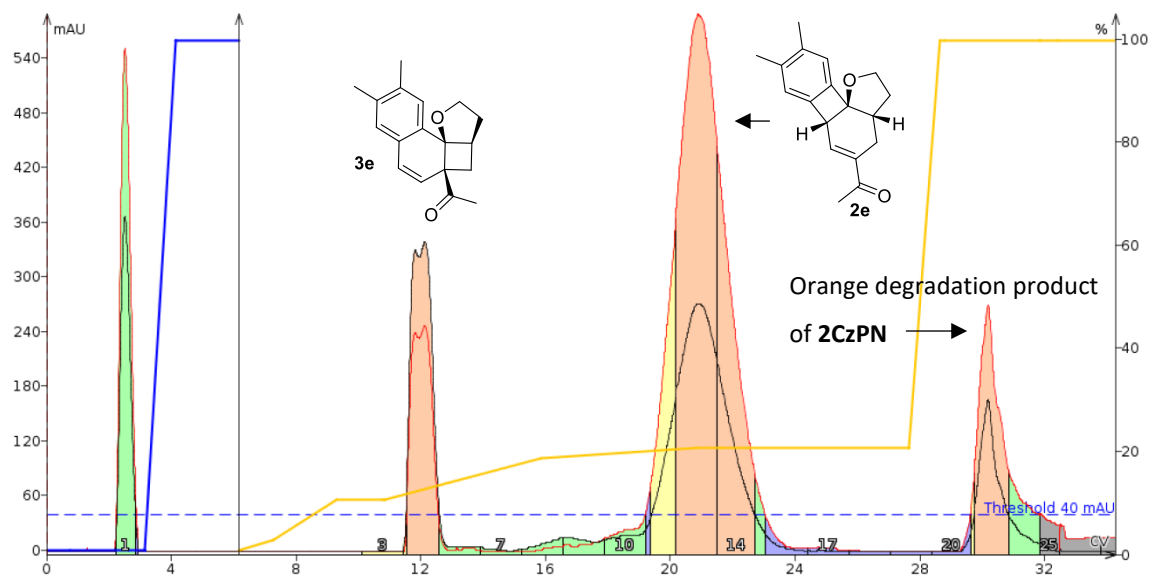


Figure S2-2: Column report of the isolation of **2e**. Reaction time: 42 h and catalyst loading: 2 mol%. Isolated yield: 70%. The high absorption of the degradation product arises from the strong color and does not correspond to the actual amount of degradation.

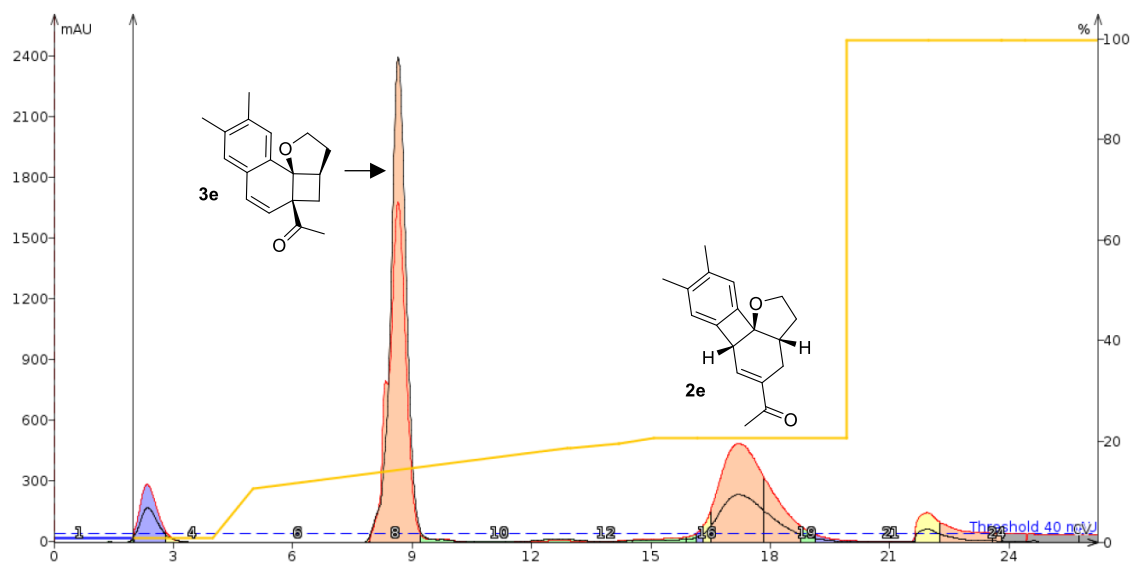
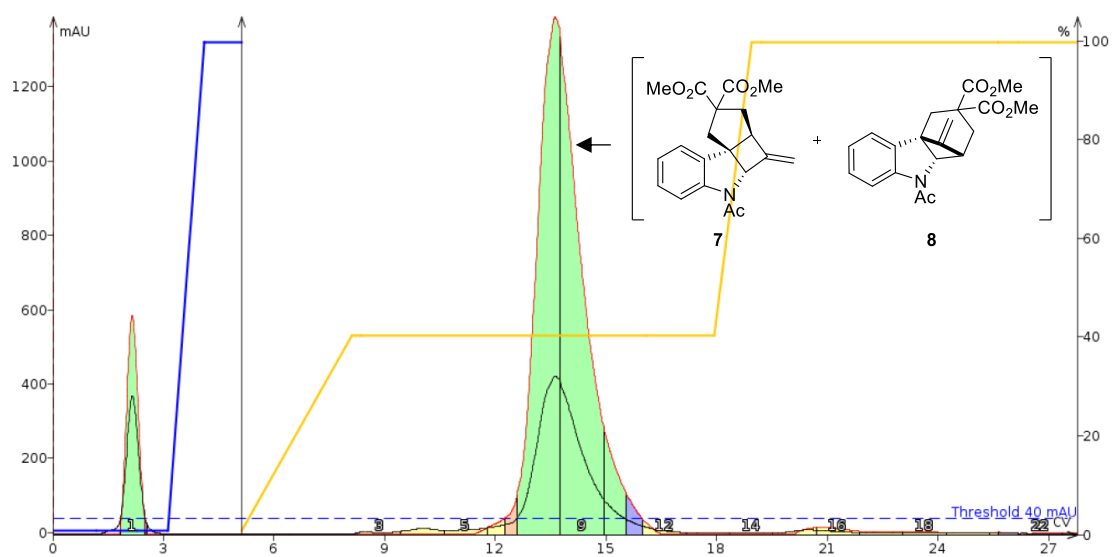
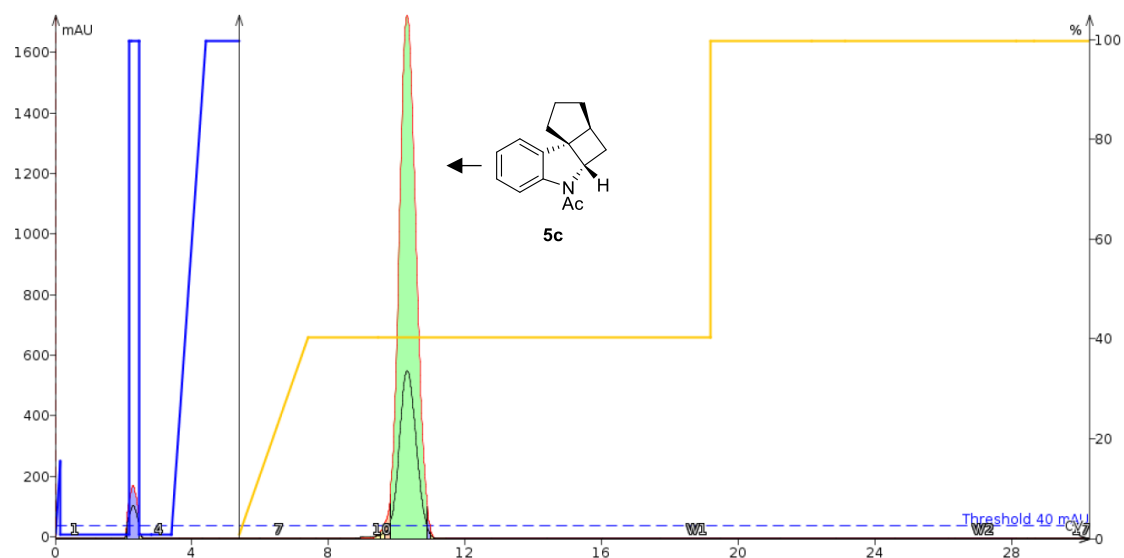


Figure S2-3: As comparison to Figure S2-2 the column report of the isolation of **2e** with a reaction time of 14 h, and 1 mol% catalyst loading. Isolated yield: 38%.

2.4.3.3.2 Indole-derivatives



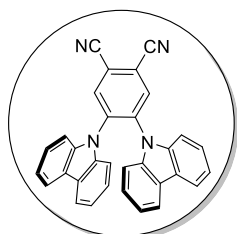
2.4.3.4 Determination of Maximum Solubility

Maximum concentration was determined using the General Procedure A of the published procedure from the group of Weaver.^{10a} 1.5 mg of **2CzPN** were weighed into a 15 mL CELLSTAR® tube with a screw cap. The respective solvent was added in steps of 50-200 μ L (depending on the solubility) by an Eppendorf pipette. After each addition, the tube was closed, sonicated for 4 min and then centrifuged for 2 min at a speed of 4.4 x 1000 rpm. This procedure was repeated until the catalyst was fully dissolved as determined by visible examination. Lastly, the fully dissolved sample was centrifuged once more for 60 min at a speed of 4.4 x 1000 rpm to ensure that the catalyst is really fully dissolved. In the case of easily volatile solvents, the amount of solvent was determined again after centrifugation, due to evaporation effects.

2.4.4 Experimental Procedures

2.4.4.1 Synthesis of Photocatalyst

1,2-bis(carbazol-9-yl)-4,5-dicyanobenzene (**2CzPN**)



This substrate was made following the procedure of Adachi et al.¹³ and Zhang et al.^{14b}

A Schlenk flask equipped with a magnetic stirring bar was charged with a solution of carbazole (3.4 g, 20 mmol) in dry THF (80 mL). NaH (60% in mineral oil, 1.2 g, 30 mmol) was slowly added under nitrogen at room temperature and the resulting solution was stirred for 30 min. Then, 4,5-difluorophthalonitrile (1.3 g, 8.0 mmol) was added and the reaction was stirred overnight. Afterwards, the reaction was quenched by addition of water (20 mL), the solvent was removed in vacuo and the residue was redissolved in DCM. After washing with EtOH, the crude mixture was first purified by flash column chromatography (DCM/PE 3:1) and then by recrystallization from acetone/hexane yielding **2CzPN** as a pale-yellow powder (710 mg, 1.5 mmol, 19%).

¹H NMR (300 MHz, CDCl₃) δ (ppm) 8.33 (s, 2H), 7.83 – 7.78 (m, 4H), 7.16 – 7.10 (m, 4H), 7.09 – 7.04 (m, 8H).

The spectroscopic data matched that reported in the literature.^{13,14b}

2.4.4.2 Synthesis of Starting Materials

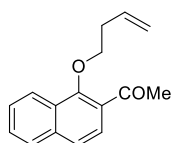
2.4.4.2.1 Synthesis of Naphthol-derivatives

These substrates were made following the procedures of Glorius et al.³

General Procedure 1 for Naphthol-derivatives

Naphthol (1.0 eq.), K₂CO₃ (2.5 eq.) and DMF were added to a crimp cap vial equipped with a magnetic stirring bar. The tube was closed, first degassed and then placed under a nitrogen atmosphere. 4-bromo-1-butene (3.0 eq.) was added via a syringe and the resulting mixture was stirred at 80 °C with a metal heating block for 16 h. The reaction was quenched with water (10 mL) and extracted with EtOAc (3 x 10 mL). The combined organics were washed with brine (2 x 20 mL), dried over Na₂SO₄ and the solvent was removed in vacuo. Purification by flash column chromatography as noted yielded the alkylated naphthol product.

1-(1-(But-3-en-1-yloxy)naphthalen-2-yl)ethan-1-one (1a)



Synthesized according to **General Procedure 1** using 2-acetyl-1-naphthol (1.86 g, 10.0 mmol), K₂CO₃ (3.46 g, 25.0 mmol) and 4-bromo-1-butene (3.05 mL, 30.0 mmol) in DMF (20 mL).

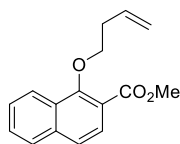
¹H NMR (300 MHz, CDCl₃) δ (ppm) 8.26 – 8.18 (m, 1H), 7.88 – 7.81 (m, 1H), 7.70 (d, *J* = 8.6 Hz, 1H), 7.64 – 7.52 (m, 3H), 5.98 (ddt, *J* = 17.1, 10.2, 6.8 Hz, 1H), 5.29 – 5.11 (m, 2H), 4.08 (t, *J* = 6.8 Hz, 2H), 2.76 (s, 3H), 2.69 (qt, *J* = 6.8, 1.3 Hz, 2H).

¹³C NMR (75 MHz, CDCl₃) δ (ppm) 200.9, 156.2, 136.9, 134.2, 128.6, 128.4, 128.3, 128.2, 126.7, 125.6, 124.2, 123.5, 117.9, 76.4, 34.9, 31.0.

Conditions for Column Chromatography: 2-→4% EtOAc in PE

Yield: 1.7 g, 7.1 mmol, 71% (pale-yellow oil)

The spectroscopic data matched that reported in the literature.³

Methyl 1-(but-3-en-1-yloxy)-2-naphthoate (1b)

Synthesized according to **General Procedure 1** using methyl 1-hydroxy-2-naphthoate (1.01 g, 5.0 mmol), K_2CO_3 (1.71 g, 12.4 mmol) and 4-bromo-1-butene (1.50 mL, 14.8 mmol) in DMF (8 mL).

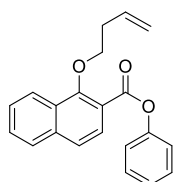
1H NMR (400 MHz, $CDCl_3$) δ (ppm) 8.34 – 8.22 (m, 1H), 7.88 – 7.82 (m, 2H), 7.64 – 7.49 (m, 3H), 6.02 (ddt, $J = 17.1, 10.2, 6.8$ Hz, 1H), 5.26 – 5.21 (m, 1H), 5.18 – 5.15 (m, 1H), 4.18 (t, $J = 6.8$ Hz, 2H), 3.98 (s, 3H), 2.72 (q, $J = 6.8$, 2H).

^{13}C NMR (101 MHz, $CDCl_3$) δ (ppm) 167.0, 157.3, 136.9, 134.8, 128.9, 128.5, 127.9, 126.9, 126.6, 123.9, 123.7, 119.4, 117.3, 75.6, 52.4, 34.9.

Conditions for Column Chromatography: 6% EtOAc in PE

Yield: 623 mg, 2.4 mmol, 49% (clear, colorless oil)

The spectroscopic data matched that reported in the literature.³

Phenyl 1-(but-3-en-1-yloxy)-2-naphthoate (1c)

Synthesized according to **General Procedure 1** using phenyl 1-hydroxy-2-naphthoate (2.64 g, 10.0 mmol), K_2CO_3 (4.15 g, 30.0 mmol) and 4-bromo-1-butene (2.54 mL, 25.0 mmol) in DMF (20 mL).

1H NMR (400 MHz, $CDCl_3$) δ (ppm) 8.41 – 8.27 (m, 1H), 8.06 (d, $J = 8.7$ Hz, 1H), 7.95 – 7.83 (m, 1H), 7.50-7.43 (m, 3H), 7.52 – 7.43 (m, 2H), 7.33 – 7.25 (m, 3H), 6.15 – 5.86 (m, 1H), 5.21 (dq, $J = 17.2$ Hz, 1.6 Hz, 1H), 5.16 – 5.09 (m, 1H), 4.27 (t, $J = 6.8$ Hz, 2H), 2.86 – 2.55 (m, 2H).

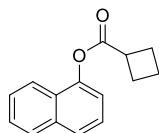
^{13}C NMR (101 MHz, $CDCl_3$) δ (ppm) 164.6, 158.4, 151.1, 137.2, 134.6, 129.7, 129.0, 128.9, 128.0, 127.0, 126.8, 126.1, 124.1, 123.9, 122.0, 118.7, 117.4, 75.8, 34.9.

Conditions for Column Chromatography: 2->4% EtOAc in PE

Yield: 2.7 g, 8.5 mmol, 85% (white solid)

The spectroscopic data matched that reported in the literature.³

Naphthalen-1-yl cyclobutanecarboxylate (**13**)

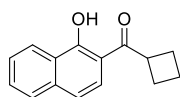


A round bottom flask equipped with a magnetic stirring bar was charged with a solution of cyclobutanecarboxylic acid (1.2 mL, 13 mmol) in DCM (20 mL) and DMF (4 drops). The reaction mixture was cooled down to 0 °C and oxalyl chloride (1.3 mL, 15 mmol) was added dropwise. After complete addition, the mixture was allowed to warm up to room temperature and was stirred for 1.5 h. The resulting solution was added dropwise via a syringe at 0 °C to another round bottom flask, containing a mixture of 1-naphthol (1.3 mL, 1.4 g, 10 mmol), DMAP (0.12 g, 10 mmol) and Et₃N (1.5 mL, 11 mmol) in DCM (10 mL). Afterwards, the resulting mixture was again allowed to warm up to room temperature and was stirred for 30 min. The reaction was quenched with 1 M HCl (20 mL) and extracted with DCM (3 x 20 mL). The combined organics were washed with NaHCO₃ (40 mL), dried over Na₂SO₄, and the solvent was removed in vacuo. Purification by flash column chromatography (6% EtOAc in pentane) yielded **13** (2.0 g, 9.0 mmol, 89%) as a colorless oil.

¹H NMR (300 MHz, CDCl₃) δ (ppm) 7.90 – 7.82 (m, 2H), 7.74 (d, J = 8.3 Hz, 1H), 7.54 – 7.42 (m, 3H), 7.23 (d, J = 1.0 Hz, 1H), 3.59 (pd, J = 8.6, 1.0 Hz, 1H), 2.66 – 2.51 (m, 2H), 2.51 – 2.38 (m, 2H), 2.23 – 1.99 (m, 2H).

¹³C NMR (75 MHz, CDCl₃) δ (ppm) 174.0, 146.7, 134.8, 128.2, 127.1, 126.5, 126.0, 125.6, 121.2, 118.2, 38.39, 25.7, 18.7.

The spectroscopic data matched that reported in the literature.³

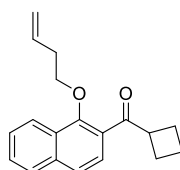
Cyclobutyl(1-hydroxynaphthalen-2-yl)methanone (14**)**

A 50 mL crimp cap vial, equipped with a magnetic stirring bar was charged with $\text{Sc}(\text{OTf})_3$ (120 mg, 2.8 mol%), degassed and placed under a nitrogen atmosphere. Naphthol **13** (2.0 g, 8.9 mmol) was transferred to the vial via a syringe using dry toluene (9 mL) and methanesulfonic acid (56 μL , 0.9 mmol) was added via a Hamilton syringe. The reaction mixture was stirred at 100 °C with a metal heating block for 16 h, before it was quenched with water (10 mL) and extracted with DCM (3 x 10 mL). The combined organics were dried over Na_2SO_4 , and the solvent was removed in vacuo. Purification by flash column chromatography (1% EtOAc in pentane) yielded **14** (1.6 g, 7.1 mmol, 80%) as a pale-yellow solid.

$^1\text{H NMR}$ (300 MHz, CDCl_3) δ (ppm) 14.14 (s, 1H), 8.46 (d, $J = 8.3$ Hz, 1H), 7.74 (d, $J = 8.1$ Hz, 1H), 7.65 – 7.57 (m, 1H), 7.51 (t, $J = 8.7$ Hz, 2H), 7.31 – 7.17 (m, 1H), 4.23 – 3.94 (m, 1H), 2.60 – 2.08 (m, 5H), 2.03 – 1.86 (m, 1H).

$^{13}\text{C NMR}$ (75 MHz, CDCl_3) δ (ppm) 207.0, 162.8, 137.2, 130.0, 127.4, 125.9, 125.5, 124.4, 124.4, 118.3, 111.7, 42.4, 25.2, 18.3.

The spectroscopic data matched that reported in the literature.³

1-(But-3-en-1-yloxy)naphthalen-2-yl)(cyclobutyl)methanone (1d**)**

A Schlenk flask equipped with a magnetic stirring bar was charged with a solution of naphthol **14** (1.5 g, 6.6 mmol), 3-buten-1-ol (0.6 mL, 8.6 mmol) and PPh_3 (1.8 g, 7.3 mmol) in THF (15 mL) and was placed under a nitrogen atmosphere. The reaction mixture was cooled down to 0 °C, and DIAD (1.42 mL, 7.3 mmol) was added dropwise via a syringe. Following complete addition, the mixture was allowed to warm up to room temperature. After stirring for 16 h, the reaction was quenched with water (10 mL) and extracted with EtOAc (3 x 20 mL). The combined organics were dried over

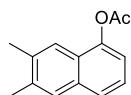
Na₂SO₄, and the solvent was removed in vacuo. Purification by flash column chromatography (20-50% DCM in pentane) yielded **1d** as a pale-yellow oil (0.33 g, 1.2 mmol, 18%).

¹H NMR (300 MHz, CDCl₃) δ (ppm) 8.29 – 8.10 (m, 1H), 7.91 – 7.74 (m, 1H), 7.66 – 7.50 (m, 4H), 5.97 (ddt, *J* = 17.1, 10.2, 6.8 Hz, 1H), 5.38 – 5.07 (m, 2H), 4.24 – 4.10 (m, 1H), 4.04 (t, *J* = 6.8 Hz, 2H), 2.65 (qt, *J* = 6.7, 1.4 Hz, 2H), 2.45 – 2.18 (m, 4H), 2.12 – 1.96 (m, 1H), 1.95 – 1.80 (m, 1H).

¹³C NMR (75 MHz, CDCl₃) δ (ppm) 205.4, 155.2, 136.4, 134.3, 128.4, 128.0, 128.0, 127.6, 126.6, 125.6, 124.1, 123.4, 117.7, 76.3, 45.4, 34.9, 25.4, 17.9.

The spectroscopic data matched that reported in the literature.³

6,7-Dimethylnaphthalen-1-yl acetate (**15**)



A Schlenk flask equipped with a magnetic stirring bar was charged with 1,2-dibromo-4,5-dimethylbenzene (2.1 g, 8.0 mmol) in THF (40 mL) and furan (20 mL) and was placed under a nitrogen atmosphere. Via a syringe *n*-BuLi (5.5 mL, 8.8 mmol, 1.6 M in hexane) was added dropwise at –78 °C and the resulting solution was stirred for 2 h at –78 °C, before the reaction was quenched with water (40 mL) and extracted with EtOAc (3 x 50 mL). The combined organics were dried over Na₂SO₄, the solvent was removed in vacuo and the residue was redissolved in DCM (8 mL).

After cooling the solution down to 0 °C, BF₃·OEt₂ (1.2 mL, 9.6 mmol) was added dropwise via a syringe and the mixture was stirred an additional hour at 0 °C, before it was once again quenched with water (10 mL) and extracted with DCM (3 x 30 mL). The combined organics were dried over Na₂SO₄, the solvent was removed in vacuo and the residue was again redissolved in DCM (24 mL).

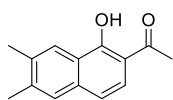
After addition of DMAP (98 mg, 0.8 mmol) and Et₃N (1.2 mL, 8.8 mmol) the crude solution was cooled down to 0 °C and acetyl chloride (0.74 mL, 10 mmol) was added dropwise via a syringe. Following complete addition, the reaction mixture was warmed to room temperature and stirred for 2 h, before it was quenched with 1 M HCl (10 mL) and extracted with DCM (3 x 10 mL). The combined organics were washed with NaHCO₃ (20 mL), dried over Na₂SO₄, and the solvent was removed in vacuo. Purification by flash column chromatography (3% EtOAc in pentane) yielded **15** as a pale-yellow solid (933 mg, 4.4 mmol, 54%).

$^1\text{H NMR}$ (300 MHz, CDCl_3) δ (ppm) 7.66 – 7.53 (m, 3H), 7.36 (t, $J = 7.8$ Hz, 1H), 7.14 (dd, $J = 7.5, 1.0$ Hz, 1H), 2.47 (s, 3H), 2.43 (d, $J = 4.7$ Hz, 6H).

$^{13}\text{C NMR}$ (75 MHz, CDCl_3) δ (ppm) 169.8, 146.2, 136.5, 136.4, 133.8, 127.7, 125.7, 125.2, 124.6, 120.6, 117.3, 21.2, 20.7, 20.3.

The spectroscopic data matched that reported in the literature.³

1-(6,7-Dimethyl-1-hydroxynaphthalen-2-yl)ethan-1-one (**16**)



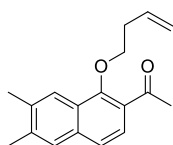
A 50 mL crimp cap vial, equipped with a magnetic stirring bar was charged with $\text{Sc}(\text{OTf})_3$ (107 mg, 0.22 mmol, 5 mol%), degassed and placed under a nitrogen atmosphere. Naphthol **15** (933 mg, 4.35 mmol) was transferred to the vial via a syringe using dry toluene (9 mL) and the reaction mixture was stirred at 100 °C with a metal heating block for 16 h. The reaction was quenched with water (10 mL) and extracted with DCM (3 x 10 mL). The combined organics were dried over Na_2SO_4 , and the solvent was removed in vacuo. Purification by flash column chromatography (3% EtOAc in pentane) yielded **16** as a yellow solid (729 mg, 3.4 mmol, 78%).

$^1\text{H NMR}$ (300 MHz, CDCl_3) δ (ppm) 14.01 (s, 1H), 8.17 (s, 1H), 7.55 – 7.44 (m, 2H), 7.12 (d, $J = 8.8$ Hz, 1H), 2.65 (s, 3H), 2.43 (d, $J = 4.1$ Hz, 6H).

$^{13}\text{C NMR}$ (75 MHz, CDCl_3) δ (ppm) 204.2, 162.2, 140.5, 136.4, 135.8, 127.4, 124.2, 124.0, 123.7, 117.6, 112.9, 26.9, 20.5, 20.3.

The spectroscopic data matched that reported in the literature.³

1-(1-(But-3-en-1-yloxy)-6,7-dimethylnaphthalen-2-yl)ethan-1-one (**1e**)



Synthesized according to **General Procedure 1** using naphthol **16** (715 mg, 3.34 mmol), K_2CO_3 (1.15 g, 8.32 mmol) and 4-bromo-1-butene (1.00 mL, 9.85 mmol) in DMF (6 mL).

¹H NMR (300 MHz, CDCl₃) δ (ppm) 7.96 (s, 1H), 7.65 – 7.55 (m, 2H), 7.48 (d, *J* = 8.6 Hz, 1H), 6.00 (ddt, *J* = 17.1, 10.2, 6.8 Hz, 1H), 5.30 – 5.15 (m, 2H), 4.06 (t, *J* = 6.7 Hz, 2H), 2.75 (s, 3H), 2.73 – 2.63 (m, 2H), 2.46 (s, 3H), 2.42 (s, 3H).

¹³C NMR (75 MHz, CDCl₃) δ (ppm) 200.7, 155.7, 138.5, 136.5, 135.9, 134.3, 127.7, 127.7, 127.0, 124.7, 123.1, 122.9, 117.7, 76.1, 34.8, 30.9, 20.6, 20.3.

Conditions for Column Chromatography: 3-→4% EtOAc in pentane

Yield: 570 mg, 2.1 mmol, 64% (yellow oil)

The spectroscopic data matched that reported in the literature.³

2.4.4.2.2 Synthesis of Indole-derivatives

These substrates were made following the procedures of You et al.⁴ unless otherwise noted.

General Procedure 2 for Indole-derivatives⁴

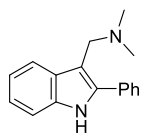
A round bottom flask equipped with a magnetic stirring bar was charged with indole (1.0 eq.) in Et₂O and closed with a rubber septum. Dimethyl malonate (1.1 eq.) was added via a syringe, followed by likewise quick addition of ethyl propiolate (1.1 eq.). The reaction mixture was stirred overnight and was then quenched with water and extracted with EtOAc (3 x 30 mL). The combined organics were washed with brine, dried over Na₂SO₄ and the solvent was removed in vacuo. Purification by flash column chromatography as noted yielded the corresponding indole intermediate.

General Procedure 3 for Indole-derivatives^{4,20}

A round bottom flask equipped with a magnetic stirring bar was charged with the corresponding indole intermediate (1.0 eq.) in THF. After the addition of NaH (60% in mineral oil, 1.2 eq.) the reaction mixture was cooled down to 0 °C and allyl bromide (1.2 eq.) was added dropwise. Following complete addition, the mixture was allowed to warm up to room temperature and was stirred overnight. It was then quenched by addition of water and was extracted with EtOAc (3 x 30 mL). The combined organics were washed with brine, dried over Na₂SO₄ and the solvent was removed in vacuo. Purification by flash column chromatography as noted yielded the corresponding indole products.

General Procedure 4 for acylation of Indole-derivatives²¹

A Schlenk flask equipped with a magnetic stirring bar was charged with a solution of indole (1.0 eq.) in dry DCM (8 mL/mmol) and was placed under a nitrogen atmosphere. Tetrabutylammonium hydrogen sulfate (10 mol%) and freshly grinded sodium hydroxide (5.0 eq.) were added and the resulting solution was stirred for 15 minutes before acetyl chloride (3.0 eq.) was added dropwise via a syringe. The resulting mixture was vigorously stirred for 4 h and then quenched by addition of water. The organic layer was separated, and the aqueous layer was extracted with DCM. The combined organics were washed with brine, dried over Na₂SO₄ and the solvent was removed in vacuo. Purification by flash column chromatography as noted yielded the corresponding acylated indole products.

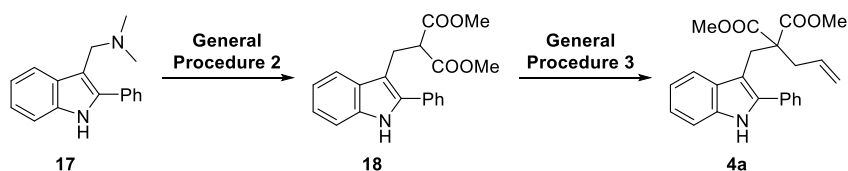
N,N-dimethyl-1-(2-phenyl-1*H*-indol-3-yl)methanamine (**17**)

Prepared according to a literature reported procedure.²²

A three-necked round bottom flask equipped with a magnetic stirring bar and a dropping funnel was charged with a mixture of formaldehyde (37 wt% in water, 2.1 mL, 28 mmol) water (2 mL) and glacial acetic acid (26 mL) in dioxane (24 mL). The reaction mixture was cooled down to 0 °C and dimethylamine (40 wt% in water, 3.5 mL, 28 mmol) was added quickly. Afterwards, phenylindole (5.0 g, 26 mmol) in dioxane (24 mL) was added dropwise via the dropping funnel. Not all phenylindole was dissolved in dioxane and the remaining phenylindole was added slowly as a solid. Following complete addition, the mixture was first stirred for 2 h at 0 °C and then for 12 h at room temperature. In the next step the reaction mixture was diluted with water (32 mL), followed by addition of Celite (1.5 g) and stirring for 10 minutes. The suspension was filtered off over Celite and the filtrate was basified by addition of 2M NaOH (400 mL) resulting in precipitation of the product. The product was filtered off, washed with water and dried in vacuo yielding **17** as a pale white solid (5.2 g, 21 mmol, 80%).

¹H NMR (300 MHz, CDCl₃) δ (ppm) 8.20 (br s, 1H), 7.88 – 7.71 (m, 3H), 7.55 – 7.45 (m, 2H), 7.42 – 7.29 (m, 2H), 7.24 – 7.07 (m, 2H), 3.64 (s, 2H), 2.30 (s, 6H).

The spectroscopic data matched that reported in the literature.²²

Dimethyl 2-allyl-2-((2-phenyl-1*H*-indol-3-yl)methyl)malonate (**4a**)

Intermediate **18** was synthesized according to **General Procedure 2** using indole **17** (4.41 g, 17.6 mmol), dimethyl malonate (2.20 mL, 19.3 mmol), and ethyl propiolate (2.00 mL, 19.3 mmol) in Et₂O (100 mL). The compound was purified via flash column chromatography (8% EtOAc in PE) to yield 2.3 g (39% yield) and was used immediately in the next step.

Compound **4a** was synthesized according to **General Procedure 3** using intermediate **18** (1.1 g, 3.4 mmol), NaH (161 mg, 4.0 mmol) and allyl bromide (0.40 mL, 4.0 mmol) in THF.

$^1\text{H NMR}$ (300 MHz, CDCl_3) δ (ppm) 8.11 (s, 1H), 7.60 – 7.51 (m, 3H), 7.48 – 7.40 (m, 2H), 7.39 – 7.28 (m, 2H), 7.22 – 7.04 (m, 2H), 5.34 (ddt, $J = 16.7, 10.3, 7.2$ Hz, 1H), 5.00 – 4.64 (m, 2H), 3.71 (s, 2H), 3.41 (s, 6H), 2.35 (d, $J = 7.2$ Hz, 2H).

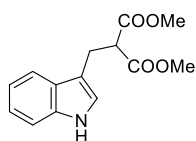
$^{13}\text{C NMR}$ (75 MHz, CDCl_3) δ (ppm) 171.7, 137.2, 135.7, 133.8, 133.0, 129.8, 129.1, 129.1, 128.2, 122.3, 119.8, 119.6, 118.3, 110.9, 106.6, 59.6, 52.2, 37.1, 27.3.

Conditions for Column Chromatography: 8% EtOAc in PE

Yield: 719 mg, 1.9 mmol, 56% (white solid)

The spectroscopic data matched that reported in the literature.²⁰

Dimethyl 2-((1*H*-indol-3-yl)methyl)malonate (**19**)



Synthesized according to a modified **General Procedure 2** using gramine (2.6 g, 15 mmol), dimethyl malonate (1.6 mL, 14 mmol), and ethyl propiolate (1.4 mL, 15 mmol) in Et_2O (5 mL). The reaction was quenched after 2 h, the phases were separated, and the aqueous layer was extracted with Et_2O (3 x 30 ml).

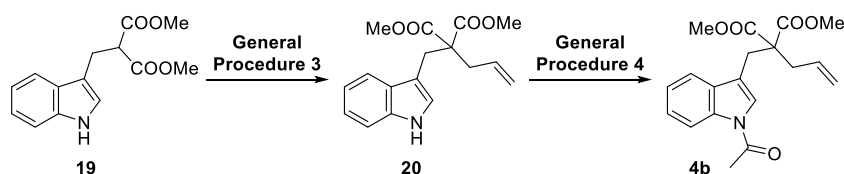
$^1\text{H NMR}$ (300 MHz, CDCl_3) δ (ppm) 8.08 (br s, 1H), 7.63 – 7.58 (m, 1H), 7.35 (dd, $J = 7.8, 1.1$ Hz, 1H), 7.24 – 7.09 (m, 2H), 7.04 (d, $J = 2.4$ Hz, 1H), 3.81 (t, $J = 7.6$ Hz, 1H), 3.70 (s, 6H), 3.40 (d, $J = 8.3$ Hz, 2H).

$^{13}\text{C NMR}$ (75 MHz, CDCl_3) δ (ppm) 169.8, 136.2, 127.1, 122.7, 122.3, 119.6, 118.6, 112.2, 111.3, 52.8, 52.7, 24.8.

Conditions for Column Chromatography: 20% EtOAc in PE

Yield: 2.2 g, 8.3 mmol, 55% (yellow oil)

The spectroscopic data matched that reported in the literature.²³

Dimethyl 2-((1-acetyl-1*H*-indol-3-yl)methyl)-2-allylmalonate (**4b**)

Intermediate **20** was synthesized according to a modified **General Procedure 3** using indole **19** (2.2 g, 8.2 mmol), NaH (0.4 g, 9.0 mmol) and allyl bromide (0.8 mL, 9.0 mmol) in THF (16 mL). After slow addition of NaH the reaction mixture was first stirred for 30 min at room temperature, before allyl bromide was added at once at 0 °C. The reaction was quenched after 5 h. The compound was purified via flash column chromatography (17% EtOAc in PE) to yield 701 mg (28% yield) and was used immediately in the next step.

Compound **4b** was synthesized according to **General Procedure 4** using intermediate **20** (620 mg, 2.1 mmol), tetrabutylammonium hydrogen sulfate (70 mg, 0.2 mmol), NaOH (412 mg, 10 mmol), acetyl chloride (0.44 mL, 6.2 mmol) and dry DCM (16 mL).

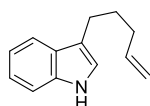
¹H NMR (300 MHz, CDCl₃) δ (ppm) 8.39 (d, *J* = 8.2 Hz, 1H), 7.48 (dd, *J* = 7.1, 1.2 Hz, 1H), 7.34 (td, *J* = 8.3, 7.8, 1.4 Hz, 1H), 7.30 – 7.23 (m, 2H), 5.77 (ddt, *J* = 17.6, 10.3, 7.3 Hz, 1H), 5.20 – 5.09 (m, 2H), 3.71 – 3.56 (m, 6H), 3.34 (s, 2H), 2.72 (dt, *J* = 7.3, 1.3 Hz, 2H), 2.61 (s, 3H).

¹³C NMR (75 MHz, CDCl₃) δ (ppm) 171.4, 168.4, 135.5, 132.5, 131.0, 125.4, 124.2, 123.5, 119.7, 119.0, 116.8, 116.7, 58.5, 52.6, 37.9, 28.1, 24.2.

Conditions for Column Chromatography: 5-10% EtOAc in PE

Yield: 610 mg, 1.8 mmol, 86% (white solid)

The spectroscopic data matched that reported in the literature.⁴

3-(pent-4-en-1-yl)-1*H*-indole (**21**)

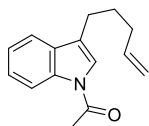
Prepared according to a literature reported procedure.^{21,24}

A crimp cap vial equipped with a magnetic stirring bar was degassed and placed under a nitrogen atmosphere before it was charged with a solution of MeMgI (3.5 ml, 10.5 mmol, 3.0M solution in Et₂O) in benzene (10 ml). A solution of indole (1.2 g, 10 mmol) in benzene was added via a syringe, followed after 10 minutes by addition of 5-bromopentene (0.8 ml, 6.6 mmol), likewise with a syringe. The mixture was heated with a metal heating block for 27 h at 112 °C, then cooled down to room temperature and quenched with saturated NH₄Cl solution. After separation of the organic phase, the aqueous phase was extracted with EtOAc and the combined organics were washed with brine, dried over Na₂SO₄ and the solvent was removed in vacuo. Purification by flash column chromatography (9% EtOAc in PE) yielded **21** (847 mg, 4.6 mmol, 46%) as a yellow oil.

¹H NMR (300 MHz, CDCl₃) δ (ppm) 7.91 (br s, 1H), 7.62 (d, *J* = 7.8 Hz, 1H), 7.36 (dt, *J* = 8.1, 0.9 Hz, 1H), 7.26 – 7.06 (m, 2H), 7.02 – 6.95 (m, 1H), 5.88 (ddt, *J* = 16.9, 10.2, 6.6 Hz, 1H), 5.20 – 4.87 (m, 2H), 2.78 (t, *J* = 8.0 Hz, 2H), 2.26 – 2.09 (m, 2H), 1.91 – 1.74 (m, 2H).

The spectroscopic data matched that reported in the literature.^{21,24}

1-(3-(pent-4-en-1-yl)-1H-indol-1-yl)ethan-1-one (4c)



Synthesized according to **General Procedure 4** using indole **21** (631 mg, 3.4 mmol), tetrabutylammonium hydrogen sulfate (115 mg, 0.3 mmol), NaOH (680 mg, 17 mmol), acetyl chloride (0.7 mL, 10 mmol) and dry DCM (27 mL).

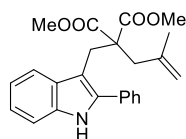
¹H NMR (300 MHz, CDCl₃) δ (ppm) 8.43 (d, *J* = 8.1 Hz, 1H), 7.58 – 7.48 (m, 1H), 7.42 – 7.24 (m, 2H), 7.18 (s, 1H), 5.87 (ddt, *J* = 16.9, 10.2, 6.6 Hz, 1H), 5.11 – 4.98 (m, 2H), 2.77 – 2.65 (m, 2H), 2.61 (s, 3H), 2.24 – 2.13 (m, 2H), 1.82 (p, *J* = 7.4 Hz, 2H).

¹³C NMR (75 MHz, CDCl₃) δ (ppm) 168.5, 138.4, 136.1, 130.9, 125.3, 123.5, 123.2, 121.8, 119.1, 116.8, 115.2, 33.7, 28.4, 24.5, 24.2.

Conditions for Column Chromatography: 5-10% EtOAc in PE

Yield: 561 mg, 2.5 mmol, 74% (pale-yellow oil)

The spectroscopic data matched that reported in the literature.²¹

Dimethyl 2-(2-methylallyl)-2-((2-phenyl-1*H*-indol-3-yl)methyl)malonate (**4e**)

Synthesized according to a modified **General Procedure 3** using indole **18** (450 mg, 1.3 mmol), NaH (64 mg, 1.6 mmol) and 3-Brom-2-methyl-1-propen (0.2 mL, 1.6 mmol) in THF (5 mL).

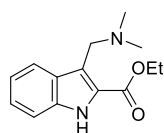
¹H NMR (300 MHz, CDCl₃) δ (ppm) 8.17 (s, 1H), 7.65 (d, $J = 7.7$ Hz, 1H), 7.56 – 7.49 (m, 2H), 7.45 – 7.23 (m, 4H), 7.22 – 7.06 (m, 2H), 4.70 (d, $J = 27.5$ Hz, 2H), 3.88 (s, 2H), 3.32 (s, 6H), 2.44 (s, 2H), 1.47 (s, 3H).

¹³C NMR (75 MHz, CDCl₃) δ (ppm) 172.0, 142.2, 136.8, 135.7, 133.8, 130.1, 129.0, 128.9, 128.0, 122.2, 119.7, 119.7, 111.9, 110.9, 106.8, 58.4, 52.1, 40.0, 28.1, 24.5.

Conditions for Column Chromatography: 8% EtOAc in PE

Yield: 370 mg, 0.95 mmol, 71% (white solid)

The spectroscopic data matched that reported in the literature.⁴

Ethyl 3-((dimethylamino)methyl)-1*H*-indole-2-carboxylate (**22**)

Prepared according to a literature reported procedure.²⁵

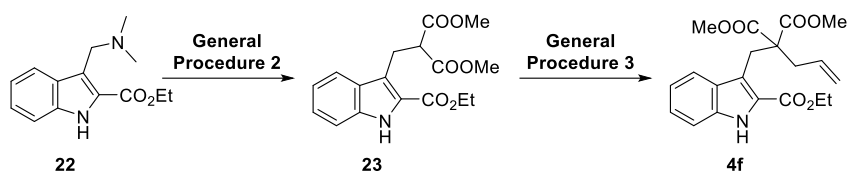
A 250 mL Schlenk flask equipped with a magnetic stirring bar was placed under a nitrogen atmosphere, charged with dimethylamine (12 mL, 2M solution in THF, 24 mmol) and cooled to 0 °C. Acetic acid (2.9 mL), formaldehyde (37 wt% in water, 1.8 mL, 24 mmol) and finally ethyl indole-2-carboxylate (2.4 g, 13 mmol) in methanol (100 mL) were added and the resulting solution was refluxed for 4 h using an oil bath. Afterwards, the reaction mixture was first concentrated to 20% of its volume, then diluted with water (33 mL) and last washed with CHCl₃ (2 x 33 mL). The aqueous phase was separated, cooled in an ice bath and 20% NaOH solution was added until a pH of 12 was obtained. The mixture was extracted with DCM (3 x 33 mL), the combined organics

washed with a saturated NaHCO₃ solution, dried over Na₂SO₄ and the solvent was removed in vacuo yielding **22** as white solid (2.3 g, 9.2 mmol, 73%).

¹H NMR (300 MHz, DMSO-*d*₆) δ (ppm) 11.62 (s, 1H), 7.81 – 7.76 (m, 1H), 7.45 – 7.40 (m, 1H), 7.29 – 7.21 (m, 1H), 7.05 (ddd, *J* = 8.0, 6.9, 1.0 Hz, 1H), 4.34 (q, *J* = 7.1 Hz, 2H), 3.89 (s, 2H), 2.16 (s, 6H), 1.36 (t, *J* = 7.1 Hz, 3H).

The spectroscopic data matched that reported in the literature.²⁵

Dimethyl 2-allyl-2-((2-(ethoxycarbonyl)-1*H*-indol-3-yl)methyl)malonate (**4f**)



Intermediate **23** was synthesized according to **General Procedure 2** using indole **22** (840 mg, 3.4 mmol), dimethyl malonate (0.4 mL, 3.7 mmol), and ethyl propiolate (0.4 mL, 3.7 mmol) in THF. The compound was purified via flash column chromatography (8% EtOAc in PE) to yield 104 mg (9% yield) and was used immediately in the next step.

Compound **4f** was synthesized according to **General Procedure 3** using intermediate **23** (104 mg, 0.31 mmol), NaH (14 mg, 0.35 mmol) and allyl bromide (33 μL, 0.38 mmol) in dry THF.

¹H NMR (300 MHz, CDCl₃) δ (ppm) 8.88 (s, 1H), 7.71 – 7.57 (m, 1H), 7.41 – 7.24 (m, 2H), 7.11 (ddd, *J* = 8.1, 6.7, 1.2 Hz, 1H), 6.03 – 5.80 (m, 1H), 5.13 – 4.93 (m, 2H), 4.41 (q, *J* = 7.1 Hz, 2H), 3.90 (s, 2H), 3.60 (s, 6H), 2.63 (d, *J* = 7.2 Hz, 2H), 1.43 (t, *J* = 7.1 Hz, 3H).

¹³C NMR (75 MHz, CDCl₃) δ (ppm) 171.7, 162.1, 135.7, 133.9, 128.5, 125.7, 125.3, 121.7, 120.3, 118.3, 117.9, 111.8, 61.2, 59.5, 52.3, 38.5, 28.8, 14.5.

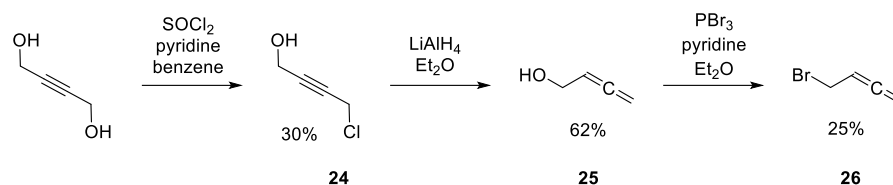
Conditions for Column Chromatography: 8% EtOAc in PE

Yield: 46 mg, 0.12 mmol, 39% (white solid)

The spectroscopic data matched that reported in the literature.⁴

2.4.4.2.3 Synthesis of Allene-derivatives

Allenyl bromide was synthesized according to a literature procedure:^{18b}

**4-Chlorobut-2-yne-1-ol (24)**

A 100 mL crimped capped vial equipped with a magnetic stirring bar was charged with but-2-yne-1,4-diol (22.50 g, 261.5 mmol). The vial was set under nitrogen and benzene (28 mL) and pyridine (23 mL) were added via a syringe. The reaction mixture was cooled down to 0 °C and thionyl chloride (21 mL, 287.7 mmol) was added dropwise via a syringe pump over 3 h. Following complete addition, the ice bath was removed, and the reaction mixture was allowed to warm to room temperature. After stirring for an additional 16 h, the reaction mixture was poured onto an ice/water mixture (75 mL) and was extracted with Et₂O (1 x 50 mL, 2 x 20 mL). The combined organics were washed with a saturated NaHCO₃ solution (2 x 100 mL) and brine, dried over Na₂SO₄ and the solvent was removed in vacuo. Fractionated distillation (1.4 mbar, 54 °C) yielded **24** as colorless liquid (8.20 g, 78.5 mmol, 30%).

¹H NMR (300 MHz, CDCl₃) δ (ppm) 4.32 (t, *J* = 2.0 Hz, 2H), 4.25 – 4.13 (m, 2H), 2.01 (s, 1H).

The spectroscopic data matched that reported in the literature.^{18b}

Buta-2,3-dien-1-ol (25)

A 250 mL three-necked round bottom flask equipped with a magnetic stirring bar and a condenser was charged with **24** (8.20 g, 78.5 mmol) in dry Et₂O (150 mL) and set under nitrogen. LiAlH₄ (3.20 g, 84.3 mmol) was added in small portions under nitrogen and after complete addition the suspension was stirred for an additional 30 min. The reaction mixture was then cooled to 0 °C in an ice bath and carefully quenched by addition of water (3.1 mL), 15% NaOH (3.1 mL) and finally an ice/water mixture (18.2 mL). The resulting grey slurry was stirred overnight at room temperature. The precipitate was filtered off, the organic phase was dried over Na₂SO₄ and the

solvent was removed in vacuo. Distillation (14 mbar, 40 °C) yielded **25** as colorless liquid (3.40 g, 48.5 mmol, 62%).

¹H NMR (300 MHz, CDCl₃) δ (ppm) 5.43 – 5.27 (m, 1H), 4.93 – 4.77 (m, 2H), 4.15 (td, *J* = 5.9, 2.9 Hz, 2H).

The spectroscopic data matched that reported in the literature.^{18b}

4-Bromobuta-1,2-diene (26)

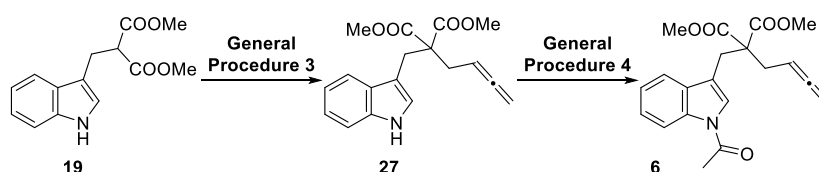
A 50 mL Schlenk flask equipped with a magnetic stirring bar was charged with a solution of PBr₃ (1.90 mL, 19.4 mmol) in Et₂O (10 mL) and was set under nitrogen. **25** (3.40 g, 48.5 mmol) was dissolved in pyridine (2 mL) and added dropwise via a syringe at -10 °C. The reaction mixture was allowed to warm to room temperature and stirred for 16 h. The reaction was quenched by addition of water (100 mL) and the organic layer was extracted with pentane (3 x 50 mL). The combined organics were washed with brine (50 mL), dried over Na₂SO₄ and the solvent was removed in vacuo. Fractionated distillation (96 mbar, 50 °C) yielded **26** as colorless liquid (1.60 g, 12.0 mmol, 25%).

¹H NMR (300 MHz, CDCl₃) δ (ppm) 5.55 – 5.28 (m, 1H), 4.94 (dt, *J* = 6.5, 2.0 Hz, 2H), 3.96 (dt, *J* = 8.2, 2.0 Hz, 2H).

¹³C NMR (75 MHz, CDCl₃) δ (ppm) 209.8, 89.4, 77.5, 30.1.

The spectroscopic data matched that reported in the literature.^{18b}

Dimethyl 2-((1-acetyl-1*H*-indol-3-yl)methyl)-2-(buta-2,3-dien-1-yl)malonate (6)



Intermediate **27** was synthesized according to a modified **General Procedure 3** using indole **19** (630 mg, 2.4 mmol), NaH (105 mg, 2.6 mmol) and **26** (400 mg, 3.0 mmol) in dry THF (10 mL) under a nitrogen atmosphere. After addition of NaH, the reaction mixture was first stirred for 30 min at 0 °C, before **26** was added dropwise as a solution in pentane at 0 °C and stirred for 10 min at 0 °C.

The reaction was quenched after stirring for 3 h at room temperature by addition of a saturated NH_4Cl solution and water. The compound was purified via flash column chromatography (13% EtOAc in PE) to yield 620 mg (83% yield) and was used immediately in the next step.

Compound **6** was synthesized according to **General Procedure 4** using intermediate **27** (620 mg, 2.0 mmol), tetrabutylammonium hydrogen sulfate (67 mg, 0.2 mmol), NaOH (396 mg, 10.0 mmol), acetyl chloride (0.42 mL, 6.2 mmol) and dry DCM (16 mL).

HRMS (ESI⁺) (m/z): calculated for $\text{C}_{20}\text{H}_{21}\text{NO}_5\text{Na}^+$ [$\text{M}+\text{Na}^+$]: 378.1312, found: 378.1313.

Melting Point: 84-85 °C

¹H NMR (300 MHz, CDCl_3) δ (ppm) 8.40 (d, $J = 7.9$ Hz, 1H), 7.55 – 7.43 (m, 1H), 7.37 – 7.20 (m, 3H), 5.12 – 4.96 (m, 1H), 4.84 – 4.69 (m, 2H), 3.65 (s, 6H), 3.38 (s, 2H), 2.69 (dt, $J = 7.9, 2.6$ Hz, 2H), 2.60 (s, 3H).

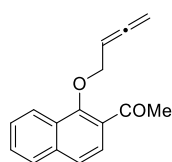
¹³C NMR (75 MHz, CDCl_3) δ (ppm) 210.5, 171.2, 168.5, 135.6, 131.0, 125.4, 124.6, 123.5, 118.9, 116.7, 116.6, 84.7, 75.2, 58.3, 52.7, 32.3, 27.6, 24.2.

IR (neat): 2944, 2363, 1960, 1710, 1606, 1446, 1244, 1203, 1073, 868, 760 cm^{-1} .

Conditions for Column Chromatography: 5-10% EtOAc in PE

Yield: 598 mg, 1.7 mmol, 85% (white solid)

1-(1-(buta-2,3-dien-1-yloxy)naphthalen-2-yl)ethan-1-one (**9a**)



Synthesized according to a modified **General Procedure 1^{18b}** using 2-acetyl-1-naphthol (279 mg, 1.5 mmol), K_2CO_3 (625 mg, 4.5 mmol) and **26** (0.3 mL) in DMF (10 mL). The reaction was stirred at room temperature overnight and under a nitrogen atmosphere. The reaction mixture was diluted with EtOAc (25 mL), washed with water (3 x 25 mL) and brine (25 mL), dried over Na_2SO_4 and the solvent was removed in vacuo.

HRMS (EI) (m/z): calculated for $\text{C}_{16}\text{H}_{14}\text{O}_2$ [M^+]: 238.0988, found: 238.0981.

¹H NMR (300 MHz, CDCl₃) δ (ppm) = 8.28 – 8.18 (m, 1H), 7.89 – 7.82 (m, 1H), 7.72 (d, *J* = 8.6 Hz, 1H), 7.64 (d, *J* = 8.3 Hz, 1H), 7.62 – 7.53 (m, 2H), 5.58 – 5.42 (m, 1H), 4.85 (dt, *J* = 6.6, 2.3 Hz, 2H), 4.60 (dt, *J* = 7.2, 2.3 Hz, 2H), 2.77 (s, 3H).

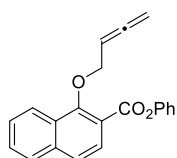
¹³C NMR (75 MHz, CDCl₃) δ (ppm) 210.1, 200.8, 155.5, 136.9, 129.0, 128.5, 128.4, 128.2, 126.8, 125.5, 124.4, 123.6, 87.0, 76.6, 74.4, 31.1.

IR (neat): 3060, 2993, 2929, 2873, 1953, 1669, 1625, 1565, 1502, 1461, 1427, 1390, 1356, 1271, 1244, 1185, 1151, 1110, 1073, 1021, 849, 816 cm⁻¹.

Conditions for Column Chromatography: 0-→20% EtOAc in PE

Yield: 303 mg, 1.3 mmol, 85% (clear oil)

Phenyl 1-(buta-2,3-dien-1-yloxy)-2-naphthoate (9b**)**



Synthesized according to a modified **General Procedure 1^{18b}** using phenyl 1-hydroxy-2-naphthoate (198 mg, 0.75 mmol), K₂CO₃ (313 mg, 2.30 mmol) and **26** (0.15 mL) in DMF (5 mL). The reaction was stirred at room temperature overnight and under a nitrogen atmosphere. The reaction mixture was diluted with EtOAc (25 mL), washed with water (3 x 25 mL) and brine (25 mL), dried over Na₂SO₄ and the solvent was removed in vacuo.

HRMS (EI) (*m/z*): calculated for C₂₁H₁₆O₃ [*M*⁺]: 316.1094, found: 316.1092.

Melting Point: 46-47 °C

¹H NMR (300 MHz, CDCl₃) δ (ppm) 8.39 – 8.33 (m, 1H), 8.06 (d, *J* = 8.7 Hz, 1H), 7.92 – 7.86 (m, 1H), 7.70 (d, *J* = 8.6 Hz, 1H), 7.66 – 7.56 (m, 2H), 7.50 – 7.42 (m, 2H), 7.33 – 7.26 (m, 3H), 5.67 – 5.51 (m, 1H), 4.82 (t, *J* = 2.2 Hz, 1H), 4.79 (s, 2H), 4.77 (t, *J* = 2.2 Hz, 1H).

¹³C NMR (75 MHz, CDCl₃) δ (ppm) 210.0, 164.7, 157.8, 151.1, 137.2, 129.7, 129.2, 128.9, 128.0, 126.9, 126.9, 126.1, 124.2, 124.1, 122.0, 119.0, 87.6, 76.4, 74.2.

IR (neat): 3060, 2944, 1956, 1725, 1625, 1490, 1453, 1330, 1274, 1230, 1200, 1129, 1069, 957, 827 cm⁻¹.

Conditions for Column Chromatography: 5->10% EtOAc in PE

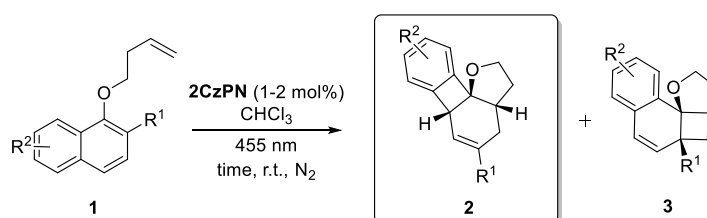
Yield: 200 mg, 0.6 mmol, 84% (white solid)

2.4.4.3 Photoreactions

General Procedure 5 for photoreactions

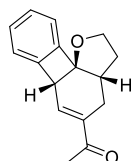
A crimp capped vial (5 mL for naphthols, 10 mL for indoles) equipped with a magnetic stirring bar was charged with either the corresponding alkylated naphthol (200 μ mol, 1.0 eq., 100 μ mol for allene-naphthols) or indole (50 μ mol, 1.0 eq.), **2CzPN** (1-4 mol%), and solvent (2.0 mL of chloroform for naphthols and 4.0 mL of anhydrous toluene for indoles). The mixture was degassed by three cycles of freeze-pump-thaw, backfilled with nitrogen and subsequently stirred under blue light irradiation ($\lambda_{\text{max}} = 455$ nm LED) through the plane bottom side of the vial at room temperature for 14-42 h. For isolation, two reactions were combined and submitted to flash column chromatography (100% DCM for removal of the catalyst, then 5->20% EtOAc in PE or 5->40% EtOAc in PE) unless otherwise noted.

2.4.4.3.1 Photocatalytic Cycloaddition of Naphthol-derivatives



Scheme S2-1: Photocycloaddition of naphthol-derivatives **1**. Product **3** is the side product of the reaction and was isolated together with product **2** in the indicated cases.

1-(3,3a,4,6a-Tetrahydro-2H-biphenyleno[8b,1-b]furan-5-yl)ethan-1-one (2a)



The **General Procedure 5** was applied using alkylated naphthol **1a** (48.1 mg), **2CzPN** (1 mol%), chloroform and irradiation with 455 nm for 14 h. Combination of two reactions and purification with flash column chromatography yielded **2a** as a white solid (90.3 mg, 94%).

Synthesis with recycled catalyst:

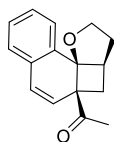
The **General Procedure 5** was applied using alkylated naphthol **1a** (48.1 mg), recycled 2CzPN (1 mol%), chloroform and irradiation with 455 nm for 14 h. Purification with flash column chromatography yielded **2a** as a white solid (43.3 mg, 90%) and **3a** as a white solid (4.7 mg, 10%).

¹H NMR (300 MHz, CDCl₃) δ (ppm) 7.30 – 7.13 (m, 4H), 7.10 – 7.00 (m, 1H), 4.36 – 4.13 (m, 3H), 2.95 (dd, *J* = 16.2, 3.1 Hz, 1H), 2.29 (s, 3H), 2.23 – 2.13 (m, 1H), 2.08 – 1.90 (m, 2H), 1.58 – 1.44 (m, 1H).

¹³C NMR (75 MHz, CDCl₃) δ (ppm) 198.6, 146.4, 145.1, 141.5, 141.2, 129.9, 128.0, 122.7, 121.5, 90.4, 68.6, 49.7, 44.0, 27.9, 25.7, 23.8.

The spectroscopic data matched that reported in the literature.³

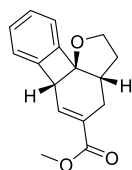
1-(2,3,3a,4-Tetrahydro-4aH-naphtho[1',2':1,4]cyclobuta[1,2-*b*]furan-4a-yl)ethan-1-one (3a)



¹H NMR (300 MHz, CDCl₃) δ (ppm) 7.29 – 7.18 (m, 3H), 7.13 – 7.04 (m, 1H), 6.52 (d, *J* = 9.7 Hz, 1H), 5.67 (d, *J* = 9.7 Hz, 1H), 4.39 (t, *J* = 8.4 Hz, 1H), 4.08 (ddd, *J* = 11.4, 8.7, 5.5 Hz, 1H), 3.18 – 3.05 (m, 1H), 2.65 (dd, *J* = 12.6, 7.4 Hz, 1H), 2.19 – 2.08 (m, 1H), 2.09 (s, 3H), 1.99 – 1.85 (m, 1H), 1.68 (dd, *J* = 12.5, 5.5 Hz, 1H).

¹³C NMR (75 MHz, CDCl₃) δ (ppm) 205.7, 135.4, 131.4, 128.9, 128.7, 128.1, 128.1, 127.3, 124.8, 87.9, 70.5, 57.4, 46.2, 32.9, 30.6, 27.0.

The spectroscopic data matched that reported in the literature.³

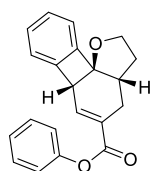
Methyl 3,3a,4,6a-tetrahydro-2H-biphenyleno[8b,1-b]furan-5-carboxylate (**2b**)

The **General Procedure 5** was applied using alkylated naphthol **1b** (51.3 mg), **2CzPN** (1 mol%), chloroform and irradiation with 455 nm for 14 h. Combination of two reactions and purification with flash column chromatography yielded **2b** as a white solid (63.5 mg, 62%) with no **3b** observed with ^1H NMR in the crude mixture.

^1H NMR (300 MHz, CDCl_3) δ (ppm) 7.31 (dd, $J = 5.4, 2.8$ Hz, 1H), 7.27 – 7.19 (m, 2H), 7.19 – 7.13 (m, 1H), 7.07 – 7.02 (m, 1H), 4.34 – 4.12 (m, 3H), 3.69 (s, 3H), 2.85 (dd, $J = 16.4, 2.8$ Hz, 1H), 2.26 – 2.15 (m, 1H), 2.12 – 1.97 (m, 2H), 1.72 – 1.59 (m, 1H).

^{13}C NMR (75 MHz, CDCl_3) δ (ppm) 167.7, 146.3, 145.4, 140.8, 131.6, 129.8, 127.8, 122.5, 121.6, 90.3, 68.5, 51.9, 49.5, 44.0, 27.8, 25.4.

The spectroscopic data matched that reported in the literature.³

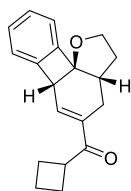
Phenyl 3,3a,4,6a-tetrahydro-2H-biphenyleno[8b,1-b]furan-5-carboxylate (**2c**)

The **General Procedure 5** was applied using alkylated naphthol **1c** (63.7 mg), **2CzPN** (1 mol%), chloroform and irradiation with 455 nm for 14 h. Combination of two reactions and purification with flash column chromatography yielded **2c** as a white powder (126 mg, 99%).

^1H NMR (300 MHz, CDCl_3) δ (ppm) 7.59 (dd, $J = 5.4, 2.8$ Hz, 1H), 7.42 – 7.35 (m, 2H), 7.33 – 7.27 (m, 1H), 7.28 – 7.20 (m, 3H), 7.15 – 7.06 (m, 3H), 4.42 – 4.19 (m, 3H), 3.00 (dd, $J = 16.3, 3.0$ Hz, 1H), 2.31 – 2.21 (m, 1H), 2.19 – 1.99 (m, 2H), 1.88 – 1.72 (m, 1H).

^{13}C NMR (75 MHz, CDCl_3) δ (ppm) 165.6, 151.0, 146.4, 145.2, 142.7, 131.2, 129.9, 129.5, 128.0, 125.6, 122.6, 121.7, 121.7, 90.3, 68.5, 49.7, 44.0, 27.8, 25.5.

The spectroscopic data matched that reported in the literature.³

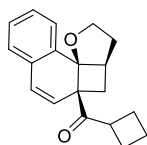
Cyclobutyl(3,3a,4,6a-tetrahydro-2H-biphenyleno[8b,1-b]furan-5-yl)methanone (**2d**)

The **General Procedure 5** was applied using alkylated naphthol **1d** (56.1 mg), **2CzPN** (2 mol%), chloroform and irradiation with 455 nm for 42 h. Combination of two reactions and purification with flash column chromatography yielded **2d** as a yellow oil (85.6 mg, 76%) and **3d** as a pale-yellow powder (22.1 mg, 20 %).

¹H NMR (300 MHz, CDCl₃) δ (ppm) 7.27 – 7.18 (m, 2H), 7.21 – 7.09 (m, 1H), 7.06 – 6.97 (m, 2H), 4.32 – 4.23 (m, 2H), 4.26 – 4.13 (m, 1H), 3.74 – 3.60 (m, 1H), 2.91 (dd, $J = 16.3, 3.2$ Hz, 1H), 2.34 – 1.89 (m, 8H), 1.85 – 1.68 (m, 1H), 1.57 – 1.39 (m, 1H).

¹³C NMR (75 MHz, CDCl₃) δ (ppm) = 201.7, 146.4, 145.2, 140.5, 138.9, 129.8, 127.9, 122.6, 121.3, 90.4, 68.5, 49.6, 44.0, 41.4, 27.9, 25.6, 25.4, 24.0, 18.2.

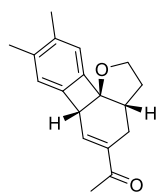
The spectroscopic data matched that reported in the literature.³

Cyclobutyl(2,3,3a,4-tetrahydro-4aH-naphtho[1',2':1,4]cyclobuta[1,2-b]furan-4a-yl)methanone (**3d**)

¹H NMR (300 MHz, CDCl₃) δ (ppm) 7.33 – 7.17 (m, 3H), 7.14 – 7.01 (m, 1H), 6.50 (d, $J = 9.7$ Hz, 1H), 5.63 (d, $J = 9.7$ Hz, 1H), 4.46 – 4.25 (m, 1H), 4.09 (ddd, $J = 11.4, 8.7, 5.4$ Hz, 1H), 3.52 – 3.26 (m, 1H), 3.11 (dt, $J = 9.2, 6.9$ Hz, 1H), 2.73 (dd, $J = 12.5, 7.4$ Hz, 1H), 2.48 – 2.24 (m, 1H), 2.11 – 1.58 (m, 8H).

¹³C NMR (75 MHz, CDCl₃) δ (ppm) 208.3, 135.7, 131.6, 128.8, 128.3, 128.0, 127.5, 127.1, 124.7, 88.1, 70.4, 56.7, 46.5, 43.4, 32.9, 30.6, 27.2, 23.8, 18.0.

The spectroscopic data matched that reported in the literature.³

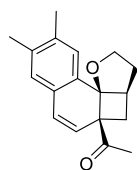
1-(8,9-dimethyl-3,3a,4,6a-tetrahydro-2*H*-biphenyleno[8*b*,1-*b*]furan-5-yl)ethan-1-one (**2e**)

The **General Procedure 5** was applied using alkylated naphthol **1e** (53.7 mg), **2CzPN** (2 mol%), chloroform and irradiation with 455 nm for 42 h. Combination of two reactions and purification with flash column chromatography yielded **2e** as a white solid (74.7 mg, 70%) and **3e** as a white powder (28.1 mg, 26%).

¹H NMR (300 MHz, CDCl₃) δ (ppm) 7.19 (dd, *J* = 5.4, 2.7 Hz, 1H), 6.94 (s, 1H), 6.84 (s, 1H), 4.31 – 4.12 (m, 3H), 2.94 (dd, *J* = 16.3, 3.1 Hz, 1H), 2.28 (s, 3H), 2.22 (s, 6H), 2.18 – 2.13 (m, 1H), 2.06 – 1.87 (m, 2H), 1.57 – 1.44 (m, 1H).

¹³C NMR (75 MHz, CDCl₃) δ (ppm) 198.7, 143.9, 142.8, 142.1, 140.9, 138.6, 136.6, 123.5, 122.5, 90.2, 68.4, 49.3, 43.9, 27.9, 25.7, 23.8, 20.8, 20.5.

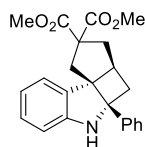
The spectroscopic data matched that reported in the literature.³

1-(8,9-dimethyl-2,3,3a,4-tetrahydro-4a*H*-naphtho[1',2':1,4]cyclobuta[1,2-*b*]furan-4a-yl)ethan-1-one (**3e**)

¹H NMR (300 MHz, CDCl₃) δ (ppm) 7.03 (s, 1H), 6.87 (s, 1H), 6.47 (d, *J* = 9.6 Hz, 1H), 5.59 (d, *J* = 9.7 Hz, 1H), 4.38 (t, *J* = 8.2 Hz, 1H), 4.06 (ddd, *J* = 11.5, 8.7, 5.5 Hz, 1H), 3.07 (dt, *J* = 9.2, 7.0 Hz, 1H), 2.63 (dd, *J* = 12.6, 7.4 Hz, 1H), 2.24 (s, 6H), 2.08 (s, 4H), 2.01 – 1.84 (m, 1H), 1.67 (dd, *J* = 12.4, 5.4 Hz, 1H).

The spectroscopic data matched that reported in the literature.³

2.4.4.3.2 Photocatalytic Cycloaddition of Indole-derivatives

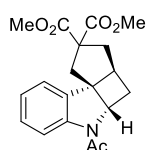
Dimethyl-4a-phenyl-3a,4,4a,5-tetrahydro-1H-cyclopenta[2,3]cyclobuta[1,2-b]indole-2,2(3H)-dicarboxylate (5a)

The **General Procedure 5** was applied using alkylated indole **4a** (18.9 mg), **2CzPN** (4 mol%), toluene (anhydrous) and irradiation with 455 nm for 24 h. Combination of two reactions and purification with flash column chromatography yielded **5a** as brown solid (36.0 mg, 95%).

¹H NMR (300 MHz, CDCl₃) δ (ppm) 7.36 – 7.29 (m, 2H), 7.28 – 7.25 (m, 1H), 7.22 – 7.16 (m, 2H), 7.03 – 7.11 (m, 2H), 6.76 (td, *J* = 7.4, 1.0 Hz, 1H), 6.59 (dt, *J* = 7.6, 0.7 Hz, 1H), 4.21 (s, 1H), 3.74 (s, 3H), 3.36 (s, 3H), 3.05 – 2.93 (m, 1H), 2.86 – 2.76 (m, 2H), 2.65 – 2.53 (m, 2H), 2.52 – 2.35 (m, 2H).

¹³C NMR (75 MHz, CDCl₃) δ (ppm) 172.8, 172.1, 152.1, 142.3, 132.9, 128.6, 128.1, 127.6, 126.7, 122.7, 118.7, 108.5, 71.4, 65.4, 63.8, 53.1, 52.7, 45.7, 40.7, 39.3, 36.8.

The spectroscopic data matched that reported in the literature.⁴

Dimethyl-5-acetyl-3a,4,4a,5-tetrahydro-1H-cyclopenta[2,3]cyclobuta[1,2-b]indole-2,2(3H)-dicarboxylate (5b)

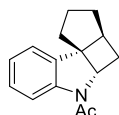
The **General Procedure 5** was applied using alkylated indole **4b** (17.2 mg), **2CzPN** (4 mol%), toluene (anhydrous) and irradiation with 455 nm for 24 h. Combination of two reactions and purification with flash column chromatography yielded **5b** as a white solid (34.1 mg, 99%).

¹H NMR (300 MHz, CDCl₃) δ (ppm) 8.25 (d, *J* = 7.8 Hz, 1H), 7.26 – 7.15 (m, 2H), 7.05 (td, *J* = 7.4, 1.1 Hz, 1H), 4.43 (t, *J* = 5.7 Hz, 1H), 3.85 (s, 3H), 3.79 (s, 3H), 2.93 – 2.79 (m, 2H), 2.68 – 2.44 (m, 3H), 2.29 – 2.22 (m, 2H), 2.08 (s, 3H).

^{13}C NMR (75 MHz, CDCl_3) δ (ppm) 172.6, 172.0, 168.5, 144.3, 134.7, 128.7, 124.2, 122.7, 117.4, 63.1, 62.4, 58.1, 53.3, 53.1, 45.6, 43.5, 40.7, 33.1, 24.0.

The spectroscopic data matched that reported in the literature.⁴

1-(1,2,3,3a,4,4a-hexahydro-5H-cyclopenta[2,3]cyclobuta[1,2-b]indol-5-yl)ethan-1-one (5c)



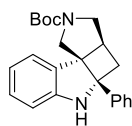
The **General Procedure 5** was applied using alkylated indole **4c** (11.4 mg), **2CzPN** (4 mol%), toluene (anhydrous) and irradiation with 455 nm for 19 h. Combination of two reactions and purification with flash column chromatography yielded **5c** as a white solid (22.5 mg, 99%).

^1H NMR (300 MHz, CDCl_3) δ (ppm) 8.27 (d, J = 8.1 Hz, 1H), 7.27 – 7.15 (m, 1H), 7.14 – 7.01 (m, 2H), 4.24 (dd, J = 6.9, 4.2 Hz, 1H), 2.80 – 2.66 (m, 1H), 2.33 (ddd, J = 13.5, 9.5, 4.2 Hz, 1H), 2.12 (s, 3H), 2.10 – 2.04 (m, 2H), 2.03 – 1.92 (m, 1H), 1.91 – 1.76 (m, 3H), 1.69 – 1.56 (m, 1H).

^{13}C NMR (75 MHz, CDCl_3) δ (ppm) 168.8, 144.9, 136.0, 128.1, 124.0, 122.3, 117.2, 62.4, 57.3, 45.0, 36.1, 33.5, 33.0, 26.1, 24.1.

The spectroscopic data matched that reported in the literature.²¹

tert-butyl 4a-phenyl-3a,4,4a,5-tetrahydro-1H-pyrrolo[3',4':2,3]cyclobuta[1,2-b]indole-2(3H) carboxylate (5d)



The **General Procedure 5** was applied using *tert*-butyl allyl((2-phenyl-1H-indol-3-yl)methyl)carbamate (18.1 mg), **2CzPN** (4 mol%), toluene (anhydrous) and irradiation with 455 nm for 24 h. Combination of three reactions and purification with flash column chromatography yielded **5d** as a clear oil (41.1 mg, 76%).

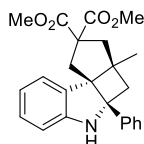
Signals of major rotamer:

¹H NMR (300 MHz, CDCl₃) δ (ppm) 7.39 – 7.24 (m, 5H), 7.10 (td, *J* = 7.7, 1.2 Hz, 1H), 7.00 (d, *J* = 6.9 Hz, 1H), 6.74 (t, *J* = 7.3 Hz, 1H), 6.67 (d, *J* = 7.8 Hz, 1H), 4.36 (s, 1H), 3.84 – 3.21 (m, 4H), 3.01 (q, *J* = 6.9 Hz, 1H), 2.87 – 2.52 (m, 2H), 1.46 (s, 3H), 1.27 (s, 6H).

¹³C NMR (75 MHz, CDCl₃) δ (ppm) 154.4, 152.9, 141.2, 128.7, 127.6, 126.5, 126.1, 122.8, 118.5, 108.4, 79.3, 70.9, 63.9, 51.7, 49.5, 43.8, 37.6, 28.6, 28.4.

The spectroscopic data matched that reported in the literature.⁴

Dimethyl -3a-methyl-4a-phenyl-3a,4,4a,5-tetrahydro-1*H*-cyclopenta[2,3]cyclobuta[1,2-*b*]indole-2,2(3*H*)-dicarboxylate (5e)



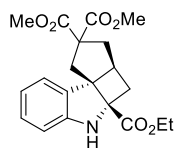
The **General Procedure 5** was applied using alkylated indole **4e** (19.6 mg), **2CzPN** (4 mol%), toluene (anhydrous) and irradiation with 455 nm for 24 h. Combination of two reactions and purification with flash column chromatography yielded **5e** as a pale-white solid (20.0 mg, 51%).

¹H NMR (300 MHz, CDCl₃) δ (ppm) 7.35 – 7.28 (m, 2H), 7.25 – 7.22 (m, 1H), 7.19 – 7.12 (m, 2H), 7.11 – 7.03 (m, 2H), 6.78 (td, *J* = 7.6, 1.0 Hz, 1H), 6.57 (dt, *J* = 7.4, 1.0 Hz, 1H), 4.13 (s, 1H), 3.70 (s, 3H), 3.21 (s, 3H), 3.09 (d, *J* = 13.0 Hz, 1H), 2.99 (d, *J* = 15.5 Hz, 1H), 2.77 (d, *J* = 13.9 Hz, 1H), 2.70 (d, *J* = 15.5 Hz, 1H), 2.17 (d, *J* = 13.0 Hz, 1H), 1.89 (d, *J* = 13.9 Hz, 1H), 0.99 (s, 3H).

¹³C NMR (75 MHz, CDCl₃) δ (ppm) 173.0, 171.9, 153.2, 142.5, 129.9, 128.6, 128.2, 127.5, 126.7, 124.1, 118.5, 108.3, 69.5, 67.4, 61.6, 53.1, 52.6, 48.6, 47.9, 42.5, 39.0, 24.4.

The spectroscopic data matched that reported in the literature.⁴

4a-ethyl 2,2-dimethyl-3a,4-dihydro-1H-cyclopenta[2,3]cyclobuta[1,2-b]indole-2,2,4a(3H,5H)-tricarboxylate (5f)



The **General Procedure 5** was applied using alkylated indole **4f** (18.7 mg), **2CzPN** (4 mol%), toluene (anhydrous) and irradiation with 455 nm for 24 h. Combination of two reactions and purification with flash column chromatography yielded **5f** as a transparent-white oil (28.3 mg, 76%).

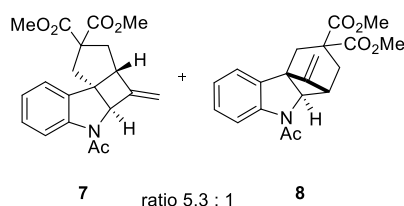
¹H NMR (300 MHz, CDCl₃) δ (ppm) 7.15 – 7.07 (m, 2H), 6.84 (td, $J = 7.6, 1.0$ Hz, 1H), 6.81 – 6.76 (m, 1H), 4.65 (s, 1H), 4.39 – 4.18 (m, 2H), 3.82 (s, 3H), 3.77 (s, 3H), 2.98 – 2.84 (m, 2H), 2.78 – 2.53 (m, 4H), 2.33 (dd, $J = 13.1, 8.7$ Hz, 1H), 1.34 (t, $J = 7.1$ Hz, 3H).

¹³C NMR (75 MHz, CDCl₃) δ (ppm) 173.0, 172.2, 171.7, 151.1, 134.4, 128.5, 123.4, 120.9, 112.2, 71.2, 66.5, 64.8, 62.1, 53.1, 52.9, 46.5, 43.1, 41.9, 37.7, 14.4.

The spectroscopic data matched that reported in the literature.⁴

2.4.4.3.3 Photocatalytic Cycloaddition of Allene-derivatives

Dimethyl-5-acetyl-4-methylene-3a,4,4a,5-tetrahydro-1H-cyclopenta[2,3]cyclobuta[1,2-b]indole-2,2(3H)-dicarboxylate (7)



The **General Procedure 5** was applied using alkylated indole **6** (17.8 mg), **2CzPN** (4 mol%), toluene and irradiation with 455 nm for 19 h. Combination of four reactions and purification with flash column chromatography yielded a mixture of **7 + 8** as a clear oil (70.5 mg, 99%).

HRMS (ESI⁺) (m/z): calculated for C₂₀H₂₂NO₅⁺ [M+H⁺]: 356.1492, found: 356.1495.

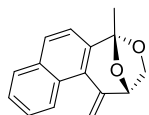
Only the peaks of the major product **7** are given:

¹H NMR (300 MHz, CDCl₃) δ (ppm) 8.28 (d, *J* = 8.1 Hz, 1H), 7.25 – 7.20 (m, 1H), 7.23 – 7.12 (m, 1H), 7.12 – 7.03 (m, 1H), 5.30 – 5.27 (m, 1H), 5.09 – 5.04 (m, 2H), 3.79 (s, 3H), 3.76 (s, 3H), 3.44 – 3.31 (m, 1H), 3.02 (d, *J* = 14.3 Hz, 1H), 2.72 (dd, *J* = 14.0, 8.5 Hz, 1H), 2.65 – 2.53 (m, 1H), 2.50 – 2.42 (m, 1H), 2.26 (s, 3H).

¹³C NMR (75 MHz, CDCl₃) δ (ppm) 172.1, 171.8, 169.1, 149.8, 144.4, 133.8, 128.7, 124.2, 122.4, 117.7, 113.8, 68.8, 62.9, 56.9, 56.1, 53.3, 53.1, 41.6, 39.8, 24.8.

IR (neat): 2952, 1729, 1662, 1599, 1479, 1382, 1252, 1203, 1084, 1058, 972, 905, 805, 752 cm⁻¹.

5-methyl-1-methylene-1,2,3,5-tetrahydro-2,5-epoxynaphtho[2,1-c]oxepine (**10a**)



The **General Procedure 5** was applied using alkylated naphthol **9a** (23.8 mg, 0.1 mmol), **2CzPN** (2 mol%), chloroform (anhydrous) and irradiation with 455 nm for 16 h. Purification with flash column chromatography yielded **10a** as a white solid (14.6 mg, 61%).

HRMS (EI) (*m/z*): calculated for C₁₆H₁₄O₂ [*M*⁺]: 238.0988, found: 238.0985.

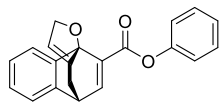
Melting Point: 116-119 °C

¹H NMR (300 MHz, CDCl₃) δ (ppm) 8.55 (dd, *J* = 8.0, 1.7 Hz, 1H), 7.91 – 7.70 (m, 2H), 7.57 – 7.42 (m, 3H), 5.94 (s, 1H), 5.57 (s, 1H), 5.14 (dd, *J* = 5.8, 1.5 Hz, 1H), 4.19 (dd, *J* = 7.3, 5.8 Hz, 1H), 3.78 (dd, *J* = 7.3, 1.5 Hz, 1H), 2.04 (s, 3H).

¹³C NMR (75 MHz, CDCl₃) δ (ppm) 143.3, 136.9, 134.1, 130.8, 129.0, 128.9, 126.9, 126.5, 125.9, 125.7, 121.1, 114.5, 106.2, 81.9, 69.7, 21.3.

IR (neat): 2940, 2993, 2885, 1625, 1587, 1509, 1461, 1394, 1341, 1274, 1241, 1215, 1099, 998, 909, 820 cm⁻¹.

Phenyl-4,5-dihydro-2H-5,9b-ethenonaphtho[1,2-b]furan-10-carboxylate (**11b**)



The **General Procedure 5** was applied using alkylated naphthol **9b** (31.6 mg, 0.1 mmol), **2CzPN** (2 mol%), chloroform (anhydrous) and irradiation with 455 nm for 16 h. Purification with flash column chromatography yielded **11b** as a white solid (25.7 mg, 81%).

HRMS (EI) (m/z): calculated for C₂₁H₁₆O₃ [M⁺]: 316.1094, found: 316.1086.

Melting Point: 141-144 °C

¹H NMR (300 MHz, CDCl₃) δ (ppm) 7.64 – 7.58 (m, 1H), 7.48 (d, *J* = 6.4 Hz, 1H), 7.41 – 7.32 (m, 2H), 7.30 – 7.17 (m, 4H), 7.16 – 7.09 (m, 2H), 5.48 (p, *J* = 1.8 Hz, 1H), 5.32 – 5.22 (m, 1H), 5.19 – 5.08 (m, 1H), 4.31 – 4.18 (m, 1H), 2.55 – 2.29 (m, 2H).

¹³C NMR (75 MHz, CDCl₃) δ (ppm) 161.8, 150.8, 144.0, 143.6, 141.0, 139.1, 138.8, 129.4, 126.4, 126.2, 125.8, 123.2, 121.9, 120.0, 114.4, 94.8, 80.1, 41.5, 28.3.

IR (neat): 2922, 2855, 1722, 1591, 1487, 1457, 1334, 1282, 1256, 1218, 1189, 1088, 1054, 1002, 939, 894, 861, 797, 745 cm⁻¹.

2.4.4.4 Large scale Reaction

Photochemical Set up

Gram-scale synthesis was performed with a custom-made Tauchschaftreaktor (University of Regensburg workshop), using water cooling and irradiation via 24 x 455 nm LEDs from the outside.

To the glass tube equipped with a magnetic stirring bar was added **2CzPN** (32.2 mg, 1 mol%) and **2c** (2.22 g, 7.00 mmol). The tube was degassed and refilled with nitrogen and chloroform (70 mL), which was degassed via three cycles of freeze-pump thaw in an extra Schlenk flask, was added via a syringe. The reaction mixture was irradiated for 19 h with 455 nm using the photochemical set up in Figure S2-6. Purification with flash column chromatography yielded **2c** as a white powder (2.04 g, 92%).

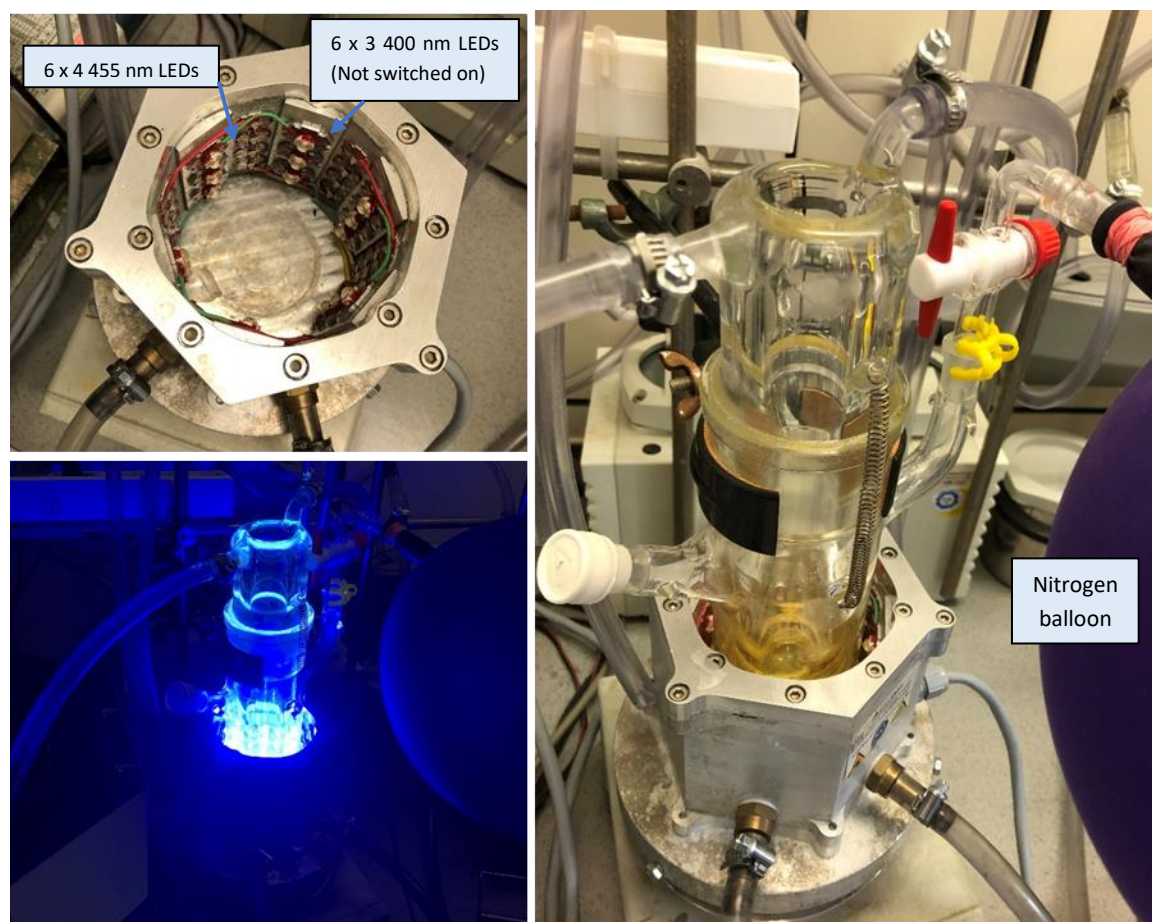
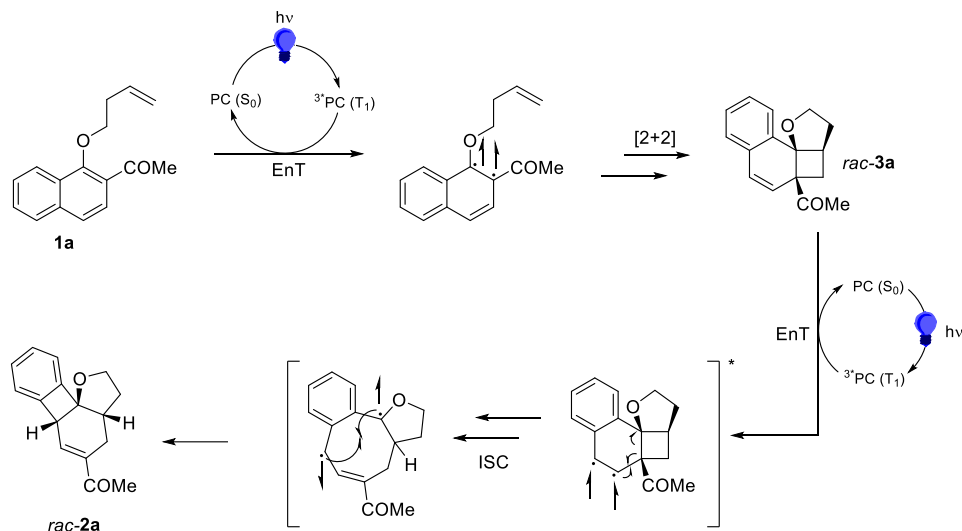


Figure S2-6: Photochemical setup for gram-scale reaction.

2.4.5 Previous Works and Mechanisms

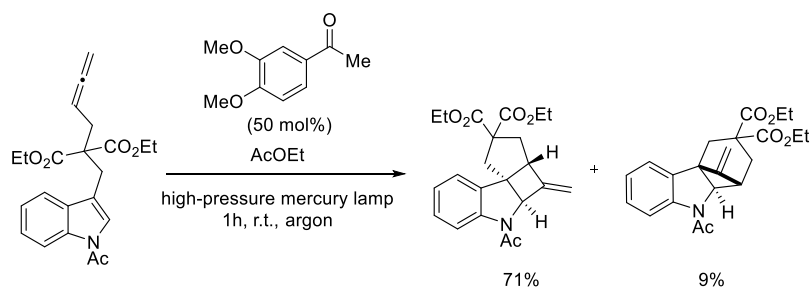
2.4.5.1 Dearomative Cycloaddition of Naphthol-derivatives



Scheme S2-2: Mechanism for the formation of **2a** via **3a** as proposed by Glorius et al.³

2.4.5.2 Dearomative Cycloaddition of Allene-substituted Indole-derivative

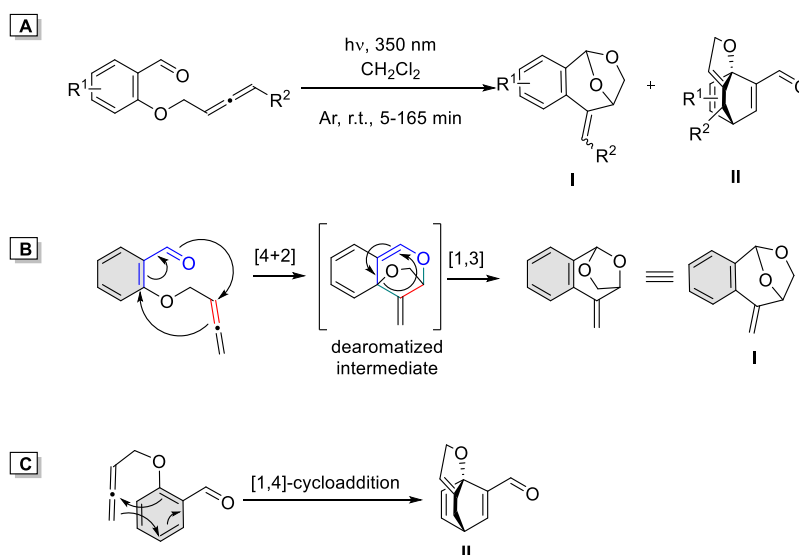
The following scheme depicts the existing work of Arai and Ohkuma.^{18e}



Scheme S2-3: Photosensitized formation of methylenecyclobutane-fused angular tetracyclic spiroindolines utilizing 50 mol% of 3',4'-dimethoxyacetophenone and a high-pressure mercury lamp.

2.4.5.3 (Dearomative) Cycloaddition of Allene-substituted Benzene-derivatives

The work of visible-light mediated and photosensitized allene-substituted naphthols was inspired by the photochemistry of allenyl salicylaldehydes^{18c} (Scheme S2-4). We believe that the products **10** and **11** are formed via a similar mechanism, but due to the triplet-excited nature of the naphthol we assume a biradical species operating, as proposed by Glorius (Scheme S2-2).



Scheme S2-4: Photochemistry of allenyl salicylaldehydes (**A**) and the mechanism for the formation of product **I** (**B**) and product **II** (**C**) as proposed by Bochet et al.^{18b,18c}

2.4.6 NMR-Spectra

The Supporting Information including NMR-spectra can be found online at:

<https://pubs.acs.org/doi/10.1021/acs.orglett.0c01622>

(https://pubs.acs.org/doi/suppl/10.1021/acs.orglett.0c01622/suppl_file/ol0c01622_si_001.pdf)

2.4.7 X-Ray Structures and Data

2.4.7.1 1-(3,3a,4,6a-Tetrahydro-2H-biphenyleno[8b,1-b]furan-5-yl)ethan-1-one (2a)

X-Ray data of this compound was first published by Glorius et al.³ The corresponding CCDC number is: [1831751](#). However, due to differences in the lattice system (presumably occurring from differences in recrystallization and temperature during data collection), it is reported here as well.

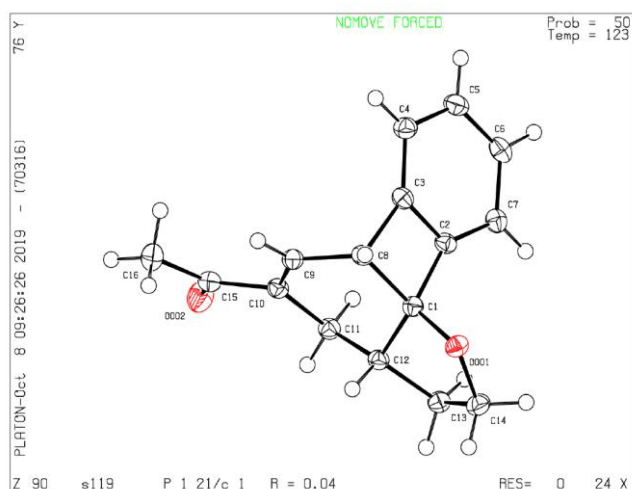


Figure S2-7: Crystal structure of compound **2a** (ellipsoids shown at 50% contour percent probability level)

Experimental. Single clear colourless prism-shaped crystals of **2a** were obtained by recrystallisation from EtOAc in Pentane. A suitable crystal $0.35 \times 0.21 \times 0.11$ mm³ was selected and mounted on a MITIGEN holder oil on an SuperNova, Single source at offset/far, Atlas diffractometer. The crystal was kept at a steady $T = 123.01(10)$ K during data collection. The structure was solved with the ShelXT²⁶ structure solution program using the Intrinsic Phasing solution method and by using Olex2²⁷ as the graphical interface. The model was refined with version 2018/3 of ShelXL²⁶ using Least Squares minimisation.

Crystal Data. C₁₆H₁₆O₂, $M_r = 240.29$, monoclinic, $P2_1/c$ (No. 14), $a = 5.19710(10)$ Å, $b = 10.2837(2)$ Å, $c = 22.6470(4)$ Å, $\beta = 90.241(2)^\circ$, $\alpha = \gamma = 90^\circ$, $V = 1210.37(4)$ Å³, $T = 123.01(10)$ K, $Z = 4$, $Z' = 1$, $\mu(\text{CuK}\alpha) = 0.680$, 8724 reflections measured, 2421 unique ($R_{int} = 0.0176$) which were used in all calculations. The final wR_2 was 0.0972 (all data) and R_1 was 0.0367 ($I > 2(I)$).

CCDC: [2000974](#)

Compound	2a
Formula	C ₁₆ H ₁₆ O ₂
$D_{calc.}/\text{g cm}^{-3}$	1.319
μ/mm^{-1}	0.680
Formula Weight	240.29
Colour	clear colourless
Shape	prism
Size/mm ³	$0.35 \times 0.21 \times 0.11$
T/K	123.01(10)
Crystal System	monoclinic
Space Group	$P2_1/c$
$a/\text{Å}$	5.19710(10)
$b/\text{Å}$	10.2837(2)
$c/\text{Å}$	22.6470(4)
$\alpha/^\circ$	90
$\beta/^\circ$	90.241(2)
$\gamma/^\circ$	90
$V/\text{Å}^3$	1210.37(4)
Z	4
Z'	1
Wavelength/Å	1.54184
Radiation type	CuK α
$\theta_{min}/^\circ$	3.904
$\theta_{max}/^\circ$	74.144
Measured Refl.	8724
Independent Refl.	2421
Reflections with $I > 2(I)$	2254
R_{int}	0.0176
Parameters	164
Restraints	0
Largest Peak	0.280
Deepest Hole	-0.210
Goof	1.056
wR_2 (all data)	0.0972
wR_2	0.0948
R_1 (all data)	0.0392
R_1	0.0367
Creation Method	
Solution	Olex2 1.2-alpha
Refinement	(compiled 2018.07.26 svn.r3523 for OlexSys, GUI svn.r5532)

2.4.7.2 Dimethyl-5-acetyl-3a,4,4a,5-tetrahydro-1*H*-cyclopenta[2,3]cyclobuta[1,2-*b*]indole-2,2(3*H*)-dicarboxylate (**5b**)

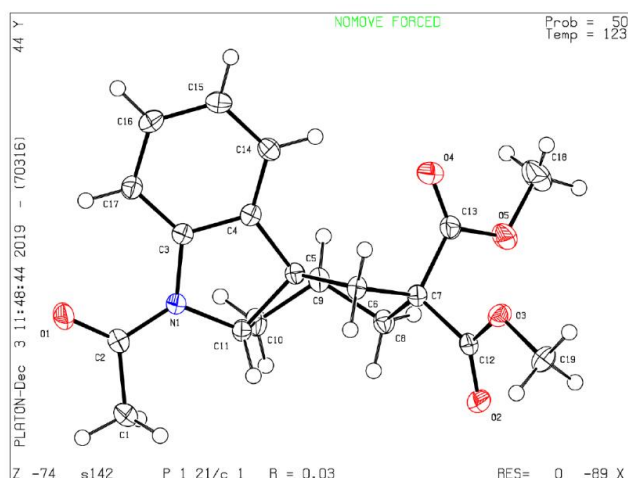


Figure S2-8: Crystal structure of compound **5b** (ellipsoids shown at 50% contour percent probability level)

Experimental. Single clear colourless prism crystals of **5b** were used as supplied. A suitable crystal with dimensions $0.20 \times 0.16 \times 0.12$ mm³ was selected and mounted on a MITIGEN holder oil on a SuperNova, Single source at offset/far, Atlas diffractometer. The crystal was kept at a steady $T = 123.01(10)$ K during data collection. The structure was solved with the ShelXT²⁶ solution program using dual methods. The model was refined with ShelXL 2018/3²⁶ using full matrix least squares minimisation on F^2 .

Crystal Data. C₁₉H₂₁NO₅, $M_r = 343.37$, monoclinic, $P2_1/c$ (No. 14), $a = 8.02106(12)$ Å, $b = 19.1796(2)$ Å, $c = 11.27263(16)$ Å, $\beta = 102.2439(14)^\circ$, $\alpha = \gamma = 90^\circ$, $V = 1694.75(4)$ Å³, $T = 123.01(10)$ K, $Z = 4$, $Z' = 1$, $\mu(\text{Cu } K\alpha) = 0.806$, 20072 reflections measured, 3486 unique ($R_{int} = 0.0203$) which were used in all calculations. The final wR_2 was 0.0868 (all data) and R_1 was 0.0338 ($I > 2(I)$).

CCDC: 1998663

Compound	5b
Formula	C ₁₉ H ₂₁ NO ₅
$D_{calc.}/\text{g cm}^{-3}$	1.346
μ/mm^{-1}	0.806
Formula Weight	343.37
Colour	clear colourless
Shape	prism
Size/mm ³	0.20×0.16×0.12
T/K	123.01(10)
Crystal System	monoclinic
Space Group	$P2_1/c$
$a/\text{Å}$	8.02106(12)
$b/\text{Å}$	19.1796(2)
$c/\text{Å}$	11.27263(16)
$\alpha/^\circ$	90
$\beta/^\circ$	102.2439(14)
$\gamma/^\circ$	90
$V/\text{Å}^3$	1694.75(4)
Z	4
Z'	1
Wavelength/Å	1.54184
Radiation type	Cu $K\alpha$
$\theta_{min}/^\circ$	4.611
$\theta_{max}/^\circ$	76.173
Measured Refl's.	20072
Ind't Refl's	3486
Refl's with $I > 2(I)$	3244
R_{int}	0.0203
Parameters	229
Restraints	0
Largest Peak	0.302
Deepest Hole	-0.179
GooF	1.037
wR_2 (all data)	0.0868
wR_2	0.0848
R_1 (all data)	0.0362
R_1	0.0338

2.4.7.3 5-methyl-1-methylene-1,2,3,5-tetrahydro-2,5-epoxynaphtho[2,1-c]oxepine (10a)

10a was recrystallized from DCM In Pentane

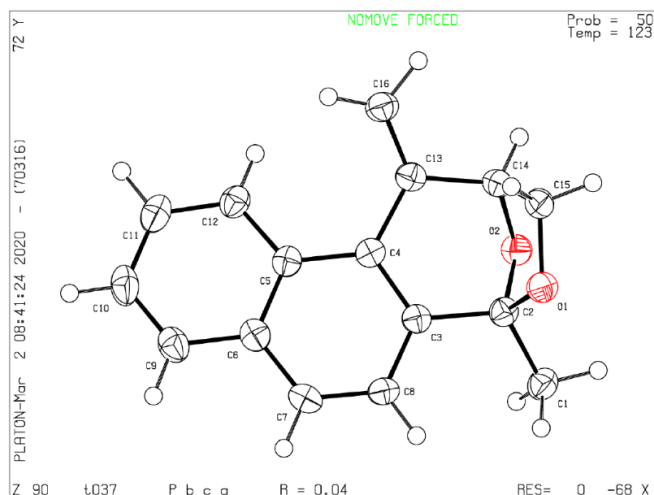


Figure S2-9: Crystal structure of compound **10a** (ellipsoids shown at 50% contour percent probability level)

Experimental. Single clear colourless irregular crystals of **10a** were used as supplied. A suitable crystal with dimensions $0.24 \times 0.12 \times 0.10 \text{ mm}^3$ was selected and mounted on a MITIGEN holder oil on a GV1000, TitanS2 diffractometer. The crystal was kept at a steady $T = 122.99(10) \text{ K}$ during data collection. The structure was solved with the ShelXT 2018/2²⁶ solution program using dual methods and by using Olex2²⁷ as the graphical interface. The model was refined with ShelXL 2018/3²⁶ using full matrix least squares minimisation on F^2 .

Crystal Data. $\text{C}_{16}\text{H}_{14}\text{O}_2$, $M_r = 238.27$, orthorhombic, $Pbca$ (No. 61), $a = 15.9520(4) \text{ \AA}$, $b = 7.5577(2) \text{ \AA}$, $c = 19.3357(5) \text{ \AA}$, $\alpha = \beta = \gamma = 90^\circ$, $V = 2331.12(10) \text{ \AA}^3$, $T = 122.99(10) \text{ K}$, $Z = 8$, $Z' = 1$, $\mu(\text{Cu K}\beta) = 0.512$, 12150 reflections measured, 2289 unique ($R_{int} = 0.0298$) which were used in all calculations. The final wR_2 was 0.0981 (all data) and R_1 was 0.0368 ($I > 2(I)$).

Compound	10a
Formula	$\text{C}_{16}\text{H}_{14}\text{O}_2$
$D_{calc.}/\text{g cm}^{-3}$	1.358
μ/mm^{-1}	0.512
Formula Weight	238.27
Colour	clear colourless
Shape	irregular
Size/ mm^3	$0.24 \times 0.12 \times 0.10$
T/K	122.99(10)
Crystal System	orthorhombic
Space Group	$Pbca$
$a/\text{\AA}$	15.9520(4)
$b/\text{\AA}$	7.5577(2)
$c/\text{\AA}$	19.3357(5)
$\alpha/^\circ$	90
$\beta/^\circ$	90
$\gamma/^\circ$	90
$V/\text{\AA}^3$	2331.12(10)
Z	8
Z'	1
Wavelength/ \AA	1.39222
Radiation type	Cu $K\beta$
$\theta_{min}/^\circ$	5.007
$\theta_{max}/^\circ$	59.827
Measured Refl's.	12150
Ind't Refl's	2289
Refl's with $I > 2(I)$	1927
R_{int}	0.0298
Parameters	219
Restraints	0
Largest Peak	0.293
Deepest Hole	-0.178
GooF	1.047
wR_2 (all data)	0.0981
wR_2	0.0920
R_1 (all data)	0.0462
R_1	0.0368

CCDC: 1998654

2.4.7.4 Phenyl-4,5-dihydro-2*H*-5,9*b*-ethenonaphtho[1,2-*b*]furan-10-carboxylate (**11b**)

11b was recrystallized from DCM in Pentane

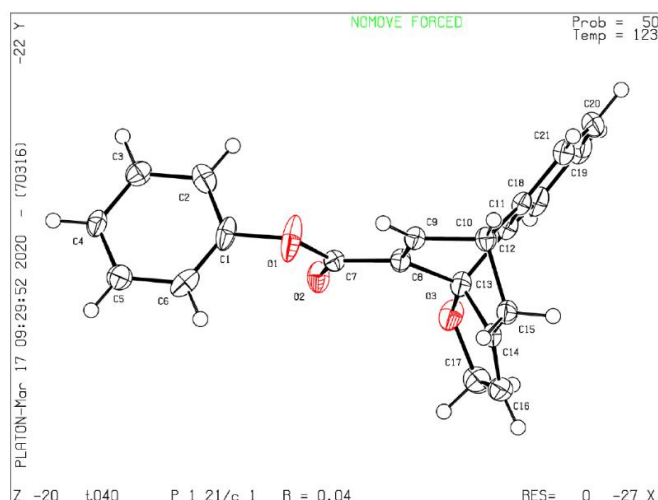


Figure S2-10: Crystal structure of compound **11b** (ellipsoids shown at 50% contour percent probability level)

Experimental. Single clear colourless plate crystals of **11b** were used as supplied. A suitable crystal with dimensions $0.31 \times 0.21 \times 0.11 \text{ mm}^3$ was selected and mounted on a MITIGEN holder oil on a SuperNova, Single source at offset/far, Atlas diffractometer. The crystal was kept at a steady $T = 123.00(10) \text{ K}$ during data collection. The structure was solved with the ShelXT²⁶ solution program using dual methods and by using Olex2²⁷ as the graphical interface. The model was refined with ShelXL 2018/3²⁶ using full matrix least squares minimisation on F^2 .

Crystal Data. $\text{C}_{21}\text{H}_{16}\text{O}_3$, $M_r = 316.34$, monoclinic, $P2_1/c$ (No. 14), $a = 17.2986(3) \text{ \AA}$, $b = 7.62192(14) \text{ \AA}$, $c = 11.5539(2) \text{ \AA}$, $\beta = 94.9094(18)^\circ$, $\alpha = \gamma = 90^\circ$, $V = 1517.78(5) \text{ \AA}^3$, $T = 123.00(10) \text{ K}$, $Z = 4$, $Z' = 1$, $\mu(\text{Cu K}\alpha) = 0.741$, 17711 reflections measured, 3011 unique ($R_{int} = 0.0274$) which were used in all calculations. The final wR_2 was 0.1040 (all data) and R_1 was 0.0401 ($I > 2(I)$).

CCDC: 1998653

Compound	11b
Formula	$\text{C}_{21}\text{H}_{16}\text{O}_3$
$D_{calc.}/\text{g cm}^{-3}$	1.384
μ/mm^{-1}	0.741
Formula Weight	316.34
Colour	clear colourless
Shape	plate
Size/ mm^3	$0.31 \times 0.21 \times 0.11$
T/K	123.00(10)
Crystal System	monoclinic
Space Group	$P2_1/c$
$a/\text{\AA}$	17.2986(3)
$b/\text{\AA}$	7.62192(14)
$c/\text{\AA}$	11.5539(2)
$\alpha/^\circ$	90
$\beta/^\circ$	94.9094(18)
$\gamma/^\circ$	90
$V/\text{\AA}^3$	1517.78(5)
Z	4
Z'	1
Wavelength/ \AA	1.54184
Radiation type	Cu $K\alpha$
$\theta_{min}/^\circ$	5.132
$\theta_{max}/^\circ$	72.898
Measured Refl's.	17711
Ind't Refl's	3011
Refl's with $I > 2(I)$	2741
R_{int}	0.0274
Parameters	217
Restraints	0
Largest Peak	0.462
Deepest Hole	-0.438
Goof	1.027
wR_2 (all data)	0.1040
wR_2	0.1010
R_1 (all data)	0.0440
R_1	0.0401

2.5 References

- [1] For a recent review on energy transfer mediated reactions, see: (a) Zhou, Q.-Q.; Zou, Y.-Q.; Lu, L.-Q.; Xiao, W.-J. Visible-Light Induced Organic Photochemical Reactions through Energy-Transfer Pathways. *Angew. Chem. Int. Ed.* **2019**, *58*, 1586-1604. For a tutorial review covering the principles and applications of energy transfer catalysis, see: (b) Strieth-Kalthoff, F.; James, M. J.; Teders, M.; Pitzer, L.; Glorius, F. Energy transfer catalysis mediated by visible light: principles, applications, directions. *Chem. Soc. Rev.* **2018**, *47*, 7190-7202.
- [2] For selected reviews, see: (a) Sarkar, D.; Bera, N.; Ghosh, S. [2+2] Photochemical Cycloaddition in Organic Synthesis. *Eur. J. Org. Chem.* **2020**, *2020*, 1310-1326. (b) Okumura, M.; Sarlah, D. Visible Light-Induced Dearomatizations. *Eur. J. Org. Chem.* **2020**, *2020*, 1259-1273. (c) Roche, S. P.; Porco, J. A. Dearomatization Strategies in the Synthesis of Complex Natural Products. *Angew. Chem. Int. Ed.* **2011**, *50*, 4068-4093.
- [3] James, M. J.; Schwarz, J. L.; Strieth-Kalthoff, F.; Wibbeling, B.; Glorius, F. Dearomative Cascade Photocatalysis: Divergent Synthesis through Catalyst Selective Energy Transfer. *J. Am. Chem. Soc.* **2018**, *140*, 8624-8628.
- [4] Zhu, M.; Zheng, C.; Zhang, X.; You, S.-L. Synthesis of Cyclobutane-Fused Angular Tetracyclic Spiroindolines via Visible Light-Promoted Intramolecular Dearomatization of Indole Derivatives. *J. Am. Chem. Soc.* **2019**, *141*, 2636-2644.
- [5] For a review covering natural cyclobutane-containing alkaloids, see (a) Dembitsky, V. M. Bioactive cyclobutane-containing alkaloids. *J. Nat. Med.* **2007**, *62*, 1-33. For selected reviews featuring the alternative synthesis of complex molecular scaffolds, see: (b) Zheng, C.; You, S.-L. Catalytic asymmetric dearomatization (CADA) reaction-enabled total synthesis of indole-based natural products. *Nat. Prod. Rep.* **2019**, *36*, 1589-1605. (c) Sebren, L. J.; Devery, J. J.; Stephenson, C. R. J. Catalytic Radical Domino Reactions in Organic Synthesis. *ACS Catal.* **2014**, *4*, 703-716. (d) Pape, A. R.; Kaliappan, K. P.; Kündig, E. P. Transition-Metal-Mediated Dearomatization Reactions. *Chem. Rev.* **2000**, *100*, 2917-2940. For selected papers featuring natural products related to the scaffolds accessed by energy transfer catalysis, see: (e) Hara, H.; Maruyama, N.; Yamashita, S.; Hayashi, Y.; Lee, K. H.; Bastow, K. F.; Marumoto, C. R.; Imakura, Y. Elecanacin, a Novel New Naphthoquinone from the Bulb of *Eleutherine americana*. *Chem. Pharm. Bull.* **1997**, *45*, 1714-1716. (f) Jamart-Grégoire, B.; Fort, Y.; Zouaoui, M. A.; Caubère, P. Efficient Synthesis of New Benzocyclobutenic Phenethylamines. *Synth. Commun.* **1993**, *23*, 885-894.

- (g) Carre, M. C.; Youlassani, A.; Caubere, P.; Saint-Aubin-Floch, A.; Blanc, M.; Advenier, C. Synthesis of a Novel Series of (Aryloxy)propanolamines: New Selective Beta 2-blocking Agents. *J. Med. Chem.* **1984**, *27*, 792-799.
- [6] For selected reviews, see: (a) Poplata, S.; Tröster, A.; Zou, Y.-Q.; Bach, T. Recent Advances in the Synthesis of Cyclobutanes by Olefin [2+2] Photocycloaddition Reactions. *Chem. Rev.* **2016**, *116*, 9748-9815. (b) Yoon, T. P.; Ischay, M. A.; Du, J. Visible light photocatalysis as a greener approach to photochemical synthesis. *Nat. Chem.* **2010**, *2*, 527-532. (c) Hoffmann, N. Photochemical Cycloaddition between Benzene Derivatives and Alkenes. *Synthesis* **2004**, *4*, 481-495. (d) Bach, T. Stereoselective Intermolecular [2+2]-Photocycloaddition Reactions and Their Application in Synthesis. *Synthesis* **1998**, *1998*, 683-705. (e) Fleming, S. A.; Bradford, C. L.; Gao, J. J. Regioselective and Stereoselective [2+2] Photocycloadditions. In *Organic Photochemistry, Molecular and Supramolecular Photochemistry*; Ramamurthy, V., Schanze, K. S., Eds.; Dekker: New York, 1997; Vol. 1, p 187. (f) Crimmins, M. T.; Reinhold, T. L. Enone Olefin [2+2] Photochemical Cycloadditions. *Org. React.* **1993**, *44*, 297. (g) Bauslaugh, P. G. Photochemical Cycloaddition Reactions of Enones to Alkenes; Synthetic Applications. *Synthesis* **1970**, *1970*, 287-300. For an example of a UV-light induced dearomatization of naphthol derivatives, see: (h) Wagner, P. J. Photoinduced Ortho [2+2] Cycloaddition of Double Bonds to Triplet Benzenes. *Acc. Chem. Res.* **2001**, *34*, 1-8.
- [7] (a) Oderinde, M. S.; Mao, E.; Ramirez, A.; Pawluczyk, J.; Jorge, C.; Cornelius, L. A. M.; Kempson, J.; Vetrichelvan, M.; Pitchai, M.; Gupta, A.; Gupta, A. K.; Meanwell, N. A.; Mathur, A.; Dhar, T. G. M. Synthesis of Cyclobutane-Fused Tetracyclic Scaffolds via Visible-Light Photocatalysis for Building Molecular Complexity. *J. Am. Chem. Soc.* **2020**, *142*, 3094-3103. Recently, an example of gadolinium photocatalysis was published: (b) Ma, J.; Schäfers, F.; Daniliuc, C.; Bergander, K.; Strassert, C. A.; Glorius, F. Gadolinium Photocatalysis: Dearomatic [2+2] Cycloaddition/Ring-Expansion Sequence with Indoles. *Angew. Chem. Int. Ed.* **2020**, *59*, 2-9. For an example of rhodium-catalyzed dearomatization of benzofuranes and benzothiophenes, see: (c) Hu, N.; Jung, H.; Zheng, Y.; Lee, J.; Zhang, L.; Ullah, Z.; Xie, X.; Harms, K.; Baik, M.-H.; Meggers, E. Catalytic Asymmetric Dearomatization by Visible-Light-Activated [2+2] Photocycloaddition. *Angew. Chem. Int. Ed.* **2018**, *57*, 6242-6246. For an example of dearomatization of molecules with a lower degree of aromaticity utilizing an organic sensitizer, see: (d) Tröster, A.; Alonso, R.; Bauer, A.; Bach, T. Enantioselective Intermolecular [2+2] Photocycloaddition Reactions

of 2(1*H*)-Quinolones Induced by Visible Light Irradiation. *J. Am. Chem. Soc.* **2016**, *138*, 7808-7811.

- [8] For selected examples utilizing [Ir-F] as an energy transfer catalyst, see: (a) Becker, M. R.; Richardson, A. D.; Schindler, C. S. Functionalized azetidines via visible light-enabled aza Paternò-Büchi reactions. *Nat. Commun.* **2019**, *10*, 5095. (b) Soni, V. K.; Lee, S.; Kang, J.; Moon, Y. K.; Hwang, H. S.; You, Y.; Cho, E. J. Reactivity Tuning for Radical–Radical Cross-Coupling via Selective Photocatalytic Energy Transfer: Access to Amine Building Blocks. *ACS Catal.* **2019**, *9*, 10454-10463. (c) Patra, T.; Mukherjee, S.; Ma, J.; Strieth-Kalthoff, F.; Glorius, F. Visible-Light-Photosensitized Aryl and Alkyl Decarboxylative Functionalization Reactions. *Angew. Chem. Int. Ed.* **2019**, *58*, 10514-10520. (d) Ma, J.; Strieth-Kalthoff, F.; Dalton, T.; Freitag, M.; Schwarz, J. L.; Bergander, K.; Daniliuc, C.; Glorius, F. Direct Dearomatization of Pyridines via an Energy-Transfer-Catalyzed Intramolecular [4+2] Cycloaddition. *Chem.* **2019**, *5*, 2854-2864. (e) Chatterjee, A.; König, B. Birch-Type Photoreduction of Arenes and Heteroarenes by Sensitized Electron Transfer. *Angew. Chem. Int. Ed.* **2019**, *58*, 14289-14294. (f) Teders, M.; Henkel, C.; Anhäuser, L.; Strieth-Kalthoff, F.; Gómez-Suárez, A.; Kleinmans, R.; Kahnt, A.; Rentmeister, A.; Guldi, D.; Glorius, F. The energy-transfer-enabled biocompatible disulfide-ene reaction. *Nat. Chem.* **2018**, *10*, 981-988. (g) Sun, Z.; Kumagai, N.; Shibasaki, M. Photocatalytic α -Acylation of Ethers. *Org. Lett.* **2017**, *19*, 3727-3730. (h) Bagal, D. B.; Park, S.-W.; Song, H.-J.; Chang, S. Visible light sensitization of benzoyl azides: cascade cyclization toward oxindoles via a non-nitrene pathway. *Chem. Commun.* **2017**, *53*, 8798-8801. (i) Pagire, S. K.; Hossain, A.; Traub, L.; Kerres, S.; Reiser, O. Photosensitized regioselective [2+2]-cycloaddition of cinnamates and related alkenes. *Chem. Commun.* **2017**, *53*, 12072-12075. (j) Zhao, J.; Brosmer, J. L.; Tang, Q.; Yang, Z.; Houk, K. N.; Diaconescu, P. L.; Kwon, O. Intramolecular Crossed [2+2] Photocycloaddition through Visible Light-Induced Energy Transfer. *J. Am. Chem. Soc.* **2017**, *139*, 9807-9810. (k) Heitz, D. R.; Tellis, J. C.; Molander, G. A. Photochemical Nickel-Catalyzed C-H Arylation: Synthetic Scope and Mechanistic Investigations. *J. Am. Chem. Soc.* **2016**, *138*, 12715-12718. (l) Xia, X.-D.; Ren, Y.-L.; Chen, J.-R.; Yu, X.-L.; Lu, L.-Q.; Zou, Y.-Q.; Wan, J.; Xiao, W.-J. Phototandem Catalysis: Efficient synthesis of 3-Ester-3-hydroxy-2-oxindoles by a Visible Light-Induced Cyclization of Diazoamides through an Aerobic Oxidation Sequence. *Chem. Asian J.* **2015**, *10*, 124-128. (m) Hurtley, A. E.; Lu, Z.; Yoon, T. P. [2+2] Cycloaddition of 1,3-Dienes by Visible Light Photocatalysis. *Angew. Chem. Int. Ed.* **2014**, *53*, 8991-8994. (n) Lu, Z.; Yoon, T. P. Visible Light Photocatalysis of [2+2] Styrene

- Cycloadditions by Energy Transfer. *Angew. Chem. Int. Ed.* **2012**, *51*, 10329-10332. For selected examples utilizing other iridium-based catalysts for energy transfer catalysis, see: (o) Nicasri, M. C.; Lehnerr, D.; Lam, Y.-H.; DiRocco, D. A.; Rovis, T. Synthesis of Sterically Hindered Primary Amines by Concurrent Tandem Photoredox Catalysis. *J. Am. Chem. Soc.* **2020**, *142*, 987-998. (p) Hörmann, F. M.; Chung, T. S.; Rodriguez, E.; Jakob, M.; Bach, T. Evidence for Triplet Sensitization in the Visible-Light-Induced [2+2] Photocycloaddition of Eniminium Ions. *Angew. Chem. Int. Ed.* **2018**, *57*, 827-831. (q) Zhu, S.; Pathigoolla, A.; Lowe, G.; Walsh, D. A.; Cooper, M.; Lewis, W.; Lam, H. W. Sulfonylative and Azidosulfonylative Cyclizations by Visible-Light-Photosensitization of Sulfonyl Azides in THF. *Chem. Eur. J.* **2017**, *23*, 17598-17604. (r) Skubi, K. L.; Kidd, J. B.; Jung, H.; Guzei, I. A.; Baik, M.-H.; Yoon, T. P. Enantioselective Excited-State Photoreactions Controlled by a Chiral Hydrogen-Bonding Iridium Sensitizer. *J. Am. Chem. Soc.* **2017**, *139*, 17186-17192. (s) Lei, T.; Zhou, C.; Huang, M.-Y.; Zhao, L.-M.; Yang, B.; Ye, C.; Xiao, H.; Meng, Q.-Y.; Ramamurthy, V.; Tung, C.-H.; Wu, L.-Z. General and Efficient Intermolecular [2+2] Photodimerization of Chalcones and Cinnamic Acid Derivatives in Solution through Visible-Light Catalysis. *Angew. Chem. Int. Ed.* **2017**, *56*, 15407-15410. (t) Scholz, S. O.; Farney, E. P.; Kim, S.; Bates, D. M.; Yoon, T. P. Spin-Selective Generation of Triplet Nitrenes: Olefin Aziridination through Visible-Light Photosensitization of Azidoformates. *Angew. Chem. Int. Ed.* **2016**, *55*, 2239-2242.
- [9] Triplet lifetime: $\tau = 2300$ ns; $E_T = 60.1$ kcal/mol, see: (a) Day, J. I.; Teegardin, K.; Weaver, J.; Chan, J. Advances in Photocatalysis: A Microreview of Visible Light Mediated Ruthenium and Iridium Catalyzed Organic Transformations. *Org. Process Res. Dev.* **2016**, *20*, 1156-1163. (b) Singh, A.; Teegardin, K.; Kelly, M.; Prasad, K. S.; Krishnan, S.; Weaver, J. D. Facile synthesis and complete characterization of homoleptic and heteroleptic cyclometalated Iridium(III) complexes for photocatalysis. *J. Organomet. Chem.* **2015**, *776*, 51-59. (c) Prier, C. K.; Rankic, D. A.; MacMillan, D. W. C. Visible Light Photoredox Catalysis with Transition Metal Complexes: Applications in Organic Synthesis. *Chem. Rev.* **2013**, *113*, 5322-5363. (d) Lowry, M. S.; Hudson, W. R.; Pascal, R. A.; Bernhard, S. Accelerated Luminophore Discovery through Combinatorial Synthesis. *J. Am. Chem. Soc.* **2004**, *126*, 14129-14135.
- [10] (a) Jespersen, D.; Keen, B.; Day, J. I.; Singh, A.; Briles, J.; Mullins, D.; Weaver, J. D. Solubility of Iridium and Ruthenium Organometallic Photoredox Catalysts. *Org. Process Res. Dev.*

- 2019**, *23*, 1087-1095. (b) Hans Wedepohl, K. The composition of the continental crust. *Geochim. Cosmochim. Acta* **1995**, *59*, 1217-1232.
- [11] (a) Hermann, J. C.; Chen, Y.; Wartchow, C.; Menke, J.; Gao, L.; Gleason, S. K.; Haynes, N.-E.; Scott, N.; Petersen, A.; Gabriel, S.; Vu, B.; George, K. M.; Narayanan, A.; Li, S. H.; Qian, H.; Beatini, N.; Niu, L.; Gan, Q.-F. Metal Impurities Cause False Positives in High Throughput Screening Campaigns. *ACS Med. Chem. Lett.* **2013**, *4*, 197-200. (b) Abernethy, D. R.; Destefano, A. J.; Cecil, T. L.; Zaidi, K.; Williams, R. L. Metal Impurities in Food and Drugs. *Pharm. Res.* **2010**, *27*, 750-755.
- [12] Recently, a few approaches focused on immobilizing the iridium catalyst on polymers to recycle the catalyst and make iridium catalysis more sustainable, underlining the need for alternatives: (a) Xu, Z.-Y.; Luo, Y.; Zhang, D.-W.; Wang, H.; Sun, X.-W.; Li, Z.-T. Iridium complex-linked porous organic polymers for recyclable, broad-scope photocatalysis of organic transformations. *Green Chem.* **2020**, *22*, 136-143. (b) Zhi, P.; Xi, Z.-W.; Wang, D.-Y.; Wang, W.; Liang, X.-Z.; Tao, F.-F.; Shen, R.-P.; Shen, Y.-M. Vilsmeier–Haack reagent mediated synthetic transformations with an immobilized iridium complex photoredox catalyst. *New J. Chem.* **2019**, *43*, 709-717.
- [13] Uoyama, H.; Goushi, K.; Shizu, K.; Nomura, H.; Adachi, C. Highly efficient organic light-emitting diodes from delayed fluorescence. *Nature* **2012**, *492*, 234-238.
- [14] For a summary of selected properties, see experimental part 2.4.2. For key references, see: (a) Lu, J.; Pattengale, B.; Liu, Q.; Yang, S.; Shi, W.; Li, S.; Huang, J.; Zhang, J. Donor-Acceptor Fluorophores for Energy-Transfer-Mediated Photocatalysis. *J. Am. Chem. Soc.* **2018**, *140*, 13719-13725. (b) Luo, J.; Zhang, J. Donor– Acceptor Fluorophores for Visible-Light-Promoted Organic Synthesis: Photoredox/Ni Dual Catalytic C(sp³)–C(sp²) Cross-Coupling. *ACS Catal.* **2016**, *6*, 873-877. (c) Lee, K.; Kim, D. Local-Excitation versus Charge-Transfer Characters in the Triplet State: Theoretical Insight into the Singlet–Triplet Energy Differences of Carbazolyl-Phthalonitrile-Based Thermally Activated Delayed Fluorescence Materials. *J. Phys. Chem. C* **2016**, *120*, 28330-28336. (d) Huang, S.; Zhang, Q.; Shiota, Y.; Nakagawa, T.; Kuwabara, K.; Yoshizawa, K.; Adachi, C. Computational Prediction for Singlet- and Triplet-Transition Energies of Charge-Transfer Compounds. *J. Chem. Theory Comput.* **2013**, *9*, 3872-3877. For a recent example of an organic sensitizer with a triplet energy lower than that of **2CzPN** used in a not-dearomative process, see: (e) Chen, D.-F.; Chrisman, C. H.; Miyake, G. M. Bromine Radical Catalysis by Energy Transfer Photosensitization. *ACS Catal.* **2020**, *10*, 2609-2614.

- [15] Zhang, Z.; Zhang, J.; Wu, B.; Li, X.; Chen, Y.; Huang, J.; Zhu, L.; Tian, H. Diarylethenes with a Narrow Singlet-Triplet Energy Gap Sensitizer: a Simple Strategy for Efficient Visible-Light Photochromism. *Adv. Opt. Mater.* **2018**, *6*, 1700847.
- [16] Iyer, A.; Clay, A.; Jockusch, S.; Sivaguru, J. Evaluating brominated thioxanthenes as organophotocatalysts. *J. Phys. Org. Chem.* **2017**, *30*, No. e3738.
- [17] Beesley, R. M.; Ingold, C. K.; Thorpe, J. F. The formation and stability of spiro-compounds. *J. Chem. Soc., Trans.* **1915**, *107*, 1080-1106.
- [18] For a review about photochemical cycloadditions of allenes, see: (a) Alcaide, B.; Almendros, P.; Aragoncillo, C. Exploiting [2+2] cycloaddition chemistry: achievements with allenes. *Chem. Soc. Rev.* **2010**, *39*, 783-816. For UV-light mediated dearomatic cycloaddition of allenes to salicylaldehydes, see: (b) Streit, U.; Birbaum, F.; Quattropani, A.; Bochet, C. G. Photocycloaddition of Arenes and Allenes. *J. Org. Chem.* **2013**, *78*, 6890-6910. (c) Birbaum, F.; Neels, A.; Bochet, C. G. Photochemistry of Allenyl Salicylaldehydes. *Org. Lett.* **2008**, *10*, 3175-3178. For triplet sensitized dearomatic cycloaddition of allenes to indoles, see: (d) Arai, N.; Ohkuma, T. Stereoselective preparation of methylenecyclobutane-fused angular tetracyclic spiroindolines via photosensitized intramolecular [2+2] cycloaddition with allene. *Tetrahedron Lett.* **2019**, *60*, 151252. (e) Arai, N.; Ohkuma, T. Stereoselective Construction of Methylenecyclobutane-Fused Indolines through Photosensitized [2+2] Cycloaddition of Allene-Tethered Indole Derivatives. *Org. Lett.* **2019**, *21*, 1506-1510. For a recent example of visible-light triplet sensitized allene chemistry, see: (f) Li, X.; Jandl, C.; Bach, T. Visible-Light-Mediated Enantioselective Photoreactions of 3-Alkylquinolones with 4-O-Tethered Alkenes and Allenes. *Org. Lett.* **2020**, *22*, 3618-3622.
- [19] Ishimatsu, R.; Matsunami, S.; Kasahara, T.; Mizuno, J.; Edura, T.; Adachi, C.; Nakano, K.; Imato, T. Electrogenenerated chemiluminescence of donor-acceptor molecules with thermally activated delayed fluorescence. *Angew. Chem. Int. Ed.* **2014**, *53*, 6993-6996.
- [20] Zhu, M.; Zhou, K.; Zhang, X.; You, S.-L. Visible-Light-Promoted Cascade Alkene Trifluoromethylation and Dearomatization of Indole Derivatives via Intermolecular Charge Transfer. *Org. Lett.* **2018**, *20*, 4379-4383.
- [21] Nandi, R. K.; Guillot, R.; Kouklovsky, C.; Vincent, G. Synthesis of 3,3-Spiroindolines via FeCl₃-Mediated Cyclization of Aryl- or Alkene-Containing 3-Substituted *N*-Ac Indoles. *Org. Lett.* **2016**, *18*, 1716-1719.

-
- [22] Li, S.-G.; Zard, S. Z. A convenient metal-free reagent for the generation and capture of trifluoromethanethiol. *Org. Lett.* **2013**, *15*, 5898-5901.
- [23] Bandini, M.; Eichholzer, A. Enantioselective gold-catalyzed allylic alkylation of indoles with alcohols. *Angew. Chem. Int. Ed.* **2009**, *48*, 9533-9537.
- [24] Youn, S. W.; Pastine, S. J.; Sames, D. Ru(III)-catalyzed cyclization of arene-alkene substrates via intramolecular electrophilic hydroarylation. *Org. Lett.* **2004**, *6*, 581-584.
- [25] Ananthan, S.; Saini, S. K.; Zhou, G.; Hobrath, J. V.; Padmalayam, I.; Zhai, L.; Bostwick, J. R.; Antonio, T.; Reith, M. E. A.; McDowell, S.; Cho, E.; McAleer, L.; Taylor, M.; Luedtke, R. R. Design, synthesis, and structure-activity relationship studies of a series of 4-(4-carboxamidobutyl)-1-arylpiperazines. *J. Med. Chem.* **2014**, *57*, 7042-7060.
- [26] (a) Sheldrick, G. M. Crystal structure refinement with *SHELXL*. *Acta Cryst. C* **2015**, *71*, 3-8.
(b) Sheldrick, G. M. *SHELXT* - Integrated space-group and crystal-structure determination. *Acta Cryst. A* **2015**, *71*, 3-8.
- [27] Dolomanov, O. V.; Bourhis, L. J.; Gildea, R. J.; Howard, J. A. K.; Puschmann, H. J. *OLEX2*: a complete structure solution, refinement and analysis program. *Appl. Cryst.* **2009**, *42*, 339-341.

3 Photocatalytic C–H Trifluoromethylthiolation by the Decatungstate Anion

This chapter has been published. Reprinted (adapted) with permission from:

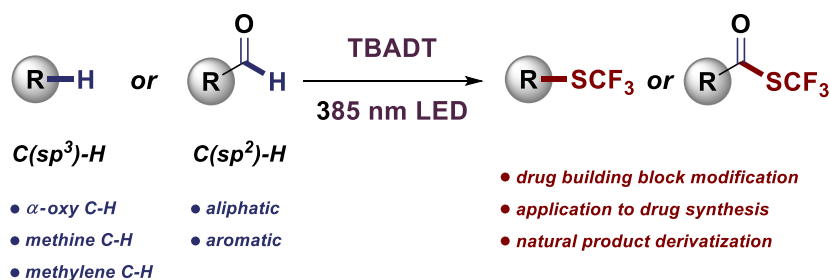
T. E. Schirmer†, A. B. Rolka†, T. A. Karl, F. Holzhausen, B. König, *Org. Lett.* **2021**, *23*, 5729-5733.

(†Authors contributed equally). Copyright 2021 American Chemical Society.

A. B. Rolka optimized the reaction conditions for alkoxy substrates, isolated compounds **2e-f**, **2m-q**, **2al**, **2am**, **3f**, **4f**, conducted the large-scale experiment, and synthesized respective starting materials. T. E. Schirmer optimized the reaction conditions for alkanes and aldehydes, contributed the compounds **2a-d**, **2g-2l**, **2r-2ak**, **2an**, **3l**, and synthesized respective starting materials. A. B. Rolka and T. E. Schirmer wrote the first draft, which was improved through suggestions from all authors. A. B. Rolka and T. E. Schirmer further wrote this work contribution statement. T. A. Karl synthesized the catalyst and helped to revise the manuscript. F. Holzhausen supported the isolation of thioesters during his internship under the supervision of T. E. Schirmer. X-ray crystallographic analysis was performed by the X-Ray structure analysis department of the University of Regensburg, particularly by B. Hischa. B. König supervised the project.

Abstract

A broadly applicable method for the trifluoromethylthiolation of methylene C(sp³)-H, methine C(sp³)-H, α -oxygen C(sp³)-H, and formyl C(sp²)-H bonds is presented using the decatungstate anion as the sole catalyst. By adjusting the substrate ratio and reaction concentration, this method was applied to 40 examples in good regioselectivities, including the derivatization of natural products. Furthermore, SCF₃-drug analogues were synthesized by subsequent functionalization of the SCF₃ products, highlighting the importance of this photocatalyzed C-H functionalization.



40 examples, up to 99% yield

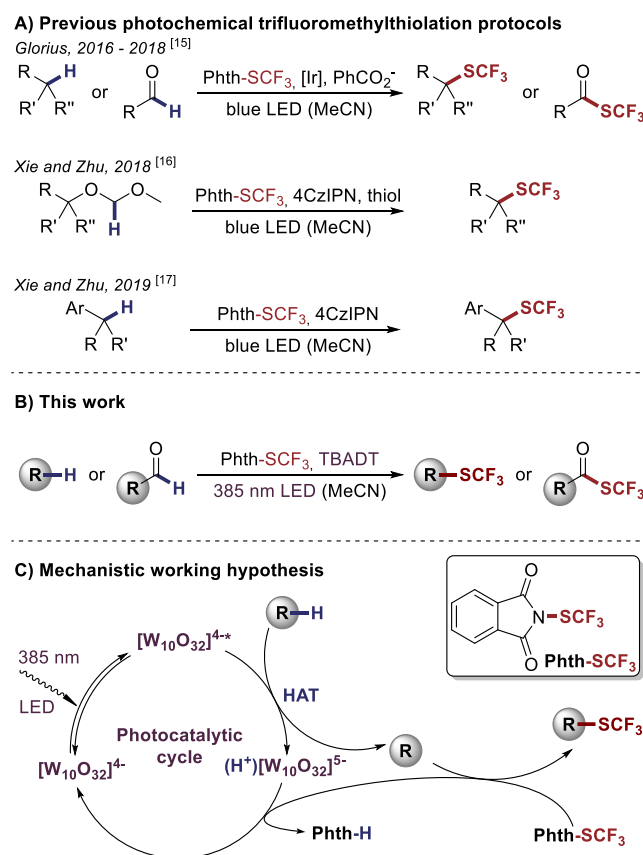
3.1 Introduction

Straightforward access to highly valuable products from abundant starting materials is a highly desirable and mutual goal for synthetic chemists across a multitude of disciplines. To this end, the activation of inert C–H bonds has gained significant attention in the field of chemistry over the past decades, as it represents a valuable tool for the functionalization of organic molecules with the potential for high atom and even higher step economy.¹

In recent years, the field of photoredox chemistry has spurred a multitude of novel hydrogen atom transfer (HAT) processes designed to facilitate such transformations. While significant success has been achieved, the vast majority of examples rely upon the functionalization of activated C–H bonds adjacent to heteroatoms or arenes.² The selective transformation of nonactivated bonds, on the other hand, is considerably more challenging due to the high bond dissociation energy of aliphatic C–H bonds coupled with the presence of only minor energetic differences between the multitude of similar C–H bonds typically present in a substrate of interest.³

Of particular focus in this field are catalysts that can serve a dual function and combine the roles of photocatalyst and HAT activation. In this context, the decatungstate anion (DT, $[W_{10}O_{32}]^{4-}$) has emerged as one of the most prominent examples of combined photo-HAT catalysts.⁴ This success has been heavily influenced by a remarkably fast HAT from C(sp³)–H centers.⁵ While advances have been made in the use of DT photo-HAT catalysis in the context of C–C,⁶ C–D,⁷ and C–F⁸ bond formation, the incorporation of the trifluoromethylthiol (–SCF₃) group by DT catalysis has thus far remained elusive.⁹ Such a development is highly desirable due to the increased application of the trifluoromethylthiol group in medicinal chemistry.¹⁰ This surge in interest results from the motif's significant electronegativity and particularly high lipophilicity (Hansch parameter of $\pi = 1.44$), which makes the SCF₃ group a powerful handle to both adjust pharmacokinetic properties and optimize interactions of an active compound with its target.¹¹ While the recent development of tailored reagents¹² has allowed for both polar¹³ and radical¹⁴ transformations for the incorporation of the SCF₃ group, use of HAT in this context is of particular interest due to its ability to selectively promote late-stage incorporation of the functionality with relatively high levels of chemoselectivity. The power of such a strategy has been demonstrated by the Glorius group using a dual catalytic system, consisting of an iridium photo- and benzoate HAT-catalyst for the selective trifluoromethylthiolation of methine and formyl C–H bonds (Scheme 3-1A).¹⁵ Xie and Zhu reported

a creative iteration of that approach to initiate the fragmentation of methoxymethyl ethers and thereby achieve deoxytrifluoromethylthiolation of tertiary alcohols.¹⁶ The same group then developed a protocol based on arene oxidation to achieve benzylic C–H trifluoromethylthiolation, which is interestingly enough not accessible via HAT catalysis.^{15b,17}



Scheme 3-1: (A) Photochemical trifluoromethylthiolation procedures reported in literature. (B) Novel DT-based trifluoromethylthiolation. (C) Mechanistic rationale behind the presented work.

Given the ongoing quest for novel trifluoromethylthiolation reactions,¹⁸ we envisioned being able to leverage the reactivity of the decatungstate anion to functionalize strong methylene- $\text{C}(\text{sp}^3)\text{-H}$, methine- $\text{C}(\text{sp}^3)\text{-H}$, and $\text{C}(\text{sp}^2)\text{-H}$ bonds with high selectivity (Scheme 3-1B). The development of operationally simple conditions coupled with the well-studied reactivity of the decatungstate anion and the use of a commercially available reagent would allow for widespread implementation of the procedure with a high level of predictability. Such a process would begin with the photoexcitation of DT, subsequent HAT from the substrate to the excited catalyst, and finally trapping of the radical by Munavalli's reagent (Phth-SCF_3)¹⁹ to yield the desired trifluoromethylthiolated product while regenerating the catalyst and forming phthalimide as the

side product through a formal electron and proton transfer from the reduced catalyst (Scheme 3-1C).

3.2 Results and discussion

We first focused our investigations of tetra-*n*-butylammonium decatungstate (TBADT)-catalyzed trifluoromethylthiolations on the optimization of nonactivated C(sp³)-H bonds, whose high bond dissociation energies create additional challenges in their functionalization. Using 2.0 eq. of cyclohexane (**1a**) as a model substrate (Table 3-1), 0.5 mol% TBADT, and Phth-SCF₃ as limiting reagent at a 0.1 mmol scale under irradiation with 385 nm LED light in dry MeCN resulted in a promising 61% crude NMR yield of the desired product **2a** (entry 1).

Table 3-1: Optimization and control reactions^a

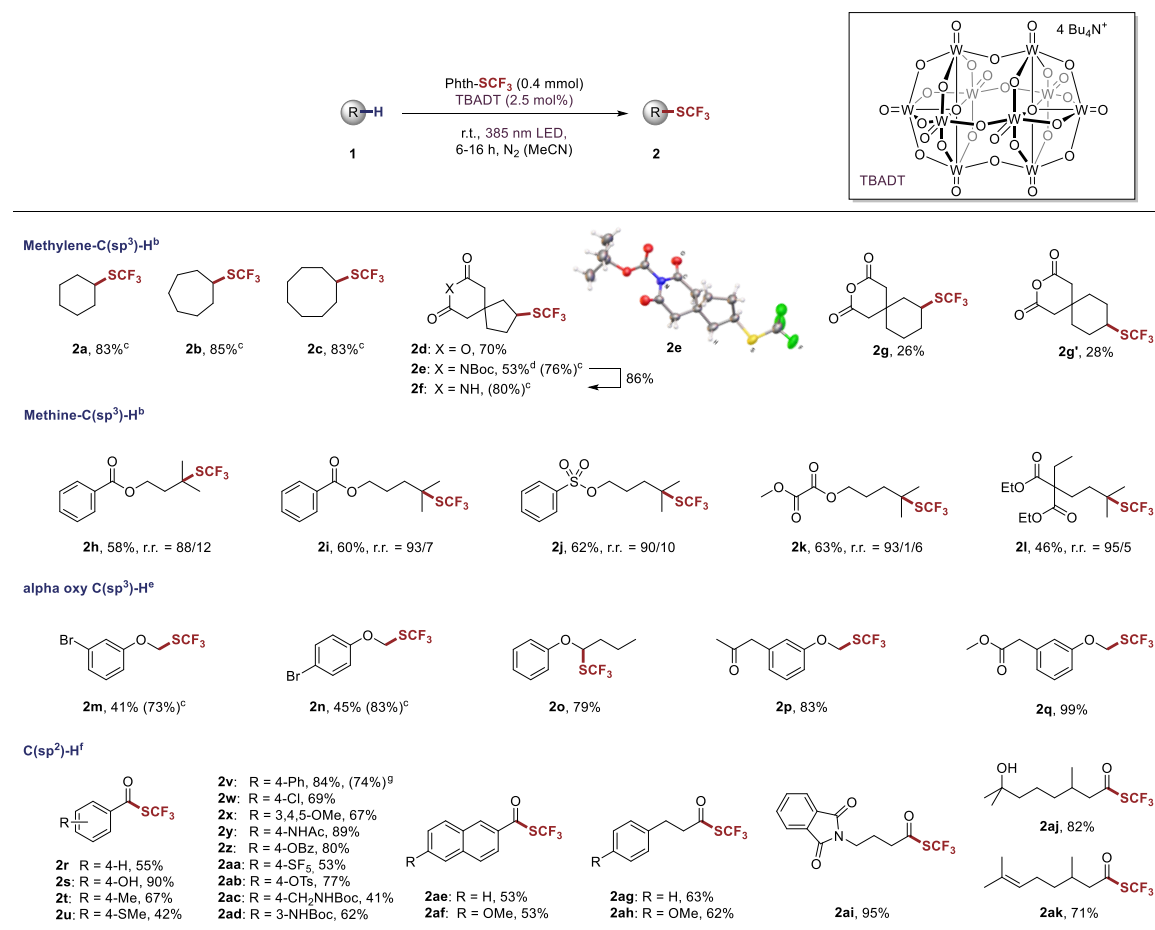
Entry	x (mol%)	y (mmol)	z (eq.)	Conc. (M)	Yield ^b (%)
1	0.5	0.1	2	0.1	61
2	1.0	0.1	2	0.1	66
3	2.5	0.1	2	0.1	67
4	5	0.1	2	0.1	69
5	5	0.1	5	0.1	82
6	5	0.1	5	0.2	88
7	5	0.4	5	0.2	85
8	2.5	0.4	5	0.2	83
9^c	2.5	0.4	5	0.2	n.d. ^e
10^{c,d}	2.5	0.4	5	0.2	n.d. ^e
11	-	0.4	5	0.2	n.d. ^e

^aReactions were run at the respective scales in anhydrous MeCN under irradiation with UV-LEDs (385 nm) and under a N₂-atmosphere for 16 h at 25 °C. ^bYield determined by ¹⁹F-crude NMR analysis with α,α,α-trifluorotoluene as internal standard. ^cNo light. ^dRun at 80 °C. ^en.d. = not detected.

Increasing the catalyst loading resulted in slightly higher yields (entries 1–4), while raising the equivalents of cyclohexane from 2 to 5 produced a significant boost in yield to 82% (entry 5). Halving both the catalyst loading and amount of solvent in order to hold catalyst concentration constant did not reduce the yield (entries 6–8). For practical considerations, the reaction scale was increased to 0.4 mmol for these reactions and all further experiments. With optimized reaction

conditions (entry 8), control experiments were run, which confirmed that the reaction requires both irradiation with light and the presence of TBADT. Based upon these results, we ruled out thermal and noncatalyzed reaction pathways (entries 9–11). For each class of substrate used in this report, a similar optimization could be carried out by adjusting only the reaction concentration and substrate-reagent ratio, allowing all other reaction conditions to remain constant (see the experimental part). Not surprisingly, C(sp³)–H bonds activated by an adjacent oxygen required a smaller excess of the substrate (2.5 eq.). In the case of aldehydes, the equivalents of substrate could be lowered even further to 1.5 eq. While an additional solvent screen for these activated substrates confirmed acetonitrile to be ideal, acetone was also a viable alternative (see the experimental part). With the ideal reaction conditions in hand for each class of C–H bond, the substrate scope was investigated (Table 3-2).

Table 3-2: Substrate scope of the decatungstate-catalyzed trifluoromethylthiolation^a



^aReactions were run at a 0.4 mmol scale in anhydrous MeCN (conc. = 0.2 M) under irradiation with UV-LEDs (385 nm) and under a N₂ atmosphere for 16 h at 25 °C. Isolated yields are given, if not stated otherwise. r.r. = regioisomeric ratio of isolated product ^b5.0 eq. of substrate was used. ^cDetermined by crude ¹⁹F NMR with α,α,α-trifluorotoluene as internal standard. ^d2.0 eq. of substrate was used. ^e2.5 eq. of ether substrate was used (conc. = 0.4 M). ^f1.5 eq. of aldehyde was used. Irradiation for 6 h. ^gPerformed at 1.2 mmol scale (see experimental part).

Challenging, strong C–H bonds in the form of both methylene and methine C(sp³)–H bonds were trifluoromethylthiolated in overall good to high yields. Selectivity in the reaction is driven both by steric accessibility and polarity matching that favors activation of the most hydridic bond present in the molecule.⁵ Compound **1g** represents an exception to this high selectivity, where two methylene positions possess similar steric and electronic environments. However, these two regioisomers **2g** and **2g'** could be separated by means of column chromatography, which gives access to two different trifluoromethylthiolated products. Additionally, the higher reactivity of spiro compound **2e** required only 2.0 eq. of substrate to obtain a high yield, and a single-crystal X-ray structure confirmed the molecular structure. Although spiro imide **2f** can be directly trifluoromethylthiolated in 80% ¹⁹F NMR yield, purification presented a challenge due to coelution of phthalimide. The isolation problem could be overcome by subjecting Boc-protected imide **2e** to the reaction conditions followed by a subsequent deprotection to obtain the free imide **2f**.

Next, we investigated activated α-oxy C(sp³)–H bonds and were delighted to achieve excellent yields of up to 99%. In several examples (**2m** and **2n**), separation of the product from the starting material via silica flash chromatography was not satisfactory, but pure material could be readily achieved via Kugelrohr distillation with slightly diminished yields. In these cases, we provide the product yields determined by ¹⁹F NMR before isolation and the isolated yields following distillation.

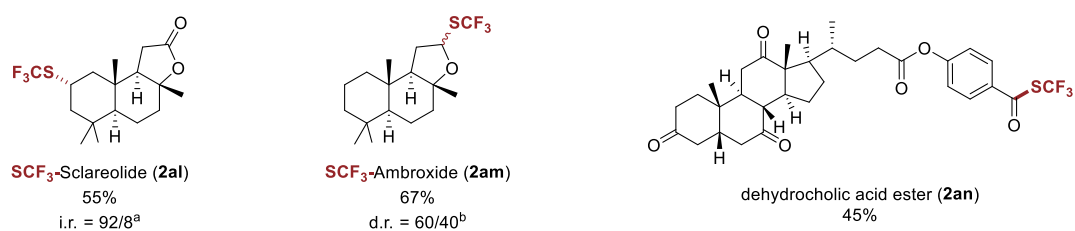
Last, the scope of formyl C–H activation for trifluoromethylthiolation was explored.^{15a,20} We were pleased to find that both aliphatic and aromatic aldehydes were functionalized in moderate to high yields. For aromatic aldehydes, electron-donating substituents on the aromatic ring increased the yield up to 90%, while electron-withdrawing groups were tolerated giving moderate to good yields (**2r–2ad**). The methodology can be upscaled to 1.2 mmol with only a minor decrease in yield of **2v**. Expanding the aromatic system to naphthaldehydes yielded the trifluoromethylthioester in slightly decreased yields (**2ae, 2af**). Aliphatic aldehydes worked equally well under the given reaction conditions (**2ag–2ai**).

To demonstrate the applicability of the method to the derivatization of natural products, several SCF₃-analogues were synthesized (Table 3-3A). The plant sesquiterpene lactone sclareolide (**1al**),²¹ representing the class of nonactivated C(sp³)–H bonds, was functionalized in 55% isolated yield (**2al**). The naturally occurring terpenoid ambroxide (**1am**), commonly used as a perfume

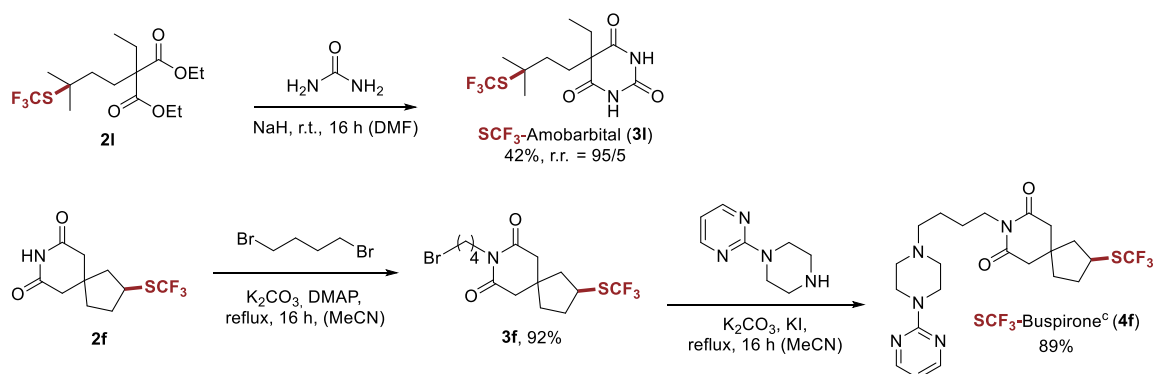
ingredient,²² contains an activated α -oxy $C(sp^3)$ -H bond, and its SCF_3 derivative (**2am**) was obtained in good yield with a d.r. of 1:1.5. Finally, the aldehyde moiety in the 4-hydroxybenzaldehyde ester of dehydrocholic acid (**1an**) could be trifluoromethylthiolated in 45% isolated yield (**2an**), presenting an application for the activation of $C(sp^2)$ -H bonds.

Table 3-3: Natural product derivatization and applications of the products as building blocks in the synthesis of drug derivatives

A) Natural product derivatization



B) Application of the products: Building blocks for drug synthesis



^ai.r. = isomeric ratio of isolated product. ^bd.r. = diastereomeric ratio of isolated product. ^c6% of *p*-chlorinated SCF_3 -bupirone was observed in the NMR spectrum of the final isolated product, presumably introduced by using deuterated chloroform during the measurement.

Furthermore, subsequent functionalization of the SCF_3 products **2l** and **2f** gave access to trifluoromethylthiol analogues of drug molecules (Table 3-3B). SCF_3 -amobarbital (**3l**), the SCF_3 derivative of the GABA receptor agonist,²³ is accessible in one step from malonate **2l** in 42% yield. We further showed that the SCF_3 analogue of bupirone - which is currently used to treat anxiety disorders - can be synthesized in two high-yielding steps (overall yield of 82%) from **2f**. The synthesis of SCF_3 -drug derivatives may be of interest in the context of recent investigations on the effect of SCF_3 groups in medicinal chemistry.^{11b}

3.3 Conclusion

In conclusion, we have shown that TBADT can be used as a catalyst in the photocatalyzed trifluoromethylthiolation of C–H bonds, eliminating the need for a dual catalytic system. Furthermore, we demonstrated the broad applicability of the method by functionalizing methine C(sp³)–H, methylene C(sp³)–H, α-oxy C(sp³)–H, and formyl C(sp²)–H groups by only adjusting the ratio of substrate to reagent and concentration, while all other reaction conditions remain unchanged. The method was applied to 40 examples and gave the products in good to excellent yields. We believe that the method will prove valuable in C–H functionalization and find applications in drug discovery by improving pharmacokinetics and target binding properties of SCF₃ drugs by providing an easy and generally applicable method for their synthesis.

3.4 Experimental part

3.4.1 General information

All NMR spectra were recorded at room temperature using one of the following devices: Bruker Avance 300 (300 MHz for ^1H , 75 MHz for ^{13}C , 282 MHz for ^{19}F), Bruker Avance 400 (400 MHz for ^1H , 100 MHz for ^{13}C , 376 MHz for ^{19}F). All chemical shifts are reported on the δ -scale in parts per million [ppm] (multiplicity, coupling constant J in Hertz [Hz], number of protons) relative to the solvent residual peaks as the internal standard.²⁴ Abbreviations used for signal multiplicity are br = broad, s = singlet, d = doublet, t = triplet, q = quartet, m = multiplet and combinations thereof.

High resolution mass spectra (HRMS) were obtained from the central analytic mass spectrometry department of the institute. The spectra were recorded on one of the following devices: Finnigan MAT 95, Thermo Quest Finnigan TSQ 7000, Finnigan MATSSQ 710 A or Agilent Q-TOF 6540 UHD. For GC-FID measurements a GC 7890 from Agilent Technologies was used, the analysis of the data was performed with Agilent ChemStation Rev.C.01.04.

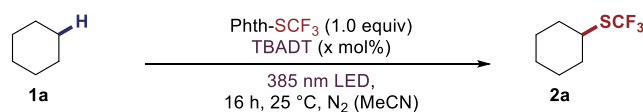
Analytical TLC was performed on silica gel coated alumina plates (MN TLC plates ALUGRAM[®] Xtra SIL G/UV254). Detection was done by UV light (254 or 366 nm). Infrared spectra were recorded neat on an Agilent Cary 630 FT-IR Spectrometer, melting points were measured in open capillary tubes by a Stanford Research System OptiMelt MPA 100 and are uncorrected. Compounds were purified by automated column chromatography with silica gel 60 M (40-63 μm , 230-440 mesh, Merck) on a Biotage[®] Isolera[™] Spektra One device. Trifluoromethylthiolation reactions were irradiated from the bottom (distance ca. 1 cm) with 385 nm LEDs (*Opulent Americas*, LST1-01G01-UV02-00, $\lambda = 385 \text{ nm}$, 3.4 V, 350 mA, 1.015 W light flux).

If not otherwise stated below, all chemicals and solvents were obtained from commercial sources. Specifically, Phth-SCF₃ was purchased from TCI Europe, dry acetonitrile was purchased from *Acros Organics* (Acetonitril, 99.9%, Extra Dry, over Molecular Sieve, AcroSeal[®]). Solid aldehydes were used as received; liquid ones were purified by distillation under reduced pressure prior use. Starting materials **1h**^{15b}, **1i**^{15b}, **1z**²⁵, **1ab**²⁶, **1ai**²⁷, **1an**²⁸ were synthesized according to literature procedures. The synthesis of relevant known (**1e**, **1l**) and unknown substrates (**1j**, **1k**) are outlined below.

3.4.2 General procedure for trifluoromethylthiolation

A crimp cap vial was charged with tetra-*n*-butylammonium decatungstate (TBADT, 33.2 mg, 0.01 mmol, 2.5 mol%), *N*-(trifluoromethylthio)phthalimide (Phth-SCF₃, 98.9 mg, 0.40 mmol, 1.0 eq.) solid substrate (2.00 mmol, 5.0 eq. for substrates with unactivated C(sp³)-H bonds; 1.00 mmol, 2.5 eq. for substrates with activated C(sp³)-H bonds; 0.60 mmol, 1.5 eq. for aldehydes) and a stirring bar. The vial was sealed, flushed with dried nitrogen (3x) before dry acetonitrile (1 mL for activated C(sp³)-H substrates, 2 mL for aldehydes and unactivated C(sp³)-H substrates) was added. At this point liquid substrates were added by syringe through the septum. The mixture was degassed by three *freeze-pump-backfill-thaw*-cycles and subsequently irradiated with LEDs (385 nm) for 16 h at 25 °C for C(sp³)-H substrates or 6 h for aldehyde substrates, respectively. The mixture was transferred into a round bottom flask and concentrated under reduced pressure. The residue was purified by automated column chromatography with indicated solvent mixtures.

3.4.3 Optimization of the reaction conditions and detailed procedures

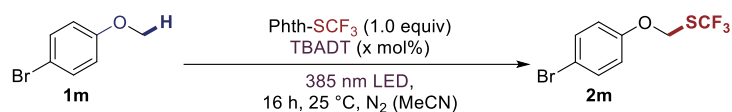
Table S3-1: Optimization for cyclohexane (**1a**)

Entry	TBADT (mol%)	1a (mmol)	Phth-SCF ₃ (mmol)	Conc. (M)	Yield (%)
1	0.5	0.2	0.1	0.1	61
2	1.0	0.2	0.1	0.1	66
3	2.5	0.2	0.1	0.1	67
4	5	0.2	0.1	0.1	69
5	5	0.5	0.1	0.1	82
6	5	0.5	0.1	0.2	88
7	5	2.0	0.4	0.2	85
8	2.5	2.0	0.4	0.2	83
9 ^a	2.5	2.0	0.4	0.2	n.d. ^c
10 ^{a,b}	2.5	2.0	0.4	0.2	n.d. ^c
11	-	2.0	0.4	0.2	n.d. ^c

Reactions were run at the respective scales in anhydrous MeCN under irradiation with UV-LEDs (385 nm) and under a N₂-atmosphere for 16 h at 25 °C. The yield was determined by ¹⁹F-crude NMR analysis with α,α,α -trifluorotoluene as internal standard. ^aNo light. ^bRun at 80 °C. ^cn.d. = not detected.

General Procedure A: A crimp cap vial was charged with tetra-*n*-butylammonium decatungstate (TBADT, 33.2 mg, 0.01 mmol, 2.5 mol%), *N*-(trifluoromethylthio)phthalimide (Phth-SCF₃, 98.9 mg, 0.40 mmol, 1.0 eq.) solid substrate (2.00 mmol, 5.0 eq.) and a stirring bar. The vial was sealed, flushed with dry nitrogen (3x) and charged with dry acetonitrile (2 mL, 0.2 M) and liquid substrates (2.00 mmol, 5.0 eq.). The mixture was degassed by three *freeze-pump-backfill-thaw*-cycles and subsequently irradiated with LEDs (385 nm) for 16 h at 25 °C. The mixture was transferred into a round bottom flask and concentrated under reduced pressure. The residue was purified by automated column chromatography with indicated solvent mixtures. Products, which are more polar than the phthalimide by-product might require a second chromatographic purification.

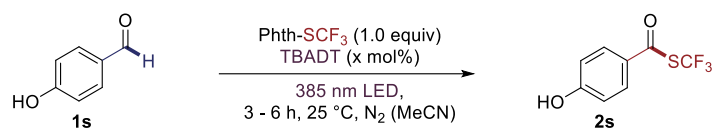
Please note: If the product was suspected to be volatile, the reaction was concentrated by passing a gentle stream of nitrogen through the vial, the residue was absorbed on silica and purified with pentane, diethylether or dichloromethane.

Table S3-2: Optimization for 4-bromoanisole (**1m**)

Entry	TBADT (mol%)	1m (mmol)	Phth-SCF ₃ (mmol)	Conc. (M)	Solvent	Yield (%)
1	2.5	0.2	0.13	0.13	PhCF ₃	n.d. ^c
2	2.5	0.2	0.13	0.13	DCE	traces
3	2.5	0.2	0.13	0.13	C ₆ D ₆	n.d. ^c
4	2.5	0.2	0.13	0.13	acetone	61
5	2.5	0.2	0.13	0.13	MeCN	62
6	2.5	0.2	0.13	0.2	MeCN	66
7	5	0.2	0.13	0.2	MeCN	66
8	2.5	0.6	0.4	0.4	MeCN	71
9	2.5	1.0	0.4	0.4	MeCN	83
10	2.5	2.0	0.4	0.4	MeCN	86
11 ^{a,b}	2.5	0.15	0.1	0.1	MeCN	n.d. ^c
12	-	0.15	0.1	0.1	MeCN	n.d. ^c

Reactions were run at the respective scales in anhydrous solvent under irradiation with UV-LEDs (385 nm) and under a N₂-atmosphere for 16 h at 25 °C. The yield was determined by ¹⁹F-crude NMR analysis with α,α,α -trifluorotoluene as internal standard. ^aNo light. ^bRun at 70 °C. ^cn.d. = not detected.

General Procedure B: A crimp cap vial was charged with tetra-*n*-butylammonium decatungstate (TBADT, 33.2 mg, 0.01 mmol, 2.5 mol%), *N*-(trifluoromethylthio)phthalimide (Phth-SCF₃, 98.9 mg, 0.40 mmol, 1.0 eq.) solid substrate (1.00 mmol, 2.5 eq.) and a stirring bar. The vial was sealed, flushed with dry nitrogen (3x) and charged with dry acetonitrile (1 mL, 0.4 M) and liquid substrates (2.00 mmol, 2.5 eq.). The mixture was degassed by three *freeze-pump-backfill-thaw*-cycles and subsequently irradiated with LEDs (385 nm) for 16 h at 25 °C. The mixture was transferred into a round bottom flask and concentrated under reduced pressure. The residue was purified by automated column chromatography with indicated solvent mixtures or distilled.

Table S3-3: Optimization for 4-hydroxybenzaldehyde (**2s**)

Entry	TBADT (mol%)	1s (mmol)	Phth-SCF ₃ (mmol)	Conc. (M)	Time (h)	Yield (%)
1	1	0.15	0.1	0.1	3	83
2	2.5	0.15	0.1	0.1	3	82
3	5	0.15	0.1	0.1	3	83
4	2.5	0.4	0.6	0.1	3	54
5	2.5	0.4	0.6	0.1	6	74
5	2.5	0.4	0.6	0.1	8	77
7	2.5	0.6	0.4	0.1	3	75
8	2.5	0.6	0.4	0.1	6	80
9	2.5	0.6	0.4	0.1	8	80
10	2.5	0.6	0.4	0.2	6	92
11	2.5	0.6	0.4	0.4	6	92
12 ^a	2.5	0.6	0.4	0.4	6	n.d. ^b
13	-	0.6	0.4	0.4	6	30

Reactions were run at the respective scales in anhydrous MeCN under irradiation with UV-LEDs (385 nm) and under a N₂-atmosphere for 3-6 h at 25 °C. The yield was determined by ¹⁹F-crude NMR analysis with α,α,α -trifluorotoluene as internal standard. ^aNo light. ^bn.d. = not detected.

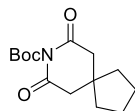
General Procedure C: A crimp cap vial was charged with tetra-*n*-butylammonium decatungstate (TBADT, 33.2 mg, 0.01 mmol, 2.5 mol%), *N*-(trifluoromethylthio)phthalimide (Phth-SCF₃, 98.9 mg, 0.40 mmol, 1.0 eq.) solid substrate (0.60 mmol, 1.5 eq.) and a stirring bar. The vial was sealed, flushed with dry nitrogen (3x) and charged with dry acetonitrile (2 mL, 0.2 M) and liquid substrates (0.60 mmol, 1.5 eq.). The mixture was degassed by three *freeze-pump-backfill-thaw*-cycles and subsequently irradiated with LEDs (385 nm) for 6 h at 25 °C. The mixture was transferred into a round bottom flask and concentrated under reduced pressure. The residue was purified by automated column chromatography with indicated solvent mixtures.

Please note: If the product was suspected to be volatile, the reaction was concentrated by passing a gentle stream of nitrogen through the vial, the residue was absorbed on silica and purified with pentane, diethylether or dichloromethane.

3.4.4 Experimental Procedures

3.4.4.1 Synthesis of starting materials

tert-butyl 7,9-dioxo-8-azaspiro[4.5]decane-8-carboxylate (1e)



Based on a literature reported procedure,²⁹ a Schlenk flask equipped with a magnetic stirring bar was charged with di-*tert*-butyl dicarbonate (2.4 g, 0.011 mol, 1.1 eq.) and DMAP (61 mg, 0.50 mmol, 5 mol%) in MeCN (10 mL) and was placed under a nitrogen atmosphere. To this mixture, a solution of tetramethylene glutarimide (1.7 g, 0.01 mol, 1.0 eq.) in MeCN (5 mL) was added at room temperature. The reaction mixture was stirred overnight and was then concentrated in vacuo. Afterwards, H₂O (15 mL) was added, and the aqueous layer was extracted with DCM (3 x 20 mL). The combined organics were washed with brine, dried over Na₂SO₄, filtered over Celite and finally the solvent was removed in vacuo. Purification by flash column chromatography (10-40% EtOAc in PE) yielded **1e** as a white solid (1.4 g, 5.2 mmol, 52%).

Melting Point: 99.7-101.6 °C.

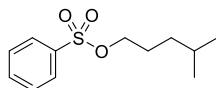
¹H NMR (400 MHz, CDCl₃) δ (ppm) 2.55 (s, 4H), 1.73 – 1.66 (m, 4H), 1.54 – 1.51 (m, 13H).

¹³C NMR (101 MHz, CDCl₃) δ (ppm) 169.9, 149.0, 86.2, 43.9, 40.1, 37.6, 27.5, 24.1.

HRMS (APCI⁺): calculated for C₁₄H₂₅N₂O₄ [M+NH₄⁺]: 285.1809, found: 285.1810.

IR (neat): 2967, 2870, 1781, 1722, 1684, 1356, 1244, 1140, 1058, 842 cm⁻¹.

4-methylpentyl benzenesulfonate (1j)



Adapting literature procedure for the benzylation of 4-methylpentanol,^{15b} a mixture of 4-methylpentan-1-ol (1.26 mL, 10.0 mmol, 1.0 eq.), 4-dimethylaminepyridine (244 mg, 2.00 mmol, 0.2 eq.) and Et₃N (2.09 mL, 15.0 mmol, 1.5 eq.) in DCM (50 mL) was cooled down to 0 °C (50 mL) and treated with benzenesulfonyl chloride (1.53 mL, 12.0 mmol, 1.2 eq.). The reaction mixture was stirred at room temperature overnight, quenched with water (50 mL), extracted with DCM (2 x 20 mL), dried over Na₂SO₄ and concentrated. The crude product was purified by column

chromatography (50 g SiO₂, PE/EA = 80/20 → 40/60) to afford the title compound as colourless oil (1.84 g, 7.59 mmol, 76%).

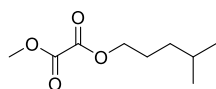
¹H NMR (400 MHz, CDCl₃) δ (ppm) 7.95 – 7.88 (m, 2H), 7.70 – 7.60 (m, 1H), 7.60 – 7.51 (m, 2H), 4.04 (t, *J* = 6.6 Hz, 2H), 1.70 – 1.58 (m, 2H), 1.53 – 1.42 (m, 1H), 1.22 – 1.12 (m, 2H), 0.83 (d, *J* = 6.6 Hz, 6H).

¹³C NMR (101 MHz, CDCl₃) δ (ppm) 136.5, 133.8, 129.4, 128.0, 71.4, 34.5, 27.6, 26.9, 22.5.

HRMS (ESI+): calculated for C₁₂H₁₉O₃S⁺ [M+H⁺]: 243.1049, found: 243.1051.

IR (neat): 2955, 2870, 1468, 1448, 1356, 1185, 1095, 954, 913, 752 cm⁻¹.

methyl (4-methylpentyl) oxalate (1k)



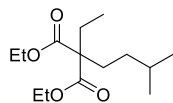
Adapting literature procedure for the benzylation of 4-methylpentanol,^{15b} a mixture of 4-methylpentan-1-ol (1.26 mL, 10.0 mmol, 1.0 eq.), 4-dimethylaminepyridine (244 mg, 2.00 mmol, 0.2 eq.) and Et₃N (2.09 mL, 15.0 mmol, 1.5 eq.) and treated with methyl 2-chloro-2-oxoacetate (1.10 mL, 12.0 mmol, 1.2 eq.). The reaction mixture was stirred at room temperature overnight, quenched with water (50 mL), extracted with DCM (2 x 20.0 mL), dried over Na₂SO₄ and concentrated. The crude product was purified by column chromatography (50 g SiO₂, PE/EA = 80/20 → 40/60) to afford the title compound as colourless oil (1.12 g, 5.95 mmol, 60%).

¹H NMR (400 MHz, CDCl₃) δ (ppm) 4.27 (t, *J* = 6.9 Hz, 2H), 3.90 (s, 3H), 1.79 – 1.67 (m, 2H), 1.65 – 1.49 (m, 1H), 1.30 – 1.20 (m, 2H), 0.89 (d, *J* = 6.6 Hz, 6H).

¹³C NMR (101 MHz, CDCl₃) δ (ppm) 158.4, 157.8, 67.7, 53.7, 34.8, 27.8, 26.3, 22.5.

HRMS (ESI+): calculated for C₉H₂₀NO₄⁺ [M+NH₄⁺]: 206.1387, found: 206.1384.

IR (neat): 2959, 2873, 1770, 1744, 1468, 1319, 1200, 1155, 957, 775 cm⁻¹.

diethyl 2-ethyl-2-isopentylmalonate (11)

Adapting literature procedure for the alkylation of 2-ethylmalonates,³⁰ diethyl 2-ethylmalonate (10.0 mmol, 1.88 g, 1.87 ml, 1.0 eq.) was dissolved in dry DMF (15 mL), cooled to 0 °C, treated with sodium hydride (60% dispersion in mineral oil, 479 mg, 12.0 mmol, 1.2 eq.) and stirred for 1.5 h. Then 1-bromo-3-methylbutane (12.0 mmol, 1.20 mL, 1.2 eq.) was added and the reaction was stirred overnight. The reaction was quenched by the addition of saturated aqueous NH₄Cl solution (50 mL) and the product was extracted with ether (3 x 25 mL). The combined organic phase was dried over Na₂SO₄ and concentrated. The crude product was purified by column chromatography (50 g SiO₂, PE/EA = 80/20 → 50/50) to afford the title compound as colourless oil (1.91 g, 7.39 mmol, 74%).

¹H NMR (300 MHz, CDCl₃) δ (ppm) 4.17 (q, *J* = 7.2 Hz, 4H), 1.97 – 1.80 (m, 4H), 1.56 – 1.44 (m, 1H), 1.23 (t, *J* = 7.1 Hz, 6H), 1.06 – 0.95 (m, 2H), 0.88 (d, *J* = 6.5 Hz, 6H), 0.80 (t, *J* = 7.5 Hz, 3H).

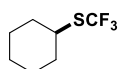
¹³C NMR (75 MHz, CDCl₃) δ (ppm) 172.1, 61.1, 58.0, 32.9, 29.4, 28.4, 25.0, 22.6, 14.3, 8.5.

HRMS (ESI+): calculated for C₁₄H₂₇O₄⁺ [M+H⁺]: 259.1904, found: 259.1904.

IR (neat): 2959, 2873, 1729, 1464, 1386, 1304, 1252, 1218, 1133, 1028 cm⁻¹.

3.4.4.2 Characterization and Synthesis of SCF₃-Products

cyclohexyl(trifluoromethyl)sulfane (2a)



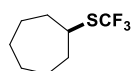
Following **Procedure A**, **2a** was obtained from cyclohexane (216 μ L, 2.00 mmol, 5.0 eq.) and Phth-SCF₃ (98.9 mg, 0.40 mmol, 1.0 eq.) in 83% NMR-Yield with trifluorotoluene as internal standard.

¹⁹F NMR (377 MHz, CD₃CN) δ (ppm) -38.5.

MS (EI, 70 eV): m/z (%) = 184 (19.8), 115 (11.7), 83 (100), 82 (21.8), 81 (8.9), 69 (17.4), 67 (24.2), 55 (81.7), 54 (12.1), 15 (9.1).

The data matches the one reported in literature.^{15b}

cycloheptyl(trifluoromethyl)sulfane (2b)



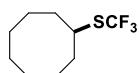
Following **Procedure A**, **2b** was obtained from cyclohexane (262 μ L, 2.00 mmol, 5.0 eq.) and Phth-SCF₃ (98.9 mg, 0.40 mmol, 1.0 eq.) in 85% NMR-Yield with trifluorotoluene as internal standard.

¹⁹F NMR (377 MHz, CD₃CN) δ (ppm) -39.1.

MS (EI, 70 eV): m/z (%) = 198 (1.7), 129 (42.7), 97 (81.9), 96 (11.7), 81 (22.9), 69 (23.9), 68 (11.7), 67 (24.8), 55 (100), 54 (13.5).

The data matches the one reported in literature.^{15b}

cyclooctyl(trifluoromethyl)sulfane (2c)



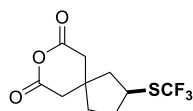
Following **Procedure A**, **2c** was obtained from cyclohexane (269 μ L, 2.00 mmol, 5.0 eq.) and Phth-SCF₃ (98.9 mg, 0.40 mmol, 1.0 eq.) in 83% NMR-Yield with trifluorotoluene as internal standard.

¹⁹F NMR (377 MHz, CD₃CN) δ (ppm) -39.0

MS (EI, 70 eV): m/z (%) = 212.1 (0.1), 143.1 (51.8), 128.0 (5.7), 111.1 (26.5), 82.1 (12.8), 81.1 (9.9), 69.1 (100), 67.1 (20.9), 55.1 (30.9), 41.1 (20.3), 39.0 (6.4).

The data matches the one reported in literature.^{18c,18d}

2-((trifluoromethyl)thio)-8-oxaspiro[4.5]decane-7,9-dione (**2d**)



Following **Procedure A**, **2d** was obtained from 8-oxaspiro[4.5]decane-7,9-dione (336 mg, 2.00 mmol, 5.0 eq.) and Phth-SCF₃ (98.9 mg, 0.40 mmol, 1.0 eq.) as colourless amorphous solid (75.3 mg, 0.28 mmol, 70%). The product was purified by automated column chromatography (*Biotage*[®] SNAP Ultra 25 g column, pentane/Et₂O = 80/20 → 20/80).

¹H NMR (400 MHz, CDCl₃) δ (ppm) 3.70 (p, J = 7.6 Hz, 1H), 2.82 – 2.75 (m, 2H), 2.71 (s, 2H), 2.43 – 2.27 (m, 1H), 2.18 (dd, J = 14.0, 7.9 Hz, 1H), 1.94 – 1.78 (m, 2H), 1.75 – 1.63 (m, 2H).

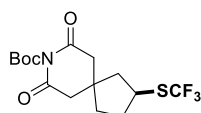
¹³C NMR (101 MHz, CDCl₃) δ (ppm) 165.4, 165.4, 130.5 (q, J = 306.8 Hz), 45.3, 42.6, 42.2, 41.1 (q, J = 1.8 Hz), 39.5, 36.6, 32.8.

¹⁹F NMR (377 MHz, CDCl₃) δ (ppm) -40.0.

HRMS (EI+): calculated for C₁₀H₁₁F₃O₃S⁺ [M^{+}]: 268.0376, found: 268.0376.

IR (neat): 2929, 2855, 1714, 1453, 1416, 1151, 1118 cm⁻¹.

tert-butyl 7,9-dioxo-2-((trifluoromethyl)thio)-8-azaspiro[4.5]decane-8-carboxylate (**2e**)



Following **Procedure A**, **2e** was obtained from *tert*-butyl 7,9-dioxo-8-azaspiro[4.5]decane-8-carboxylate (294 mg, 0.80 mmol, 2.0 eq.) and Phth-SCF₃ (98.9 mg, 0.40 mmol, 1.0 eq.) as colourless solid (78.0 mg, 0.21 mmol, 53%). The product was purified twice by automated column chromatography (*Biotage*[®] SNAP Ultra 25 g column, PE/EA = 90/10 → 80/20 and *Biotage*[®] Sfär Silica HC D 10 g column, P/Et₂O = 65/35). Tough separation of the product from phthalimide

caused the isolated yield to be significant lower compared to the ^{19}F NMR yield (76%) of the crude reaction with PhCF_3 as internal standard.

Melting Point: 122.4-125.1 °C.

^1H NMR (400 MHz, CDCl_3) δ (ppm) 3.68 (p, $J = 7.8$ Hz, 1H), 2.67 (s, 2H), 2.60 (s, 2H) 2.37 – 2.26 (m, 1H), 2.18 (dd, $J = 13.9, 7.9$ Hz, 1H), 1.90 – 1.78 (m, 2H), 1.67 (dd, $J = 13.5, 7.9$ Hz, 2H), 1.56 (s, 9H).

^{13}C NMR (101 MHz, CDCl_3) δ (ppm) 168.9, 148.6, 130.6 (q, $J = 306.5$ Hz), 86.7, 45.3, 44.5, 44.0, 41.1, 40.0, 36.6, 32.8, 27.6.

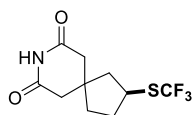
^{19}F NMR (376 MHz, CDCl_3) δ (ppm) -41.0.

HRMS (ESI+): calculated for $\text{C}_{15}\text{H}_{24}\text{F}_3\text{N}_2\text{O}_4\text{S}^+$ [$\text{M}+\text{NH}_4^+$]: 385.1403, found: 385.1409.

X-Ray Structure CCDC: 2046602.

IR (neat): 2959, 2926, 2855, 1766, 1729, 1692, 1461, 1244, 1107, 842 cm^{-1} .

2-((trifluoromethyl)thio)-8-azaspiro[4.5]decane-7,9-dione (**2f**)



tert-butyl 7,9-dioxo-2-((trifluoromethyl)thio)-8-azaspiro[4.5]decane-8-carboxylate (**2e**, 78.0 mg, 0.21 mmol) was dissolved in DCM (1 mL) and TFA (0.2 mL) was added. The solution was stirred for 2 h at room temperature until complete conversion as monitored by TLC. The solvent was evaporated, and the crude mixture was again redissolved in DCM and was washed with sat. NaHCO_3 solution (3x). Evaporation of the solvent yielded **2f** as a white solid (47.6 mg, 0.18 mmol, 86%).

Melting Point: 129.7-130.3 °C.

^1H NMR (400 MHz, CDCl_3) δ (ppm) 8.44 (s, 1H), 3.68 (p, $J = 7.7$ Hz, 1H), 2.63 (s, 2H), 2.56 (s, 2H), 2.37 – 2.26 (m, 1H), 2.17 (dd, $J = 13.9, 7.9$ Hz, 1H), 1.91 – 1.76 (m, 2H), 1.73 – 1.60 (m, 2H).

^{13}C NMR (101 MHz, CDCl_3) δ (ppm) 171.5, 130.6 (q, $J = 306.7$ Hz), 45.5, 44.4, 43.9, 41.1 (q, $J = 1.8$ Hz), 40.7, 36.8, 32.8.

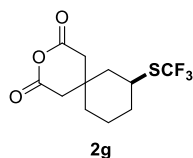
^{19}F NMR (376 MHz, CDCl_3) δ (ppm) -41.0.

HRMS (ESI+): calculated for $C_{10}H_{16}F_3N_2O_2S^+$ [$M+NH_4^+$]: 285.0879, found: 285.0878.

IR (neat): 3190, 3090, 2952, 2866, 1729, 1673, 1379, 1267, 1095, 849 cm^{-1} .

8-((trifluoromethyl)thio)-3-oxaspiro[5.5]undecane-2,4-dione (**2g**) and
9-((trifluoromethyl)thio)-3-oxaspiro[5.5]undecane-2,4-dione (**2g'**)

Following **Procedure A**, **2g** and **2g'** were obtained from 3-oxaspiro[5.5]undecane-2,4-dione (364 mg, 2.00 mmol, 5.0 eq.) and Phth-SCF₃ (98.9 mg, 0.40 mmol, 1.0 eq.) as colourless oil (**2g**, 28.9 mg, 0.10 mmol, 26%) and colourless solid (**2g'**, 31.5 mg, 0.11 mmol, 28 %), respectively. The products were purified by automated column chromatography twice (*Biotage*[®] *SNAP Ultra* 25 g column, P/Et₂O = 80/20 → 20/80 and *Biotage*[®] *Sfär Silica* 10 g column, P/Et₂O = 80/20 → 30/70).



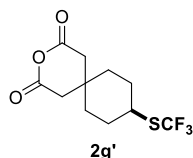
¹H NMR (400 MHz, CDCl₃) δ (ppm) 3.26 (tt, $J = 12.3, 3.9$ Hz, 1H), 2.87 (dd, $J = 17.3, 1.3$ Hz, 1H), 2.68 (d, 1H), 2.62 (s, 2H), 2.24 – 2.15 (m, 1H), 2.01 – 1.93 (m, 1H), 1.89 – 1.79 (m, 1H), 1.66 – 1.50 (m, 3H), 1.41 – 1.30 (m, 2H).

¹³C NMR (101 MHz, CDCl₃) δ (ppm) 165.2, 165.2, 130.7 (q, $J = 306.9$ Hz), 44.6, 43.5, 39.0, 38.3, 34.3, 33.8, 32.8, 21.4.

¹⁹F NMR (376 MHz, CDCl₃) δ (ppm) -39.3.

HRMS (EI+): calculated for $C_{11}H_{13}F_3O_3S^{*+}$ [M^{*+}]: 282.0532, found: 282.05235.

IR (neat): 2937, 2870, 1703, 1446, 1408, 1293, 1215, 1110, 928 cm^{-1} .



¹H NMR (400 MHz, CDCl₃) δ (ppm) 3.28 (ddt, $J = 13.0, 8.6, 3.4$ Hz, 1H), 2.73 (d, $J = 1.2$ Hz, 2H), 2.62 (d, $J = 1.2$ Hz, 2H), 2.12 – 2.03 (m, 2H), 1.75 – 1.61 (m, 4H), 1.57 – 1.46 (m, 2H).

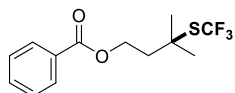
¹³C NMR (101 MHz, CDCl₃) δ (ppm) 165.6, 165.5, 130.9 (q, $J = 306.5$ Hz), 42.9, 42.0, 39.4, 34.6, 31.6, 28.4.

^{19}F NMR (376 MHz, CDCl_3) δ (ppm) -39.6.

HRMS (EI+): calculated for $\text{C}_{11}\text{H}_{13}\text{F}_3\text{O}_3\text{S}^{*+}$ [M^{*+}]: 282.0532, found: 282.0526.

IR (neat): 2929, 2862, 1811, 1759, 1707, 1453, 1237, 1103, 1058, 946 cm^{-1} .

3-methyl-3-((trifluoromethyl)thio)butyl benzoate (2h)



Following **Procedure A**, **2h** was obtained from isopentyl benzoate (385 mg, 2.00 mmol, 5.0 eq.) and Phth- SCF_3 (98.9 mg, 0.40 mmol, 1.0 eq.) as colourless oil (67.4 mg, 0.23 mmol, 58%, r.r. = 88/12). The product was purified by chromatography (*Biotage*[®] *SNAP Ultra* 25 g column, P/Et₂O = 97/3).

^1H NMR (400 MHz, CDCl_3) δ (ppm) 8.06 – 8.00 (m, 2H), 7.61 – 7.53 (m, 1H), 7.45 (t, J = 7.7 Hz, 2H), 4.52 (t, J = 6.7 Hz, 2H), 2.21 (t, J = 6.7 Hz, 2H), 1.56 (s, 6H).

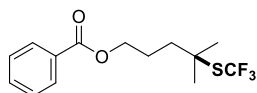
^{13}C NMR (101 MHz, CDCl_3) δ (ppm) 166.6, 133.2, 130.9 (d, J = 307.8 Hz), 130.2, 129.7, 128.6, 61.8, 50.5, 41.5, 29.9 (q, J = 1.7 Hz).

^{19}F NMR (376 MHz, CDCl_3) δ (ppm) -36.2.

HRMS (EI+): calculated for $\text{C}_{13}\text{H}_{19}\text{F}_3\text{NO}_2\text{S}$ [M^{*+}]: 292.0739, found: 292.0743.

The data matches the one reported in literature.^{15b}

4-methyl-4-((trifluoromethyl)thio)pentyl benzoate (2i)



Following **Procedure A**, **2i** was obtained from 4-methylpentyl benzoate (413 mg, 2.00 mmol, 5.0 eq.) and Phth- SCF_3 (98.9 mg, 0.40 mmol, 1.0 eq.) as colourless oil (73.3 mg, 0.24 mmol, 60%, r.r. = 93/7). The product was purified by column chromatography (*Biotage*[®] *SNAP Ultra* 25 g column, P/Et₂O = 95/5).

$^1\text{H NMR}$ (400 MHz, CDCl_3) δ (ppm) 8.13 – 7.85 (m, 1H), 7.66 – 7.48 (m, 1H), 7.45 (dd, $J = 8.4, 7.1$ Hz, 1H), 4.34 (t, $J = 6.2$ Hz, 1H), 2.01 – 1.88 (m, 1H), 1.87 – 1.78 (m, 1H).

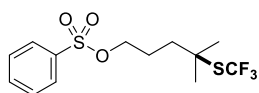
$^{13}\text{C NMR}$ (101 MHz, CDCl_3) δ (ppm) 166.7, 133.1, 131.1 (q, $J = 307.6$ Hz), 130.4, 129.7, 128.5, 64.8, 51.8, 39.6, 29.6 (q, $J = 1.9$ Hz), 24.5.

$^{19}\text{F NMR}$ (376 MHz, CDCl_3) δ (ppm) -36.3.

HRMS (APCI+): calculated for $\text{C}_{14}\text{H}_{21}\text{F}_3\text{NO}_2\text{S}$ [$\text{M}+\text{NH}_4^+$]: 324.1245, found: 324.1242.

The data matches the one reported in literature.^{15b}

4-methyl-4-((trifluoromethyl)thio)pentyl benzenesulfonate (**2j**)



Following **Procedure A**, **2j** was obtained from 4-methylpentyl benzenesulfonate (484 mg, 2.00 mmol, 5.0 eq.) and Phth- SCF_3 (98.9 mg, 0.40 mmol, 1.0 eq.) as colourless oil (85.5 mg, 0.25 mmol, 62%, r.r. = 90/10). The product was purified by automated column chromatography (*Biotage*[®] SNAP Ultra 25 g column, $\text{P}/\text{Et}_2\text{O} = 95/5 \rightarrow 80/20$).

$^1\text{H NMR}$ (300 MHz, CDCl_3) δ (ppm) 7.95 – 7.87 (m, 2H), 7.74 – 7.61 (m, 1H), 7.62 – 7.51 (m, 2H), 4.06 (q, $J = 6.2$ Hz, 2H), 1.79 (tdd, $J = 9.8, 4.8, 1.6$ Hz, 2H), 1.72 – 1.59 (m, 2H), 1.40 (d, $J = 1.0$ Hz, 5H).

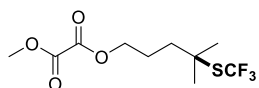
$^{13}\text{C NMR}$ (75 MHz, CDCl_3) δ (ppm) 136.2, 134.0, 130.9 (d, $J = 307.7$ Hz), 129.4, 128.0, 70.7, 51.4, 39.0, 29.5 (d, $J = 1.7$ Hz), 24.7.

$^{19}\text{F NMR}$ (282 MHz, CDCl_3) δ -36.32.

HRMS (EI+): calculated for $\text{C}_{13}\text{H}_{17}\text{F}_3\text{NaO}_2\text{S}_2^+$ [$\text{M}+\text{Na}^+$]: 365.0463, found: 365.0466.

IR (neat): 2970, 2933, 1475, 1449, 1360, 1185, 1095, 969, 916, 752 cm^{-1} .

methyl (4-methyl-4-((trifluoromethyl)thio)pentyl) oxalate (**2k**)



Following **Procedure A**, **2k** was obtained from methyl (4-methylpentyl) oxalate (376 mg, 2.00 mmol, 5.0 eq.) and Phth-SCF₃ (98.9 mg, 0.40 mmol, 1.0 eq.) as colourless oil (73.0 mg, 0.25 mmol, 63%, r.r. = 93/1/6). The product was purified by chromatography (25 g SiO₂, P/Et₂O = 95/5 → 80/20).

¹H NMR (300 MHz, CDCl₃) δ (ppm) 4.30 (t, *J* = 6.4 Hz, 2H), 3.90 (s, 3H), 1.99 – 1.85 (m, 2H), 1.79 – 1.70 (m, 2H), 1.45 (q, *J* = 0.8 Hz, 6H).

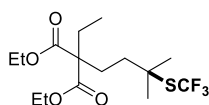
¹³C NMR (75 MHz, CDCl₃) δ (ppm) 158.2, 157.7, 131.0 (q, *J* = 307.5 Hz), 66.9, 53.7, 51.5, 39.1 (d, *J* = 1.8 Hz), 29.5 (d, *J* = 1.7 Hz), 24.0.

¹⁹F NMR (282 MHz, CDCl₃) δ (ppm) δ -36.34.

HRMS (EI+): calculated for C₁₀H₁₅F₃NaO₄S⁺ [M+Na⁺]: 311.0535, found: 311.0538.

IR (neat): 2970, 1770, 1744, 1468, 1319, 1095, 965, 723 cm⁻¹.

diethyl 2-ethyl-2-(3-methyl-3-((trifluoromethyl)thio)butyl)malonate (2l)



Following **Procedure A**, **2l** was obtained from diethyl 2-ethyl-2-isopentylmalonate (517 mg, 2.00 mmol, 5.0 eq.) and Phth-SCF₃ (98.9 mg, 0.40 mmol, 1.0 eq.) as colourless oil (65.7 mg, 0.18 mmol, 46%, r.r. = 95/5). The product was purified by automated column chromatography (Biotage® SNAP Ultra 25 g column, P/Et₂O = 80/20 → 80/20).

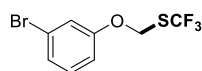
¹H NMR (400 MHz, CDCl₃) δ (ppm) 4.18 (q, *J* = 7.1 Hz, 4H), 2.06 – 1.97 (m, 2H), 1.92 (q, *J* = 7.6 Hz, 2H), 1.57 – 1.48 (m, 2H), 1.45 (d, *J* = 0.9 Hz, 6H), 1.24 (t, *J* = 7.1 Hz, 6H), 0.82 (t, *J* = 7.6 Hz, 3H).

¹³C NMR (101 MHz, CDCl₃) δ (ppm) 171.6, 131.1 (d, *J* = 307.6 Hz), 61.3, 57.6, 51.6, 37.4, 29.4 (q, *J* = 1.3 Hz), 26.8, 25.3, 14.2, 8.4.

¹⁹F NMR (377 MHz, CDCl₃) δ (ppm) -36.18.

HRMS (ESI+): calculated for C₁₄H₂₁F₃NO₂S [M+NH₄⁺]: 324.1245, found: 324.1242.

IR (neat): 2948, 2873, 1811, 1759, 1449, 1237, 1103, 1058, 946, 756 cm⁻¹.

((3-bromophenoxy)methyl)(trifluoromethyl)sulfane (2m)

Following **Procedure B**, **2m** was obtained from 1-bromo-3-methoxybenzene (127 μ L, 187 mg, 1.00 mmol, 2.5 eq.) and Phth-SCF₃ (98.9 mg, 0.40 mmol, 1.0 eq.) as colourless oil (47.1 mg, 0.16 mmol, 41%). The product was purified by automated column chromatography (*Biotage*[®] *SNAP Ultra* 10 g column, pentane) to obtain a mixture of product and starting material, which was subsequently separated by Kugelrohr distillation (7 mbar, 65 °C).

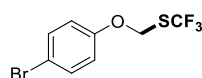
¹H NMR (400 MHz, CDCl₃) δ (ppm) 7.24 – 7.17 (m, 2H), 7.12 – 7.09 (m, 1H), 6.87 (dt, J = 6.6, 2.4 Hz, 1H), 5.49 (s, 2H).

¹³C NMR (101 MHz, CDCl₃) δ (ppm) 156.8, 131.0, 130.1 (q, J = 308.2 Hz), 126.3, 123.1, 120.0, 115.2, 68.3 (q, J = 2.7 Hz).

¹⁹F NMR (376 MHz, CDCl₃) δ (ppm) -40.8.

HRMS (EI+): calculated for C₈H₆⁷⁹BrF₃OS⁺ [M⁺]: 285.9269, found: 285.9261.

IR (neat): 2970, 2926, 2855, 1461, 1379, 1162, 1080, 1021 cm⁻¹.

((4-bromophenoxy)methyl)(trifluoromethyl)sulfane (2n)

Following **Procedure B**, **2n** was obtained from 1-bromo-4-methoxybenzene (125 μ L, 187 mg, 1.00 mmol, 2.5 eq.) and Phth-SCF₃ (98.9 mg, 0.40 mmol, 1.0 eq.) as colourless oil (51.4 mg, 0.18 mmol, 45%). The product was purified by automated column chromatography (*Biotage*[®] *SNAP Ultra* 10 g column, pentane) to obtain a mixture of product and starting material, which was subsequently separated by Kugelrohr distillation (7 mbar, 70 °C).

¹H NMR (400 MHz, CDCl₃) δ (ppm) 7.50 – 7.41 (m, 2H), 6.89 – 6.76 (m, 2H), 5.48 (s, 2H).

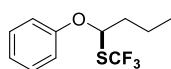
¹³C NMR (101 MHz, CDCl₃) δ (ppm) 155.1, 132.8, 130.1 (q, J = 308.2 Hz), 118.4, 115.7, 68.5 (q, J = 2.8 Hz).

¹⁹F NMR (376 MHz, CDCl₃) δ (ppm) -40.7.

HRMS (EI+): calculated for $C_8H_6^{79}BrF_3OS^{*+}$ [M^{*+}]: 285.9269, found: 285.9270.

IR (neat): 1584, 1483, 1442, 1326, 1207, 1103, 1025, 820, 756, 678 cm^{-1} .

(1-phenoxybutyl)(trifluoromethyl)sulfane (2o)



Following **Procedure B**, **2o** was obtained from butoxybenzene (162 μ L, 150 mg, 1.00 mmol, 2.5 eq.) and Phth-SCF₃ (98.9 mg, 0.40 mmol, 1.0 eq.) as colourless oil (78.8 mg, 0.31 mmol, 79%). The product was purified by automated column chromatography (*Biotage*[®] *SNAP Ultra* 10 g column, pentane).

¹H NMR (400 MHz, CDCl₃) δ (ppm) 7.37 – 7.30 (m, 2H), 7.08 (t, J = 7.4 Hz, 1H), 7.05 – 6.93 (m, 2H), 5.66 (dd, J = 7.3, 5.4 Hz, 1H), 2.21 (dq, J = 14.4, 7.0 Hz, 1H), 2.13 – 2.02 (m, 1H), 1.69 – 1.54 (m, 2H), 1.01 (t, J = 7.4 Hz, 3H).

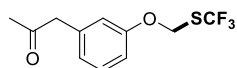
¹³C NMR (101 MHz, CDCl₃) δ (ppm) 156.5, 130.5 (q, J = 307.6 Hz), 129.8, 123.3, 117.6, 84.4 (q, J = 1.8 Hz), 39.4, 19.3, 13.6.

¹⁹F NMR (376 MHz, CDCl₃) δ (ppm) -38.0.

HRMS (EI+): calculated for $C_{11}H_{13}F_3OS^{*+}$ [M^{*+}]: 250.0634, found: 250.0627.

IR (neat): 2955, 2922, 2855, 1722, 1461, 1379, 1274, 1080, 969 cm^{-1} .

1-(3-(((trifluoromethyl)thio)methoxy)phenyl)propan-2-one (2p)



Following **Procedure B**, **2p** was obtained from 1-(3-methoxyphenyl)propan-2-one (153 μ L, 164 mg, 2.00 mmol, 2.5 eq.) and Phth-SCF₃ (98.9 mg, 0.40 mmol, 1.0 eq.) as colourless oil (87.3 mg, 0.33 mmol, 83%). The product was purified by automated column chromatography (*Biotage*[®] *SNAP Ultra* 10 g column, PE/EA = 90/10 \rightarrow 80/20).

¹H NMR (400 MHz, CDCl₃) δ (ppm) 7.30 (t, J = 7.9 Hz, 1H), 6.92 (d, J = 7.9 Hz, 1H), 6.84 (dd, J = 8.2, 2.4 Hz, 1H), 6.80 – 6.77 (m, 1H), 5.51 (s, 2H), 3.69 (s, 2H), 2.17 (s, 3H).

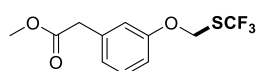
^{13}C NMR (101 MHz, CDCl_3) δ (ppm) 205.9, 156.3, 136.2, 130.2 (q, $J = 308.1$ Hz), 130.1, 124.2, 117.7, 114.9, 68.3 (q, $J = 2.8$ Hz), 50.9, 29.5.

^{19}F NMR (376 MHz, CDCl_3) δ (ppm) -40.8.

HRMS (EI+): calculated for $\text{C}_{11}\text{H}_{11}\text{F}_3\text{O}_2\text{S}^{*+}$ [M^{*+}]: 264.0426, found: 264.0418.

IR (neat): 2929, 2855, 1699, 1587, 1490, 1453, 1114, 1036, 756, 678 cm^{-1} .

methyl 2-(3-(((trifluoromethyl)thio)methoxy)phenyl)acetate (2q)



Following **Procedure B**, **2q** was obtained from methyl 2-(3-methoxyphenyl)acetate (161 μL , 180 mg, 1.00 mmol, 2.5 eq.) and Phth- SCF_3 (98.9 mg, 0.40 mmol, 1.0 eq.) as colourless oil (111 mg, 0.40 mmol, 99%,). The product was purified by automated column chromatography (*Biotage*[®] SNAP Ultra 25 g column, P/DCM = 50/50).

^1H NMR (400 MHz, CDCl_3) δ (ppm) 7.29 (t, $J = 7.9$ Hz, 1H), 7.03 – 6.96 (m, 1H), 6.89 – 6.87 (m, 1H), 6.85 (dd, $J = 8.2, 2.3$ Hz, 1H), 5.53 – 5.48 (m, 2H), 3.70 (s, 3H), 3.62 (s, 2H).

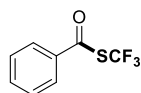
^{13}C NMR (101 MHz, CDCl_3) δ (ppm) 171.7, 156.2, 136.0, 130.3 (q, $J = 308.0$ Hz), 129.9, 124.0, 117.5, 115.0, 68.2 (q, $J = 2.8$ Hz), 52.2, 41.2.

^{19}F NMR (376 MHz, CDCl_3) δ (ppm) -40.8.

HRMS (EI+): calculated for $\text{C}_{11}\text{H}_{11}\text{F}_3\text{O}_3\text{S}^{*+}$ [M^{*+}]: 280.0375, found: 280.0374.

IR (neat): 2955, 1736, 1587, 1490, 1438, 1259, 1103, 1036, 756, 678 cm^{-1} .

S-(trifluoromethyl) benzothioate (2r)



Following **Procedure C**, **2r** was obtained from benzaldehyde (61.2 μL mg, 0.60 mmol, 1.5 eq.) and Phth- SCF_3 (98.9 mg, 0.40 mmol, 1.0 eq.) as colourless oil (75.3 mg, 0.28 mmol, 55%, NMR-Yield: 76%). The product was purified by automated column chromatography (*Biotage*[®] SNAP Ultra 25 g

column, pentane). The compound is volatile, evaporation of the solvent at room temperature is recommended.

¹H NMR (400 MHz, CDCl₃) δ (ppm) 7.89 – 7.83 (m, 2H), 7.73 – 7.63 (m, 1H), 7.57 – 7.46 (m, 2H).

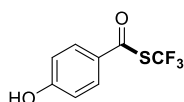
¹³C NMR (101 MHz, CDCl₃) δ (ppm) δ 183.4, 135.3 (q, *J* = 2.9 Hz), 135.2, 129.4, 128.2 (q, *J* = 309.6 Hz), 127.8.

¹⁹F NMR (377 MHz, CDCl₃) δ (ppm) -40.2.

HRMS (APCI): calculated for C₈H₉F₃NOS⁺ [M+NH₄⁺]: 224.0351, found: 224.0353

The data matches the one reported in literature.^{15a}

S-(trifluoromethyl) 4-hydroxybenzothioate (2s)



Following **Procedure C**, **2s** was obtained from 4-hydroxybenzaldehyde (73.3 mg, 0.6 mmol, 1.5 eq.) and Phth-SCF₃ (98.9 mg, 0.40 mmol, 1.0 eq.) as slightly yellow solid (80.0 mg, 0.360 mmol, 90%) after purification by automated column chromatography (25 g SiO₂, PE/EA = 90/10 → 84/16).

Melting Point: 82.9-84.0 °C.

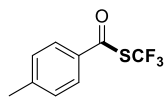
¹H NMR (300 MHz, CDCl₃) δ (ppm) 7.79 (d, *J* = 8.8 Hz, 2H), 6.94 (d, *J* = 8.9 Hz, 2H), 6.47 (br, 1H).

¹³C NMR (75 MHz, CDCl₃) δ (ppm) δ 182.9, 162.1, 130.6, 128.2 (q, *J* = 309.4 Hz), 127.9 (q, *J* = 2.8 Hz), 116.2.

¹⁹F NMR (282 MHz, CDCl₃) δ (ppm) -39.9.

HRMS (EI+): calculated for C₈H₅F₃O₂S⁺ [M⁺]: 221.9957, found: 221.9957.

IR (neat): 3444, 2926, 2855, 1677, 1610, 1580, 1510, 1442, 1297, 1211, 1140, 1095, 887, 846 cm⁻¹.

S-(trifluoromethyl) 4-methylbenzothioate (2t)

Following **Procedure C**, **2t** was obtained from 4-methylbenzaldehyde (70.7 μ L, 0.6 mmol, 1.5 eq.) and Phth-SCF₃ (98.9 mg, 0.40 mmol, 1.0 eq.) as colourless oil (59.2 mg, 0.27 mmol, 67%) after purification by automated column chromatography (10 g SiO₂, pentane). As the product is quite volatile, evaporation of the solvent at room temperature is recommended.

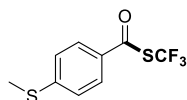
¹H NMR (400 MHz, CDCl₃) δ (ppm) 7.75 (d, J = 8.3 Hz, 1H), 7.30 (d, J = 8.1 Hz, 1H), 2.44 (s, 2H).

¹³C NMR (101 MHz, CDCl₃) δ (ppm) 182.9, 146.6, 132.7 (q, J = 2.7 Hz), 130.0, 128.3 (q, J = 309.3 Hz), 127.9, 21.9.

¹⁹F NMR (377 MHz, CDCl₃) δ (ppm) -40.1.

HRMS (APCI): calculated for C₉H₁₁F₃NOS⁺ [M+NH₄⁺]: 238.0508, found: 238.0511.

The data matches the one reported in literature.^{15a}

S-(trifluoromethyl) 4-(methylthio)benzothioate (2u)

Following **Procedure C**, **2u** was obtained from 4-(methylthio)benzaldehyde (91.3 mg, 0.6 mmol, 1.5 eq.) and Phth-SCF₃ (98.9 mg, 0.40 mmol, 1.0 eq.) as colourless amorphous solid (43.0 mg, 0.17 mmol, 42%) after purification by automated column chromatography (10g SiO₂, PE/EA = 100/0 \rightarrow 95/05).

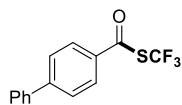
¹H NMR (400 MHz, CDCl₃) δ (ppm) 7.71 (d, J = 8.6 Hz, 2H), 7.44 – 7.06 (m, 2H), 2.50 (s, 3H).

¹³C NMR (101 MHz, CDCl₃) δ (ppm) 182.2, 149.3, 131.2 (q, J = 2.8 Hz), 128.2 (q, J = 309.3 Hz), 128.1, 125.3, 14.7.

¹⁹F NMR (377 MHz, CDCl₃) δ (ppm) -39.9.

HRMS (APCI): calculated for C₉H₁₁F₃NOS₂⁺ [M+NH₄⁺]: 270.0229, found: 270.0232.

IR (neat): 3373, 2929, 1692, 1580, 1487, 1438, 1401, 1222, 1118, 1088, 820, 719 cm⁻¹.

S-(trifluoromethyl) [1,1'-biphenyl]-4-carbothioate (**2v**)

Following **Procedure C**, **2v** was obtained from 4-phenylbenzaldehyde (109 mg, 0.6 mmol, 1.5 eq.) and Phth-SCF₃ (98.9 mg, 0.40 mmol, 1.0 eq.) as colourless solid (95.0 mg, 0.34 mmol, 84%) after purification by automated column chromatography (*Biotage*[®] *SNAP Ultra* 10 g column, PE/EA = 100/0 → 98/02). Alternatively, **2v** was obtained from 4-phenylbenzaldehyde (327 mg, 1.8 mmol, 1.5 eq.) and Phth-SCF₃ (297 mg, 1.2 mmol, 1.0 eq.) with TBADT (99.6 mg, 0.03 mmol, 2.5mol%) after irradiation overnight in MeCN (3 mL, 0.4 M) in 74% yield (250 mg, 0.88 mmol).

Melting Point: 61.1-65.8 °C.

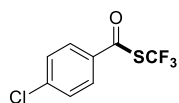
¹H NMR (400 MHz, CDCl₃) δ (ppm) 7.96 – 7.90 (m, 2H), 7.73 (d, *J* = 8.3 Hz, 2H), 7.66 – 7.60 (m, 2H), 7.54 – 7.41 (m, 3H).

¹³C NMR (101 MHz, CDCl₃) δ 182.8, 148.0, 139.2, 133.8 (q, *J* = 2.6 Hz), 129.2, 128.9, 128.4, 128.2 (q, *J* = 309.7 Hz), 127.9, 127.4.

¹⁹F NMR (377 MHz, CDCl₃) δ (ppm) -40.0.

HRMS (EI+): calculated for C₁₄H₉ F₃OS⁺ [*M*⁺]: 282.0321, found: 282.0318.

The data matches the one reported in literature.^{15a}

S-(trifluoromethyl) 4-chlorobenzothioate (**2w**)

Following **Procedure C**, **2w** was obtained from 4-chlorobenzaldehyde (118 mg, 0.6 mmol, 1.5 eq.) and Phth-SCF₃ (98.9 mg, 0.40 mmol, 1.0 eq.) as colourless amorphous solid (66.0 mg, 0.27 mmol, 69%) after purification by automated column chromatography (10g SiO₂, 100% pentane). Albeit solid at room temperature, the product was found to be volatile at 40 °C under the reduced pressure. Evaporation the solvent at room temperature is recommended.

¹H NMR (400 MHz, CDCl₃) δ (ppm) 7.84 – 7.77 (m, 2H), 7.53 – 7.46 (m, 2H).

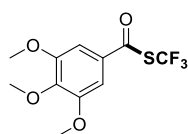
^{13}C NMR (101 MHz, CDCl_3) δ (ppm) 182.3, 141.9, 133.6 (q, $J = 2.8$ Hz), 129.7, 129.1, 127.95 (q, $J = 309.9$ Hz).

^{19}F NMR (377 MHz, CDCl_3) δ (ppm) -40.1.

HRMS (EI+): calculated for $\text{C}_8\text{H}_4\text{ClF}_3\text{OS}^{*+}$ [M^{*+}]: 239.9618, found: 239.9624.

The data matches the one reported in literature.^{15a}

S-(trifluoromethyl) 3,4,5-trimethoxybenzothioate (2x)



Following **Procedure C**, **2x** was obtained from 3,4,5-trimethoxybenzaldehyde (118 mg, 0.6 mmol, 1.5 eq.) and Phth- SCF_3 (98.9 mg, 0.40 mmol, 1.0 eq.) as colourless solid (79.6 mg, 0.27 mmol, 67%) after purification by automated column chromatography (25 g SiO_2 , PE/EA = 95/05 \rightarrow 91/09).

Melting Point: 53.8-56.8 °C.

^1H NMR (400 MHz, CDCl_3) δ (ppm) 7.26 (s, 2H), 4.11 (s, 3H), 4.08 (s, 6H).

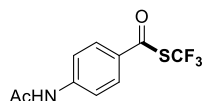
^{13}C NMR (101 MHz, CDCl_3) δ (ppm) 182.3, 153.6, 144.3, 130.1 (q, $J = 2.8$ Hz), 128.1 (q, $J = 309.5$ Hz), 105.2, 61.2.

^{19}F NMR (377 MHz, CDCl_3) δ (ppm) -40.2.

HRMS (EI+): calculated for $\text{C}_{11}\text{H}_{11}\text{F}_3\text{O}_4\text{S}^{*+}$ [M^{*+}]: 296.0325, found: 296.0316.

IR (neat): 2944, 2840, 1699, 1580, 1498, 1464, 1416, 1319, 1248, 1125, 1088, 991, 760 cm^{-1} .

S-(trifluoromethyl) 4-acetamidobenzothioate (2y)



Following **Procedure C**, **2y** was obtained from *N*-(4-formylphenyl)acetamide (97.9 mg, 0.6 mmol, 1.5 eq.) and Phth- SCF_3 (98.9 mg, 0.40 mmol, 1.0 eq.) as colourless solid (94.2 mg, 0.357 mmol, 89%) after purification by automated column chromatography (25 g SiO_2 , PE/EA = 90/10 \rightarrow 84/16).

Melting Point: 162.5-165.1 °C.

¹H NMR (400 MHz, CDCl₃) δ (ppm) 7.83 (d, *J* = 8.8 Hz, 2H), 7.67 (d, *J* = 8.8 Hz, 2H), 7.52 (br, 1H), 2.23 (s, 3H).

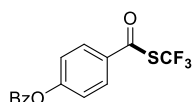
¹³C NMR (101 MHz, CDCl₃) δ (ppm) δ 182.0, 168.7, 144.1, 130.6, 129.4, 128.2 (d, *J* = 309.3 Hz), 119.3, 24.5.

¹⁹F NMR (377 MHz, CDCl₃) δ (ppm) -40.0.

HRMS (EI+): calculated for C₁₀H₈F₃NO₂S⁺ [*M*⁺]: 263.0222, found: 263.0229.

IR (neat): 3246, 3179, 3108, 3049, 2363, 1699, 1587, 1539, 1408, 1323, 1155, 1099, 879, 682 cm⁻¹.

4-(((trifluoromethyl)thio)carbonyl)phenyl benzoate (**2z**)



Following **Procedure C**, **2z** was obtained from 4-formylphenyl benzoate (136 mg, 0.6 mmol, 1.5 eq.) and Phth-SCF₃ (98.9 mg, 0.40 mmol, 1.0 eq.) as colourless solid (105 mg, 0.32 mmol, 80%) after purification by automated column chromatography (*Biotage*[®] *SNAP Ultra* 10 g column, PE/DCM = 95/5).

Melting Point: 95.6-97.3 °C.

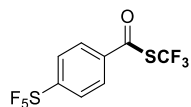
¹H NMR (400 MHz, CDCl₃) δ (ppm) 8.20 (dd, *J* = 8.4, 1.4 Hz, 2H), 7.96 (d, *J* = 8.8 Hz, 2H), 7.68 (ddt, *J* = 8.7, 7.0, 1.2 Hz, 1H), 7.58 – 7.51 (m, 2H), 7.44 – 7.38 (m, 2H).

¹³C NMR (101 MHz, CDCl₃) δ (ppm) 182.2, 164.4, 156.3, 134.3, 132.7 (q, *J* = 2.8 Hz), 130.4, 129.5, 128.9, 128.8, 128.1 (q, *J* = 309.7 Hz), 122.8.

¹⁹F NMR (377 MHz, CDCl₃) δ (ppm) -40.1.

HRMS (APCI): calculated for C₁₅H₁₃F₃NO₃S⁺ [*M*+NH₄⁺]: 344.0563, found: 344.0566.

IR (neat): 1736, 1695, 1595, 1502, 1267, 1218, 1162, 1125, 1058, 872 cm⁻¹.

S-(trifluoromethyl) 4-(pentafluoro- λ^6 -sulfaneyl)benzothioate (**2aa**)

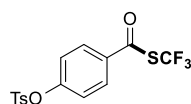
Following **Procedure C**, **2aa** was obtained from 4-(pentafluorosulfanyl)benzaldehyde (99.5 μ L, 139 mg, 0.6 mmol, 1.5 eq.) and Phth-SCF₃ (98.9 mg, 0.40 mmol, 1.0 eq.) as colourless amorphous solid (69.8 mg, 0.13 mmol, 53%) after purification by automated column chromatography (10g SiO₂, pentane).

¹H NMR (400 MHz, CDCl₃) δ (ppm) 7.99 – 7.89 (m, 4H).

¹³C NMR (101 MHz, CDCl₃) δ (ppm) 182.3, 158.3 (t, J = 18.7 Hz), 137.4, 128.2, 127.7 (q, J = 310.4 Hz), 127.3 (p, J = 4.8 Hz).

¹⁹F NMR (377 MHz, CDCl₃) δ (ppm) 81.0 (q, J = 150.5 Hz), 61.7 (d, J = 150.5 Hz), -40.1.

HRMS (EI+): calculated for C₈H₄F₇OS₂⁺ [M^{+} - F^{*}]: 312.9586, found: 312.9581.

S-(trifluoromethyl) 4-(tosyloxy)benzothioate (**2ab**)

Following **Procedure C**, **2ab** was obtained from 4-formylphenyl 4-methylbenzenesulfonate (166 mg, 0.6 mmol, 1.5 eq.) and Phth-SCF₃ (98.9 mg, 0.40 mmol, 1.0 eq.) as yellowish amorphous solid (116 mg, 0.31 mmol, 77%) after purification by column chromatography (*Biotage*[®] SNAP Ultra 10 g column, PE/DCM = 95/5).

¹H NMR (400 MHz, CDCl₃) δ (ppm) 7.85 – 7.77 (m, 2H), 7.75 – 7.68 (m, 2H), 7.37 – 7.31 (m, 2H), 7.18 – 7.13 (m, 2H).

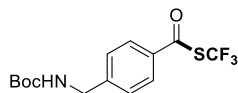
¹³C NMR (101 MHz, CDCl₃) δ (ppm) 182.1, 154.5, 146.2, 133.6 (q, J = 2.6 Hz), 132.0, 130.2, 129.6, 128.6, 127.9 (d, J = 310.0 Hz), 123.3, 21.9.

¹⁹F NMR (377 MHz, CDCl₃) δ (ppm) -40.1.

HRMS (ESI+): calculated for C₁₅H₁₁F₃NaO₄S₂⁺ [M + Na⁺]: 398.9943, found: 398.9943.

The data matches the one reported in literature.^{20a}

S-(trifluoromethyl) 4-(((*tert*-butoxycarbonyl)amino)methyl)benzothioate (**2ac**)



Following **Procedure C**, **2ac** was obtained from *tert*-butyl (4-formylbenzyl)carbamate (141 mg, 0.6 mmol, 1.5 eq.) and Phth-SCF₃ (98.9 mg, 0.40 mmol, 1.0 eq.) as colourless solid (55.6 mg, 0.17 mmol, 41%) after purification by automated column chromatography (*Biotage*[®] *SNAP Ultra* 10 g column, PE/EA = 95/05 → 75/25).

Melting Point: 129.0-131.1 °C.

¹H NMR (400 MHz, CDCl₃) δ (ppm) 7.81 (d, *J* = 8.3 Hz, 2H), 7.41 (d, *J* = 8.1 Hz, 2H), 5.04 (s, 1H), 4.38 (d, *J* = 5.3 Hz, 2H), 1.45 (s, 9H).

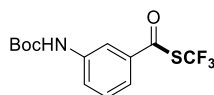
¹³C NMR (101 MHz, CDCl₃) δ (ppm) 182.9, 156.0, 147.2, 134.2 (q, *J* = 2.4 Hz), 128.1 (q, *J* = 309.6 Hz), 128.1, 127.9, 80.2, 44.3, 28.5.

¹⁹F NMR (377 MHz, CDCl₃) δ (ppm) -40.1.

HRMS (ESI+): calculated for C₁₄H₁₆F₃NNaO₃S⁺ [M+Na⁺]: 358.0695, found: 358.0696.

IR (neat): 3358, 1684, 1513, 1077, 790 cm⁻¹.

S-(trifluoromethyl) 3-(((*tert*-butoxycarbonyl)amino)benzothioate (**2ad**)



Following **Procedure C**, **2ad** was obtained from *tert*-butyl (3-formylphenyl)carbamate (133 mg, 0.6 mmol, 1.5 eq.) and Phth-SCF₃ (98.9 mg, 0.40 mmol, 1.0 eq.) as colourless solid (80.3 mg, 0.25 mmol, 62%) after purification by automated column chromatography (*Biotage*[®] *SNAP Ultra* 10 g column, PE/EA = 95/05 → 90/10).

Melting Point: 111.7-114.1 °C.

¹H NMR (400 MHz, CDCl₃) δ (ppm) 7.91 (t, *J* = 2.0 Hz, 1H), 7.67 (d, *J* = 8.1 Hz, 1H), 7.50 (ddd, *J* = 7.8, 1.8, 1.1 Hz, 1H), 7.41 (t, *J* = 7.9 Hz, 1H), 6.76 (s, 1H), 1.53 (s, 9H).

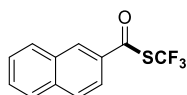
¹³C NMR (101 MHz, CDCl₃) δ (ppm) 183.3, 152.6, 139.7, 135.9 (q, *J* = 2.7 Hz), 130.0, 128.1 (q, *J* = 309.7 Hz), 124.7, 122.0, 117.1, 81.6, 28.4.

¹⁹F NMR (377 MHz, CDCl₃) δ (ppm) -40.3.

HRMS (EI+): calculated for C₁₃H₁₄F₃NNaO₃S⁺ [M+Na⁺]: 344.0539, found: 344.0543.

IR (neat): 3339, 2974, 1699, 1587, 1543, 1431, 1244, 1155, 1099, 887, 693 cm⁻¹.

S-(trifluoromethyl) naphthalene-2-carbothioate (**2ae**)



Following **Procedure C**, **2ae** was obtained from 2-naphthaldehyde (93.7 mg, 0.6 mmol, 1.5 eq.) and Phth-SCF₃ (98.9 mg, 0.40 mmol, 1.0 eq.) as yellow amorphous solid (54.5 mg, 0.21 mmol, 53%) after purification by automated column chromatography (25 g SiO₂, PE/EA = 100/0 → 98/02).

¹H NMR (400 MHz, CDCl₃) δ (ppm) 8.38 (d, *J* = 1.8 Hz, 1H), 7.96 (d, *J* = 8.1 Hz, 1H), 7.90 (t, *J* = 8.8 Hz, 2H), 7.84 (dd, *J* = 8.7, 1.9 Hz, 1H), 7.67 (ddd, *J* = 8.2, 6.8, 1.4 Hz, 1H), 7.60 (ddd, *J* = 8.2, 6.9, 1.4 Hz, 1H).

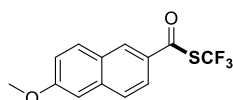
¹³C NMR (101 MHz, CDCl₃) δ (ppm) 183.3, 132.5 (q, *J* = 2.7 Hz), 130.0, 129.8, 128.3 (q, *J* = 309.6 Hz), 129.7, 129.4, 128.1, 127.7, 122.6.

¹⁹F NMR (377 MHz, CDCl₃) δ (ppm) -40.0.

HRMS (EI+): calculated for C₁₂H₇F₃OS⁺ [M⁺]: 256.0164, found: 256.0161.

The data matches the one reported in literature.^{20a}

S-(trifluoromethyl) 6-methoxynaphthalene-2-carbothioate (**2af**)



Following **Procedure C**, **2af** was obtained from 6-methoxy-2-naphthaldehyde (109 mg, 0.6 mmol, 1.5 eq.) and Phth-SCF₃ (98.9 mg, 0.40 mmol, 1.0 eq.) as yellow solid (60.7 mg, 0.21 mmol, 53%) after purification by chromatography (25 g SiO₂, PE/EA = 100/0 → 97/03).

Melting Point: 78.4-80.4 °C.

¹H NMR (400 MHz, CDCl₃) δ (ppm) 8.31 (d, *J* = 1.7 Hz, 1H), 7.90 – 7.69 (m, 3H), 7.25 (dd, *J* = 8.9, 2.4 Hz, 1H), 7.16 (d, *J* = 2.5 Hz, 1H), 3.96 (s, 3H).

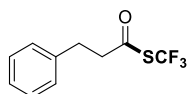
¹³C NMR (101 MHz, CDCl₃) δ (ppm) 182.8, 160.8, 138.5, 131.5, 130.44 (q, *J* = 2.7 Hz), 129.9, 128.4 (q, *J* = 309.1 Hz), 127.9, 127.7, 123.5, 120.7, 106.0, 55.7.

¹⁹F NMR (377 MHz, CDCl₃) δ (ppm) -39.9.

HRMS (EI+): calculated for C₁₃H₉F₃O₂S⁺ [*M*⁺]: 286.0270, found: 286.0277.

IR (neat): 2940, 2847, 1703, 1621, 1479, 1390, 1271, 1151, 1099, 1025, 689 cm⁻¹.

S-(trifluoromethyl) 3-phenylpropanethioate (**2ag**)



Following **Procedure C**, **2ag** was obtained from 3-phenylpropanal (79.7 μL, 80.5 mg, 0.6 mmol, 1.5 eq.) and Phth-SCF₃ (98.9 mg, 0.40 mmol, 1.0 eq.) as colourless oil (59.4 mg, 0.25 mmol, 63%) after purification by automated column chromatography (*Biotage*[®] *SNAP Ultra* 10 g column, pentane). As the product is quite volatile, evaporation of the solvent at room temperature is recommended.

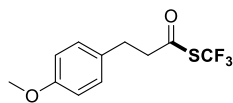
¹H NMR (300 MHz, CDCl₃) δ (ppm) 7.37 – 7.29 (m, 2H), 7.29 – 7.24 (m, 1H), 7.20 (m, 2H), 3.09 – 2.99 (m, 2H), 2.98 – 2.90 (m, 2H).

¹³C NMR (75 MHz, CDCl₃) δ (ppm) 189.7, 138.9, 128.9, 128.4, 127.7 (q, *J* = 310.2 Hz), 126.9, 46.2 (q, *J* = 2.7 Hz), 30.6.

¹⁹F NMR (282 MHz, CDCl₃) δ (ppm) -40.9.

HRMS (EI+): calculated for C₁₀H₉F₃OS⁺ [*M*⁺]: 234.0321, found: 234.0315.

IR (neat): 3063, 3030, 2926, 2855, 1710, 1453, 1155, 1110, 1028, 700 cm⁻¹.

S-(trifluoromethyl) 3-(4-methoxyphenyl)propanethioate (2ah)

Following **Procedure C**, **2ah** was obtained from 3-(4-methoxyphenyl)propanal (95.0 μL , 98.5 mg, 0.6 mmol, 1.5 eq.) and Phth-SCF₃ (98.9 mg, 0.40 mmol, 1.0 eq.) as colourless oil (65.0 mg, 0.25 mmol, 62%) after purification by automated column chromatography (*Biotage*[®] SNAP Ultra 10 g column, pentane). As the product might quite volatile, evaporation of the solvent at room temperature is recommended.

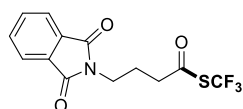
¹H NMR (400 MHz, CDCl₃) δ (ppm) 7.10 (d, J = 8.6 Hz, 2H), 6.85 (d, J = 8.6 Hz, 2H), 3.79 (s, 3H), 2.99 – 2.87 (m, 4H).

¹³C NMR (101 MHz, CDCl₃) δ (ppm) 189.7, 158.6, 130.9, 129.4, 127.7 (q, J = 310.0 Hz), 114.3, 55.4, 46.5 (q, J = 2.7 Hz), 29.8.

¹⁹F NMR (376 MHz, CDCl₃) δ (ppm) -40.7.

HRMS (EI+): calculated for C₁₁H₁₁F₃O₂S⁺ [M^{+}]: 264.0426, found: 264.0423.

IR (neat): 3004, 2937, 2840, 1736, 1613, 1513, 1464, 1244, 1148, 1103, 1028, 954 cm⁻¹.

S-(trifluoromethyl) 4-(1,3-dioxisoindolin-2-yl)butanethioate (2ai)

Following **Procedure C**, **2ai** was obtained from 4-(1,3-dioxisoindolin-2-yl)butanal (130 mg, 0.6 mmol, 1.5 eq.) and Phth-SCF₃ (98.9 mg, 0.40 mmol, 1.0 eq.) as colourless solid (121 mg, 0.378 mmol, 95%) after purification by chromatography (10 g SiO₂, PE/DCM = 80/20 \rightarrow 0/100).

Melting Point: 64.3-66.7 °C.

¹H NMR (300 MHz, CDCl₃) δ (ppm) 7.87 – 7.79 (m, 2H), 7.75 – 7.68 (m, 2H), 3.74 (t, J = 6.6 Hz, 2H), 2.71 (t, J = 7.3 Hz, 2H), 2.14 – 2.00 (m, 2H).

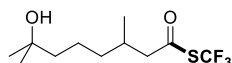
¹³C NMR (75 MHz, CDCl₃) δ (ppm) 189.5, 168.4, 134.3, 132.0, 127.6 (q, J = 310.1 Hz), 123.5, 42.0 (q, J = 2.8 Hz), 36.7, 23.6.

^{19}F NMR (282 MHz, CDCl_3) δ (ppm) -40.66.

HRMS (APCI): calculated for $\text{C}_{13}\text{H}_{11}\text{F}_3\text{NO}_3\text{S}^+$ [$\text{M}+\text{H}^+$]: 318.0406, found: 318.0410.

IR (neat): 2940, 2911, 1781, 1699, 1442, 1397, 1341, 1110, 1058, 950, 883, 715 cm^{-1} .

S-(trifluoromethyl) 7-hydroxy-3,7-dimethyloctanethioate (2aj)



Following **Procedure C**, **2aj** was obtained from 7-hydroxy-3,7-dimethyloctanal (103 mg, 0.6 mmol, 1.5 eq.) and Phth- SCF_3 (98.9 mg, 0.40 mmol, 1.0 eq.) as colourless oil (88.8 mg, 0.33 mmol, 82%) after column chromatography (*Biotage*[®] SNAP Ultra 10g, PE/DCM = 80/20 \rightarrow 0/100).

^1H NMR (400 MHz, CDCl_3) δ (ppm) 2.61 (dd, J = 15.2, 6.0 Hz, 1H), 2.43 (dd, J = 15.2, 7.9 Hz, 1H), 2.15 – 1.94 (m, 2H), 1.51 – 1.23 (m, 4H), 1.21 (s, 6H), 1.00 (d, J = 6.7 Hz, 3H).

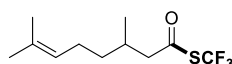
^{13}C NMR (75 MHz, CDCl_3) δ (ppm) 190.0, 127.8 (q, J = 309.9 Hz), 71.0, 51.8 (d, J = 2.6 Hz), 43.8, 36.9, 30.9, 29.4 (d, J = 6.9 Hz), 21.6, 19.5.

^{19}F NMR (376 MHz, CDCl_3) δ (ppm) δ -40.8.

HRMS (EI+): calculated for $\text{C}_{11}\text{H}_{23}\text{F}_3\text{NO}_2\text{S}^+$ [$\text{M}+\text{NH}_4^+$]: 290.1396, found: 290.1398.

IR (neat): 3377, 2937, 2967, 1744, 1710, 1461, 1379, 1151, 1110, 987, 931, 760 cm^{-1} .

S-(trifluoromethyl) 3,7-dimethyloct-6-enethioate (2ak)



Following **Procedure C**, **2ak** was obtained from 3,7-dimethyloct-6-enal (92.5 mg, 0.6 mmol, 1.5 eq.) and Phth- SCF_3 (98.9 mg, 0.40 mmol, 1.0 eq.) as colourless oil (72.1 mg, 0.28 mmol, 71%) after purification by automated column chromatography (*Biotage*[®] SNAP Ultra 10 g column, pentane). As the product is quite volatile, evaporation of the solvent at room temperature is recommended.

^1H NMR (400 MHz, CDCl_3) δ (ppm) 5.07 (tt, $J = 7.1, 1.4$ Hz, 1H), 2.62 (dd, $J = 15.2, 5.8$ Hz, 1H), 2.41 (dd, $J = 15.2, 8.1$ Hz, 1H), 2.09 – 1.94 (m, 3H), 1.69 (q, $J = 1.3$ Hz, 3H), 1.60 (s, 3H), 1.43 – 1.33 (m, 1H), 1.31 – 1.21 (m, 1H), 0.99 (d, $J = 6.7$ Hz, 3H).

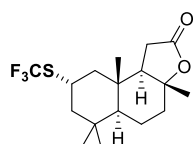
^{13}C NMR (101 MHz, CDCl_3) δ (ppm) 190.0, 132.3, 127.9 (q, $J = 309.8$ Hz), 123.8, 51.8 (q, $J = 2.7$ Hz), 36.5, 30.5, 25.8, 25.4, 19.5, 17.8.

^{19}F NMR (376 MHz, CDCl_3) δ (ppm) -40.8.

HRMS (EI⁺): calculated for $\text{C}_{10}\text{H}_{17}\text{O}^+$ [$\text{M}-\text{SCF}_3^+$] 153.1274, found: 153.1272.

IR (neat): 2926, 2855, 1710, 1461, 1379, 1159, 1114, 984 cm^{-1} .

SCF₃-Sclareoide (2aI)



Following **Procedure A**, **2aI** was obtained from Sclareoide (501 mg, 2.0 mmol, 5.0 eq.) and Phth-SCF₃ (98.9 mg, 0.40 mmol, 1.0 eq.) as colourless amorphous solid (76.9 mg, 0.22 mmol, 55%) after purification by automated column chromatography (*Biotage*[®] *SNAP Ultra* 25 g column, PE/EtOAc = 95/5 → 80/20).

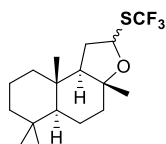
^1H NMR (400 MHz, CDCl_3) δ (ppm) 3.52 (tt, $J = 12.8, 3.8$ Hz, 1H), 2.50 – 2.37 (m, 1H), 2.26 (dd, $J = 16.2, 6.5$ Hz, 1H), 2.10 (dt, $J = 12.0, 3.3$ Hz, 1H), 1.99 (dd, $J = 14.7, 6.5$ Hz, 1H), 1.94 – 1.83 (m, 3H), 1.70 (td, $J = 12.5, 4.1$ Hz, 1H), 1.41 – 1.30 (m, 5H), 1.23 (d, $J = 13.0$ Hz, 1H), 1.10 (dd, $J = 12.6, 2.4$ Hz, 1H), 0.97 (d, $J = 10.4$ Hz, 6H), 0.92 (s, 3H).

^{13}C NMR (101 MHz, CDCl_3) δ (ppm) 176.1, 131.1 (q, $J = 306.6$ Hz), 85.9, 58.7, 55.9, 49.2, 46.8, 38.6, 37.6, 37.2, 35.1, 33.0, 28.7, 21.8, 21.3, 20.4, 15.7.

^{19}F NMR (377 MHz, CDCl_3) δ (ppm) -39.3.

HRMS (APCI⁺): calculated for $\text{C}_{17}\text{H}_{29}\text{F}_3\text{NO}_2\text{S}^+$ [$\text{M}+\text{NH}_4^+$] 368.1866, found: 368.1869.

The data matches the one reported in literature.^{18b}

SCF₃-Ambroxide (2am)

Following **Procedure B**, **2am** was obtained from (-)-Ambroxide (236 mg, 1.0 mmol, 2.5 eq.) and Phth-SCF₃ (98.9 mg, 0.40 mmol, 1.0 eq.) as colourless amorphous solid (90.6 mg, 0.27 mmol, 67%, d.r.: 60/40) after purification by automated column chromatography (*Biotage*[®] *SNAP Ultra 25 g* column, P/Et₂O = 98/2 → 97/3).

Mixture diastereomers:

¹H NMR (400 MHz, CDCl₃) δ (ppm) 5.73 – 5.66 (m, 1H), 2.41 – 2.25 (m, 1H), 2.00 (ddt, *J* = 11.3, 7.8, 3.1 Hz, 1H), 1.90 – 1.74 (m, 2H), 1.70 – 1.60 (m, 1H), 1.58 – 1.28 (m, 6H), 1.25 – 1.12 (m, 4H), 1.10 – 1.02 (m, 1H), 1.01 – 0.93 (m, 1H), 0.89 – 0.81 (m, 9H).

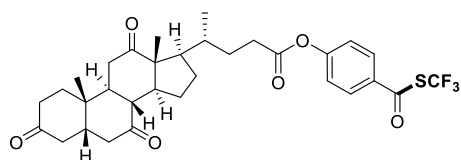
¹³C NMR (101 MHz, CDCl₃) δ (ppm) 130.6 (q, *J* = 307.1 Hz), 130.5 (q, *J* = 307.1 Hz), 85.1, 84.1, 81.5 (q, *J* = 2.1 Hz), 80.9 (q, *J* = 2.0 Hz), 60.3, 58.5, 57.2, 57.1, 42.4, 40.1, 40.0, 40.0, 39.9, 36.4, 36.3, 33.6, 33.2, 31.7, 31.1, 22.7, 22.4, 21.2, 21.2, 20.9, 20.5, 18.4, 15.5, 15.3.

¹⁹F NMR (376 MHz, CDCl₃) δ (ppm) -39.6 (*minor diastereomer*), -40.4 (*major diastereomer*).

HRMS (APCI⁺): calculated for C₁₇H₃₁F₃NOS⁺ [M+NH₄⁺]: 354.2073, found: 354.2075.

The data matches the literature reported data.^{15b}

4-(((trifluoromethyl)thio)carbonyl)phenyl (R)-4-((5S,8R,9S,10S,13R,14S,17R)-10,13-dimethyl-3,7,12-trioxohexadecahydro-1H-cyclopenta[a]phenanthren-17-yl)pentanoate (2an)



Following **Procedure C**, **2an** was obtained from 4-formylphenyl (R)-4-((5S,8R,9S,10S,13R,14S,17R)-10,13-dimethyl-3,7,12-trioxohexadecahydro-1H-cyclopenta[a]phenanthren-17-yl)pentanoate (**1an**, 304 mg, 0.6 mmol, 1.5 eq.) and Phth-SCF₃ (98.9 mg, 0.40 mmol, 1.0 eq.) as colourless solid

(109 mg, 0.18 mmol, 45%) after purification by automated column chromatography (*Biotage*[®] *SNAP Ultra* 25 g column, PE/EtOAc = 80/20 → 0/100).

Melting Point: 207.2-212.3 °C.

¹H NMR (400 MHz, CDCl₃) δ (ppm) 7.89 (d, *J* = 8.7 Hz, 2H), 7.25 (d, *J* = 8.8 Hz, 2H), 2.95 – 2.81 (m, 3H), 2.68 (ddd, *J* = 16.2, 9.3, 5.3 Hz, 1H), 2.55 (ddd, *J* = 16.1, 9.0, 7.1 Hz, 1H), 2.40 – 1.79 (m, 15H), 1.69 – 1.47 (m, 3H), 1.40 (s, 3H), 1.30 – 1.24 (m, 1H), 1.09 (s, 3H), 0.92 (d, *J* = 6.7 Hz, 3H).

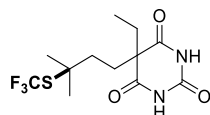
¹³C NMR (101 MHz, CDCl₃) δ (ppm) 212.0, 209.1, 208.8, 182.2, 171.8, 156.07, 132.5 (q, *J* = 3.1 Hz), 129.4, 128.0 (q, *J* = 309.6 Hz), 122.6, 57.0, 51.9, 49.1, 46.9, 45.7, 45.1, 42.9, 38.8, 36.6, 36.1, 35.6, 35.4, 31.6, 30.3, 27.8, 25.2, 22.0, 18.8, 12.0.

¹⁹F NMR (376 MHz, CDCl₃) δ (ppm) -40.0.

HRMS (ESI+): calculated for C₃₂H₃₇F₃NaO₆S⁺ [M+Na⁺]: 629.2155, found: 629.2153.

IR (neat): 2959, 1770, 1699, 1599, 1502, 1427, 1215, 1159, 1099, 887 cm⁻¹.

SCF₃-Amobarbital (3I)



Adapting literature procedure for the synthesis of barbiturates,³⁰ a suspension of urea (60.1 mg, 1.00 mmol, 10.0 eq.) in dry DMF (2 mL) was treated with sodium hydride (60% dispersion in mineral oil, 24.0 mg, 0.60 mmol, 6.0 eq.) at 0 °C and stirred for 1 hour. A solution of **2I** (0.1 mmol) in dry DMF (1 mL) was added, the mixture was stirred overnight and the reaction was quenched by the addition of saturated aqueous ammonium chloride solution (5 mL). The product was extracted into ether (3 x 10 mL), which was dried over anhydrous Na₂SO₄ and subsequently evaporated under reduced pressure. The title compound was purified by automated column chromatography (*Biotage*[®] *SNAP Ultra* 10 g column, PE/EtOAc = 60/40 → 0/100) to yield a colourless solid (13.6 mg, 41.7 μmol, 42%).

Melting Point: 132.6-138.7 °C.

¹H NMR (400 MHz, CDCl₃) δ (ppm) 8.52 (s, 2H), 2.20 – 2.11 (m, 2H), 2.07 (q, *J* = 7.5 Hz, 2H), 1.60 – 1.52 (m, 2H), 1.42 (d, *J* = 1.0 Hz, 6H), 0.92 (t, *J* = 7.5 Hz, 3H).

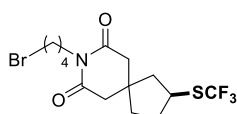
¹³C NMR (101 MHz, CDCl₃) δ (ppm) 171.8, 148.4, 130.7 (d, *J* = 308.1 Hz), 56.7, 50.8, 37.9, 33.1, 32.8, 29.1, 9.3.

¹⁹F NMR (376 MHz, CDCl₃) δ (ppm) -36.2.

HRMS (ESI+): calculated for C₁₂H₁₇F₃N₂NaO₃S⁺ [M+Na⁺]: 349.0810, found: 349.0804.

IR (neat): 3220, 3108, 2926, 2855, 1699, 1423, 1353, 1304, 1095, 756 cm⁻¹.

8-(4-bromobutyl)-2-((trifluoromethyl)thio)-8-azaspiro[4.5]decane-7,9-dione (3f**)**



Adapting literature procedure,³¹ a crimp capped vial (20 mL) equipped with **2f** (20 mg, 0.075 mmol, 1.0 eq.), DMAP (2 mol% 0.2 mg), and K₂CO₃ (31.1 mg, 0.23 mmol, 3.0 eq.) was set under a nitrogen atmosphere. 1,4-dibromobutane (11.2 μL, 0.094 mmol, 1.25 eq.) was added via a syringe, followed by MeCN (0.5-1 mL, anhydrous) and the reaction mixture was heated overnight at 95 °C. The next day, the reaction was filtered, concentrated and purified by column chromatography (PE/EtOAc = 75/25 → 60/40) to yield **3f** as clear oil (27.8 mg, 0.069 mmol, 92%).

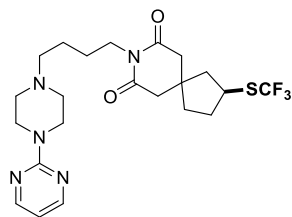
¹H NMR (400 MHz, CDCl₃) δ (ppm) 3.78 (t, *J* = 7.2 Hz, 2H), 3.66 (p, *J* = 7.8 Hz, 1H), 3.40 (t, *J* = 6.7 Hz, 2H), 2.68 (s, 2H), 2.62 (s, 2H), 2.34 – 2.24 (m, 1H), 2.11 (dd, *J* = 13.8, 7.8 Hz, 1H), 1.89 – 1.72 (m, 4H), 1.71 – 1.57 (m, 4H).

¹³C NMR (101 MHz, CDCl₃) δ (ppm) 171.2, 130.6 (q, *J* = 306.7 Hz). 45.5, 45.4, 44.9, 41.2 (q, *J* = 1.8 Hz) 39.5, 38.8, 36.6, 33.1, 32.9, 30.2, 26.8.

¹⁹F NMR (377 MHz, CDCl₃) δ (ppm) -41.0.

HRMS (ESI+): calculated for C₁₄H₂₀⁷⁹BrF₃NO₂S⁺ [M⁺H⁺]: 402.0345, found: 402.0347.

IR (neat): 2955, 2866, 1729, 1669, 1435, 1390, 1353, 1267, 1233, 1110, 756 cm⁻¹.

SCF₃-Buspirone (4f)

Adapting literature procedure,³¹ a crimp capped vial (20 mL) equipped with **3f** (27.6 mg, 68.6 μ mol), KI (0.6 mg, 5 mol%), 1-(2-pyrimidyl)piperazine (11.3 mg, 9.8 μ L, 0.069 mmol, 1.0 eq.) and K₂CO₃ (28.6 mg, 0.21 mmol, 3.0 eq.) was set under a nitrogen atmosphere and MeCN (1 mL, anhydrous) was added via a syringe. The reaction mixture was heated overnight at 95 °C. The next day, the reaction was filtered while hot, concentrated and purified by column chromatography (5% MeOH in DCM) to yield Buspirone-SCF₃ as white amorphous solid (29.4 mg, 61 μ mol, 89%). The ¹H NMR spectrum shows an impurity (at 8.20 ppm, ~ 6%), which was identified by HRMS as the *p*-chloro derivative, probably originating in the use of chlorinated solvents.

¹H NMR (400 MHz, CDCl₃) δ (ppm) 8.29 (d, *J* = 4.7 Hz, 2H), 6.49 (t, *J* = 4.7 Hz, 1H), 3.92 (s, 4H), 3.78 (t, *J* = 7.0 Hz, 2H), 3.65 (p, *J* = 7.8 Hz, 1H), 2.69 (s, 3H), 2.62 (s, 5H), 2.51 (s, 2H), 2.34 – 2.22 (m, 1H), 2.10 (dd, *J* = 13.8, 7.8 Hz, 1H), 1.87 – 1.71 (m, 2H), 1.66 – 1.49 (m, 6H).

¹³C NMR (101 MHz, CDCl₃) δ (ppm) 171.3, 161.6, 157.9, 130.6 (q, *J* = 306.8 Hz), 110.3, 58.1, 52.9, 45.4, 45.4, 44.9, 43.0, 41.2 (q, *J* = 1.7 Hz), 39.5, 39.3, 36.6, 32.9, 25.9, 23.5.

¹⁹F NMR (376 MHz, CDCl₃) δ (ppm) -41.0.

HRMS (ESI+): calculated for C₂₂H₃₁F₃N₅O₂S⁺ [M+H⁺]: 486.2145, found: 486.2146.

HRMS (ESI+): calculated for C₂₂H₃₀ClF₃N₅O₂S⁺ [M_{Cl}+H⁺]: 520.17555, found: 520.1756.

IR (neat): 2922, 2851, 2363, 1722, 1669, 1625, 1587, 1554, 1438, 1349, 1267, 1207, 1103, 969, 793, 760 cm⁻¹.

3.4.5 NMR-Spectra

The Supporting Information including NMR-spectra can be found online at:

<https://pubs.acs.org/doi/10.1021/acs.orglett.1c01870>

(https://pubs.acs.org/doi/suppl/10.1021/acs.orglett.1c01870/suppl_file/ol1c01870_si_001.pdf)

3.4.6 X-Ray Structures and Data

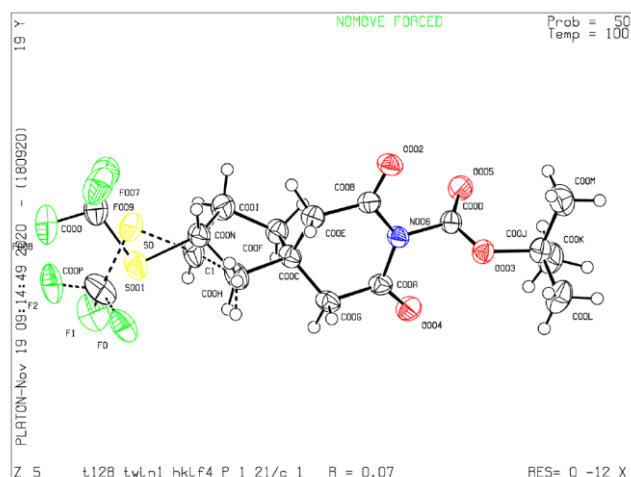


Figure S3-1: Crystal structure of **2e**. (ellipsoids shown at 50% contour percent probability level).

Experimental. Single colourless plate crystals of **2e** (recrystallized from EtOAc in pentane) were used. A suitable crystal with dimensions $0.38 \times 0.24 \times 0.12 \text{ mm}^3$ was selected and mounted on a MITIGEN holder oil on a XtaLAB Synergy R, DW system, HyPix-Arc 150 diffractometer. The crystal was kept at a steady $T = 100.00(10) \text{ K}$ during data collection. The structure was solved with the ShelXT³² solution program using dual methods and by using Olex2 1.3-alpha³³ as the graphical interface. The model was refined with ShelXL 2018/3³² using full matrix least squares minimisation on F^2 . **2e** was refined as a 2-component twin. Twin ratio 0.605(2) : 0.395(2).

Crystal Data. $\text{C}_{15}\text{H}_{20}\text{F}_3\text{NO}_4\text{S}$, $M_r = 367.38$, monoclinic, $P2_1/c$ (No. 14), $a = 13.9942(6) \text{ \AA}$, $b = 10.5800(3) \text{ \AA}$, $c = 12.1529(5) \text{ \AA}$, $\beta = 102.212(4)^\circ$, $\alpha = \gamma = 90^\circ$, $V = 1758.63(12) \text{ \AA}^3$, $T = 100.00(10) \text{ K}$, $Z = 4$, $Z' = 1$, $\mu(\text{Cu K}\alpha) = 2.096$, 5498 reflections measured, 5498 unique ($R_{\text{int}} = .$) which were used in all calculations. The final wR_2 was 0.2140 (all data) and R_1 was 0.0723 ($I \geq 2 \sigma(I)$).

CCDC: 2046602

Compound	2e
Formula	$\text{C}_{15}\text{H}_{20}\text{F}_3\text{NO}_4\text{S}$
$D_{\text{calc.}} / \text{g cm}^{-3}$	1.388
μ / mm^{-1}	2.096
Formula Weight	367.38
Colour	colourless
Shape	plate
Size/ mm^3	$0.38 \times 0.24 \times 0.12$
T / K	100.00(10)
Crystal System	monoclinic
Space Group	$P2_1/c$
$a / \text{Å}$	13.9942(6)
$b / \text{Å}$	10.5800(3)
$c / \text{Å}$	12.1529(5)
α°	90
β°	102.212(4)
γ°	90
$V / \text{Å}^3$	1758.63(12)
Z	4
Z'	1
Wavelength/ Å	1.54184
Radiation type	Cu $K\alpha$
$\theta_{\text{min}}^\circ$	3.231
$\theta_{\text{max}}^\circ$	74.876
Measured Refl's.	5498
Indep't Refl's	5498
Refl's $I \geq 2 \sigma(I)$	5083
R_{int}	.
Parameters	285
Restraints	0
Largest Peak	0.505
Deepest Hole	-0.313
Goof	1.094
wR_2 (all data)	0.2140
wR_2	0.2063
R_1 (all data)	0.0765
R_1	0.0723

3.5 References

- [1] (a) Trost, B. M. Atom Economy – A Challenge for Organic Synthesis: Homogeneous Catalysis Leads the Way. *Angew. Chem. Int. Ed.* **1995**, *34*, 259-281. (b) Newhouse, T.; Baran, P. S.; Hoffmann, R. W. The economies of synthesis. *Chem. Soc. Rev.* **2009**, *38*, 3010-3021.
- [2] (a) Capaldo, L.; Ravelli, D. Hydrogen Atom Transfer (HAT): A Versatile Strategy for Substrate Activation in Photocatalyzed Organic Synthesis. *Eur. J. Org. Chem.* **2017**, *2017*, 2056-2071. (b) Capaldo, L.; Quadri, L. L.; Ravelli, D. Photocatalytic hydrogen atom transfer: the philosopher's stone for late-stage functionalization? *Green Chem.* **2020**, *22*, 3376-3396.
- [3] Xue, X. S.; Ji, P.; Zhou, B.; Cheng, J. P. The Essential Role of Bond Energetics in C-H Activation/Functionalization. *Chem. Rev.* **2017**, *117*, 8622-8648.
- [4] (a) Tzirakis, M. D.; Lykakis, I. N.; Orfanopoulos, M. Decatungstate as an efficient photocatalyst in organic chemistry. *Chem. Soc. Rev.* **2009**, *38*, 2609-2621. (b) Ravelli, D.; Protti, S.; Fagnoni, M. Decatungstate Anion for Photocatalyzed "Window Ledge" Reactions. *Acc. Chem. Res.* **2016**, *49*, 2232-2242. (c) Crespi, S.; Fagnoni, M. Generation of Alkyl Radicals: From the Tyranny of Tin to the Photon Democracy. *Chem. Rev.* **2020**, *120*, 9790-9833.
- [5] Ravelli, D.; Fagnoni, M.; Fukuyama, T.; Nishikawa, T.; Ryu, I. Site-Selective C-H Functionalization by Decatungstate Anion Photocatalysis: Synergistic Control by Polar and Steric Effects Expands the Reaction Scope. *ACS Catal.* **2018**, *8*, 701-713.
- [6] (a) Perry, I. B.; Brewer, T. F.; Sarver, P. J.; Schultz, D. M.; DiRocco, D. A.; MacMillan, D. W. C. Direct arylation of strong aliphatic C-H bonds. *Nature* **2018**, *560*, 70-75. (b) Laudadio, G.; Deng, Y.; van der Wal, K.; Ravelli, D.; Nuno, M.; Fagnoni, M.; Guthrie, D.; Sun, Y.; Noel, T. C(sp³)-H functionalizations of light hydrocarbons using decatungstate photocatalysis in flow. *Science* **2020**, *369*, 92-96. (c) Cao, H.; Kuang, Y.; Shi, X.; Wong, K. L.; Tan, B. B.; Kwan, J. M. C.; Liu, X.; Wu, J. Photoinduced site-selective alkenylation of alkanes and aldehydes with aryl alkenes. *Nat. Commun.* **2020**, *11*, 1956. (d) Sarver, P. J.; Bacauanu, V.; Schultz, D. M.; DiRocco, D. A.; Lam, Y. H.; Sherer, E. C.; MacMillan, D. W. C. The merger of decatungstate and copper catalysis to enable aliphatic C(sp³)-H trifluoromethylation. *Nat. Chem.* **2020**, *12*, 459-467.
- [7] (a) Kuang, Y.; Cao, H.; Tang, H.; Chew, J.; Chen, W.; Shi, X.; Wu, J. Visible light driven deuteration of formyl C-H and hydridic C(sp³)-H bonds in feedstock chemicals and

- pharmaceutical molecules. *Chem. Sci.* **2020**, *11*, 8912-8918. (b) Dong, J.; Wang, X.; Wang, Z.; Song, H.; Liu, Y.; Wang, Q. Formyl-selective deuteration of aldehydes with D₂O via synergistic organic and photoredox catalysis. *Chem. Sci.* **2020**, *11*, 1026-1031.
- [8] (a) Halperin, S. D.; Fan, H.; Chang, S.; Martin, R. E.; Britton, R. A convenient photocatalytic fluorination of unactivated C-H bonds. *Angew. Chem. Int. Ed.* **2014**, *53*, 4690-4693. (b) Meanwell, M.; Lehmann, J.; Eichenberger, M.; Martin, R. E.; Britton, R. Synthesis of acyl fluorides via photocatalytic fluorination of aldehydic C-H bonds. *Chem. Commun.* **2018**, *54*, 9985-9988.
- [9] See ref 20c.
- [10] Toulgoat, F.; Alazet, S.; Billard, T. Direct Trifluoromethylthiolation Reactions: The “Renaissance” of an Old Concept. *Eur. J. Org. Chem.* **2014**, *2014*, 2415-2428.
- [11] (a) Leroux, F.; Jeschke, P.; Schlosser, M. α -Fluorinated Ethers, Thioethers, and Amines: Anomerically Biased Species. *Chem. Rev.* **2005**, *105*, 827-856. (b) Landelle, G.; Panossian, A.; Leroux, F. R. Trifluoromethyl ethers and -thioethers as tools for medicinal chemistry and drug discovery. *Curr. Top. Med. Chem.* **2014**, *14*, 941-951. (c) Boiko, V. N. Aromatic and heterocyclic perfluoroalkyl sulfides. Methods of preparation. *Beilstein J. Org. Chem.* **2010**, *6*, 880-921.
- [12] Chachignon, H.; Cahard, D. State-of-the-Art in Electrophilic Trifluoromethylthiolation Reagents. *Chin. J. Chem.* **2016**, *34*, 445-454.
- [13] (a) Liang, T.; Neumann, C. N.; Ritter, T. Introduction of fluorine and fluorine-containing functional groups. *Angew. Chem. Int. Ed.* **2013**, *52*, 8214-8264. (b) Tlili, A.; Billard, T. Formation of C-SCF₃ bonds through direct trifluoromethylthiolation. *Angew. Chem. Int. Ed.* **2013**, *52*, 6818-6819. (c) Yang, X.; Wu, T.; Phipps, R. J.; Toste, F. D. Advances in catalytic enantioselective fluorination, mono-, di-, and trifluoromethylation, and trifluoromethylthiolation reactions. *Chem. Rev.* **2015**, *115*, 826-870. (d) Barata-Vallejo, S.; Bonesi, S.; Postigo, A. Late stage trifluoromethylthiolation strategies for organic compounds. *Org. Biomol. Chem.* **2016**, *14*, 7150-7182. (e) Xu, X. H.; Matsuzaki, K.; Shibata, N. Synthetic methods for compounds having CF₃-S units on carbon by trifluoromethylation, trifluoromethylthiolation, triflylation, and related reactions. *Chem. Rev.* **2015**, *115*, 731-764.
- [14] (a) Ghiazza, C.; Billard, T.; Tlili, A. Merging Visible-Light Catalysis for the Direct Late-Stage Group-16-Trifluoromethyl Bond Formation. *Chem. Eur. J.* **2019**, *25*, 6482-6495. (b) Yerien, D. E.; Barata-Vallejo, S.; Postigo, A. New visible light organo(metal)-photocatalyzed

- fluoroalkylsulfanylation (RFS-) and fluoroalkylselenolation (RFSe-) reactions of organic substrates. *J. Fluorine Chem.* **2020**, *240*, 109652. (c) Nobile, E.; Castanheiro, T.; Besset, T. Radical-Promoted Distal C-H Functionalization of C(sp³) Centers with Fluorinated Moieties. *Angew. Chem. Int. Ed.* **2021**, *60*, 12170-12191. (d) Zhang, F. G.; Wang, X. Q.; Zhou, Y.; Shi, H. S.; Feng, Z.; Ma, J. A.; Marek, I. Remote Fluorination and Fluoroalkyl(thiol)ation Reactions. *Chem. Eur. J.* **2020**, *26*, 15378-15396.
- [15] (a) Mukherjee, S.; Patra, T.; Glorius, F. Cooperative Catalysis: A Strategy To Synthesize Trifluoromethyl-thioesters from Aldehydes. *ACS Catal.* **2018**, *8*, 5842-5846. (b) Mukherjee, S.; Maji, B.; Tlahuext-Aca, A.; Glorius, F. Visible-Light-Promoted Activation of Unactivated C(sp³)-H Bonds and Their Selective Trifluoromethylthiolation. *J. Am. Chem. Soc.* **2016**, *138*, 16200-16203.
- [16] Xu, W.; Ma, J.; Yuan, X. A.; Dai, J.; Xie, J.; Zhu, C. Synergistic Catalysis for the Umpolung Trifluoromethylthiolation of Tertiary Ethers. *Angew. Chem. Int. Ed.* **2018**, *57*, 10357-10361.
- [17] Xu, W.; Wang, W.; Liu, T.; Xie, J.; Zhu, C. Late-stage trifluoromethylthiolation of benzylic C-H bonds. *Nat. Commun.* **2019**, *10*, 4867.
- [18] (a) Wang, D.; Carlton, C. G.; Tayu, M.; McDouall, J. J. W.; Perry, G. J. P.; Procter, D. J. Trifluoromethyl Sulfoxides: Reagents for Metal-Free C-H Trifluoromethylthiolation. *Angew. Chem. Int. Ed.* **2020**, *59*, 15918-15922. (b) Guo, S.; Zhang, X.; Tang, P. Silver-mediated oxidative aliphatic C-H trifluoromethylthiolation. *Angew. Chem. Int. Ed.* **2015**, *54*, 4065-4069. (c) Wu, H.; Xiao, Z.; Wu, J.; Guo, Y.; Xiao, J. C.; Liu, C.; Chen, Q. Y. Direct trifluoromethylthiolation of unactivated C(sp³)-H using silver(I) trifluoromethanethiolate and potassium persulfate. *Angew. Chem. Int. Ed.* **2015**, *54*, 4070-4074. (d) Zhao, Y.; Lin, J. H.; Hang, X. C.; Xiao, J. C. Ag-Mediated Trifluoromethylthiolation of Inert C(sp³)-H Bond. *J. Org. Chem.* **2018**, *83*, 14120-14125. (e) Xia, Y.; Wang, L.; Studer, A. Site-Selective Remote Radical C-H Functionalization of Unactivated C-H Bonds in Amides Using Sulfone Reagents. *Angew. Chem. Int. Ed.* **2018**, *57*, 12940-12944. (f) Modak, A.; Pinter, E. N.; Cook, S. P. Copper-Catalyzed, N-Directed C(sp³)-H Trifluoromethylthiolation (-SCF₃) and Trifluoromethylselenation (-SeCF₃). *J. Am. Chem. Soc.* **2019**, *141*, 18405-18410.
- [19] Munavalli, S.; Rohrbaugh, D. K.; Rossman, D. I.; Berg, F. J.; Wagner, G. W.; Durst, H. D. Trifluoromethylsulfenylation of Masked Carbonyl Compounds. *Synth. Commun.* **2000**, *30*, 2847-2854.

- [20] (a) Wang, M. Y.; Zhu, X. Q.; Zhang, X. L.; Guo, R. L.; Jia, Q.; Wang, Y. Q. Synthesis of trifluoromethylthioesters from aldehydes via a visible light-promoted radical process. *Org. Biomol. Chem.* **2020**, *18*, 5918-5926. (b) Dong, J.; Yue, F.; Wang, X.; Song, H.; Liu, Y.; Wang, Q. Light-Mediated Difluoromethylthiolation of Aldehydes with a Hydrogen Atom Transfer Photocatalyst. *Org. Lett.* **2020**, *22*, 8272-8277. (c) During the first submission of our manuscript, a DT-based protocol for the synthesis of trifluoromethylthioesters from aromatic aldehydes was published: 8 mol% TBADT (instead of 2.5 mol%), 3.0 eq. of PhthSCF₃ (instead of 1.5 eq. of ArCHO (inverse stoichiometry)), and 1.5 eq. of Na₂HPO₄ (instead of base-free) are required to achieve comparable yields (e.g., **2v** (78% instead of 84%), **2ae** (55% instead of 53%)) after 96 h (instead of 6 h). Neither aliphatic aldehydes nor alkanes are functionalized in this report. Wang, X.; Dong, J.; Liu, Y.; Song, H.; Wang, Q. Decatungstate as a direct hydrogen atom transfer photocatalyst for synthesis of trifluoromethylthioesters from aldehydes. *Chin. Chem. Lett.* **2021**, *32*, 3027-3030.
- [21] Topcu, G.; Ulubelen, A.; Tam, T. C.-M.; Che, C.-T. Norditerpenes and Norsesterterpenes from *Salvia yosgadensis*. *J. Nat. Prod.* **1996**, *59*, 113-116.
- [22] Fahlbusch, K.-G.; Hammerschmidt, F.-J.; Panten, J.; Pickenhagen, W.; Schatkowski, D.; Bauer, K.; Garbe, D.; Surburg, H. *Ullmann's Encyclopedia of Industrial Chemistry*; Wiley-VCH: Weinheim, Germany, **2000**.
- [23] Pearson, C. M.; Parks, A.; Landazuri, P. *Neurosurgical Neuropsychology* (Eds.: C. M. Pearson, E. Ecklund-Johnson, S. D. Gale), Academic Press: San Diego, **2019**; pp 99-112.
- [24] (a) Fulmer, G. R.; Miller, A. J. M.; Sherden, N. H.; Gottlieb, H. E.; Nudelman, A.; Stoltz, B. M.; Bercaw, J. E.; Goldberg, K. I. NMR Chemical Shifts of Trace Impurities: Common Laboratory Solvents, Organics, and Gases in Deuterated Solvents Relevant to the Organometallic Chemist. *Organometallics* **2010**, *29*, 2176-2179; (b) Gottlieb, H. E.; Kotlyar, V.; Nudelman, A. NMR Chemical Shifts of Common Laboratory Solvents as Trace Impurities. *J. Org. Chem.* **1997**, *62*, 7512-7515.
- [25] Nasri, S.; Zahou, I.; Turowska-Tyrk, I.; Roisnel, T.; Loiseau, F.; Saint-Amant, E.; Nasri, H. Synthesis, Electronic Spectroscopy, Cyclic Voltammetry, Photophysics, Electrical Properties and X-ray Molecular Structures of *meso*-{Tetrakis[4-(benzoyloxy)phenyl]porphyrinato}zinc(II) Complexes with Aza Ligands. *Eur. J. Inorg. Chem.* **2016**, *2016*, 5004-5019.

- [26] Andersen, T. L.; Donslund, A. S.; Neumann, K. T.; Skrydstrup, T. Carbonylative Coupling of Alkyl Zinc Reagents with Benzyl Bromides Catalyzed by a Nickel/ NN_2 Pincer Ligand Complex. *Angew. Chem. Int. Ed.* **2018**, *57*, 800-804.
- [27] Pansuwan, H.; Ditmangklo, B.; Vilaivan, C.; Jiangchareon, B.; Pan-In, P.; Wanichwecharungruang, S.; Palaga, T.; Nuanyai, T.; Suparpprom, C.; Vilaivan, T. Hydrophilic and Cell-Penetrable Pyrrolidinyl Peptide Nucleic Acid via Post-synthetic Modification with Hydrophilic Side Chains. *Bioconjug. Chem.* **2017**, *28*, 2284-2292.
- [28] Schwarz, J. L.; Huang, H.-M.; Paulisch, T. O.; Glorius, F. Dialkylation of 1,3-Dienes by Dual Photoredox and Chromium Catalysis. *ACS Catal.* **2019**, *10*, 1621-1627.
- [29] Kurimoto, Y.; Nasu, T.; Fujii, Y.; Asano, K.; Matsubara, S. Asymmetric Cycloetherification of in Situ Generated Cyanohydrins through the Concomitant Construction of Three Chiral Carbon Centers. *Org. Lett.* **2019**, *21*, 2156-2160.
- [30] Calamai, E.; Dall'Angelo, S.; Koss, D.; Domarkas, J.; McCarthy, T. J.; Mingarelli, M.; Riedel, G.; Schweiger, L. F.; Welch, A.; Platt, B.; Zanda, M. ^{18}F -barbiturates are PET tracers with diagnostic potential in Alzheimer's disease. *Chem. Commun.* **2013**, *49*, 792-794.
- [31] Bonacorsi, S. J.; Burrell, R. C.; Luke, G. M.; DePue, J. S.; Kent Rinehart, J.; Balasubramanian, B.; Christopher, L. J.; Iyer, R. A. S. Synthesis of the anxiolytic agent [^{14}C] 6-hydroxy-buspirone for use in a human ADME study. *J. Label. Compd. Rad.* **2007**, *50*, 65-71.
- [32] (a) Sheldrick, G. M. Crystal structure refinement with *SHELXL*. *Acta Cryst. C* **2015**, *71*, 3-8.
(b) Sheldrick, G. M. *SHELXT* - Integrated space-group and crystal-structure determination. *Acta Cryst. A* **2015**, *71*, 3-8.
- [33] Dolomanov, O. V.; Bourhis, L. J.; Gildea, R. J.; Howard, J. A. K.; Puschmann, H. *J. OLEX2*: a complete structure solution, refinement and analysis program. *Appl. Cryst.* **2009**, *42*, 339-341.

CHAPTER 4

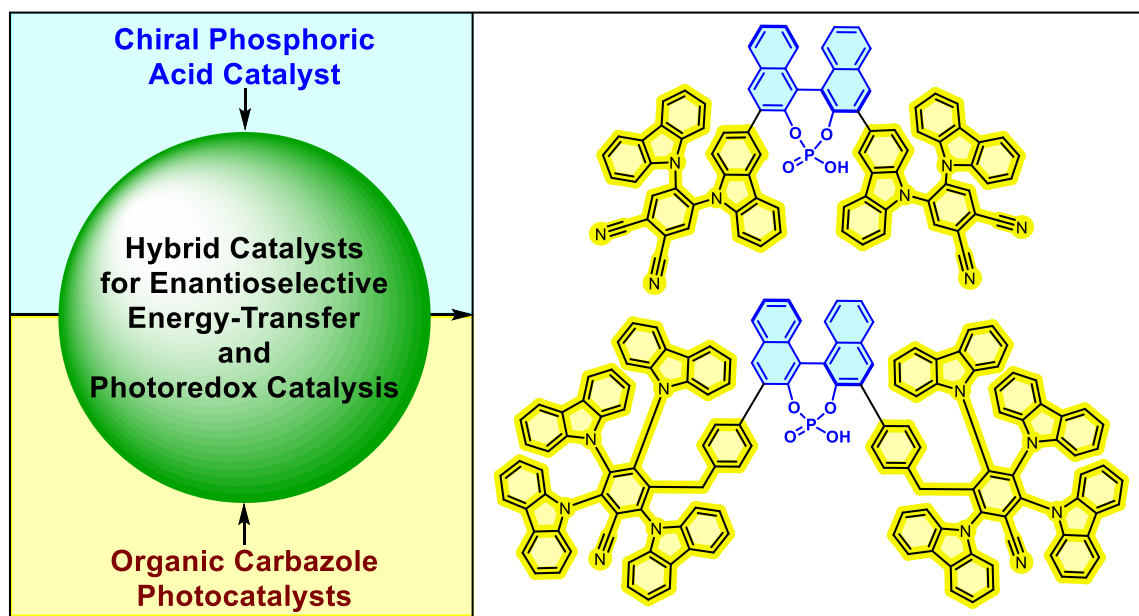
4 Hybrid Catalysts for Enantioselective Photo-Phosphoric Acid Catalysis

At the date of submission of this thesis, a version of this chapter has been submitted for publication and is undergoing revision. Additionally, it was submitted to ChemRxiv and can be found under: A. B. Rolka, F. D. Toste, B. König, **2023**, DOI: 10.26434/chemrxiv-2023-0v38p.

A. B. Rolka conceived the project, conducted the experiments, and wrote the manuscript. F. D. Toste and B. König supervised the project.

Abstract

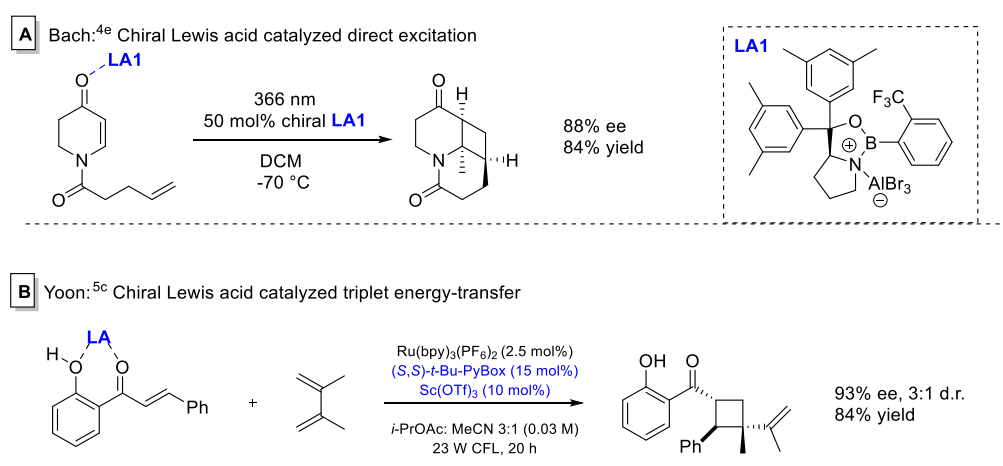
The syntheses of two novel, organic and chiral photocatalysts are presented. By combining donor-acceptor cyanoarene-based photocatalysts with a chiral phosphoric acid, bifunctional catalysts have been designed. In preliminary proof-of-concept reactions, their use in both enantioselective energy-transfer and photoredox catalysis was demonstrated.



4.1 Introduction

Within the rapidly expanding field of photocatalysis, the development of enantioselective transformations remains challenging due to the high reactivity and transient nature of photo-excited intermediates. A particular challenge in this area is the suppression of uncatalyzed background processes that give rise to undesired racemic product. To tackle this problem, creative strategies have been developed¹⁻³ such as utilizing chiral Lewis acid catalysis in conjunction with a separate photocatalyst or via direct excitation of the substrate. Within these strategies, the role of the chiral Lewis acid for the enantioselectivity of the photocatalyzed reaction can be manifold as has been elegantly shown by pioneering work of the groups of Bach⁴, Yoon⁵ and Meggers.⁶

One such mode of enantioinduction via a chiral Lewis acid was shown by the Bach group in the [2+2] photocycloaddition of enones (Scheme 4-1A).^{4e} In this example, coordination of chiral Lewis acid **LA1** to the substrate results in a change in the substrate's absorption properties and leads to a red shift by lowering the energy of the LUMO, rendering an uncoordinated racemic background reaction less feasible as compared to excitation of the chiral Lewis acid substrate complex. While this strategy relies on direct excitation of the substrate, the work of Yoon introduced the use of a chiral Lewis acid for enantioselective triplet energy-transfer catalysis that proceeds with a discrete photocatalyst separate from the Lewis acid (Scheme 4-1B).^{5c} In this case, the coordination of the chiral Lewis acid complex to 2'-hydroxychalcones causes a significant lowering of the triplet energy of the substrate, allowing for selective excitation and subsequent enantioselective control.



Scheme 4-1: Chiral Lewis acid catalysis for enantioselective photocatalysis.

In addition to utilizing Lewis acids to enable enantioselective photocatalytic processes, the use of another secondary mode of catalysis is of particular importance in this field: hydrogen bonding catalysis.^{1b,3} This non-covalent interaction has been established as a powerful method to control the selectivity of photocatalytic transformations leading to the existence of a multitude of chiral catalysts containing a hydrogen bonding site. The first bifunctional hydrogen bonding photocatalyst for an intramolecular enantioselective [2+2] photocycloaddition of quinolones was introduced in 2002 by Krische et al. and utilized benzophenone as a sensitizing moiety (Figure 4-1).⁷

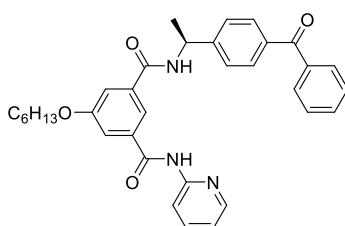
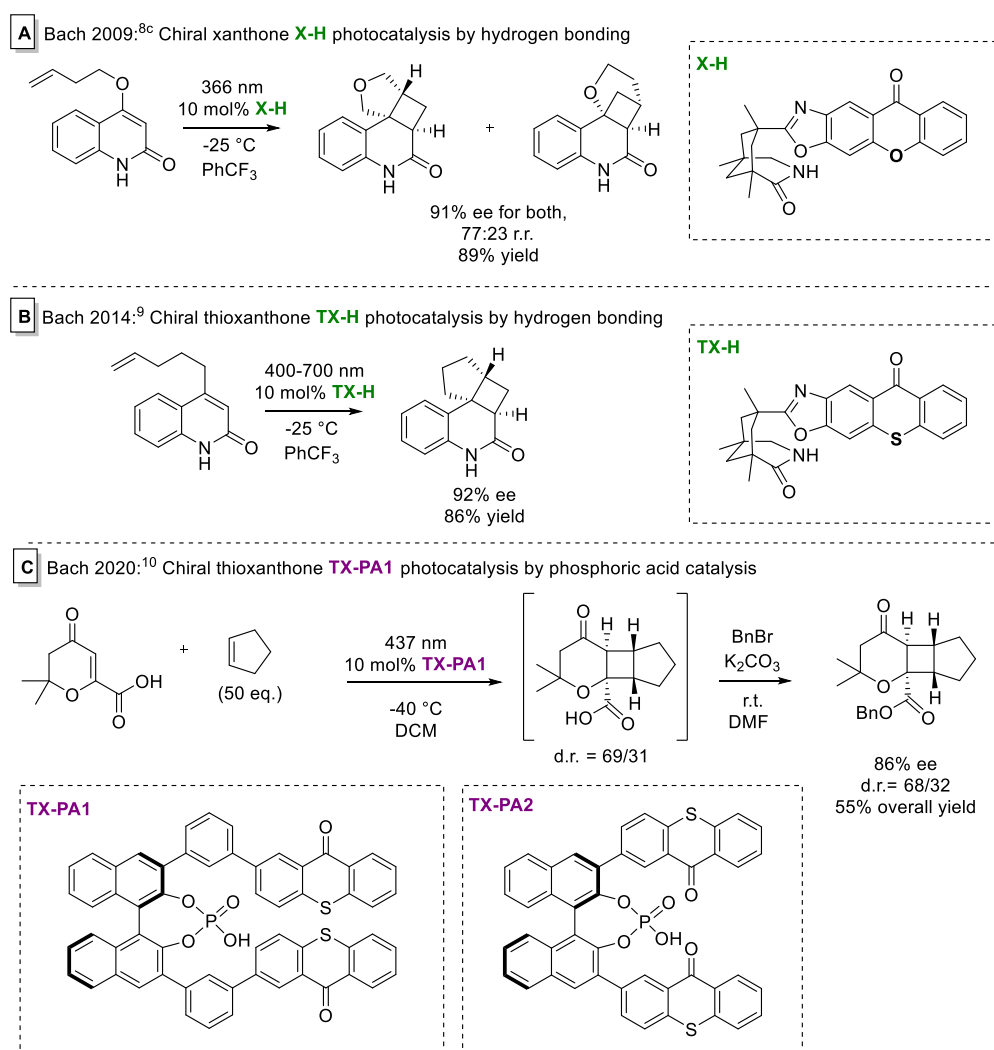


Figure 4-1: Structure of the chiral hydrogen bonding catalyst introduced by Krische.⁷

While this example was important in demonstrating the potential of enantioselective catalysis via sensitization by a photocatalyst with a pendant chiral motif, it suffers from relatively poor enantioselectivities. Since then, the Bach group has developed modified catalysts that result in higher selectivities, first by attaching a benzophenone photosensitizer to a lactam backbone and later by improving on this structure through the incorporation of a xanthone photosensitizer (xanthone catalyst shown in Scheme 4-2A).^{3,8}

Despite the success of these catalysts in chiral photocatalysis, their ability to promote competing hydrogen atom abstraction reactions results in decomposition of the catalyst that limits their long-term stability. Further, both benzophenone and xanthone absorb light in the ultraviolet region, which often has sufficiently high energy to directly excite substrates resulting in undesired background reactions. In 2014, the Bach group overcame this wavelength limitation by presenting the synthesis of a chiral thioxanthone, allowing for the use of visible light in an enantioselective [2+2] photocycloaddition (Scheme 4-2B).⁹



Scheme 4-2: Chiral xanthere and thioxanthere catalysts for enantioselective photocatalysis.

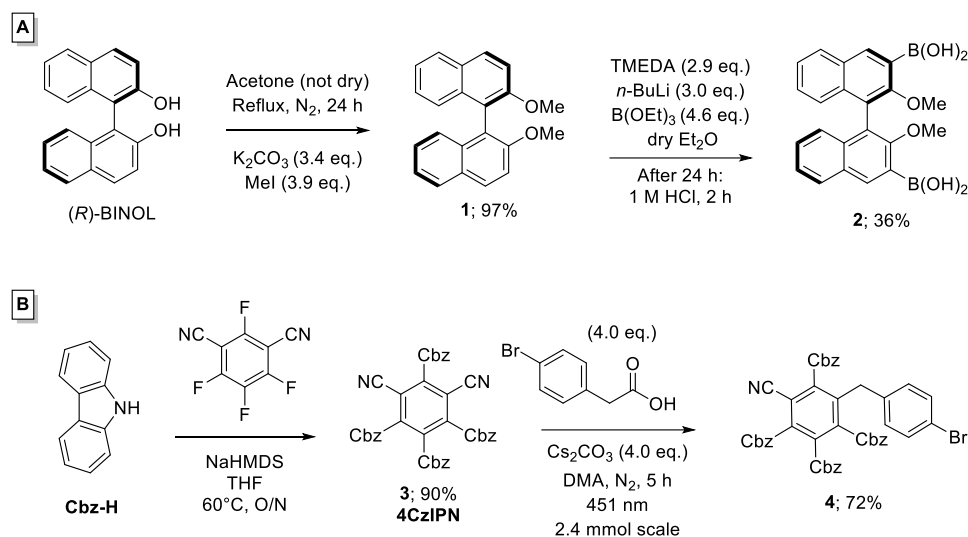
Building on the thioxanthere scaffold six years later, the group further enhanced its reactivity by combining this photocatalyst with a different hydrogen-bonding motif in the form of chiral phosphoric acids to yield novel bifunctional catalysts **TX-PA1** and **TX-PA2** (Scheme 4-2C).¹⁰ Shortly thereafter, the group of Masson independently reported the synthesis of **TX-PA2** and its monosubstituted C₁-symmetric-derivate featuring only one thioxanthere moiety.^{11h} The utility of **TX-PA1** to promote enantioselective processes was demonstrated in a [2+2] intermolecular cycloaddition reaction with β -carboxyl-substituted cyclic enones. The chiral phosphoric acid moiety binds to the carboxylic acid by means of two hydrogen bonds, allowing for the transference of chirality, while the attached thioxanthere moieties induce the energy transfer process. Enantiomeric ratios of up to 93:7 were achieved, albeit with only a relatively small substrate scope

and with overall low yields. Despite the achievements of bifunctional thioxanthone-based catalysts in the field of enantioselective photocatalysis,¹¹ the ability to further modifying the thioxanthone photocatalyst core of these chiral catalysts has proven limited and modifications are usually focusing on the attached chiral backbone, and not the photocatalyst itself. This has so far restricted the ability to address limitations resulting from the photophysical properties of these chiral thioxanthone-photocatalysts, such as unmatched redox potentials or insufficient triplet energies.¹² For example, in the case of **TX-PA1**, the authors noted that the triplet energy of this modified thioxanthone was significantly lowered as compared to the parent thioxanthone **thioxanthen-9-one** (from 272 kJ/mol to 235 kJ/mol). This need for bifunctional phosphoric acid photocatalysts with more readily tuned photophysical properties inspired us to think about alternative catalyst structures that would allow for increased design flexibility.

Specifically, we were interested in the introduction of well-known donor-acceptor cyanoarene-based photocatalysts into the backbone of chiral phosphoric acids. We were especially attracted to this family of photocatalysts because of their extensively studied photophysical properties and their known understanding of how structural changes result in a tuning of these properties. This tuning is achieved by changing the donors and acceptors, which in turn change the charge transfer characteristics of the catalyst and therefore their redox and photophysical properties.¹³ Within this wide class of carbazole-based photocatalysts, we were particularly excited by the inexpensive organic dye **4CzIPN** which has found tremendous applications in photocatalysis¹⁴ since its introduction in 2012 originally in the context of OLED research.¹⁵ The widespread adoption of this catalyst is due to its promising photophysical properties, including a high photoluminescence quantum yield (up to 94.6%) and a long lifetime in the excited state. Additionally, the wide redox potential window that is comparable to that of commonly utilized Ru- and Ir-polypyridyl catalysts combined with a high chemical stability make this system a particularly robust catalyst choice. Furthermore, carbazole-based photocatalysts have found utility as both effective photoredox catalysts as well as highly efficient energy transfer catalysts.^{16, 17} On the basis of these promising features, we hypothesized that novel chiral catalysts derived from the union of chiral phosphoric acids and donor-acceptor cyanoarene-based photocatalysts would open new chemical space in both enantioselective visible light-mediated photoredox and energy transfer catalysis.

4.2 Synthesis and challenges

For the reasons discussed above, we started our synthetic approach with the goal of attaching a **4CzIPN** derived moiety to a BINOL-based chiral phosphoric acid. We envisioned starting our synthesis of this new chiral photocatalyst from the literature reported chiral BINOL boronic acid **2** (Scheme 4-3A).^{18,19}

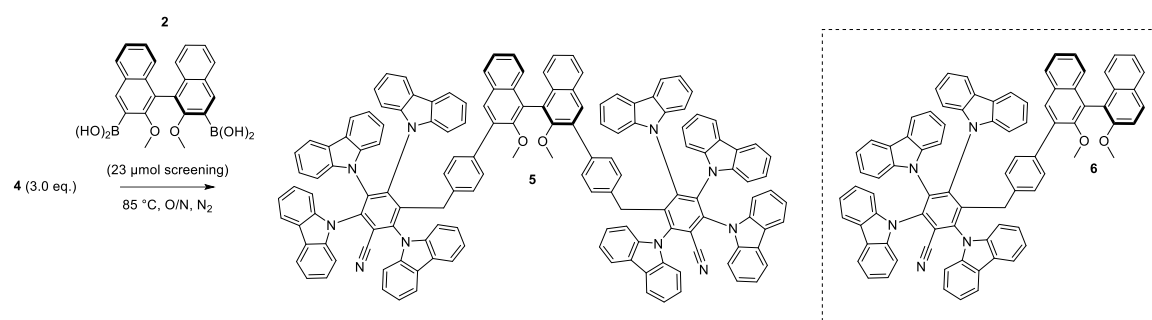


Scheme 4-3: Synthesis of chiral boronic acid **2** (A) and brominated **4CzIPN**-derivative **4** (B).

From this intermediate, a Suzuki coupling with a brominated analogue **4** of **4CzIPN** was envisioned to allow for the desired union of the photocatalyst with the BINOL backbone of what will become the phosphoric acid.¹⁹ Inspired by earlier reports from our group about photosubstitution reactions of the nitrile group at **4CzIPN** and **2CzPN**, we considered leveraging this photoredox radical coupling for the synthesis of the necessary brominated **4CzIPN** derivative **4**.²⁰ To our delight, the previously unreported reaction of **4CzIPN** (**3**) with 4-bromophenylacetic acid gave the desired product **4** without any detrimental effects due to the presence of the potentially reactive aryl bromide (Scheme 4-3B, second step). This functionalization reaction proceeded in good yield when performed on a small scale (60 μ mol) using irradiation from below via a 451 nm LED plate through the bottom of 5 mL crimp cap vials; however, scaling up the reaction to a synthetically useful 2.4 mmol using a Kessil lamp ($\lambda_{\text{max}} = 440$ nm), yielded just 42% of the desired substrate after 1 h reaction time, in contrast to the 70% observed on the 60 μ mol scale under otherwise identical conditions. By doubling the concentration and increasing the time to 5 h, a 72% isolated yield was achieved on a 2.4 mmol scale (Scheme 4-3B).

Next, the palladium cross coupling of **4** and **2** was investigated (Table 4-1). Solubility issues of **4** in commonly used solvents for Suzuki coupling, such as 1,4 dioxane/water (entry 1), resulted in low yield; therefore, DMF was added as a third co-solvent (entry 2) to increase solubility and yield. Using only a DMF/water mixture (entry 3) resulted in similar yields as 1,4-dioxane/water and provided worse results than the three solvent system. Doubling the catalyst loading (entry 4) or increasing the equivalents of base (entry 5) did not have major impacts on the yield.

Table 4-1: Optimization of the cross coupling of **4** with **2**.

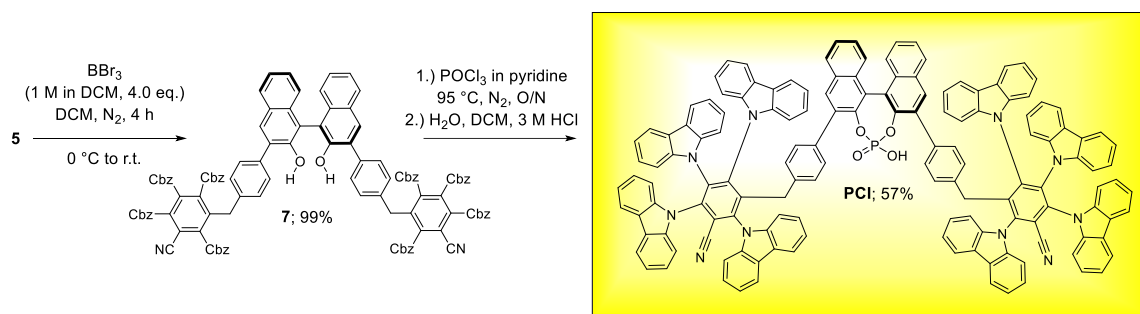


Entry	Pd (10 mol%)	Base (3.0 eq.)	Solvent	Yield (%)
1	Pd(PPh ₃) ₄	Ba(OH) ₂ ·8H ₂ O	1,4-dioxane: water (3:1)	26 ^a
2	Pd(PPh ₃) ₄	Ba(OH) ₂ ·8H ₂ O	1,4-dioxane: water: DMF (3:1:2)	42 ^a
3	Pd(PPh ₃) ₄	Ba(OH) ₂ ·8H ₂ O	water: DMF (3:1)	27 ^a
4	^c Pd(PPh ₃) ₄	Ba(OH) ₂ ·8H ₂ O	1,4-dioxane: water: DMF (3:1:2)	35 ^b
5	Pd(PPh ₃) ₄	^d Ba(OH) ₂ ·8H ₂ O	1,4-dioxane: water: DMF (3:1:2)	37 ^b
6	Pd(PPh ₃) ₄	Na ₂ CO ₃	1,4-dioxane: water: DMF (3:1:2)	20 ^a
7	Pd(PPh₃)₄	Cs₂CO₃	1,4-dioxane: water: DMF (3:1:2)	45^b

^a ¹H NMR yield based upon mesitylene as internal standard. ^b Isolated yield. ^c Catalyst loading of 20 mol%. ^d 10.0 eq. instead of 3.0 eq. were used.

Testing different palladium sources (e.g. Pd(dppf)Cl₂·DCM) and different solvents (e.g. dichloroethane) also gave very low yields. Changing the base to sodium carbonate decreased the yield (entry 6), while using cesium carbonate in the solvent system gave the best result with 45% isolated yield (entry 7) of the desired coupled product **5**. The remaining mass balance was attributed to the formation of monocoupled product **6** (26% isolated yield) and a mixture of starting material **4** and debrominated starting material. With sufficiently optimized conditions in hand, the Suzuki coupling was scaled up from the optimization scale of 23 μmol to a 0.7 mmol scale without significant impact on the yield (43% isolated yield).

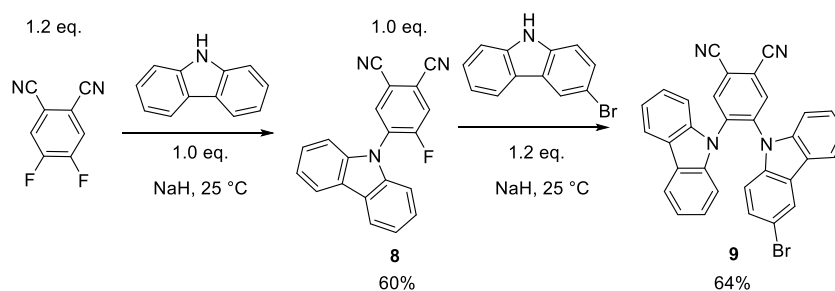
Next, demethylation to produce the free binaphthol necessary for the introduction of the phosphoric acid was explored. Using BBr_3 (4.0 eq., 1 M in DCM),^{10,19} the demethylation of **5** proceeded smoothly and resulted in quantitative formation of **7** without the need for purification by column chromatography (Scheme 4-4, first step).



Scheme 4-4: Synthesis of **PCI** via demethylation of **5** to **7**.

In the final step, the phosphoric acid moiety was introduced (Scheme 4-4, second step).²¹ After purification via recrystallization induced selective precipitation of impurities from hot MeCN followed by column chromatography, the final desired bifunctional catalyst **PCI** was obtained as bright yellow crystals.

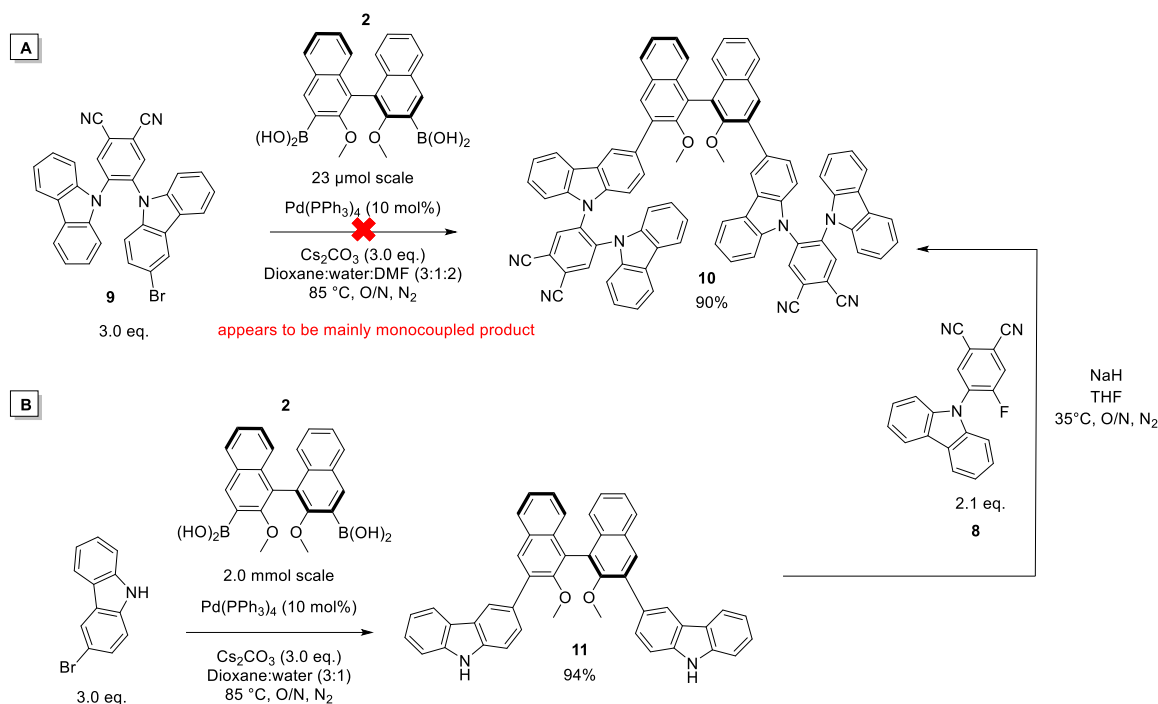
Next, we envisioned a synthetic route towards a bifunctional catalyst consisting of the chiral phosphoric acid backbone and **2CzPN** as the attached photocatalyst, motivated by positive reports on the performance of **2CzPN** as an energy transfer catalyst.²² To achieve this, a slightly different approach was used to access a brominated derivative of **2CzPN** (**9**) as depicted in Scheme 4-5. Even though the synthesis of **9** was described in the literature,²³ our attempts at replicating the reported procedure for the synthesis of intermediate **8** were hindered by both incomplete reactivity and over addition of the carbazole, which presented challenging issues related to purification. Attempts to optimize the reaction conditions to give **8** in a quantitative yield were unsuccessful and instead a mixture of **8**, starting material and double substituted material (**2CzPN**) was obtained in all cases. Purification of this mixture by column chromatography was not trivial. By observing that the desired molecule **8** displayed lower solubilities in chloroform and DCM than the symmetric unwanted products (difluoro starting material and **2CzPN**), we were able to develop a new purification process to obtain clean **8** through multiple rounds of washes with chloroform/DCM.



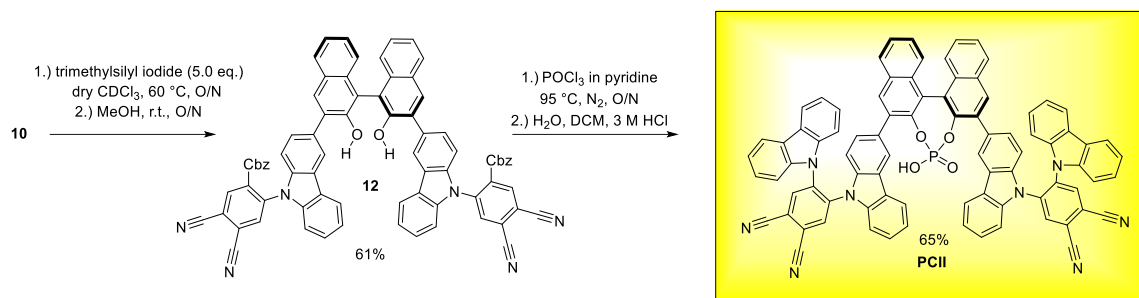
Scheme 4-5: Synthesis of brominated **2CzPN**-derivative **9** and monosubstituted **8**.

Pure **9** was then submitted to the previously optimized conditions of the Suzuki coupling of **4**; namely a solvent mixture of 1,4-dioxane, water and DMF with Cs_2CO_3 as base and $\text{Pd}(\text{PPh}_3)_4$ as the palladium catalyst (Scheme 4-6A). Surprisingly, no desired cross-coupled product **10** was observed, and only what was assigned to be the monocoupled product was obtained. We hypothesized that this lack of bis-coupling may be due to the increased steric hindrance of attaching the photocatalyst moiety directly at the carbazole, rather than by an additional benzylic linker as it was the case in the synthesis for **5**.

As such, an alternative route was explored, allowing a stepwise introduction of the steric bulk (Scheme 4-6B). First, the sterically less demanding 3-bromocarbazole was submitted to a Suzuki coupling, yielding **11** in an excellent yield of 94%. We envisioned taking advantage of the reduced steric bulk surrounding the carbazole nitrogen to introduce the remainder of the photocatalyst through a nucleophilic aromatic coupling strategy. Gratifyingly, this coupling of **11** with aryl fluoride **8** was successful and produced desired intermediate **10** in 90% yield. It is noteworthy that the nucleophilic substitution leading to **10** was only achieved using NaH and not when using NaHMDS, the latter of which is often used in the synthesis of **2CzPN** or **4CzIPN**.^{20a}

Scheme 4-6: Strategies to access **10**.

After obtaining the desired coupled product **10**, the demethylation conditions that worked well for catalyst **PCI** precursor **5** were applied (1 M BBr_3 in DCM, 4.0 eq.). Unfortunately, these conditions only led to the decomposition of **10**. Utilizing less harsh reaction conditions, such as lowering the temperature of the BBr_3 reaction to -78 °C before quenching at room temperature or using AlCl_3 ²⁴ in place of BBr_3 , also failed to give the desired product and only resulted in the formation of decomposition products. The use of pyridinium hydrochloride neat at 200 °C was next explored²⁵ but resulted in no conversion of the starting material **10**. By doubling the equivalents of BBr_3 from 4 to 8 at a reaction temperature of -78 °C, while also quenching the reaction mixture at this low temperature, a new compound was obtained that was identified to be monodemethylated **10**. However, neither longer reaction times (1-6 h) nor more equivalents of BBr_3 were able to push the reaction to complete demethylation. Finally, it was found that using trimethylsilyl iodide²⁶ in dry deuterated chloroform followed by quenching with methanol overnight produced the desired doubly demethylated catalyst precursor **12** in a moderate yield of 61% (Scheme 4-7, step 1).



Scheme 4-7: Synthesis of **PCII** via demethylation of **10** to **12**.

Targeting the formation of **PCII**, the free binaphthol **12** was then submitted to the same phosphorylation conditions as was used previously on **7** for the synthesis of **PCI**. However, in this case it is worth mentioning that the resulting ^{31}P -NMR showed three singlet phosphorus signals in proximity at ppm = 0.56, 0.76, 0.92 in $\text{DMSO}-d_6$. Conformational restrictions resulting in the formation of diastereomers at phosphorus were suspected to be a potential cause of this observation. Therefore, high temperature NMR studies in DMSO were carried out. However, these experiments proved inconclusive as heating the sample to 368 K (95 °C) did not result in coalescence of the signals. Further, neither different column chromatographic purification conditions nor recrystallization led to any observable change in the ratio of the signals in the NMR spectra (^1H and ^{31}P).

We next wanted to confirm that none of these observed phosphorus peaks correspond to the intermediate phosphoryl chloride that is formed before hydrolysis to the desired phosphoric acid. To do so, the phosphoryl chloride was selectively synthesized, and a ^{31}P -NMR was recorded²⁷ (See experimental part). The measured shift significantly differs from the acid (by around 2 ppm in CDCl_3), but also showed multiple peaks. Therefore, it can be concluded that the chloride is not the source for the three signals. Since HRMS and ^1H -NMR indicate that the desired phosphoric acid photo catalyst **PCII** was synthesized, we believe that **PCII** was obtained, and that splitting was caused by conformational effects. **PCII** was therefore used in the following proof-of-concept reactions.

4.3 Proof-of-concept reactions

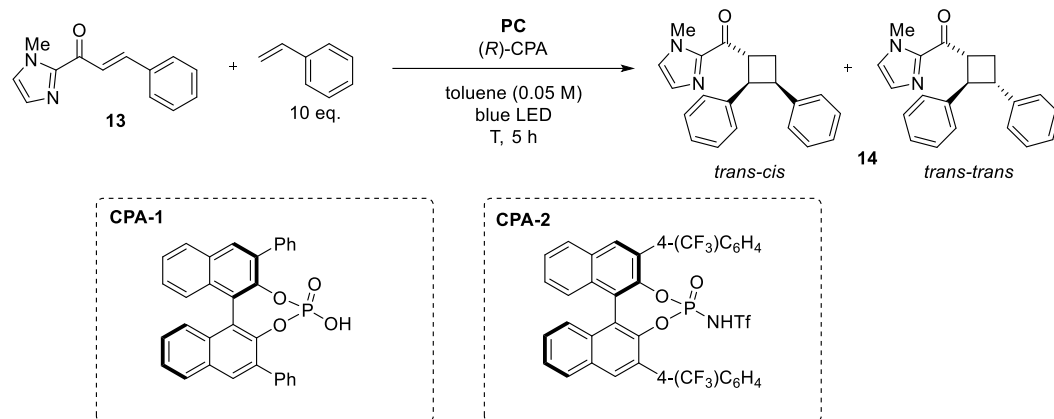
After the successful synthesis of the two novel bifunctional catalysts **PCI** and **PCII**, we first wanted to test their ability to induce chirality in known photochemical reactions. We were particularly interested in investigating whether the two catalysts can promote both asymmetric energy transfer and photoredox catalysis. For this purpose, two proof-of-concept dual catalytic reactions were picked from the literature to evaluate the competency and performance of our catalysts. In both reactions, the original conditions relied upon a chiral phosphoric acid for asymmetric induction and a discrete photocatalyst for substrate activation.

The first investigated reaction was the energy transfer-catalyzed [2+2] cycloaddition depicted in Table 4-2 that was first published in a racemic fashion in 2020 by the group of Yoon.²⁸ In the achiral version, a ruthenium catalyst can only effectively excite the imidazole substrate **13** in the presence of the acid *p*-TsOH (20 mol%), as the acid co-catalyst facilitates the triplet energy transfer of the photocatalyst (Table 4-2, entries 1-4). A year later, the group published a chiral version of this reaction utilizing 1 mol% of [Ir(Fppy)₂(dtbbpy)]PF₆ as photocatalyst with 20 mol% chiral BINOL-derived phosphoric acids **CPA-1** and **CPA-2** (entries 5-7).²⁹ At room temperature, their initial conditions utilizing **CPA-1** resulted in 72% yield with 37% enantiomeric excess (ee) and a diastereomeric ratio (d.r.) of 1:2 favoring the *trans-trans* **14** over the *trans-cis* product **14** (entry 5). Interestingly, when switching to the more acidic *N*-triflyl phosphoramidate derivative of the chiral acid (**CPA-2**), they observed that no photocatalyst is needed at all and they can achieve similar yields via direct excitation with 20 mol% acid in high ee (97%) and high, but reversed, d.r. (6:1 for the *trans-cis* product) when the temperature is lowered to -78 °C (entry 8).

Utilizing solely 5 mol% of **PCI** with the same solvent system as reported by the Yoon group, an ee of 35% was achieved at room temperature (entry 9) with a yield of 70% while slightly favoring the *trans-trans* product **14** with a d.r. of 1:1.3 (*trans-cis:trans-trans*). **PCII** achieves similar yields (72%), albeit with a slightly lower enantioselectivity of 27% ee at room temperature but with better diastereoselectivity of 1:1.6 favoring the *trans-trans* product of **14** (entry 11). As higher enantiomeric values and better d.r.'s were observed by the Yoon group when lowering the reaction temperature to -78 °C, we investigated the effects of low temperature for our catalysts as well (entries 10 and 12). We were delighted to find that upon lowering the temperature to -78 °C, both photocatalysts gave improved enantioselectivities, with **PCII** producing 65% ee with a simultaneously improved yield of 80% (entry 12). As observed in the original publication by the

Yoon group, the diastereoselectivity also improved, now favoring the *trans-cis* product of **14** with a moderate d.r. of 3.8:1.

Table 4-2: Energy transfer-catalyzed [2+2]-cycloaddition as a proof-of-concept reaction.



Entry	PC	CPA ^c	Temp. T (°C)	Yield (%) ^e	ee (%)	d.r. ⁱ
1 ^a	None	None	r.t.	0	nd ^f	-
2 ^a	Ru(bpy) ₃ Cl ₂ (2.5 mol%)	None	r.t.	11	nd ^f	1:2
3 ^a	None	<i>p</i> -TsOH	r.t.	Trace	nd ^f	-
4 ^a	Ru(bpy) ₃ Cl ₂ (2.5 mol%)	<i>p</i> -TsOH	r.t.	75	nd ^f	1:2
5 ^b	Ir(Fppy) ₂ (dtbbpy)PF ₆ (1 mol%)	CPA-1	r.t.	72	37 ^g	1:2
6 ^b	Ir(Fppy) ₂ (dtbbpy)PF ₆ (1 mol%)	CPA-1	-78	83	81 ^g	4:1
7 ^b	Ir(Fppy) ₂ (dtbbpy)PF ₆ (1 mol%)	CPA-2	-78	74	95 ^g	7:1
8 ^b	None	CPA-2	-78	71	97 ^g	6:1
9	PCI (5 mol%)	None	r.t. ^d	70	35 ^h	1:1.3
10	PCI (5 mol%)	None	-78	63	54 ^h	2.2:1
11	PCII (5 mol%)	None	r.t. ^d	72	27 ^h	1:1.6
12	PCII (5 mol%)	None	-78	80	65 ^h	3.8:1

^aEntries and values from the original publication of the Yoon group.²⁸ Reaction was carried out in MeCN for 16 h with non-chiral acids.

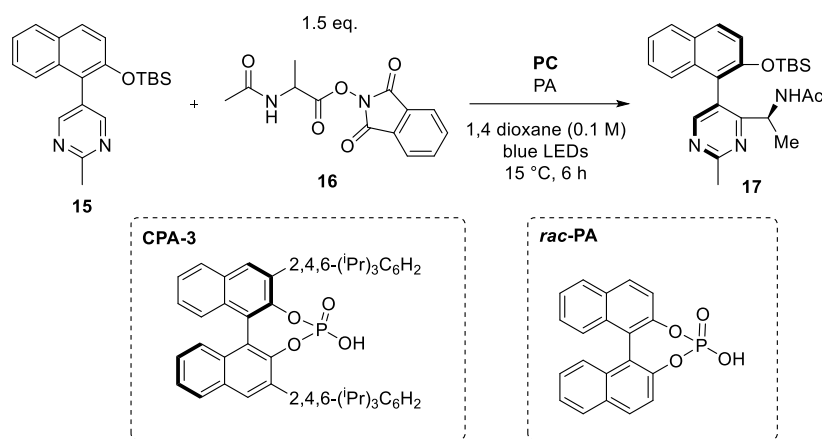
^bEntries and values from the original publication of the Yoon group.²⁹ ^c20 mol% when used. ^dReactions were run overnight. ^eYield determined by ¹H NMR analysis of crude reaction mixture with phenanthrene as internal standard. ^fnot determined. ^gEnantiomeric excess of the major diastereomer determined by chiral HPLC. ^hEnantiomeric excess of the *trans-cis* diastereomer determined by chiral HPLC. ⁱDiastereomeric ratios determined by ¹H NMR analysis of crude reaction mixture.

Highly motivated by these promising results indicating that **PCI** and **PCII** impart enantioselectivity in a visible-light mediated energy-transfer-catalyzed reaction, we wanted to further explore their performance as photoredox catalysts. To study this ability, we were especially interested in a recently published example of a chiral photoredox-catalyzed Minisci reaction (Table 4-3).³⁰ The reported example utilized 2 mol% of **4CzIPN** along with 10 mol% of a chiral phosphoric acid at 15 °C to construct chiral heterobiaryls **17** in good yields with excellent ee and diastereoselectivity (entry 1). We chose this example to test whether the novel bifunctional catalysts can replace the

dual catalytic system and fulfill the role of both chiral phosphoric acid and photocatalyst in an enantioselective fashion in this photoredox-catalyzed reaction. By subjecting both **PCI** and **PCII** to the literature reported reaction conditions, albeit at a slightly higher temperature (room temperature), we were delighted to find that without any optimization, an enantioselectivity of 21% with a yield of 33% was achieved with **PCI** (entry 4). Using only **4CzIPN** gave no product formation (entry 2), indicating that the phosphoric moiety of **PCI** is necessary for the reaction. Indeed, by adding in 10 mol% racemic phosphoric acid *rac*-**PA**, racemic product **17** could be obtained with **4CzIPN** in low yields (entry 3).

This initial hit with **PCI** (entry 4) shows evidence of achieving chirality with our novel catalyst in reactions operating by a photoredox mechanism and we are optimistic that better enantioselectivity could be achieved by optimizing the reaction conditions for this specific catalyst.

Table 4-3: Photoredox-catalyzed Minisci reaction as a proof-of-concept reaction.



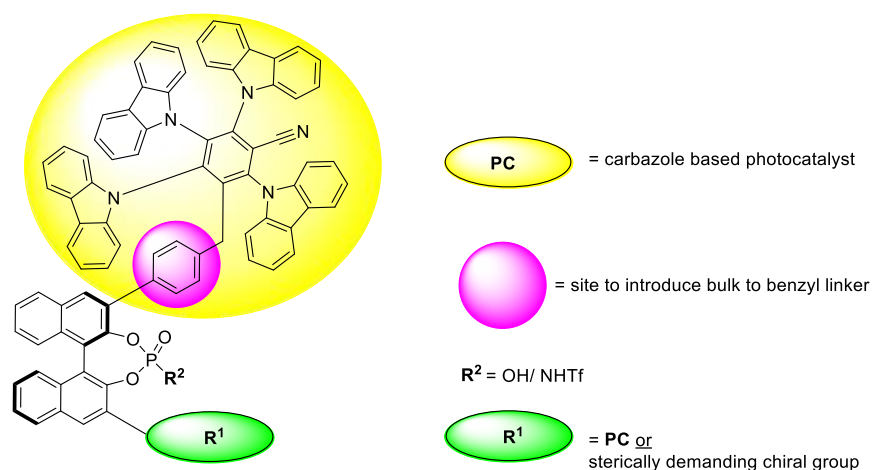
Entry	PC	PA	Yield (%) ^c	ee (%) ^d	d.r. ^f
1 ^a	4CzIPN (2 mol%)	CPA-3 (10 mol%)	64	>99	>19:1
2 ^b	4CzIPN (10 mol%)	None	-	-	-
3 ^b	4CzIPN (2 mol%)	<i>rac</i> -PA (10 mol%)	17	-	nd ^e
4 ^b	PCI (10 mol%)	None	33	21	>19:1
5 ^b	PCII (10 mol%)	None	13	14	>10:1 ^g

^aEntries and values from the publication of the Xiao group.^{30a} ^bReactions were run overnight at room temperature. ^c¹H NMR analysis with 1,3,5-trimethoxybenzene as the internal standard. ^dEnantiomeric excess was determined by chiral HPLC. ^enot determined. ^fDiastereomeric ratios determined by ¹H NMR analysis. ^gDue to low conversion and formation of undesired and unidentifiable products, we were unable to define a d.r. greater than 10:1 with high levels of confidence.

4.4 Conclusion and outlook

In summary, we have synthesized two novel catalysts that combine a chiral phosphoric acid with an organic, donor-acceptor cyanoarene-based photocatalyst moiety. Both are accessible in seven-step syntheses and all the synthetic challenges in accessing these catalysts have been overcome. In proof-of-concept reactions, the bifunctional catalysts have shown potential for both enantioselective energy transfer catalysis and photoredox catalysis. To explore the full potential of these novel catalysts, optimization studies need to be carried out to improve both yield and selectivity in the proof-of-concept examples.

Going forward, a potential library of donor-acceptor cyanoarene-based chiral photocatalysts can be envisioned to tailor the photophysical properties of the catalysts to the reactions. A possible potential pathway to modulate the enantioselectivity of these catalysts is the introduction of only one photocatalyst unit (**PC**) and replacement of the second photocatalyst unit with a bulky group that better extends the chirality of the BINOL backbone into the substrate-binding pocket of the chiral phosphoric acid (Scheme 4-8-R¹). Further, enantioselectivity might be improved by increasing the acidity of the phosphoric acid through conversion to the *N*-triflyl phosphoramidate (Scheme 4-8-R²).³¹ We believe that this new class of highly modular catalysts will help open new avenues of research in chiral photocatalysis.



Scheme 4-8: Possible points of modulating the catalyst's reactivity to build up a chiral library.

4.5 Experimental part

4.5.1 General information

All reagents were purchased from commercial suppliers and used without further purification. Anhydrous solvents were obtained from Acros Organics in form of an AcroSeal bottle (“anhydrous”) or purified by passage through an activated alumina column under argon. Air sensitive reactions were performed in Schlenk vials or crimp capped vials under nitrogen (N₂) using plastic syringes and cannulas to transfer solvents or liquid reagents. Photoreactions were weighed in under air but degassed by three cycles of freeze pump thaw to ensure complete exclusion of air.

Analytical thin-layer chromatography (TLC) was performed using Merck silica gel 60 F254 TLC plates and visualized under UV or by staining with KMnO₄. Purification by flash column chromatography was performed on a Teledyne Isco CombiFlash.

Enantiomeric excess was determined by chiral HPLC using Daicel OD-H, OJ-H, IA, and IB columns (0.46 x 25 cm).

All NMR spectra were recorded at room temperature unless otherwise noted using Bruker AV 600, Neo-500, AVB-400 and AVQ-400 spectrometers. These CoC-NMR instruments at UC Berkeley are funded in part by the NIH (S10OD024998). All chemical shifts are reported in δ -scale as parts per million [ppm] (multiplicity, coupling constant J , number of protons), relative to the solvent residual peaks as the internal standard (CHCl₃; δ H = 7.268 ppm and δ C = 77.16 ppm). Coupling constants J are given in Hertz [Hz]. Abbreviations used for signal multiplicity: ¹H-NMR: b = broad, s = singlet, d = doublet, t = triplet, q = quartet, dd = doublet of doublets, ddd = doublet of doublet of doublets, dt = doublet of triplets, dq = doublet of quartets and m = multiplet;

UV-Vis spectroscopic measurements were recorded using a Shimadzu UV-2600i spectrophotometer.

HRMS (high resolution mass spectra) were measured at the QB3 mass spectra facility at the University of California, Berkeley.

Photoreactions were performed using blue light LT-1960 royal blue (blue, λ_{max} = 451 nm) as irradiation source or a Kessil PR160L-440 nm. Reactions were performed in crimp capped vials in a water-cooled metal cooling block.

4.5.2 UV-VIS and Emission Spectra

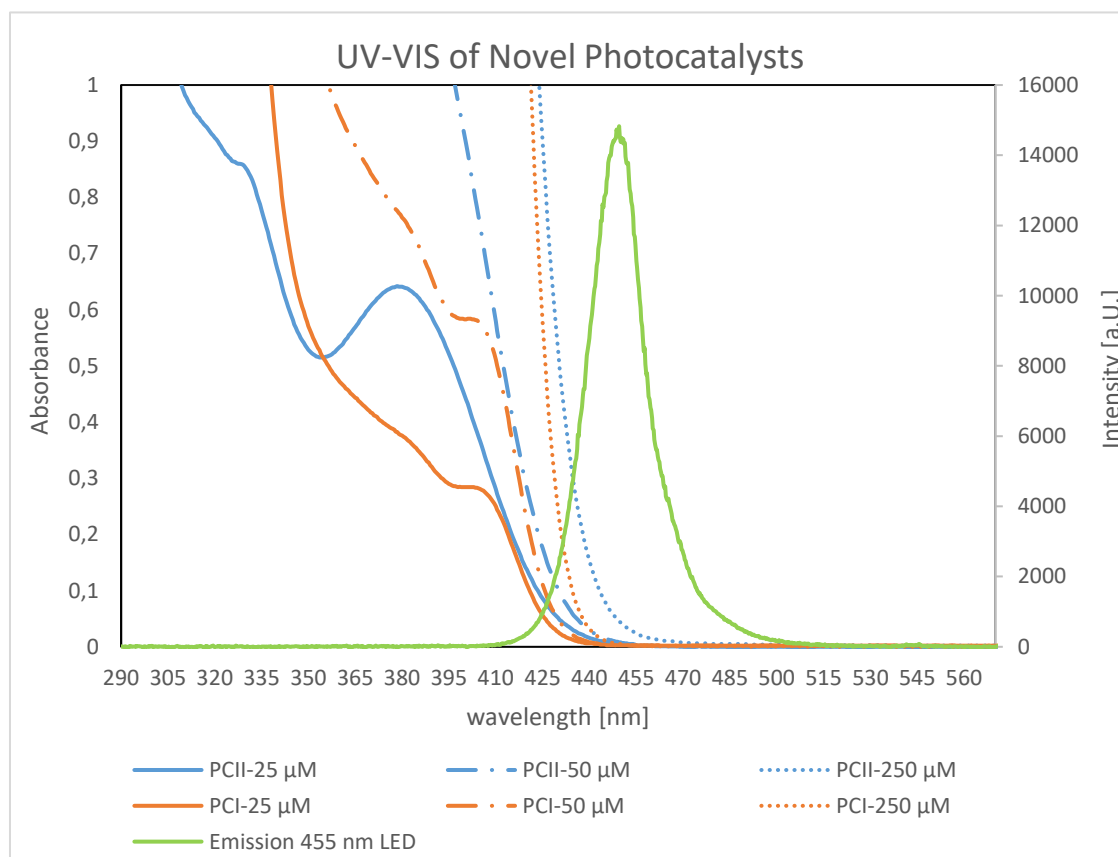
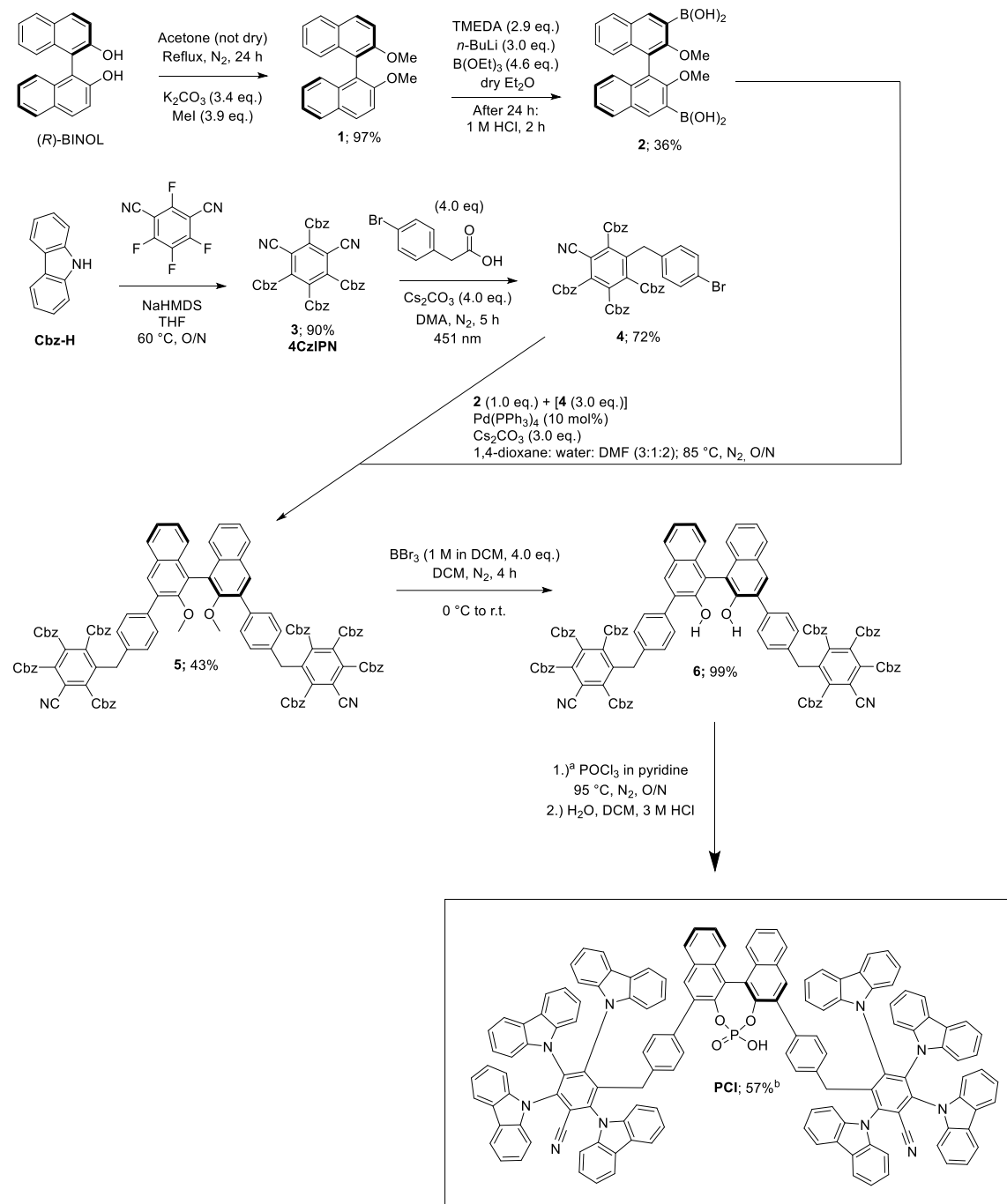


Figure S4-1: Emission spectra of a blue 455 nm LED light source and absorbance spectra of novel catalysts **PCI** and **PCII** at different concentrations in toluene. Control experiments using a 400 nm LED and 385 nm LED light source did not increase yield or enantioselectivity in the intermolecular cycloaddition of **13**, therefore 451 nm was used as preferred light source.

4.5.3 Overview of Synthesis

4.5.3.1 Synthesis of PCI

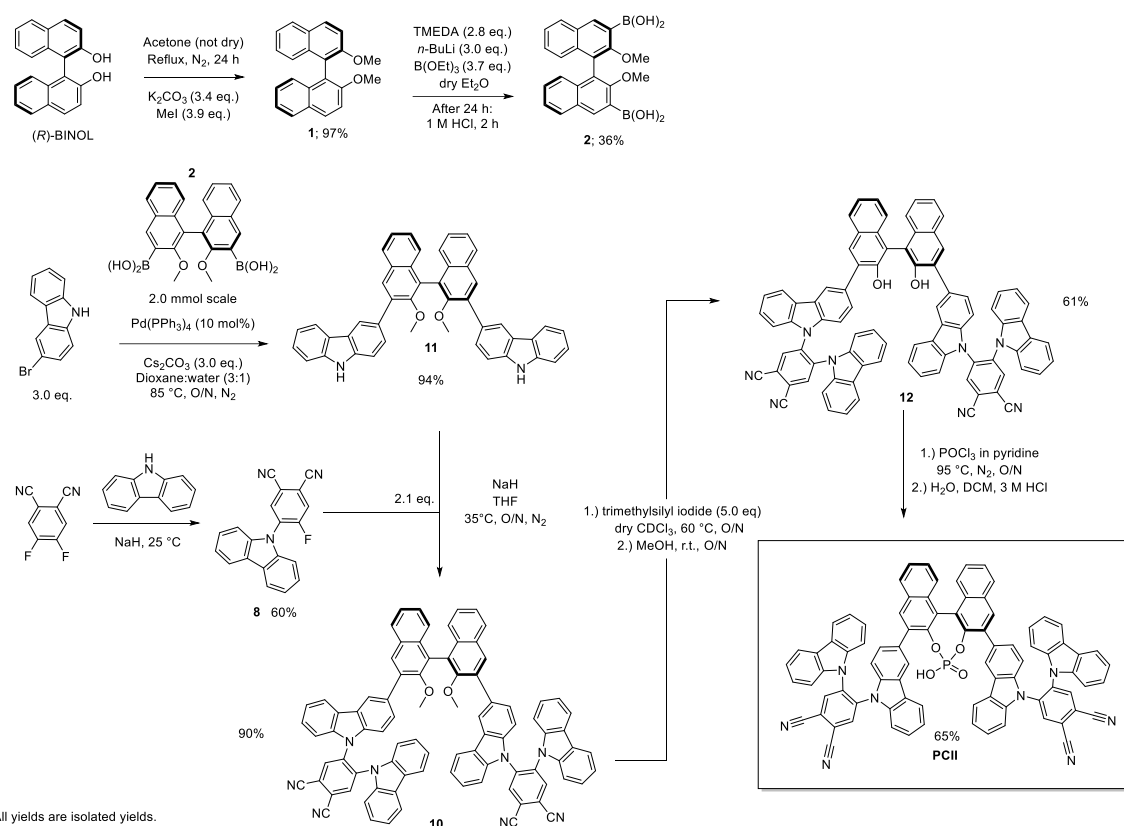


All yields are isolated yields.

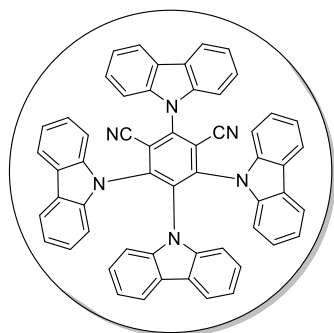
^aCan also be synthesized using Et_3N in DCM and then adding pyridine.

^bMaterial loss due to purification issues; first recrystallized from MeCN (76% yield) and then columned twice with $^1\text{H-NMRs}$ taken inbetween

4.5.3.2 Synthesis of PCII



4.5.4 Synthesis of Literature Reported Compounds

2,4,5,6-Tetrakis(carbazol-9-yl)-4,6-dicyanobenzene **4CzIPN** (**3**)

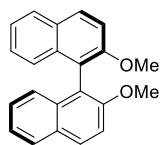
This substrate was made following a literature reported procedure.^{15,20a}

A round bottom flask equipped with a magnetic stirring bar was charged with a solution of carbazole (14.7 g, 88.0 mmol, 4.4 eq.) in dry THF (100 mL) and was cooled to 0 °C. NaHMDS (2 M in THF, 44 mL, 88 mmol, 4.4 eq.) was added under nitrogen and the resulting solution was stirred for 30 min at room temperature. Tetrafluoroisophthalonitrile (4.00 g, 20.0 mmol, 1.0 eq.) dissolved in dry THF was then added dropwise under nitrogen and the reaction was stirred overnight at 60 °C. Afterwards, the solvent was removed in vacuo and the residue was redissolved in Et₂O. The suspension was filtered, and the solid was washed with Et₂O. The crude product was then dissolved in chloroform and filtered until the remaining solid did not color the solution anymore. The solvent was removed in vacuo and the remaining solid was washed first with acetone/ hexane (9:1 mixture) and then with hexane. The pure product was dried in vacuo overnight, yielding **4CzIPN** as a bright yellow powder (14.1 g, 17.9 mmol, 90%).

¹H NMR (500 MHz, CDCl₃) δ (ppm) 8.23 (d, *J* = 7.8 Hz, 2H), 7.75 – 7.66 (m, 8H), 7.49 (ddd, *J* = 7.9, 6.7, 1.5 Hz, 2H), 7.33 (d, *J* = 7.7 Hz, 2H), 7.25 – 7.19 (m, 4H), 7.09 (tt, *J* = 7.4, 5.7 Hz, 8H), 6.87 – 6.79 (m, 4H), 6.64 (ddd, *J* = 8.4, 7.2, 1.2 Hz, 2H).

Contains acetone solvent peak. Carbazole based photocatalysts tend to incorporate solvent molecules.

The spectroscopic data matched that reported in the literature.^{15,20a}

(R)-2,2'-Dimethoxy-1,1'-binaphthalene (1)

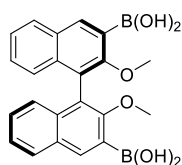
This substrate was made following a literature reported procedure.^{10,18}

(R)-1,1'-binaphthalene-2,2'-diol (14.3 g, 50.0 mmol, 1.0 eq.) was added under nitrogen to a three-necked round bottom flask equipped with a magnetic stirring bar and a reflux condenser. Acetone (50 mL) was added and after stirring at room temperature until all solid was dissolved, potassium carbonate (23.5 g, 170 mmol, 3.4 eq.) and methyl iodide (12.2 mL, 27.8 g, 196 mmol, 3.9 eq.) were added. The resulting suspension was refluxed overnight. The next day, acetone was removed by blowing nitrogen through the slurry and water (20 mL) was added. The mixture was stirred overnight, the precipitate was filtered, washed with water, and dried in vacuo yielding **1** as a white solid (15.2 g, 48.3 mmol, 97%).

¹H NMR (500 MHz, CDCl₃) δ (ppm) 7.98 (d, *J* = 8.9 Hz, 2H), 7.87 (d, *J* = 8.2 Hz, 2H), 7.47 (d, *J* = 9.0 Hz, 2H), 7.32 (ddd, *J* = 8.0, 6.6, 1.2 Hz, 2H), 7.21 (ddd, *J* = 8.2, 6.7, 1.4 Hz, 2H), 7.12 (d, *J* = 8.5 Hz, 2H), 3.77 (s, 6H).

¹³C NMR (126 MHz, CDCl₃) δ (ppm) 155.1, 134.2, 129.5, 129.4, 128.1, 126.4, 125.4, 123.7, 119.8, 114.4, 57.1.

The spectroscopic data matched that reported in the literature.^{10,18}

(R)-2,2'-Dimethoxy-[1,1'-binaphthalene]-3,3'-diyl)diboronic acid (2)

This substrate was made following a literature reported procedure.^{10,19}

n-BuLi (2.5 M solution in hexane, 7.6 mL, 19 mmol, 3.0 eq.) was added at room temperature and under nitrogen to a rigorously stirred solution of TMEDA (2.7 mL, 18 mmol, 2.9 eq.) in anhydrous Et₂O (100 mL). After the solution was stirred for 1 h, **1** (2.00 g, 6.36 mmol, 1.0 eq.) was added at once and the mixture was stirred for 4 h. After this time the solution was cooled to -78 °C and

B(OEt)₃ (5.0 mL, 29 mmol, 4.6 eq.) was added via a syringe pump over 10 minutes. The cooling bath was removed, and the resulting mixture was stirred overnight at room temperature before it was cooled to 0 °C and was quenched with 1 M HCl (50 mL). The solution was once again stirred for 2 h at room temperature and was then extracted three times with Et₂O. The combined organics were washed with brine, dried over Na₂SO₄ and the solvent was removed in vacuo. Recrystallization from boiling toluene yielded the desired product **2** as white solid (920 mg, 2.29 mmol, 36%).

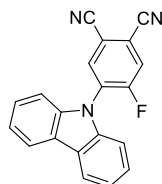
¹H NMR (500 MHz, Acetone-*d*₆) δ (ppm) 8.55 (s, 2H), 8.04 (d, *J* = 8.2 Hz, 2H), 7.45 (t, *J* = 7.5 Hz, 2H), 7.33 (t, *J* = 7.6 Hz, 2H), 7.11 (d, *J* = 8.4 Hz, 2H), 3.41 (s, 6H).

¹³C NMR (126 MHz, Acetone-*d*₆) δ (ppm) 161.2, 139.0, 136.6, 131.4, 129.7, 128.2, 126.3, 125.7, 124.2, 61.8.

Contains toluene solvent peaks.

The spectroscopic data matched that reported in the literature.^{10,19,32}

4-(9*H*-carbazol-9-yl)-5-fluorophthalonitrile (**8**)



This substrate was made following a modified literature reported procedure.²³

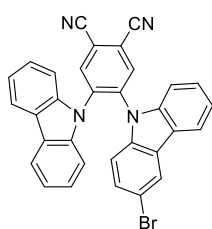
A three-necked round bottom flask equipped with a magnetic stirring bar was charged with a solution of carbazole (1.04 g, 6.22 mmol, 1.0 eq.) in dry THF (37 mL). NaH (60% in mineral oil, 496 mg, 12.4 mmol, 2.0 eq.) was slowly added under nitrogen at room temperature and the resulting solution was stirred for 30 min. Then, 4,5-difluorophthalonitrile (1.21 g, 7.37 mmol, 1.2 eq.) in dry THF (37 mL) was added and the reaction was stirred overnight. Afterwards, the reaction was quenched by addition of water and was extracted with DCM. The combined organics were washed with brine (2x) dried over MgSO₄ and the solvent was removed in vacuo. The crude mixture was first purified by flash column chromatography (70% DCM in hexanes) and then by dissolving remaining starting material (4,5-difluorophthalonitrile) and **2CzPN** in DCM and/or Chloroform (yellow solution) and filtering off pure **8** since **8** displays a lower solubility in

chloroform and DCM than the symmetric unwanted products (starting material and **2CzPN**). This procedure was repeated until no more **8** remained in the mixture. White solid (1.16 g, 3.73 mmol, 60%).

¹H NMR (400 MHz, CDCl₃) δ (ppm) 8.16 – 8.11 (m, 3H), 7.87 (d, $J = 9.0$ Hz, 1H), 7.48 (ddd, $J = 8.3, 7.3, 1.2$ Hz, 2H), 7.39 (td, $J = 7.5, 1.0$ Hz, 2H), 7.26 – 7.18 (m, 2H).

The spectroscopic data matched that reported in the literature.²³

4-(3-Bromo-9H-carbazol-9-yl)-5-(9H-carbazol-9-yl)phthalonitrile (**9**)

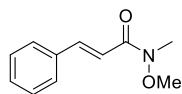


This substrate was made following a literature reported procedure.²³

A three-necked round bottom flask equipped with a magnetic stirring bar was charged with a solution of 3-bromocarbazole (0.34 g, 1.4 mmol, 1.2 eq.) in dry THF (30 mL). NaH (60% in mineral oil, 60.0 mg, 1.36 mmol, 1.2 eq.) was slowly added under nitrogen at room temperature and the resulting solution was stirred for 30 min. Then, **8** (0.35 g, 1.1 mmol, 1.0 eq.) in dry THF (30 mL) was added and the reaction was stirred overnight. Afterwards, the reaction was quenched by addition of water and was extracted with DCM. The combined organics were washed with brine (2x) dried over MgSO₄ and the solvent was removed in vacuo. The crude mixture was purified by flash column chromatography (50-70% DCM in hexanes) yielding **9** as a pale-yellow solid (89:11 mixture of **9** and **2CzPN**, 441 mg combined isolated yield corresponding to 64% yield of **9**, 0.713 mmol, 383 mg).

¹H NMR (500 MHz, CDCl₃) δ (ppm) 8.33 (s, 1H), 8.29 (s, 1H), 7.90 (d, $J = 1.9$ Hz, 1H), 7.85 – 7.79 (m, 2H), 7.78 – 7.75 (m, 1H), 7.21 – 7.06 (m, 8H), 7.02 (ddd, $J = 8.3, 7.1, 1.2$ Hz, 1H), 6.97 (dt, $J = 8.2, 1.0$ Hz, 1H), 6.87 (d, $J = 8.7$ Hz, 1H).

The spectroscopic data matched that reported in the literature.²³

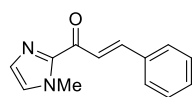
***N*-Methoxy-*N*-methylcinnamamide (**S4-1**)**

This substrate was made following a literature reported procedure.^{28,29}

Cinnamoyl chloride (4.32 g, 26.0 mmol, 1.0 eq.), and *N,O*-dimethylhydroxylamine hydrochloride (2.67 g, 27.4 mmol, 1.05 eq.) were added to a round bottom flask equipped with a magnetic stirring bar. After the flask was closed with a septum and placed under a nitrogen atmosphere, DCM (75 mL) was added and the flask was cooled to 0 °C. Pyridine (4.6 mL, 57 mmol, 2.2 eq.) was added slowly via a syringe and the resulting mixture was warmed to room temperature and stirred overnight. After the reaction was quenched with 1 M HCl, the organic layer was separated, and the aqueous layer was extracted with EtOAc (3x). The combined organics were washed with sat. NaHCO₃ and brine, dried over MgSO₄ and the solvent was removed in vacuo. Purification by flash column chromatography (20% EtOAc in hexanes) yielded **S4-1** as an off-white solid (4.31 g, 22.5 mmol, 87%).

¹H NMR (400 MHz, CDCl₃) δ (ppm) 7.74 (d, *J* = 15.9 Hz, 1H), 7.61 – 7.54 (m, 2H), 7.44 – 7.32 (m, 3H), 7.04 (d, *J* = 15.8 Hz, 1H), 3.77 (s, 3H), 3.32 (s, 3H).

The spectroscopic data matched that reported in the literature.^{28,29}

***(E)*-1-(1-Methyl-1*H*-imidazol-2-yl)-3-phenylprop-2-en-1-one (**13**)**

This substrate was made following a literature reported procedure.^{28,29}

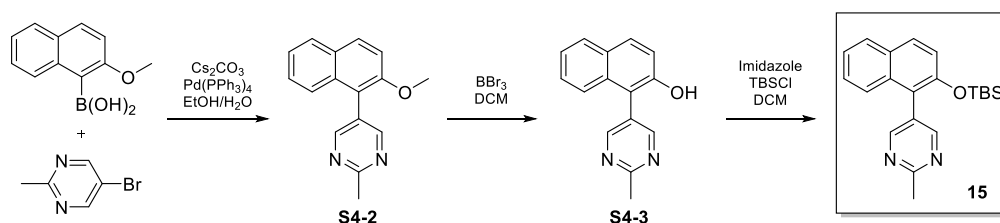
A round bottom flask equipped with a magnetic stirring bar was closed with a septum and placed under a nitrogen atmosphere. *N*-methylimidazole (0.71 mL, 8.9 mmol, 1.05 eq.) and dry THF (30 mL) were added, and the flask was cooled to -78 °C. *n*-BuLi (2.5 M in hexanes, 3.6 mL, 8.9 mmol, 1.05 eq.) was added slowly via a syringe. After complete addition, the flask was stirred at 0 °C for 30 minutes, before it was once more cooled to -78 °C and *N*-methoxy-*N*-methylcinnamamide (**S4-1**) (1.62 g, 8.50 mmol, 1.0 eq.) dissolved in dry THF (10 mL) was added. The resulting mixture was warmed to room temperature and stirred overnight. The next day, glacial

acetic acid (2 mL) was added dropwise under vigorous stirring. The resulting solution was diluted with EtOAc and washed with water. The organic layer was separated, and the aqueous layer was extracted with EtOAc (3x). The combined organics were washed with sat. NaHCO₃ and brine, dried over MgSO₄ and the solvent was removed in vacuo. Purification by flash column chromatography (25%-50% EtOAc in hexanes) yielded **13** as a white solid (1.23 g, 5.79 mmol, 68%).

¹H NMR (400 MHz, CDCl₃) δ (ppm) 8.08 (d, *J* = 16.0 Hz, 1H), 7.83 (d, *J* = 16.0 Hz, 1H), 7.73 – 7.67 (m, 2H), 7.43 – 7.37 (m, 3H), 7.23 (s, 1H), 7.09 (s, 1H), 4.10 (s, 3H).

The spectroscopic data matched that reported in the literature.^{28,29}

5-(2-((*tert*-Butyldimethylsilyl)oxy)naphthalen-1-yl)-2-methylpyrimidine (**15**)



This substrate was made following a literature reported procedure.^{30a}

(2-Methoxynaphthalen-1-yl)boronic acid (1.0 g, 5.0 mmol, 1.0 eq.), 5-bromo-2-methyl-pyrimidine (0.87 g, 5.0 mmol, 1.0 eq.), Pd(PPh₃)₄ (144 mg, 0.125 mmol, 0.025 eq.) and Cs₂CO₃ (4.10 g, 12.6 mmol, 2.5 eq.) were added to a round bottom flask equipped with a magnetic stirring bar. After the flask was closed with a septum and placed under a nitrogen atmosphere, Ethanol (10 mL) and water (5.0 mL) were added, and the flask was heated to 80 °C overnight. The reaction mixture was cooled to room temperature, diluted with Et₂O (50 mL) and washed with water. The organic layer was washed with brine, dried over MgSO₄ and the solvent was removed in vacuo. Purification by flash column chromatography (EtOAc in hexanes) yielded **S4-2**.

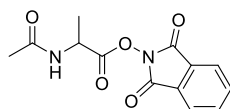
S4-2 (0.75 g, 3.0 mmol, 1.0 eq.) was redissolved in DCM (30 mL) and BBr₃ (1 M solution in DCM, 3.6 mL, 3.6 mmol, 1.2 eq.) was slowly added under nitrogen at room temperature. The mixture was stirred for 5 h before it was quenched with water. The aqueous layer was extracted with DCM and the combined organic layer were washed with brine, dried over MgSO₄ and the solvent was removed in vacuo. Purification by flash column chromatography (EtOAc in hexanes) yielded **S4-3**.

In the final step **S4-3** (438 mg, 1.85 mmol, 1.0 eq.) and imidazole (379 mg, 5.56 mmol, 3.0 eq.) in DCM (18.5 mL) were added to a round bottom flask equipped with a magnetic stirring bar. Under a nitrogen atmosphere, TBSCl (558 mg, 3.70 mmol, 2.0 eq.) was slowly added and stirred at room temperature overnight. The reaction mixture was filtered, and the solvent was removed in vacuo. Purification by flash column chromatography (EtOAc in hexanes) yielded **15** as white solid (632 mg).

¹H NMR (400 MHz, CDCl₃) δ (ppm) 8.69 (s, 2H), 7.87 – 7.81 (m, 2H), 7.50 – 7.44 (m, 1H), 7.43 – 7.37 (m, 2H), 7.19 (d, *J* = 8.9 Hz, 1H), 2.85 (s, 3H), 0.77 (s, 9H), 0.05 (s, 6H).

The spectroscopic data matched that reported in the literature.^{30a}

1,3-Dioxoisindolin-2-yl acetylalaninate (**16**)



This substrate was made following a literature reported procedure.^{30b}

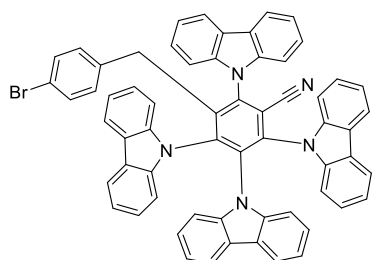
A round bottom flask equipped with a magnetic stirring bar was charged with a solution of *N*-acetyl-*L*-alanine (500 mg, 3.81 mmol, 1.0 eq.), *N*-Hydroxyphthalimide (684 mg, 4.19 mmol, 1.1 eq.), *N,N'*-dicyclohexylcarbodiimide (DCC, 943 mg, 4.57 mmol, 1.2 eq.) and DMAP (47 mg, 0.38 mmol, 0.1 eq.) in DCM (19 mL). The reaction mixture was stirred under nitrogen at room temperature overnight. Afterwards, the reaction was filtered and rinsed with DCM and the solvent was removed in vacuo. The crude mixture was purified by flash column chromatography (40% EtOAc in hexanes) yielding **16** as a white solid (115 mg, 0.416 mmol, 11%). Low yield due to purification issues.

¹H NMR (400 MHz, CDCl₃) δ (ppm) 7.91 (dd, *J* = 5.5, 3.1 Hz, 2H), 7.82 (dd, *J* = 5.5, 3.1 Hz, 2H), 6.05 – 5.99 (m, 1H), 5.10 (p, *J* = 7.3 Hz, 1H), 2.07 (s, 3H), 1.67 (d, *J* = 7.3 Hz, 3H).

The spectroscopic data matched that reported in the literature.^{30b}

4.5.5 Synthesis of Novel Compounds

3-(4-Bromobenzyl)-2,4,5,6-tetra(9*H*-carbazol-9-yl)benzonitrile (**4**)



This substrate was made following a modified literature reported procedure.^{20a}

Small scale with blue LED ($\lambda_{\text{max}} = 451 \text{ nm LED}$):

A 5 mL crimp capped vial equipped with a magnetic stirring bar was charged with **4CzIPN** (47 mg, 60 μmol , 1.0 eq.), Cs_2CO_3 (78.2 mg, 240 μmol , 4.0 eq.) and 4-bromophenylacetic acid (51.6 mg, 240 μmol , 4.0 eq.). The mixture was degassed by three cycles of vacuum and nitrogen backfills, before DMA (4 mL, not dry, 0.015 M) was added. The resulting mixture was stirred for 1 h under blue light irradiation ($\lambda_{\text{max}} = 451 \text{ nm LED}$) through the plane bottom side of the vial at room temperature. The end of the reaction was visible by a color change from yellow to pink. For isolation, 12 reactions were first diluted with DCM and were then combined and washed once with water and once with brine. After drying over MgSO_4 the solvent was removed in vacuo in a 65 °C water bath to remove remaining DMA. The solid crude material was dissolved in DCM and then equal amounts of EtOAc were added. Pure material crystallized over 48 hrs and **4** was obtained as yellow solid (473 mg, 507 μmol , 70%).

Larger scale with Kessil Lamp ($\lambda_{\text{max}} = 440 \text{ nm}$):

A 250 mL round bottom flask equipped with a magnetic stirring bar was charged with **4CzIPN** (1.88 g, 2.38 mmol, 1.0 eq.), Cs_2CO_3 (3.12 g, 9.58 mmol, 4.0 eq.) and 4-bromophenylacetic acid (2.06 g, 9.58 mmol, 4.0 eq.). The mixture was degassed by three cycles of vacuum and nitrogen backfills, before DMA (80 mL, not dry, 0.03 M) was added. The resulting mixture was stirred for 5 h under blue light irradiation ($\lambda_{\text{max}} = 440 \text{ nm}$) with a Kessil Lamp. After 5 h the reaction was first diluted with DCM and then washed with water (3 times) and once with brine. After drying over MgSO_4 the solvent was removed in vacuo in a 65 °C water bath to remove remaining DMA. The solid crude material was dissolved in DCM (17 mL) and then equal amounts of EtOAc (17 mL) were added. Pure material crystallized out and **4** was obtained as yellow solid (1.60 g, 1.72 mmol, 72%).

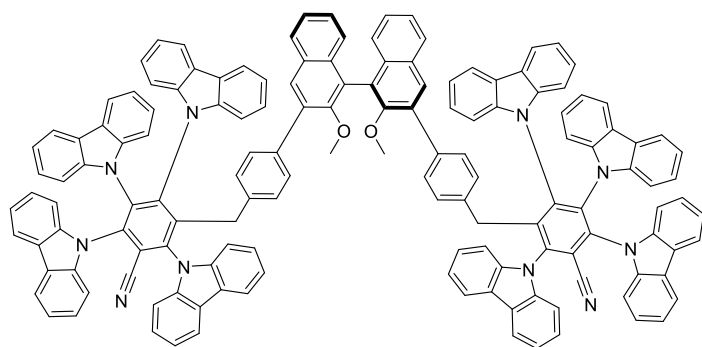
$^1\text{H NMR}$ (400 MHz, CDCl_3) δ (ppm) 8.19 (d, $J = 7.5$ Hz, 2H), 7.72 – 7.60 (m, 6H), 7.48 – 7.39 (m, 4H), 7.31 – 7.23 (m, 4H), 7.11 – 6.99 (m, 10H), 6.91 (d, $J = 8.2$ Hz, 2H), 6.76 (t, $J = 7.9$ Hz, 2H), 6.67 – 6.58 (m, 2H), 6.58 – 6.54 (m, 2H), 5.77 (d, $J = 8.4$ Hz, 2H), 3.70 (s, 2H).

$^{13}\text{C NMR}$ (126 MHz, CDCl_3) δ (ppm) 144.9, 142.1, 140.9, 140.3, 140.1, 138.9, 138.7, 137.9, 136.4, 135.6, 130.9, 129.1, 127.0, 125.6, 125.6, 124.4, 124.3, 124.2, 123.8, 123.7, 121.6, 121.3, 121.3, 121.0, 120.4, 120.4, 120.3, 120.1, 119.5, 117.8, 112.7, 110.2, 110.1, 109.8, 109.1, 34.5.

Contains Dimethylacetamide solvent peaks. Carbazole based photocatalysts tend to incorporate solvent molecules. Contains ^1H -grease impurity.

HRMS (ESI $^+$)(m/z): calculated for $\text{C}_{62}\text{H}_{38}\text{N}_5^{79}\text{Br}_1^{23}\text{Na}_1^+$ [$\text{M}+\text{Na}^+$]: 954.2203, found: 954.2207.

(*R*)-5,5'-(((2,2'-Dimethoxy-[1,1'-binaphthalene]-3,3'-diyl)bis(4,1-phenylene))bis(methylene))bis(2,3,4,6-tetra(9*H*-carbazol-9-yl)benzonitrile) (5)



This substrate was made following a modified literature reported procedure.¹⁹

A round bottom flask equipped with a magnetic stirring bar was charged with **4** (1.92 g, 2.06 mmol 3.0 eq.), **2** (276 mg, 0.687 mmol, 1.0 eq.), Cs_2CO_3 (671 mg, 2.06 mmol, 3.0 eq.) and $\text{Pd}(\text{PPh}_3)_4$ (79 mg, 0.068 mmol, 10 mol%). The flask was degassed and backfilled with nitrogen three times, before degassed solvent [dioxane (12.2 mL), water (4.1 mL) and DMF (7.5 mL)] was added. After stirring overnight at 85 °C, the reaction mixture was cooled to room temperature, diluted with 1 M HCl and extracted with DCM twice. The combined organic phases were washed with water and brine, dried over MgSO_4 and the solvent was removed in vacuo. The crude reaction mixture was purified with flash column chromatography (0-70% DCM in hexanes) yielding **5** (589 mg, 0.292 mmol, 43%) as a yellow solid.

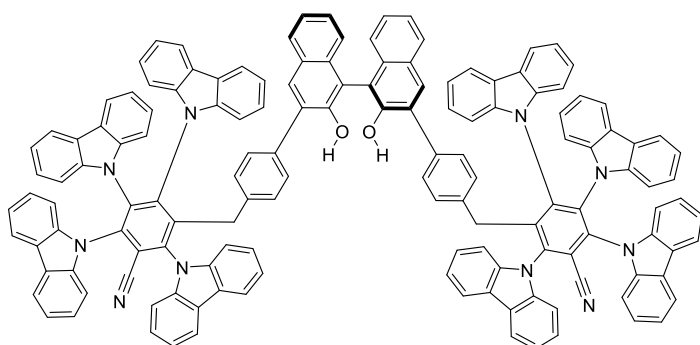
$^1\text{H NMR}$ (600 MHz, CDCl_3) δ (ppm) 8.22 (dd, $J = 7.7, 2.5$ Hz, 4H), 7.80 (d, $J = 8.4$ Hz, 2H), 7.71 – 7.61 (m, 12H), 7.50 (d, $J = 9.1$ Hz, 4H), 7.43 (td, $J = 7.4, 6.9, 3.7$ Hz, 4H), 7.38 (s, 2H), 7.36 – 7.32 (m, 2H), 7.28 (dd, $J = 7.9, 3.6$ Hz, 8H), 7.16 (ddd, $J = 8.2, 6.8, 1.3$ Hz, 2H), 7.10 – 6.98 (m, 22H), 6.91 (d, $J = 8.1$ Hz, 4H), 6.85 (d, $J = 8.2$ Hz, 4H), 6.78 – 6.73 (m, 4H), 6.65 – 6.59 (m, 4H), 6.07 (d, $J = 8.2$ Hz, 4H), 3.89 (s, 4H), 2.68 (s, 6H).

$^{13}\text{C NMR}$ (151 MHz, CDCl_3) δ (ppm) 153.8, 145.4, 142.2, 141.1, 140.3, 140.2, 139.0, 138.8, 137.9, 136.8, 136.3, 136.1, 134.2, 133.4, 130.6, 128.7, 128.0, 127.5, 127.0, 126.2, 125.7, 125.6, 125.6, 125.5, 125.0, 124.4, 124.4, 124.3, 123.9, 123.7, 121.5, 121.5, 121.3, 121.2, 120.9, 120.9, 120.4, 120.3, 119.5, 117.7, 112.7, 110.2, 110.1, 110.0, 109.3, 60.5, 34.9.

Contains ^1H -grease impurity.

HRMS (ESI+)(m/z): calculated for $\text{C}_{146}\text{H}_{92}\text{O}_2\text{N}_{10}^{23}\text{Na}_1^+$ [$\text{M}+\text{Na}^+$]: 2039.7297, found: 2039.7280.

(*R*)-5,5'-((2,2'-Dihydroxy-[1,1'-binaphthalene]-3,3'-diyl)bis(4,1-phenylene))bis(methylene))bis(2,3,4,6-tetra(9*H*-carbazol-9-yl)benzonitrile) (7)



This substrate was made following a modified literature reported procedure.^{10,19}

A round bottom flask equipped with a magnetic stirring bar was charged with **5** (558 mg, 276 μmol 1.0 eq.) and was degassed and backfilled with nitrogen three times, before anhydrous DCM (2.1 mL) was added. The reaction mixture was cooled to 0 $^\circ\text{C}$ and BBr_3 (1 M solution in DCM, 1.1 mL, 1.1 mmol, 4.0 eq.) was added dropwise. The reaction was stirred for four hours at room temperature, cooled to 0 $^\circ\text{C}$ again and quenched by slow addition of water. The mixture was diluted with DCM and the aqueous phase was extracted with DCM three more times. The combined organic phases were dried over MgSO_4 , and the solvent was removed in vacuo. The

demethylated product **7** was obtained in quantitative yield (549 mg, 276 μmol) as a yellow solid without further purification.

$^1\text{H NMR}$ (500 MHz, CDCl_3) δ (ppm) 8.06 (d, $J = 7.7$ Hz, 4H), 7.65 (d, $J = 8.1$ Hz, 2H), 7.56 – 7.47 (m, 12H), 7.36 (t, $J = 8.0$ Hz, 4H), 7.28 (d, $J = 8.1$ Hz, 5H), 7.20 – 7.06 (m, 13H), 6.91 (ddt, $J = 21.7, 18.2, 7.3$ Hz, 22H), 6.81 (d, $J = 8.1$ Hz, 4H), 6.65 (d, $J = 8.0$ Hz, 4H), 6.61 (t, $J = 6.5$ Hz, 4H), 6.50 (t, $J = 7.7$ Hz, 4H), 5.94 (d, $J = 7.9$ Hz, 4H), 4.66 (s, 2H), 3.70 (s, 4H).

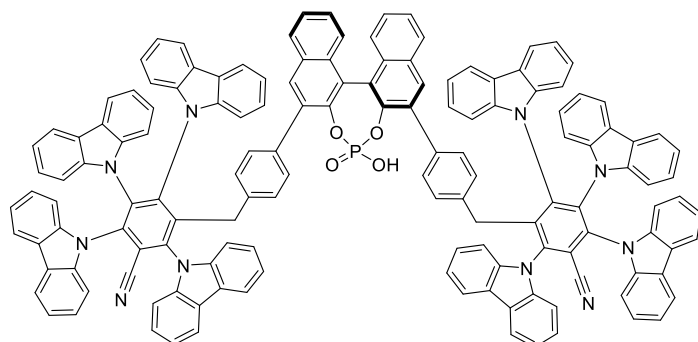
$^{13}\text{C NMR}$ (126 MHz, CDCl_3) δ (ppm) 149.5, 145.4, 142.2, 141.0, 140.3, 140.2, 140.2, 139.0, 138.7, 138.7, 137.9, 136.5, 136.4, 135.2, 132.9, 131.0, 129.9, 129.2, 128.9, 128.3, 127.7, 127.0, 126.9, 125.6, 125.6, 124.4, 124.4, 124.3, 124.3, 124.2, 124.2, 123.8, 123.8, 123.6, 121.5, 121.5, 121.3, 121.2, 120.9, 120.4, 120.3, 119.5, 117.7, 113.0, 112.7, 110.2, 110.1, 109.9, 109.2, 34.9.

The number of observed carbon peaks is higher than what would be expected based on symmetry, and it is believed to be due to rotameric and/or other conformational effects, that disrupt the symmetry.

Contains DCM solvent peaks. Carbazole based photocatalysts tend to incorporate solvent molecules. Contains ^1H -grease impurity.

HRMS (ESI-)(m/z): calculated for $\text{C}_{144}\text{H}_{87}\text{O}_2\text{N}_{10}^-$ [$\text{M}-\text{H}^+$]: 1987.7019, found: 1987.7009.

5,5'-((((11bR)-4-Hydroxy-4-oxidodinaphtho[2,1-d:1',2'-f][1,3,2]dioxaphosphepine-2,6-diyl)bis(4,1-phenylene))bis(methylene))bis(2,3,4,6-tetra(9H-carbazol-9-yl)benzonitrile) (PCI)



This substrate was made following a modified literature reported procedure.^{10,21}

A round bottom flask equipped with a magnetic stirring bar was charged with **7** (509 mg, 256 μmol , 1.0 eq.) and was degassed and backfilled with nitrogen three times, before anhydrous pyridine (0.82 mL) was added. Phosphorus(V)oxychloride (48 μL , 0.51 mmol, 2.0 eq.) was added and the

reaction mixture was stirred overnight at 95 °C before the mixture was cooled to 0 °C and degassed water (0.8 mL) was added. Afterwards, the mixture was heated up to 95 °C again and stirred overnight. The next day, the reaction mixture was cooled to room temperature, diluted with DCM and washed with 3 M HCl (x 4). The solvent was removed in vacuo and the brownish solid was redissolved in hot acetonitrile. After letting the reaction mixture cool down to room temperature, it was allowed to stand undisturbed (approximately 2 days) until brown solid formed on the bottom of the flask. The clear yellow solution was filtered, and the solvent was once again removed in vacuo. The obtained yellow solid was further purified by flash column chromatography (0-3% methanol in DCM). Finally, pure catalyst **PCI** was obtained as yellow solid (300 mg, 146 μ mol, 57%) by removing the solvent, redissolving it in DCM, washing it with 6 M HCl and removing the solvent once again in vacuo.

^1H NMR (600 MHz, DMSO- d_6) δ (ppm) 8.29 (dd, $J = 7.7, 5.2$ Hz, 4H), 8.16 (d, $J = 8.1$ Hz, 2H), 8.11 (d, $J = 8.1$ Hz, 2H), 8.04 (d, $J = 8.2$ Hz, 2H), 7.93 (dd, $J = 21.1, 8.2$ Hz, 4H), 7.85 – 7.63 (m, 20H), 7.47 (t, $J = 7.6$ Hz, 2H), 7.44 – 7.33 (m, 10H), 7.25 – 7.13 (m, 8H), 7.07 (dq, $J = 15.7, 7.7$ Hz, 6H), 7.02 (t, $J = 7.5$ Hz, 2H), 6.96 (dd, $J = 21.7, 8.1$ Hz, 4H), 6.82 – 6.71 (m, 12H), 6.16 (d, $J = 7.9$ Hz, 4H), 5.08 (s, 1H), 3.58 (s, 4H).

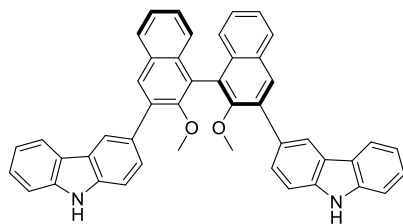
^{13}C NMR (151 MHz, DMSO- d_6) δ (ppm) 144.7, 144.6, 144.5, 142.7, 141.2, 140.2, 140.2, 139.3, 139.3, 138.7, 138.7, 138.5, 137.6, 135.2, 134.3, 133.2, 131.1, 131.0, 130.3, 128.6, 128.4, 126.6, 126.5, 125.9, 125.7, 125.2, 125.1, 124.9, 124.8, 123.8, 123.1, 123.0, 122.8, 122.7, 122.6, 122.4, 121.4, 120.8, 120.74, 120.69, 120.5, 120.1, 120.1, 119.9, 119.8, 119.7, 119.1, 117.5, 113.1, 111.8, 111.4, 111.4, 110.6, 110.6, 33.9.

The number of observed carbon peaks is higher than what would be expected based on symmetry, and it is believed to be due to rotameric and/or other conformational effects, that disrupt the symmetry.

Contains ^1H -grease impurity.

^{31}P NMR (243 MHz, DMSO- d_6) δ (ppm) 0.57.

HRMS (ESI+)(m/z): calculated for $\text{C}_{144}\text{H}_{87}\text{O}_4\text{N}_{10}\text{P}_1^{23}\text{Na}_1^+$ [$\text{M}+\text{Na}^+$]: 2073.6542, found: 2073.6517.

(R)-3,3'-(2,2'-Dimethoxy-[1,1'-binaphthalene]-3,3'-diyl)bis(9H-carbazole) (**11**)

This substrate was made following a modified literature reported procedure.¹⁹

A round bottom flask equipped with a magnetic stirring bar was charged with 3-Bromocarbazole (1.48 g, 6.00 mmol 3.0 eq.), **2** (804 mg, 2.00 mmol, 1.0 eq.), Cs₂CO₃ (1.95 g, 6.00 mmol, 3.0 eq.) and Pd(PPh₃)₄ (0.23 g, 0.20 mmol, 10 mol%). The flask was degassed and backfilled with nitrogen three times, before degassed solvent [dioxane (37.6 mL) and water (12.6 mL)] was added. After stirring overnight at 85 °C, the reaction mixture was cooled to room temperature, diluted with 1 M HCl and extracted with DCM twice. The combined organic phases were washed with water and brine, dried over MgSO₄ and the solvent was removed in vacuo. The crude reaction mixture was purified with flash column chromatography (0-70% DCM in hexanes, then up to 100% DCM) yielding **11** (1.21 g, 1.87 mmol, 94%) as a white solid.

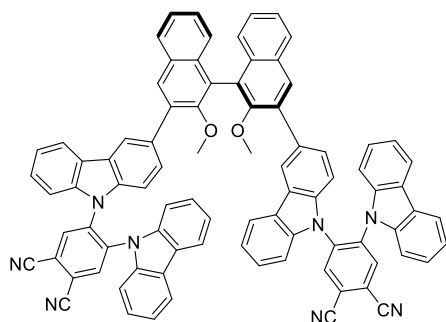
¹H NMR (500 MHz, CDCl₃) δ (ppm) 8.52 (s, 2H), 8.13 (t, *J* = 4.0 Hz, 4H), 8.06 (s, 2H), 7.98 (d, *J* = 8.2 Hz, 2H), 7.87 (dd, *J* = 8.4, 1.7 Hz, 2H), 7.48 – 7.38 (m, 8H), 7.38 – 7.34 (m, 2H), 7.33 – 7.30 (m, 2H), 7.30 – 7.24 (m, 2H), 3.25 (s, 6H).

¹³C NMR (126 MHz, CDCl₃) δ (ppm) 154.5, 140.0, 139.0, 135.9, 133.6, 131.1, 130.8, 130.4, 128.1, 127.7, 126.2, 126.2, 126.0, 126.0, 125.1, 123.6, 123.6, 121.2, 120.6, 119.7, 110.9, 110.5, 60.6.

Contains DCM solvent peaks. Carbazole based photocatalysts tend to incorporate solvent molecules.

HRMS (ESI-)(*m/z*): calculated for C₄₆H₃₁O₂N₂⁻ [M-H⁺]: 643.2391. found: 643.2392.

(R)-5,5'-((2,2'-Dimethoxy-[1,1'-binaphthalene]-3,3'-diyl)bis(9H-carbazole-3,9-diyl))bis(4-(9H-carbazol-9-yl)phthalonitrile) (**10**)



This substrate was made following a modified literature reported procedure.¹⁵

NaH (60% in oil, 148 mg, 3.70 mmol, 4.0 eq.) was added slowly to a stirred solution of **11** (596 mg, 0.924 mmol, 1.0 eq.) in dry THF (10 mL) under inert conditions. The reaction mixture was heated to 35 °C and stirred for one hour before **8** (619 mg, 1.98 mmol, 2.1 eq.) was added. Afterwards it was stirred overnight at 35 °C. The next day the reaction mixture was cooled to room temperature and H₂O (0.7 mL) was added to quench excess NaH. The resulting mixture was then concentrated under reduced pressure, the crude product was redissolved in DCM and washed with brine (2x). Purification by flash column chromatography (70-100% DCM in hexanes) yielded **10** (1.02 g, 0.831 mmol, 90%) as yellow solid.

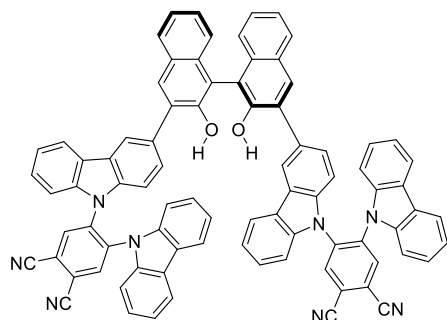
¹H NMR (600 MHz, CDCl₃) δ (ppm) 8.37 – 8.33 (m, 2H), 8.29 (t, *J* = 2.0 Hz, 2H), 8.19 – 8.15 (m, 2H), 7.93 – 7.83 (m, 6H), 7.76 – 7.71 (m, 2H), 7.71 – 7.66 (m, 2H), 7.49 – 7.43 (m, 2H), 7.42 – 7.36 (m, 2H), 7.28 – 7.01 (m, 20H), 7.00 – 6.95 (m, 4H), 2.98 (dd, *J* = 11.7, 4.4 Hz, 6H).

¹³C NMR (151 MHz, CDCl₃) δ (ppm) 154.1, 154.1, 154.0, 154.0, 138.7, 138.7, 138.4, 138.3, 138.3, 138.3, 138.3, 138.2, 138.2, 137.6, 137.6, 135.6, 135.5, 134.9, 134.8, 134.8, 133.6, 133.5, 132.5, 132.4, 130.9, 130.9, 130.5, 130.5, 130.5, 129.1, 128.3, 128.1, 128.0, 127.7, 127.7, 127.7, 126.5, 126.4, 126.3, 126.3, 126.3, 126.2, 126.1, 125.9, 125.9, 125.8, 125.8, 125.4, 125.2, 125.1, 124.5, 124.5, 124.4, 124.2, 124.2, 121.9, 121.9, 121.8, 121.8, 121.7, 121.3, 121.3, 121.2, 120.7, 120.7, 120.7, 120.5, 120.5, 120.4, 120.3, 120.3, 114.8, 114.7, 114.6, 109.2, 109.1, 109.1, 109.0, 109.0, 60.3, 60.3.

The number of observed carbon peaks is higher than what would be expected based on symmetry, and it is believed to be due to rotameric and/or other conformational effects, that disrupt the symmetry.

HRMS (ESI+)(m/z): calculated for $C_{86}H_{51}O_2N_8^+$ [M+H⁺]: 1227.4129. found: 1227.4109.

(R)-5,5'-((2,2'-Dihydroxy-[1,1'-binaphthalene]-3,3'-diyl)bis(9H-carbazole-3,9-diyl))bis(4-(9H-carbazol-9-yl)phthalonitrile) (12)



This substrate was made following a modified literature reported procedure.²⁶

A small Schlenk vial equipped with a magnetic stirring bar was charged with **10** (921 mg, 750 μ mol, 1.0 eq.) and anhydrous deuterated chloroform (2.5 mL). Under nitrogen, trimethylsilyl iodide (0.50 mL, 3.8 mmol, 5.0 eq) was added and the reaction was heated to 60 °C overnight. The next day, the mixture was filtered through a celite pad, rinsed with chloroform and methanol was added. This mixture was left to stir another night at room temperature under nitrogen. After removing the solvent in vacuo, purification by column chromatography (DCM in hexane; 0 to 100%) and washing with hexane, **12** was obtained as yellow solid (551 mg, 459 μ mol, 61%).

¹H NMR (600 MHz, CDCl₃) δ (ppm) 8.26 – 8.23 (m, 4H), 8.16 (d, J = 4.5 Hz, 1H), 8.13 (d, J = 12.2 Hz, 1H), 7.93 (d, J = 5.6 Hz, 2H), 7.91 – 7.86 (m, 2H), 7.82 – 7.72 (m, 6H), 7.49 – 7.35 (m, 4H), 7.31 (q, J = 6.2, 4.2 Hz, 2H), 7.28 – 7.22 (m, 2H), 7.18 – 7.04 (m, 20H), 5.40 – 5.29 (m, 2H).

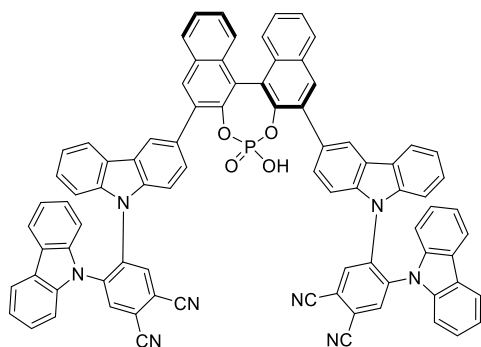
¹³C NMR (151 MHz, CDCl₃) δ (ppm) 150.2, 150.1, 138.8, 138.4, 138.4, 138.4, 138.3, 137.9, 135.5, 135.5, 135.4, 133.0, 133.0, 131.3, 131.0, 130.6, 130.5, 129.5, 128.4, 127.9, 127.3, 126.5, 126.4, 126.3, 124.6, 124.4, 124.4, 124.3, 121.9, 121.8, 121.8, 121.6, 120.6, 120.5, 114.8, 114.8, 114.8, 114.6, 112.8, 112.8, 109.3, 109.1.

Contains ¹H-grease impurity and ethyl acetate solvent peaks. Carbazole based photocatalysts tend to incorporate solvent molecules.

HRMS (ESI+)(m/z): calculated for $C_{84}H_{47}O_2N_8^+$ [M+H⁺]: 1199.3816, found: 1199.3805.

HRMS (ESI-)(m/z): calculated for $C_{84}H_{45}O_2N_8$ [M-H⁺]: 1197.3671, found: 1197.3666.

(4*r*,4'*r*)-5,5'-(((11*b**S*)-4-Hydroxy-4-oxidodiphospho[2,1-*d*:1',2'-*f*][1,3,2]dioxaphosphepine-2,6-diyl)bis(9*H*-carbazole-3,9-diyl))bis(4-(9*H*-carbazol-9-yl)phthalonitrile) (PCII)



This substrate was made following a literature reported procedure.^{10,21}

A round bottom flask equipped with a magnetic stirring bar was charged with **12** (185 mg, 155 μmol , 1.0 eq.) and was degassed and backfilled with nitrogen three times, before anhydrous pyridine (0.50 mL) was added. Phosphorus(V)oxychloride (29 μL , 0.31 mmol, 2.0 eq.) was added and the reaction mixture was stirred overnight at 95 °C before the mixture was cooled to 0 °C and degassed water was added. Afterwards, the mixture was heated up to 95 °C again and stirred overnight. The next day, the reaction mixture was cooled to room temperature, diluted with DCM and washed with 3 M HCl (x4). The solvent was removed in vacuo and the brownish solid was redissolved in hot acetonitrile. After letting the reaction mixture cool down to room temperature, it was allowed to stand undisturbed (approximately 2 days) until brown solid formed on the bottom of the flask. The clear yellow solution was filtered, and the solvent was once again removed in vacuo yielding **PCII** as yellow solid (127 mg, 100 μmol , 65%).

¹H NMR (600 MHz, DMSO-*d*₆) δ (ppm) 8.88 (dd, $J = 11.4, 6.0$ Hz, 2H), 8.86 – 8.81 (m, 2H), 8.49 (d, $J = 15.8$ Hz, 1H), 8.44 (d, $J = 15.0$ Hz, 1H), 8.20 (d, $J = 4.7$ Hz, 1H), 8.17 (d, $J = 3.7$ Hz, 1H), 8.12 (dd, $J = 8.3, 4.9$ Hz, 2H), 8.00 – 7.88 (m, 6H), 7.85 (d, $J = 8.5$ Hz, 1H), 7.68 – 7.63 (m, 1H), 7.60 (dd, $J = 8.6, 2.9$ Hz, 1H), 7.57 – 7.48 (m, 5H), 7.38 – 7.32 (m, 2H), 7.28 – 7.13 (m, 10H), 7.10 – 7.01 (m, 6H), 7.03 – 6.94 (m, 2H).

¹³C NMR (151 MHz, DMSO-*d*₆) δ (ppm) 145.4, 145.3, 145.3, 145.2, 145.2, 138.9, 138.8, 138.5, 138.4, 138.3, 138.1, 138.1, 138.1, 136.6, 136.5, 136.4, 136.4, 133.9, 133.8, 131.3, 131.1, 131.1, 130.9, 130.8, 130.0, 128.6, 128.2, 128.0, 126.6, 126.2, 126.1, 125.9, 125.8, 125.8, 125.7, 123.6, 123.4, 123.2, 122.3, 122.2, 121.9, 121.7, 121.1, 121.0, 120.3, 120.2, 120.1, 115.4, 115.1, 110.0, 110.0, 109.9, 109.6, 109.4.

The number of observed carbon peaks is higher than what would be expected based on symmetry, and it is believed to be due to rotameric and/or other conformational effects, that disrupt the symmetry.

^{31}P NMR (243 MHz, DMSO- d_6) δ (ppm) 0.92, 0.76, 0.56.

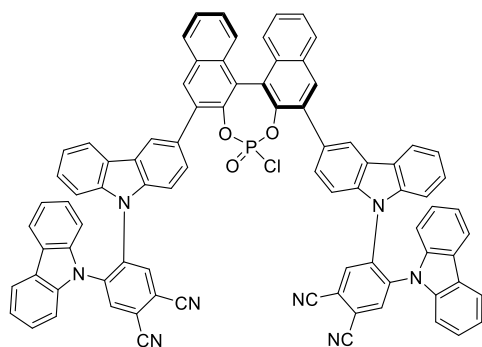
The number of observed phosphorus peaks is higher than what would be expected based on symmetry, and it is believed to be due to rotameric and/or other conformational effects, that disrupt the symmetry, explicitly that could result in the formation of diastereomers at phosphorus.

HRMS (ESI+)(m/z): calculated for $\text{C}_{84}\text{H}_{46}\text{O}_4\text{N}_8\text{P}_1^+$ [M+H $^+$]: 1261.3374, found: 1261.3365.

HRMS (ESI-)(m/z): calculated for $\text{C}_{84}\text{H}_{44}\text{O}_4\text{N}_8\text{P}_1^-$ [M-H $^+$]: 1259.3229, found: 1259.3215.

Comparison of ^{31}P of PCII and the chloride intermediate PCII-Cl intermediate

(4*r*,4'*r*)-5,5'-(((11*b*S)-4-Chloro-4-oxidodino[2,1-*d*:1',2'-*f*][1,3,2]dioxaphosphepine-2,6-diyl)bis(9*H*-carbazole-3,9-diyl))bis(4-(9*H*-carbazol-9-yl)phthalonitrile) (PCII-Cl intermediate)



This substrate was made following a literature reported procedure.²⁷

A round bottom flask equipped with a magnetic stirring bar was charged with **12** (128.7 mg, 107.0 μmol 1.0 eq.) and was degassed and backfilled with nitrogen three times, before anhydrous DCM (0.4 mL) was added. Phosphorus(V)oxychloride (20 μL , 0.22 mmol, 2.0 eq.) was added, followed by Et_3N (45 μL , 0.32 mmol, 3.0 eq.) and the reaction mixture was stirred overnight at room temperature. The next day, the reaction mixture was diluted with DCM and washed with water. The combined organic phases were dried over MgSO_4 and the solvent was removed in vacuo giving the crude chloride as yellow solid.

^{31}P of PCII: ^{31}P NMR (202 MHz, CDCl_3) δ (ppm) 6.14, 5.93, 5.71, 5.57.

^{31}P of PCII-Cl intermediate: ^{31}P NMR (202 MHz, CDCl_3) δ (ppm) 8.16, 8.02, 7.96.

4.5.6 Proof-of-Concept Photoreactions

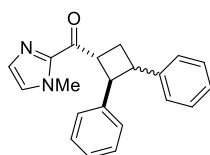
General Procedure A for photoreactions

A 5 mL crimp capped vial equipped with a magnetic stirring bar was charged with the corresponding starting materials, photocatalyst, and solvent. The mixture was degassed by three cycles of freeze-pump-thaw, backfilled with dinitrogen, and subsequently stirred under blue light irradiation ($\lambda_{\text{max}} = 451 \text{ nm LED}$) through the plane bottom side of the vial at room temperature for the respective time.

General Procedure B for photoreactions

A Schlenk flask equipped with a magnetic stirring bar was charged with the corresponding starting materials, photocatalyst, and solvent. The mixture was degassed by three cycles of freeze-pump-thaw, backfilled with dinitrogen, and subsequently stirred under blue light irradiation from within ($\lambda_{\text{max}} = 451 \text{ nm LED}$) with a single spot LED and a glass rod at $-78 \text{ }^\circ\text{C}$ for the respective time.

Enantioselective (2,3-diphenylcyclobutyl)(1-methyl-1*H*-imidazol-2-yl)methanone (**14**)



For the racemic version, either **4CzIPN** (10 mol%) in toluene (2.0 mL) or $\text{Ru}(\text{bpy})_3\text{Cl}_2 \cdot 6\text{H}_2\text{O}$ (2.5 mol%) with *p*-toluenesulfonic acid monohydrate (20 mol%) in MeCN (2.0 mL) was used.

With PCI at r.t.:

The **General Procedure A** was applied using **13** (21.2 mg, 99.9 μmol , 1.0 eq.), freshly distilled styrene (104 mg, 999 μmol , 10 eq.), **Photocatalyst PCI** (5 mol%), and dry toluene and irradiation with 451 nm for 16 h. Yield and d.r. were determined by crude $^1\text{H-NMR}$ yield with phenanthrene (17.8 mg, 99.9 μmol , 1.0 eq.) as internal standard. Purification with Prep-TLC (20% EtOAc in hexanes) yielded **14** as a colorless oil.

The diastereomers have not yet been separated and since the $^1\text{H-NMR}$ exhibited a complex mixture of the diastereomers in the aromatic region, integrals are not accurate for the aromatic region.

Major Diastereomer:

¹H NMR (400 MHz, CDCl₃) δ (ppm) 7.35 – 7.07 (m, 8H), 7.06 (d, *J* = 6.6 Hz, 3H), 7.03 – 6.92 (m, 1H), 4.65 – 4.54 (m, 1H), 4.10 (t, *J* = 9.8 Hz, 1H), 4.04 (s, 3H), 3.70 – 3.60 (m, 1H), 2.91 – 2.82 (m, 1H), 2.33 (q, *J* = 10.2 Hz, 1H).

Minor Diastereomer:

¹H NMR (400 MHz, CDCl₃) δ (ppm) 7.35 – 7.07 (m, 8H), 7.06 (d, *J* = 6.6 Hz, 3H), 7.03 – 6.92 (m, 1H), 5.07 (q, *J* = 9.0, 8.4 Hz, 1H), 4.48 (t, *J* = 9.3 Hz, 1H), 4.05 (s, 3H), 4.03 – 3.96 (m, 1H), 2.80 – 2.75 (m, 2H).

The spectroscopic data matched that reported in the literature.²⁹

HPLC conditions: Daicel CHIRALCEL® OD-H, 5% i-PrOH in hexane, 1 mL/min, major: t₁ = 9.84 min, t₂ = 11.37 min; area% = 34.89 : 26.08 (14% ee) minor: t₁ = 14.09 min, t₂ = 23.41 min; area% = 26.35 : 12.68 (35% ee).

With PCII at -78 °C:

The **General Procedure B** was applied using **13** (21.2 mg, 99.9 μmol, 1.0 eq), freshly distilled styrene (104 mg, 999 μmol 10 eq.), **Photocatalyst PCII** (5 mol%), and dry toluene and irradiation with 451 nm for 5 h. Yield and d.r. were determined by crude ¹H-NMR yield with phenanthrene (17.8 mg, 99.9 μmol, 1.0 eq.) as internal standard. Purification with Prep-TLC (20% EtOAc in hexanes) yielded **14** as a colorless oil.

The diastereomers have not yet been separated and since the ¹H-NMR exhibited a complex mixture of the diastereomers in the aromatic region, integrals are not accurate for the aromatic region. The d.r. of the isolated mixture is decreased to 2.4:1 compared to the 3.8:1 d.r. based on the crude ¹H-NMR.

Major Diastereomer:

¹H NMR (400 MHz, CDCl₃) δ (ppm) 7.35 – 7.25 (m, 2H), 7.22 – 7.00 (m, 8H), 7.01 – 6.95 (m, 2H), 5.07 (q, *J* = 9.2 Hz, 1H), 4.48 (t, *J* = 9.3 Hz, 1H), 4.03 (s, 3H), 4.02 – 3.96 (m, 1H), 2.80 – 2.72 (m, 2H),

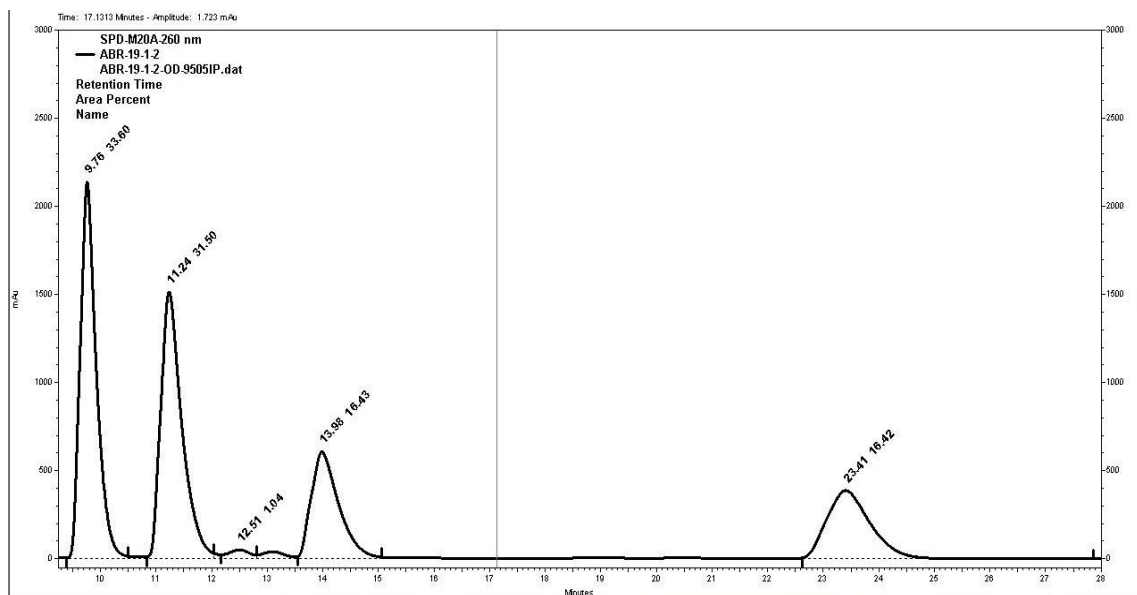
Minor Diastereomer:

¹H NMR (400 MHz, CDCl₃) δ (ppm) 7.35 – 7.25 (m, 2H), 7.22 – 7.00 (m, 8H), 7.01 – 6.95 (m, 2H), 4.63 – 4.53 (m, 1H), 4.10 (t, *J* = 9.8 Hz, 1H), 4.03 (s, 3H), 3.64 (td, *J* = 10.1, 8.1 Hz, 1H), 2.86 (dd, *J* = 10.4, 8.4 Hz, 1H), 2.32 (q, *J* = 10.2 Hz, 1H).

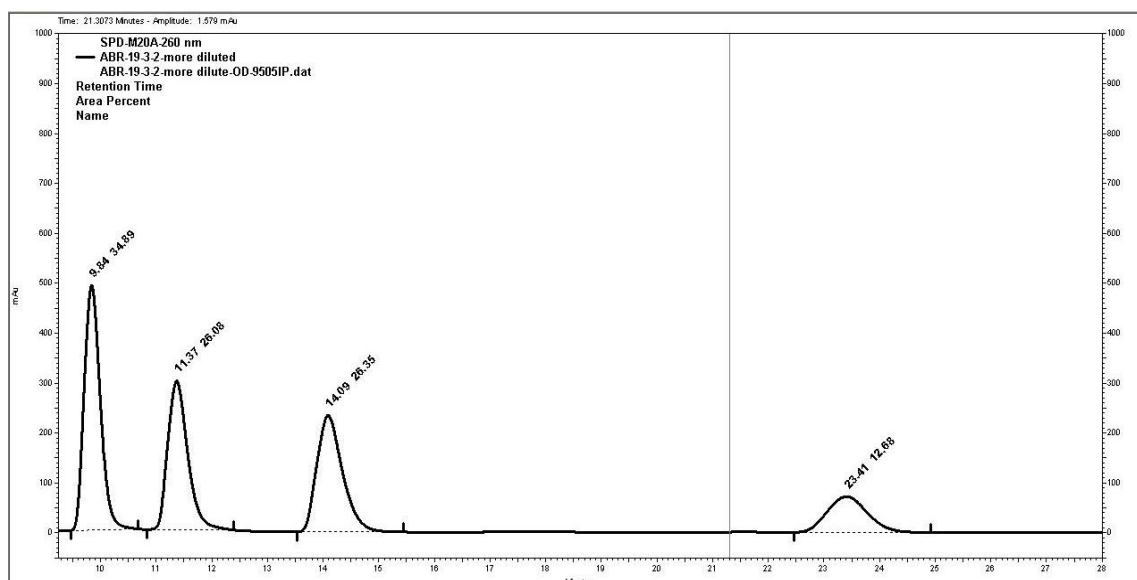
The spectroscopic data matched that reported in the literature.²⁹

HPLC conditions: Daicel CHIRALCEL® OD-H, 5% i-PrOH in hexane, 1 mL/min, Major: t₁ = 13.85 min, t₂ = 22.09 min; area% = 56.63 : 11.83 (65% ee).

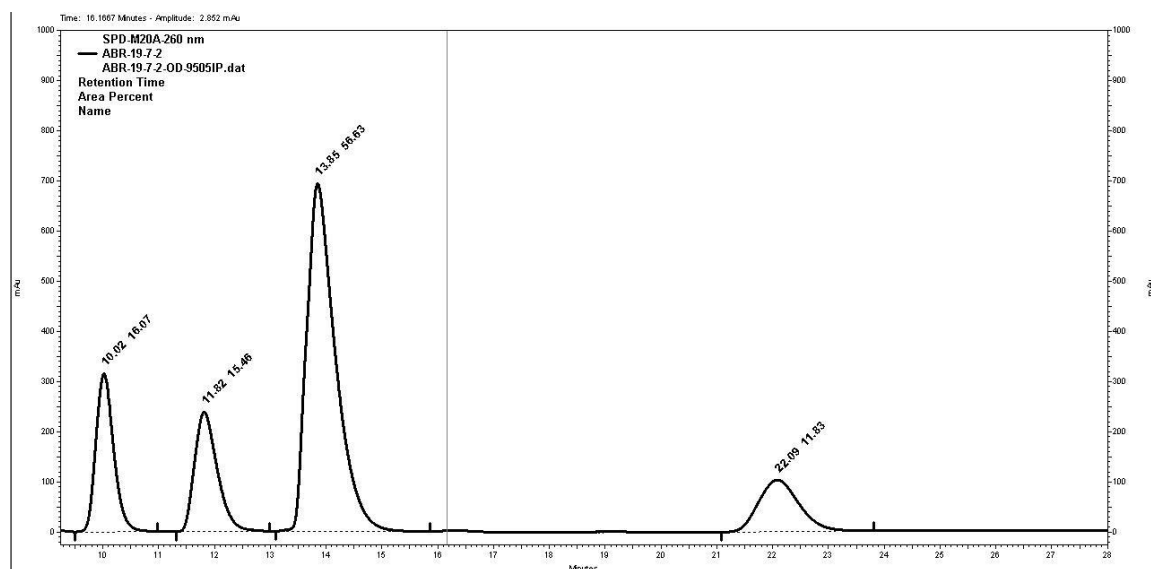
Racemic trace:



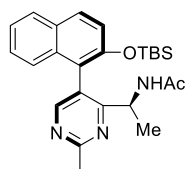
Non-racemic trace of the reaction with PCI at r.t.:



Non-racemic trace of the reaction with PCII at -78 °C:



N-((1*S*)-1-(5-(2-((*tert*-Butyldimethylsilyl)oxy)naphthalen-1-yl)-2-methylpyrimidin-4-yl)ethyl)acetamide (**17**)



For the racemic version, **4CzIPN** (2 mol%) in dry 1,4 dioxane (0.5 mL) with *racemic PA* (10 mol%) was used.

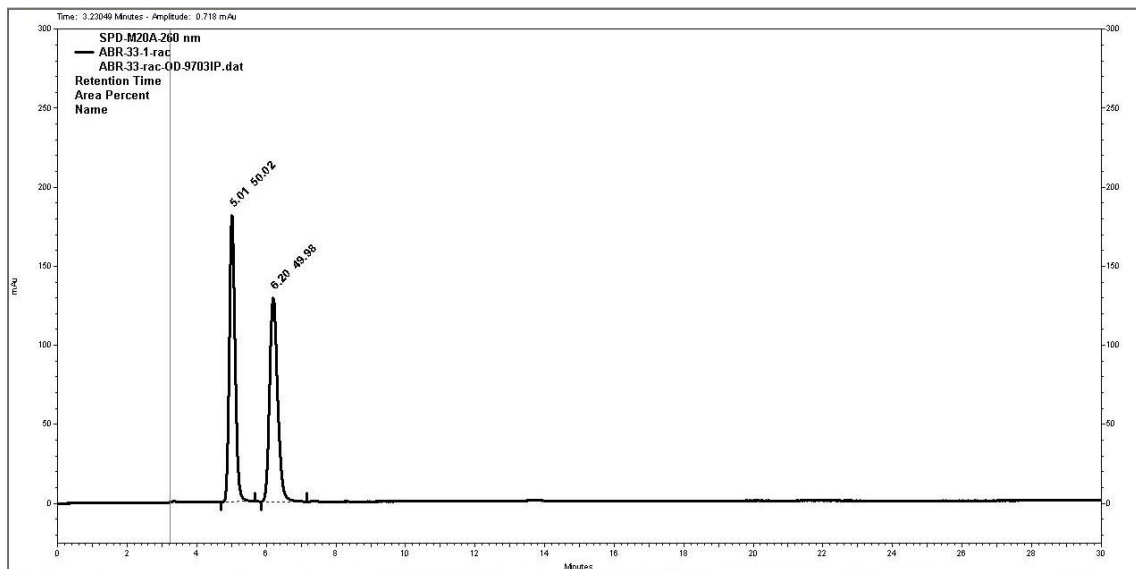
The **General Procedure A** was applied using **15** (17.5 mg, 49.9 μ mol, 1.0 eq), and **16** (20.7 mg, 74.9 μ mol, 1.5 eq.), **Photocatalyst PCI** (10 mol%), and dry 1,4-dioxane (0.5 mL) and irradiation with 451 nm for 16 h. Yield and d.r. were determined by crude $^1\text{H-NMR}$ yield with 1,3,5-trimethoxybenzene (2.8 mg, 17 μ mol, 1/3 eq.) as internal standard. Purification with Prep-TLC (50% EtOAc in hexanes) yielded **17** as white solid.

$^1\text{H NMR}$ (400 MHz, CDCl_3) δ (ppm) 8.42 (s, 1H), 7.89 – 7.81 (m, 2H), 7.37 (dt, $J = 6.8, 3.4$ Hz, 2H), 7.28 (s, 1H), 7.22 (dd, $J = 6.2, 3.5$ Hz, 1H), 7.18 (d, $J = 8.9$ Hz, 1H), 5.03 (p, $J = 6.7$ Hz, 1H), 2.85 (s, 3H), 1.99 (s, 3H), 0.98 (d, $J = 6.7$ Hz, 3H), 0.65 (s, 9H), 0.22 (s, 3H), -0.07 (s, 3H).

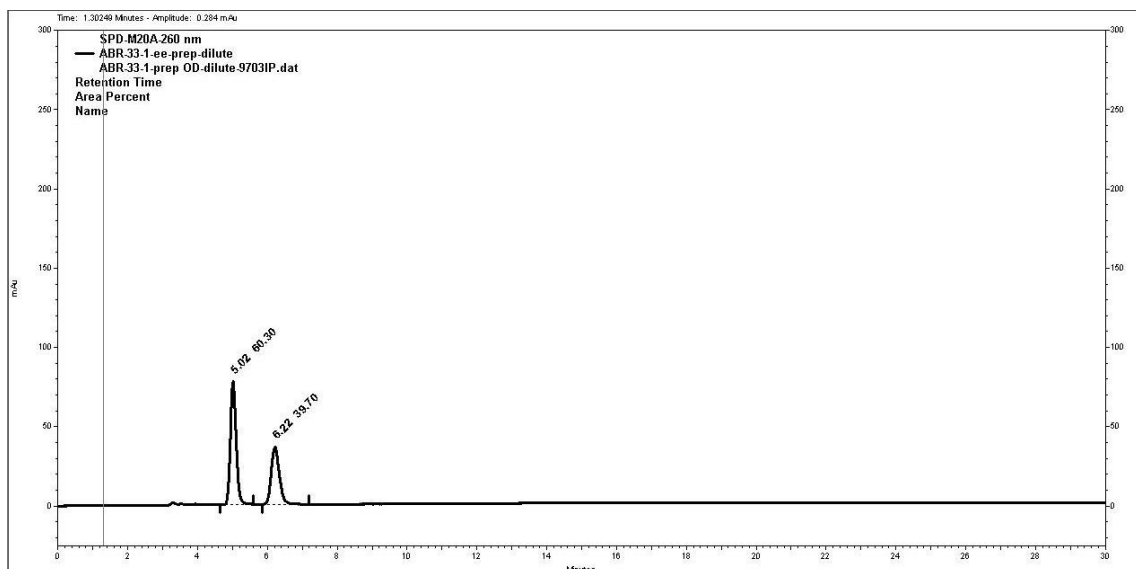
The spectroscopic data matched that reported in the literature.^{30a}

HPLC conditions: Daicel CHIRALCEL® OD-H, 3% i-PrOH in hexane, 1 mL/min: t₁ = 5.02 min, t₂ = 6.22 min; area% = 60.30 : 39.70 (21% ee)

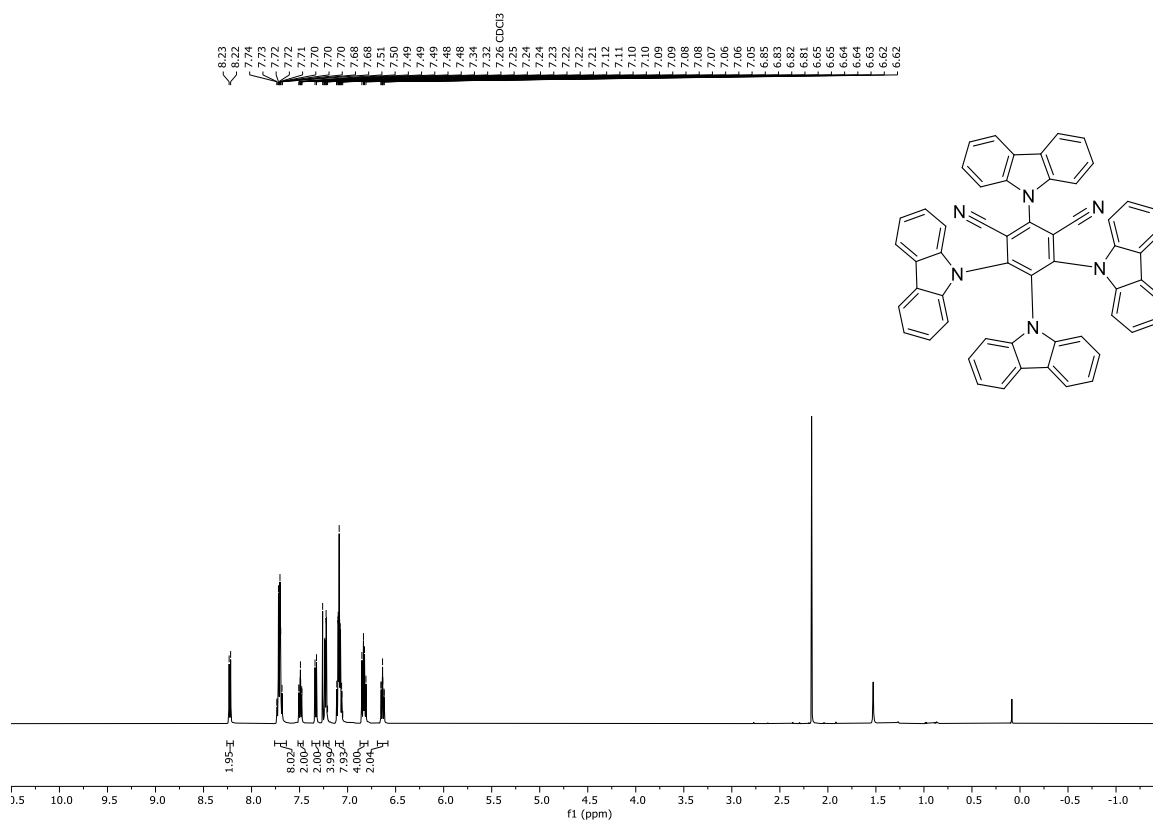
Racemic trace:

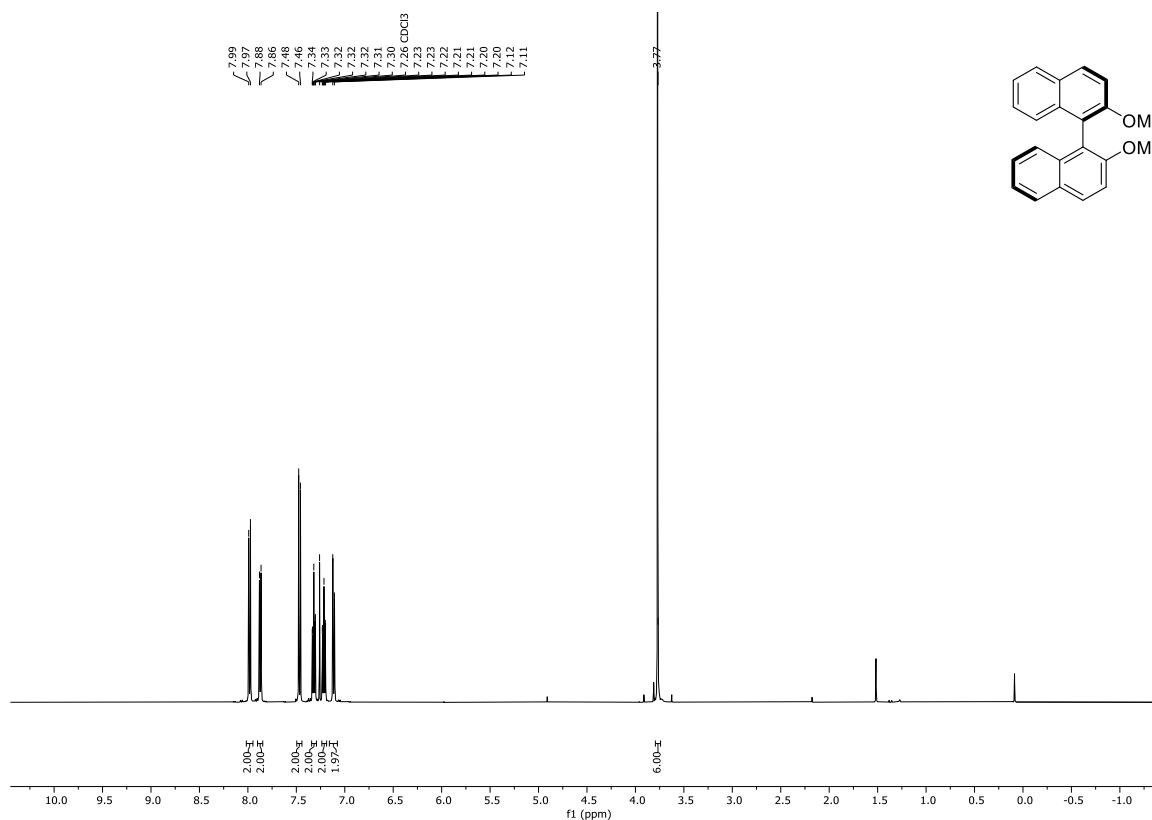
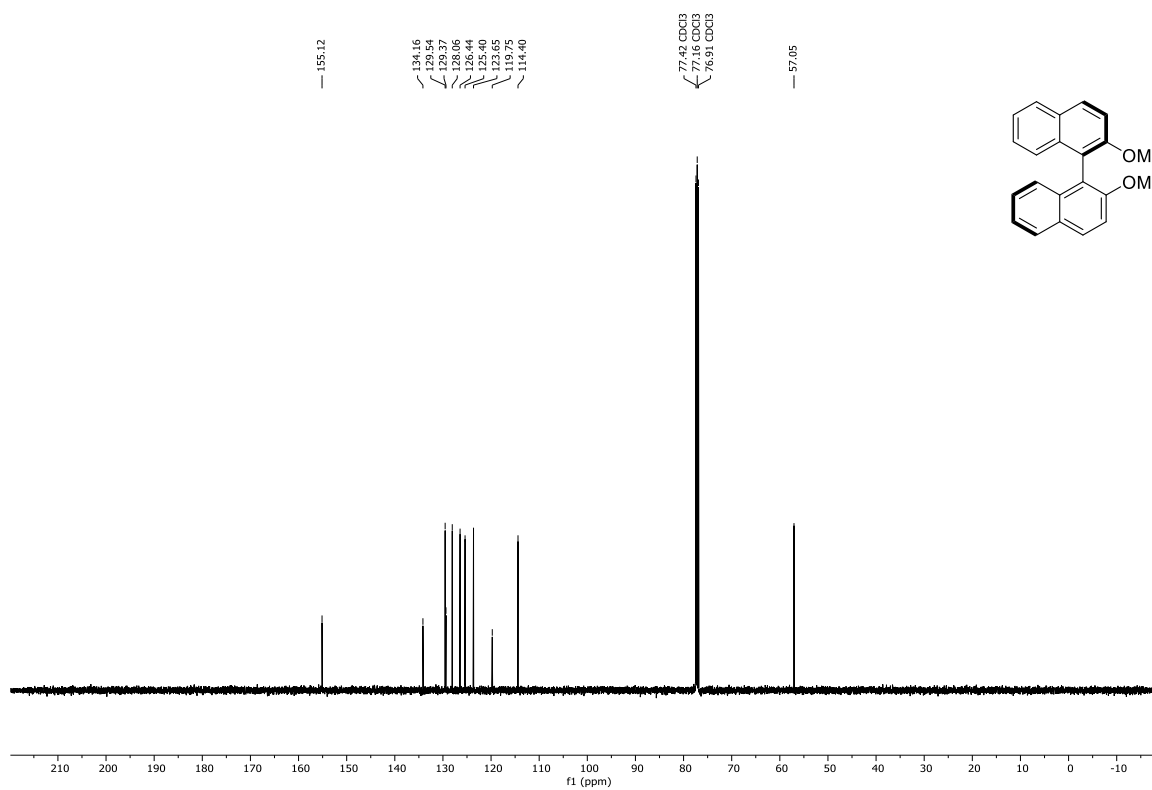


Non-racemic trace:

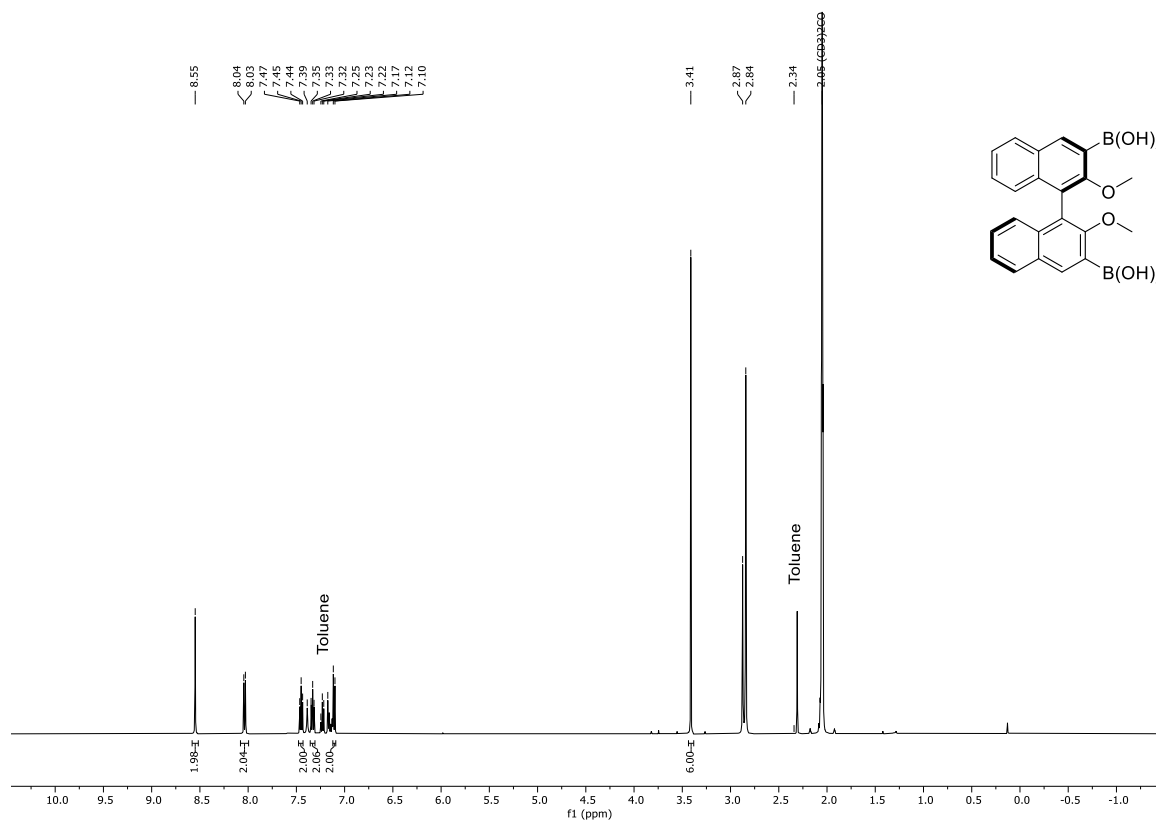


4.5.7 NMR-Spectra

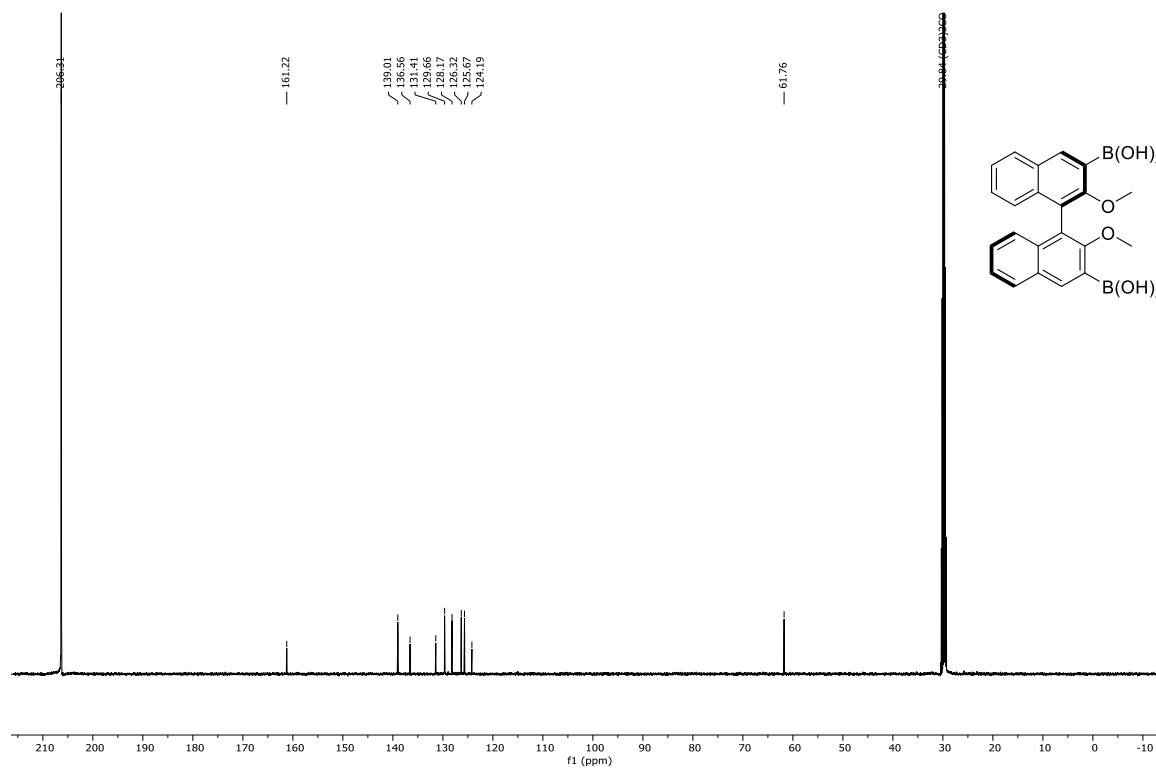
 ^1H NMR (500 MHz, CDCl_3) of **4CzIPN (3)**

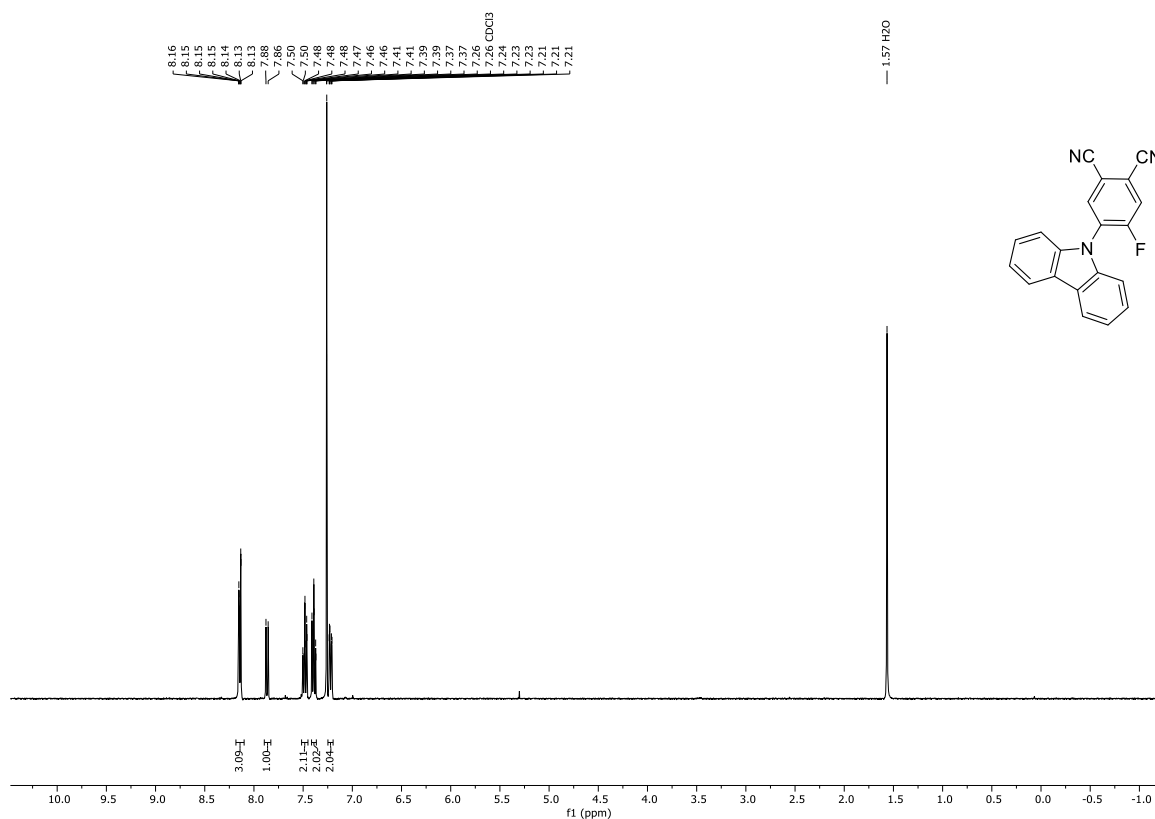
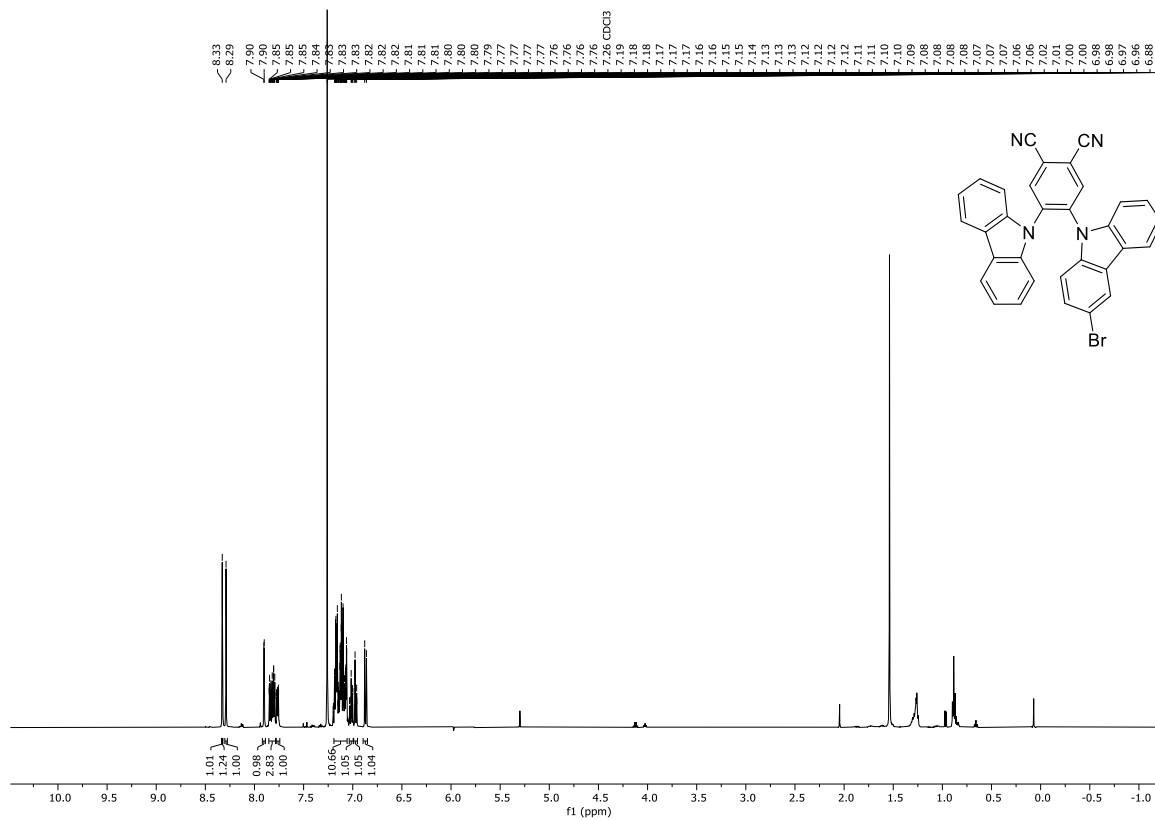
^1H NMR (500 MHz, CDCl_3) of (*R*)-2,2'-Dimethoxy-1,1'-binaphthalene (1**)** **^{13}C NMR (126 MHz, CDCl_3) of (*R*)-2,2'-Dimethoxy-1,1'-binaphthalene (**1**)**

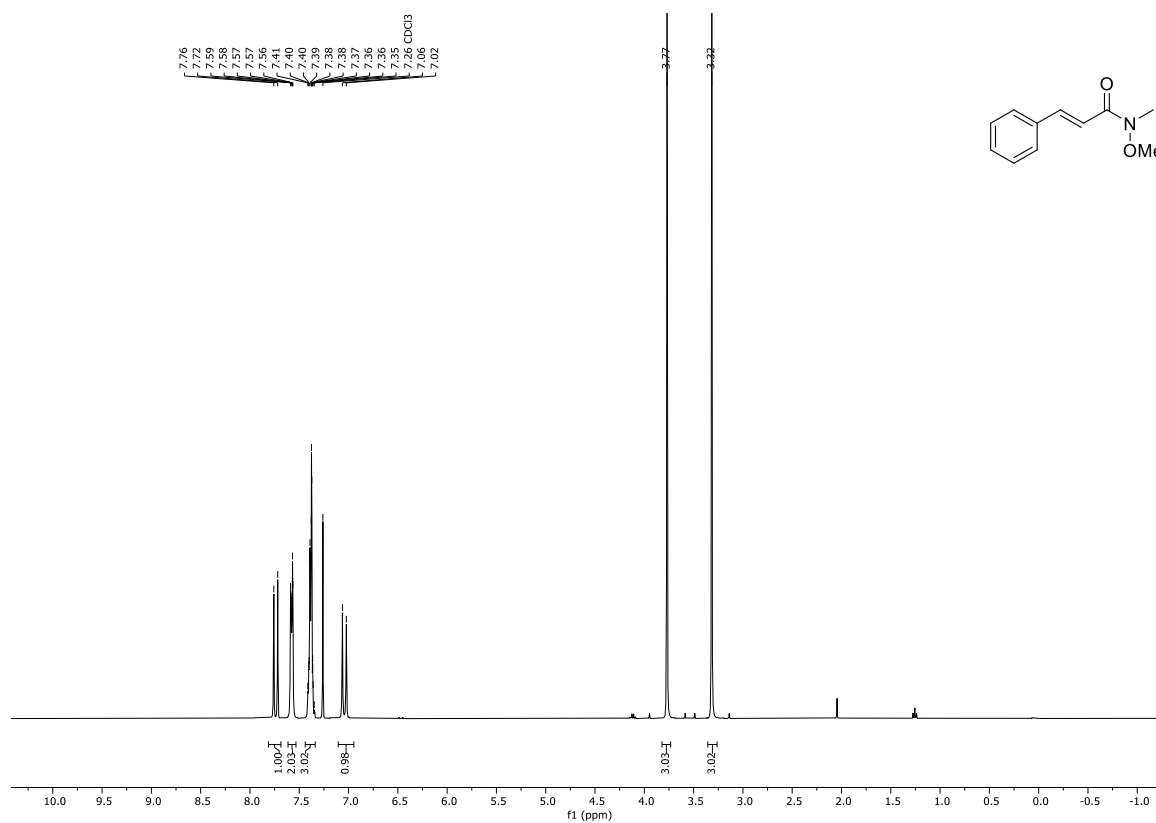
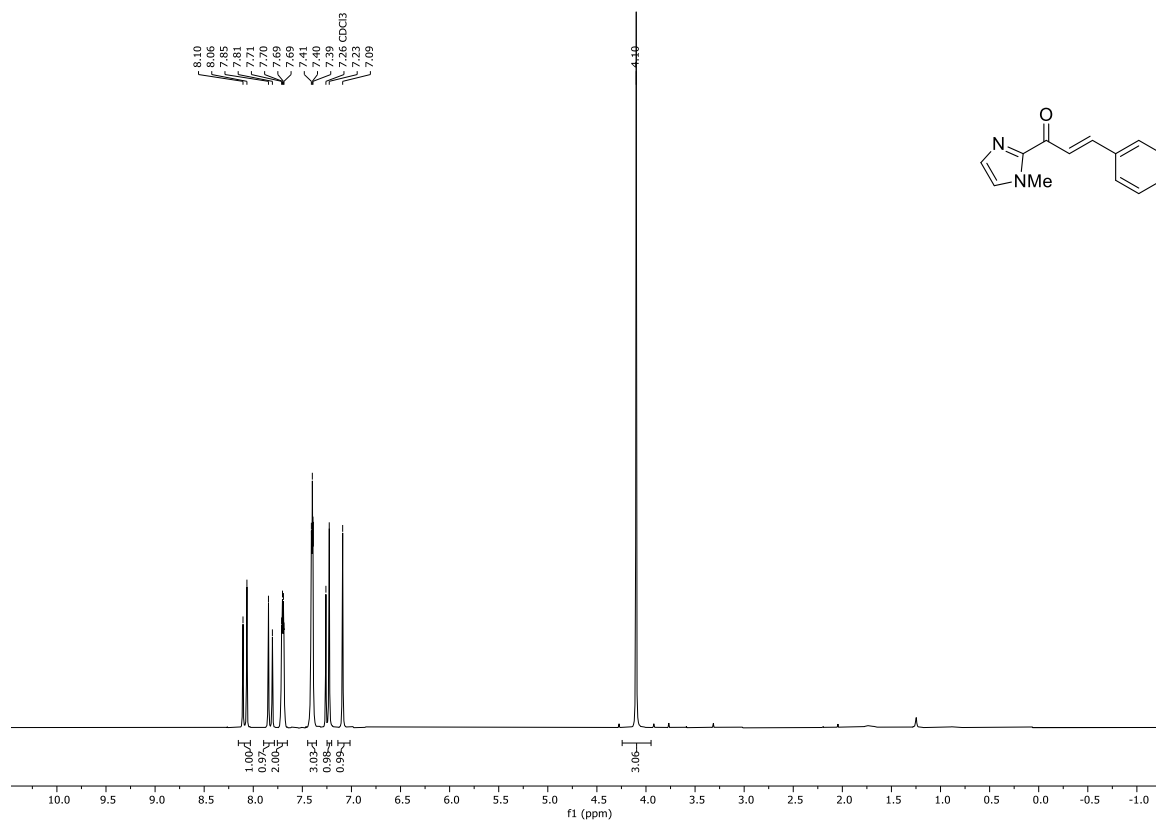
^1H NMR (500 MHz, Acetone- d_6) of (*R*)-2,2'-Dimethoxy-[1,1'-binaphthalene]-3,3'-diyl)diboronic acid (**2**)

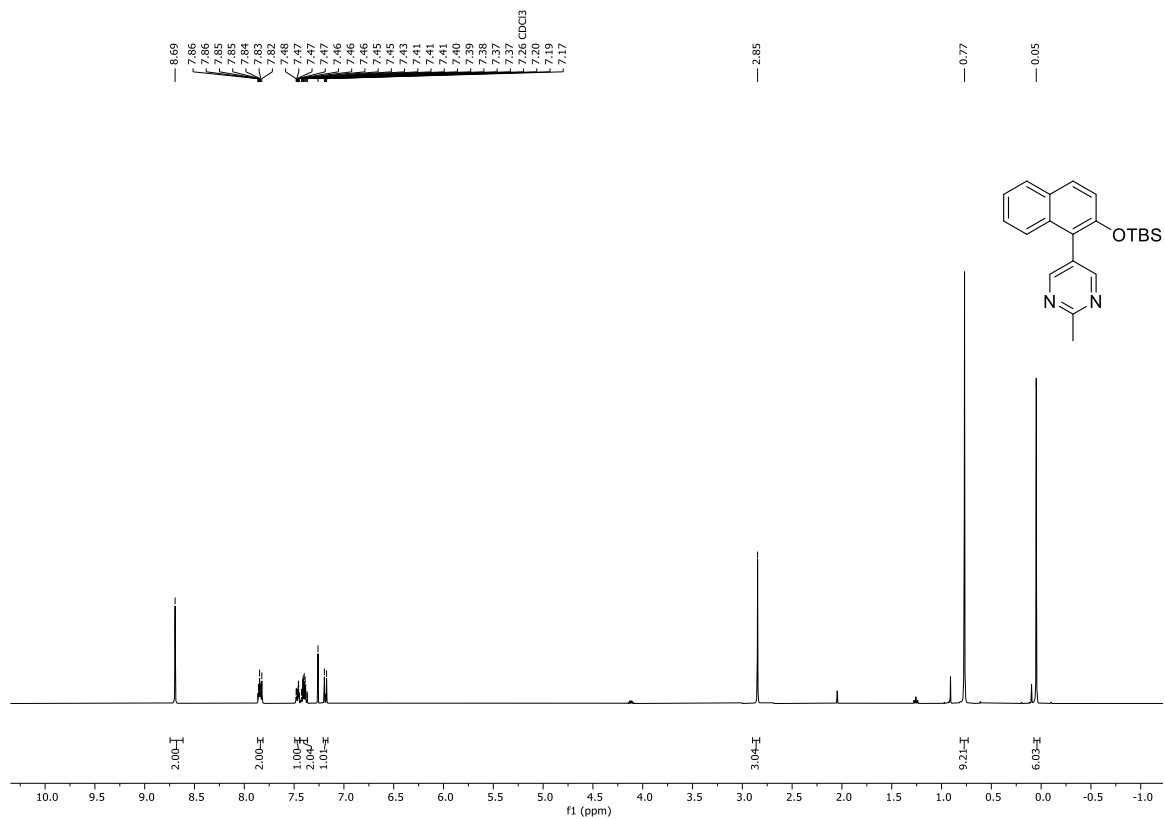
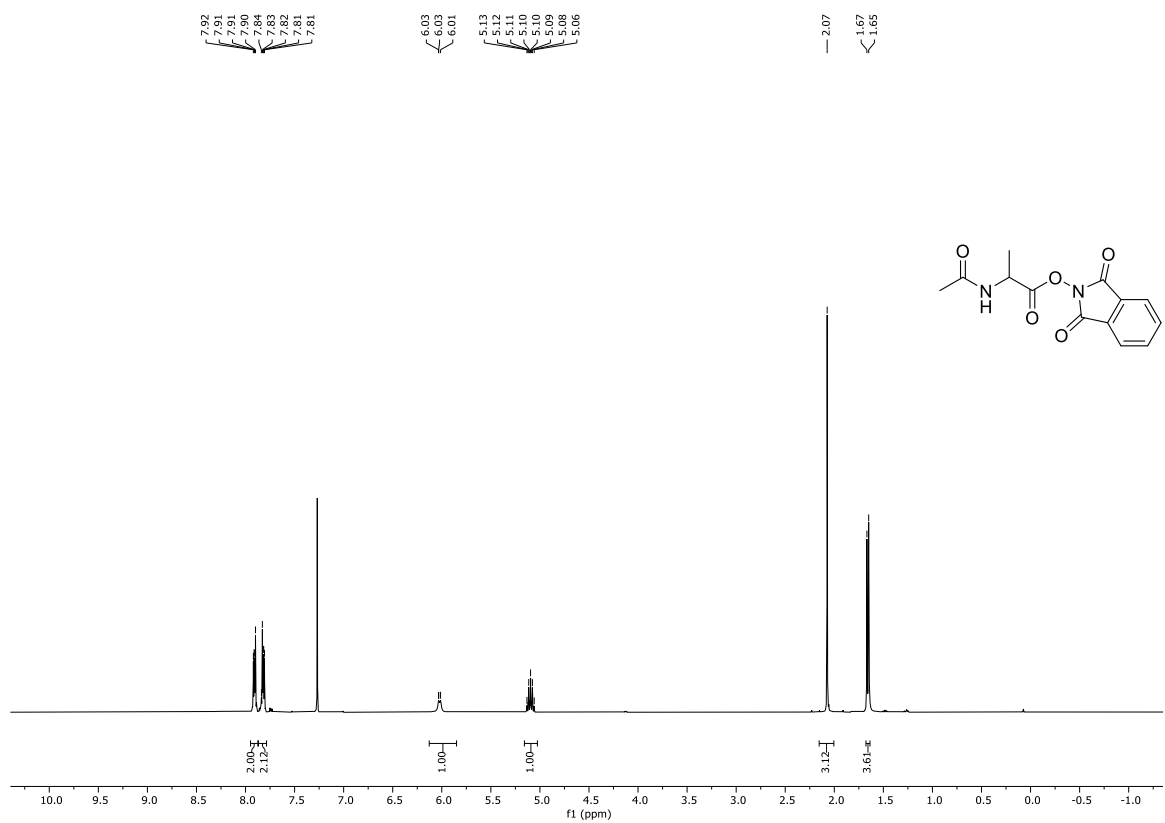


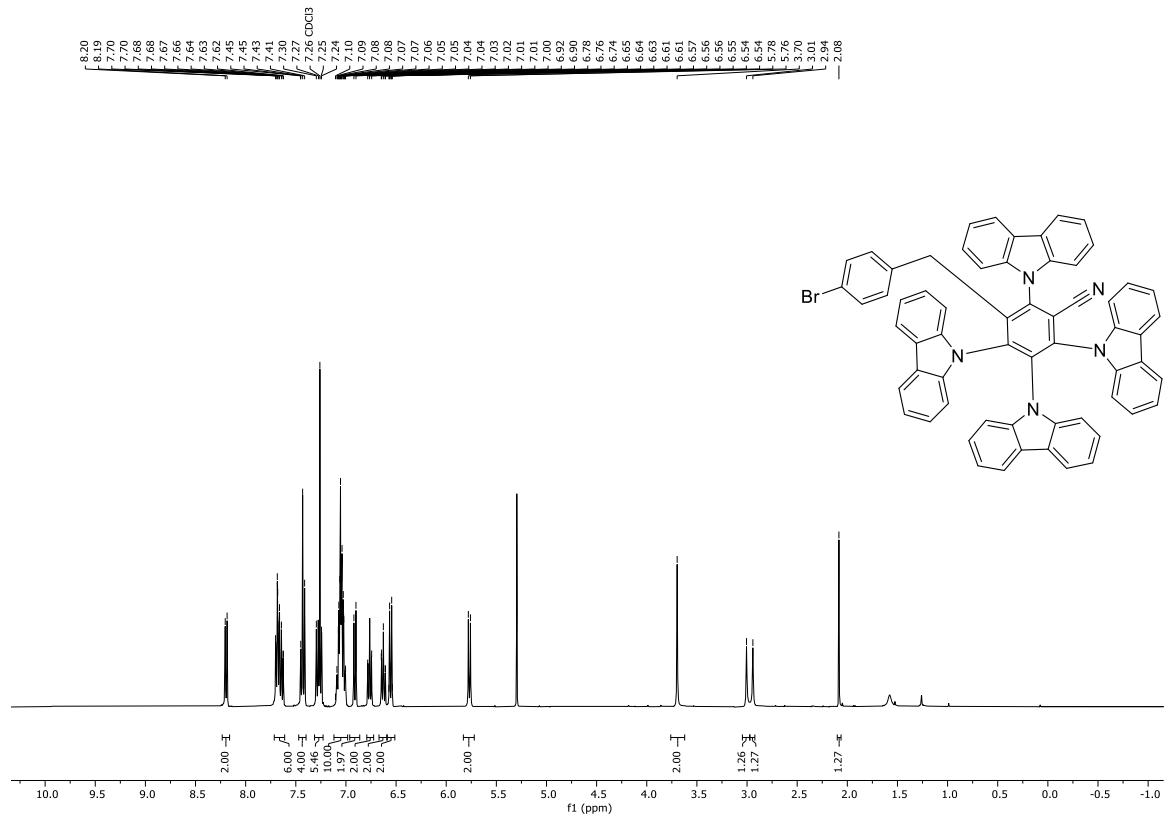
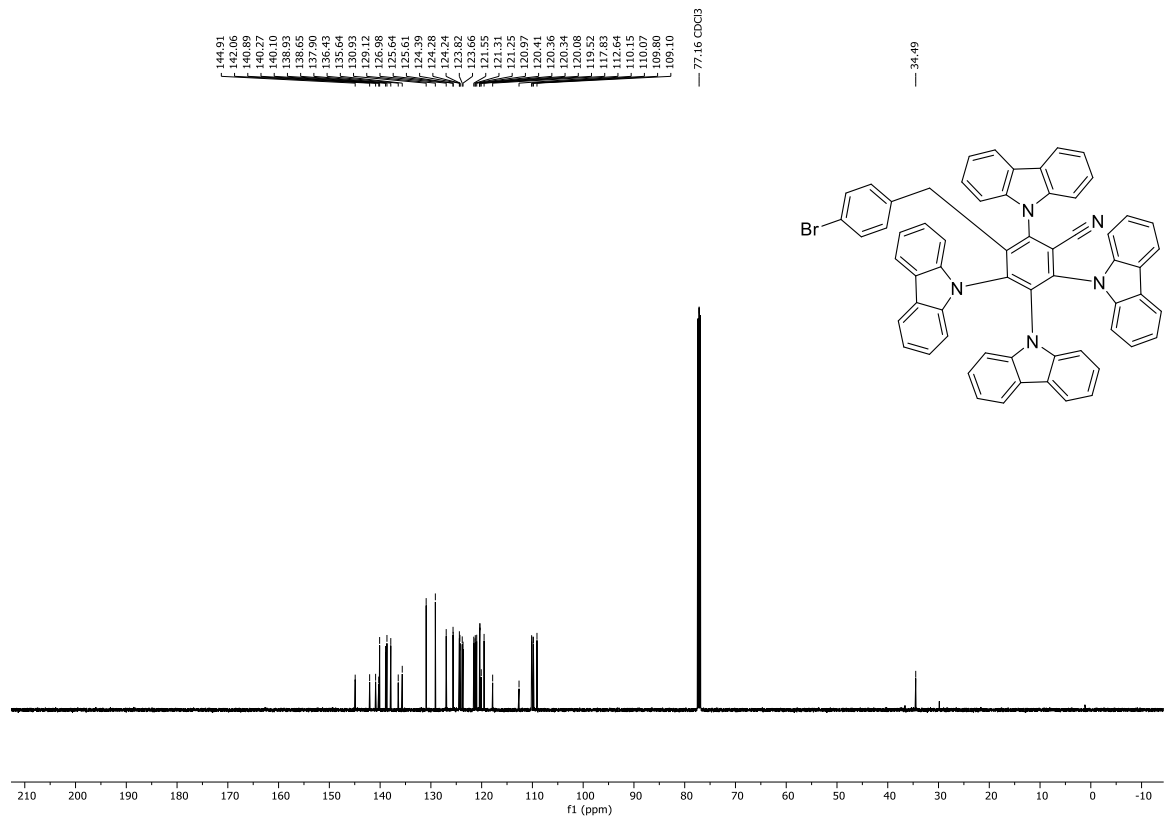
^{13}C NMR (126 MHz, Acetone- d_6) of (*R*)-2,2'-Dimethoxy-[1,1'-binaphthalene]-3,3'-diyl)diboronic acid (**2**)



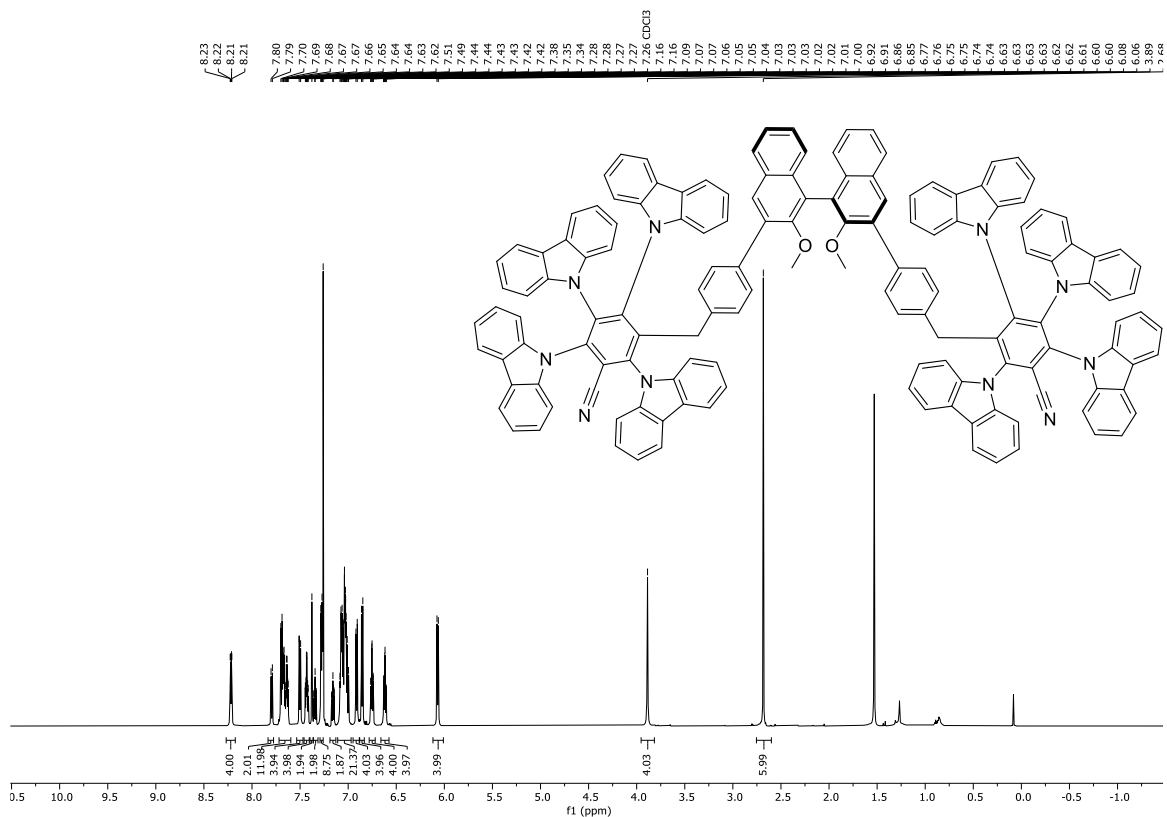
^1H NMR (400 MHz, CDCl_3) of 4-(9H-Carbazol-9-yl)-5-fluorophthalonitrile (8) **^1H NMR (500 MHz, CDCl_3) of 4-(3-Bromo-9H-carbazol-9-yl)-5-(9H-carbazol-9-yl)phthalonitrile (9)**

^1H NMR (400 MHz, CDCl_3) of *N*-Methoxy-*N*-methylcinnamamide (4-S1**)** **^1H NMR (400 MHz, CDCl_3) of (*E*)-1-(1-Methyl-1*H*-imidazol-2-yl)-3-phenylprop-2-en-1-one (**13**)**

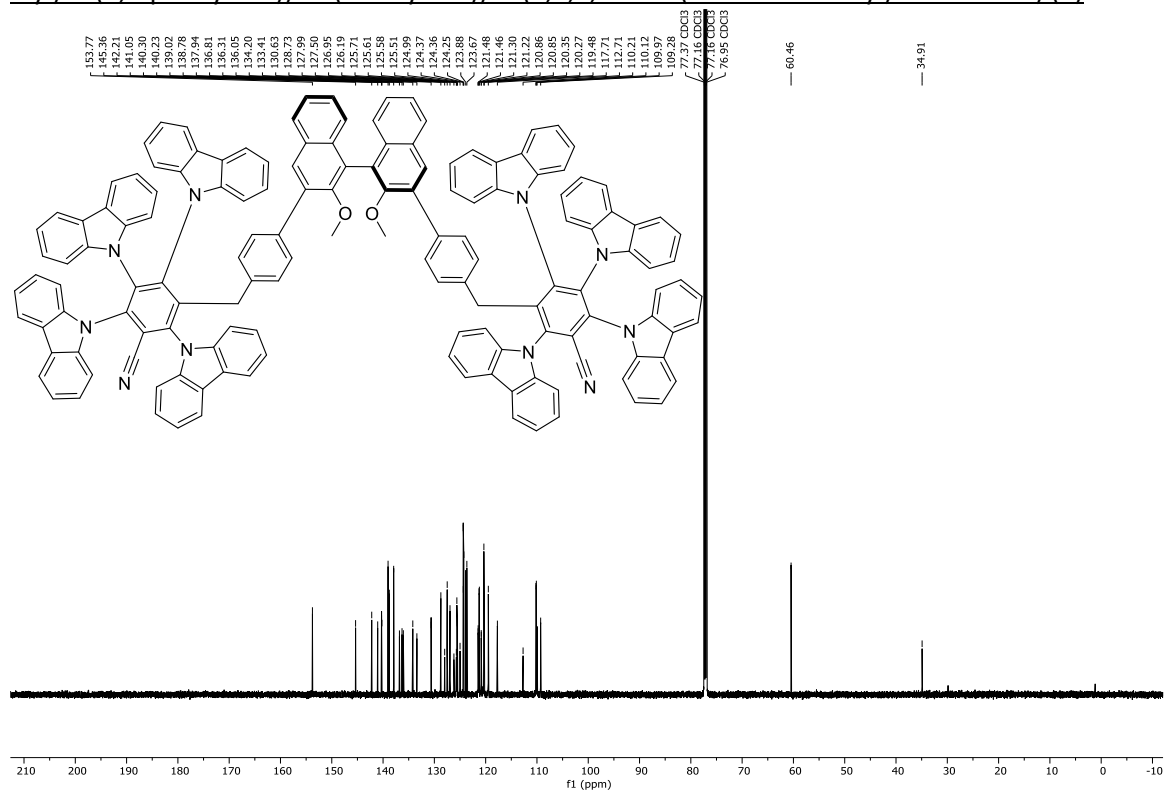
^1H NMR (400 MHz, CDCl_3) of 5-(2-((*tert*-Butyldimethylsilyloxy)naphthalen-1-yl)-2-methylpyrimidine (15) **^1H NMR (400 MHz, CDCl_3) of 1,3-Dioxoisindolin-2-yl acetyl-L-alaninate (16)**

${}^1\text{H}$ NMR (400 MHz, CDCl_3) of 3-(4-Bromobenzyl)-2,4,5,6-tetra(9*H*-carbazol-9-yl)benzonitrile (**4**) ${}^{13}\text{C}$ NMR (126 MHz, CDCl_3) of 3-(4-Bromobenzyl)-2,4,5,6-tetra(9*H*-carbazol-9-yl)benzonitrile (**4**)

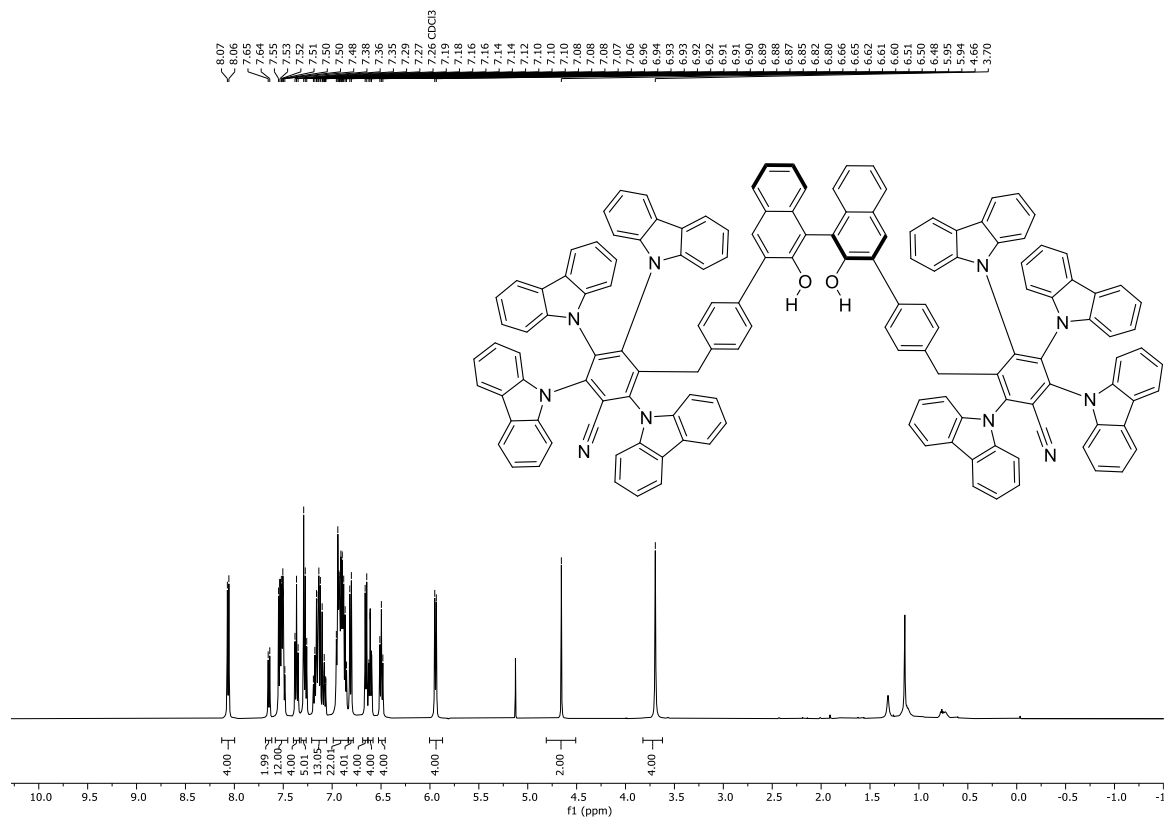
^1H NMR (600 MHz, CDCl_3) of (*R*)-5,5'-(((2,2'-Dimethoxy-[1,1'-binaphthalene]-3,3'-diyl)bis(4,1-phenylene)) bis(methylene))bis(2,3,4,6-tetra(9*H*-carbazol-9-yl)benzocnitrile) (5)



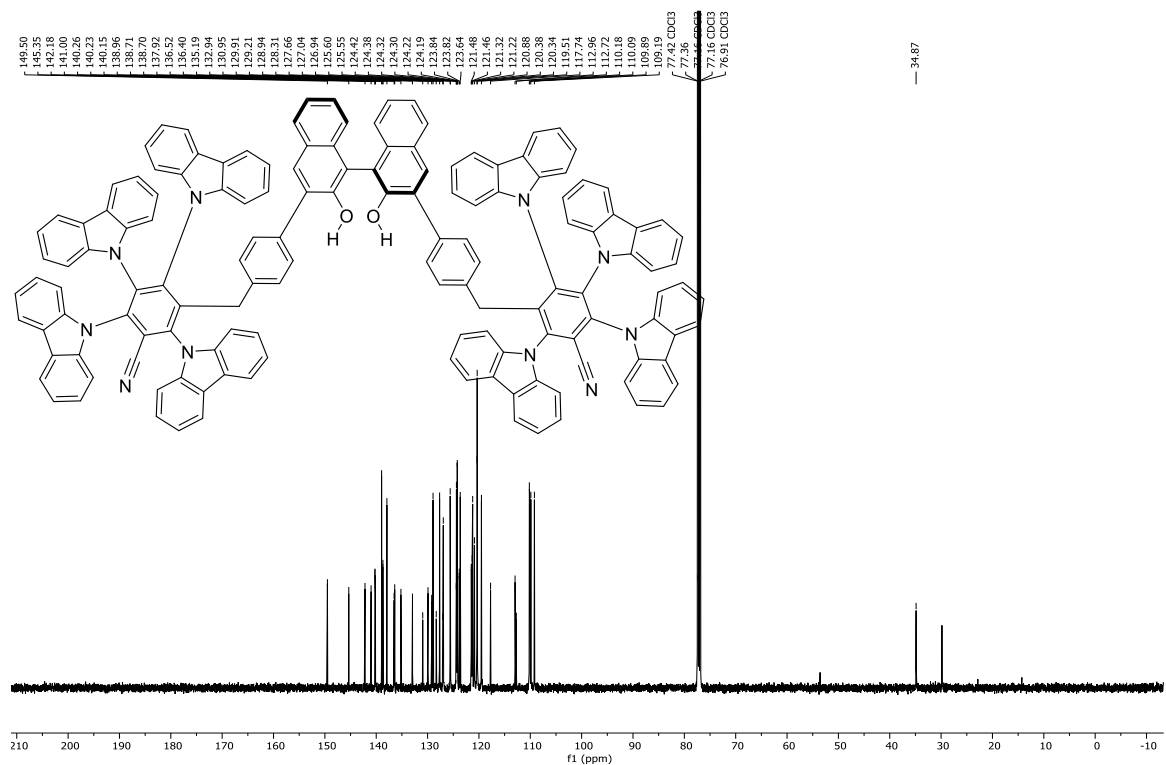
^{13}C NMR (151 MHz, CDCl_3) of (*R*)-5,5'-(((2,2'-Dimethoxy-[1,1'-binaphthalene]-3,3'-diyl)bis(4,1-phenylene)) bis(methylene))bis(2,3,4,6-tetra(9*H*-carbazol-9-yl)benzocnitrile) (5)



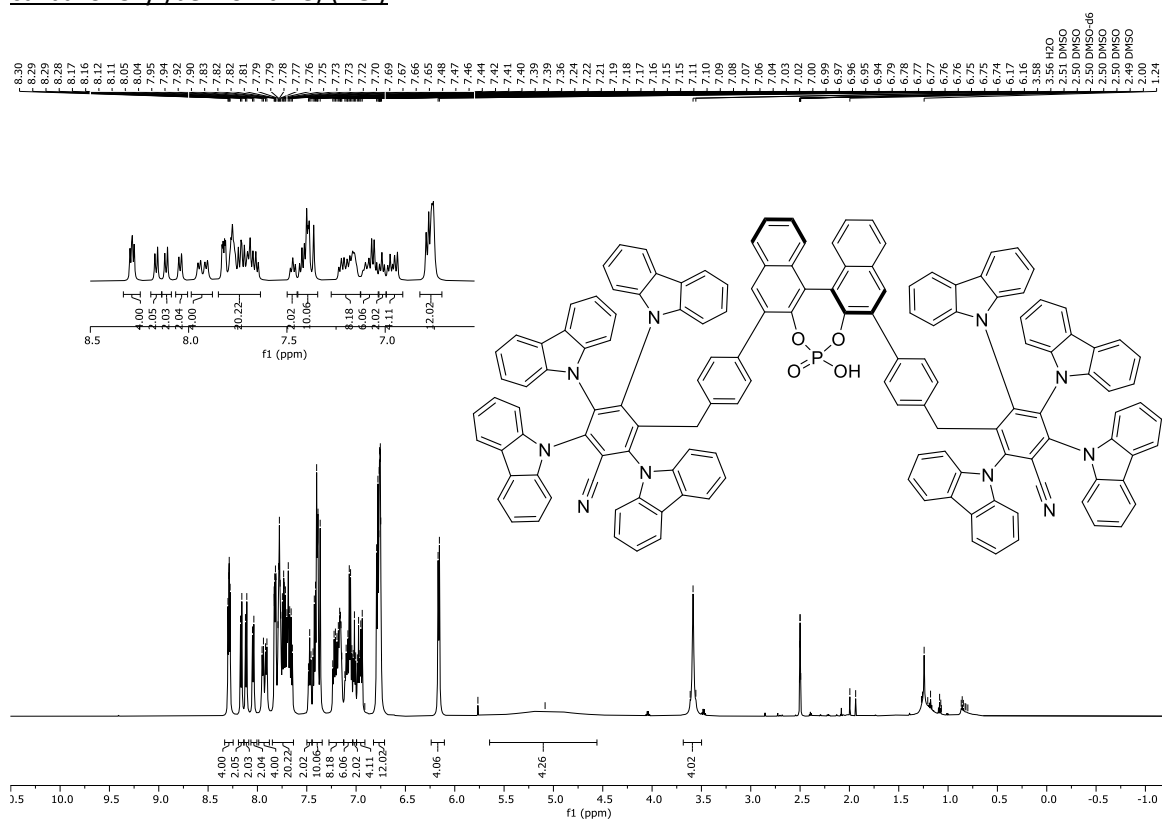
^1H NMR (500 MHz, CDCl_3) of (*R*)-5,5'-(((2,2'-Dihydroxy-[1,1'-binaphthalene]-3,3'-diyl)bis(4,1-phenylene)) bis(methylene))bis(2,3,4,6-tetra(9*H*-carbazol-9-yl)benzocnitrile) (7**)**



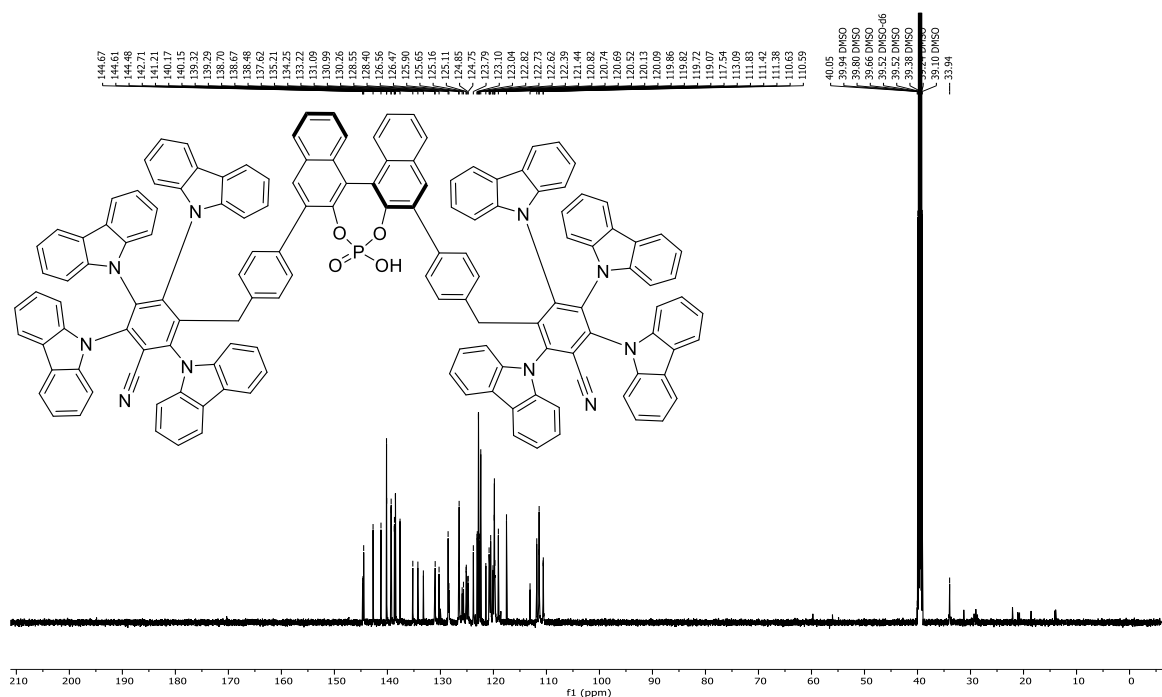
^{13}C NMR (126 MHz, CDCl_3) of (*R*)-5,5'-(((2,2'-Dihydroxy-[1,1'-binaphthalene]-3,3'-diyl)bis(4,1-phenylene)) bis(methylene))bis(2,3,4,6-tetra(9*H*-carbazol-9-yl)benzocnitrile) (7**)**



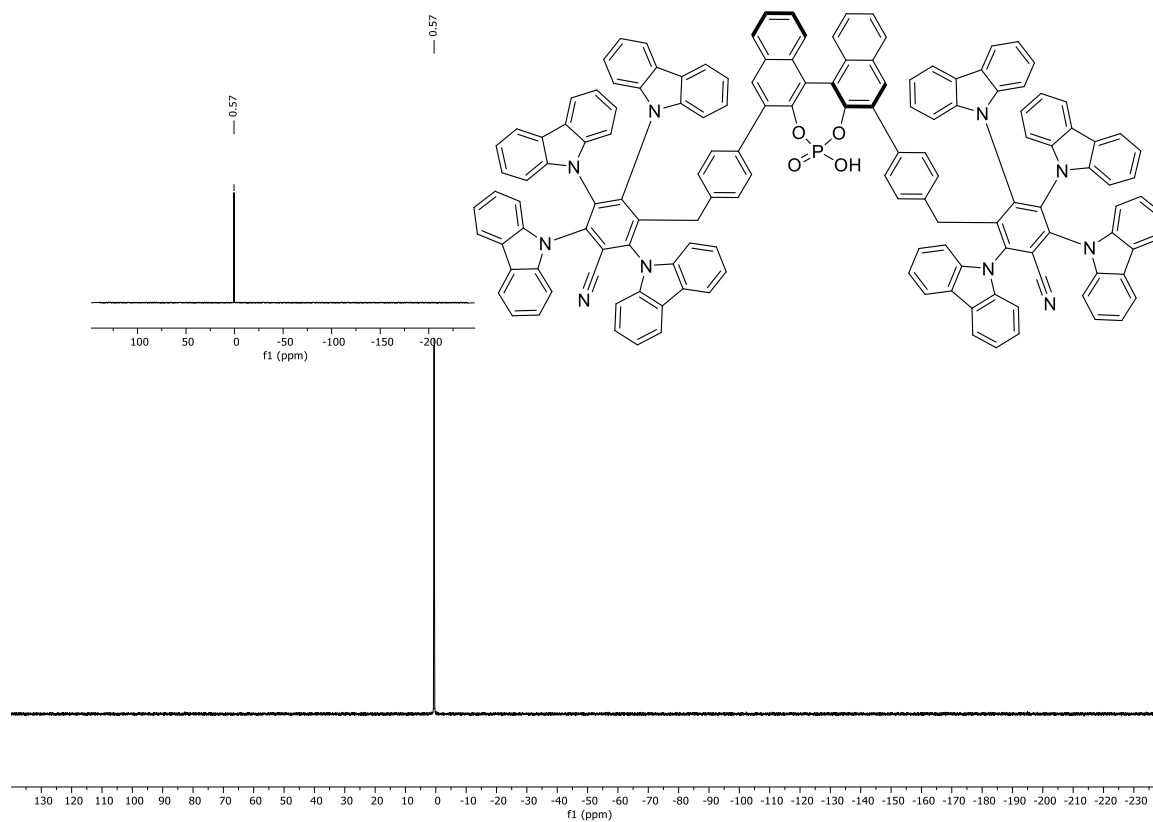
¹H NMR (600 MHz, DMSO-*d*₆) of 5,5'-((((11*b*R)-4-Hydroxy-4-oxidodiphtho[2,1-*d*:1',2'-f][1,3,2]dioxaphosphepine-2,6-diyl)bis(4,1-phenylene))bis(methylene))bis(2,3,4,6-tetra(9*H*-carbazol-9-yl)benzotrile) (PCI)

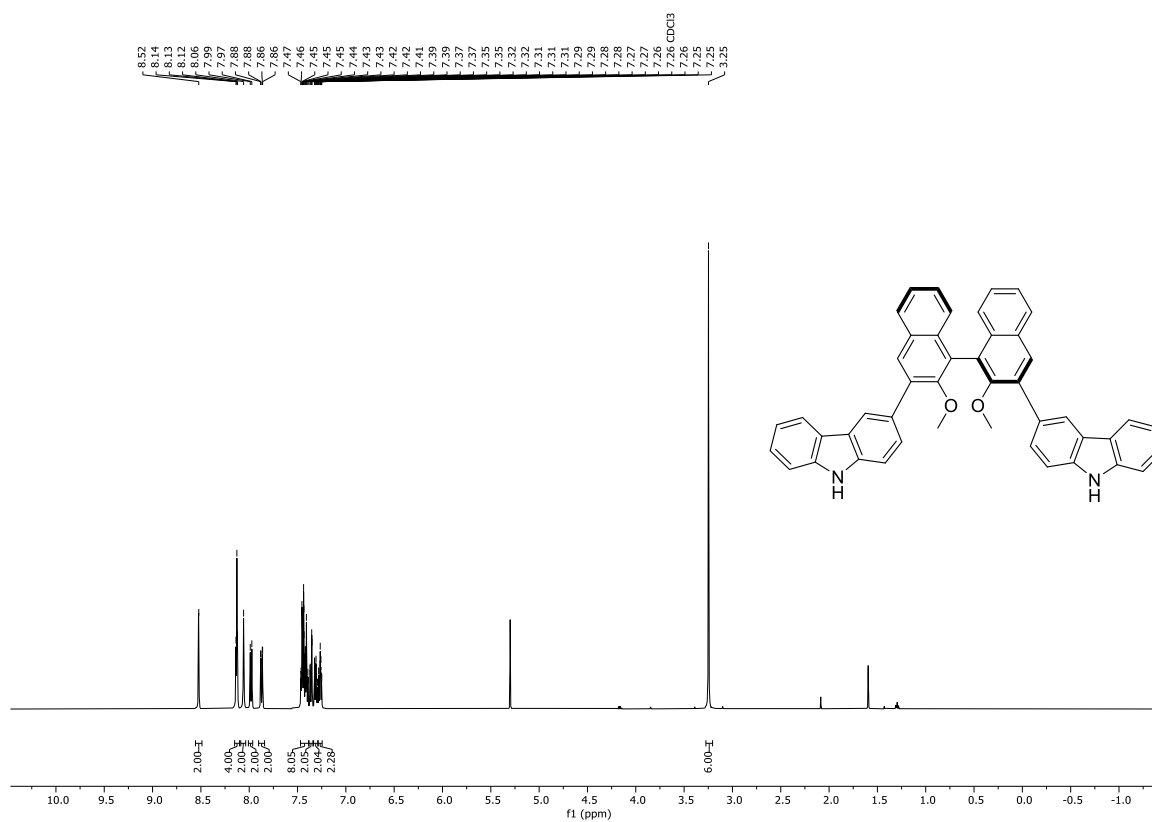
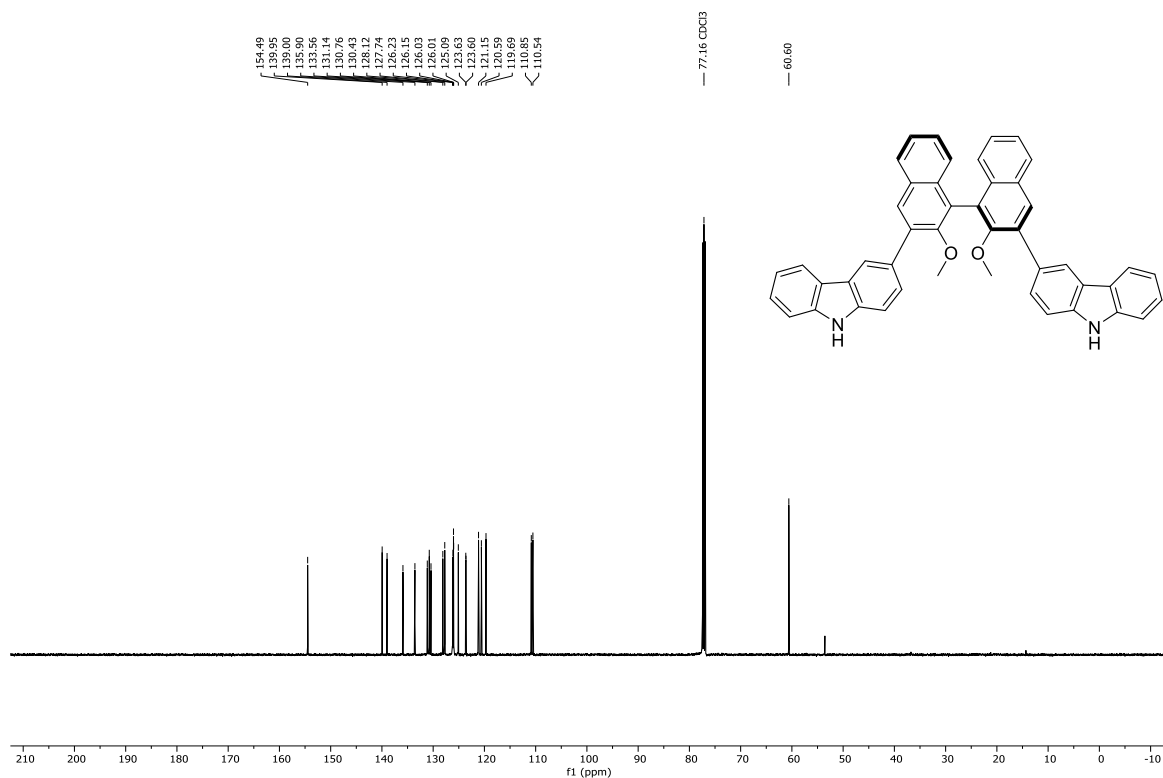


¹³C NMR (151 MHz, DMSO-*d*₆) of 5,5'-((((11*b*R)-4-Hydroxy-4-oxidodiphtho[2,1-*d*:1',2'-f][1,3,2]dioxaphosphepine-2,6-diyl)bis(4,1-phenylene))bis(methylene))bis(2,3,4,6-tetra(9*H*-carbazol-9-yl)benzotrile) (PCI)

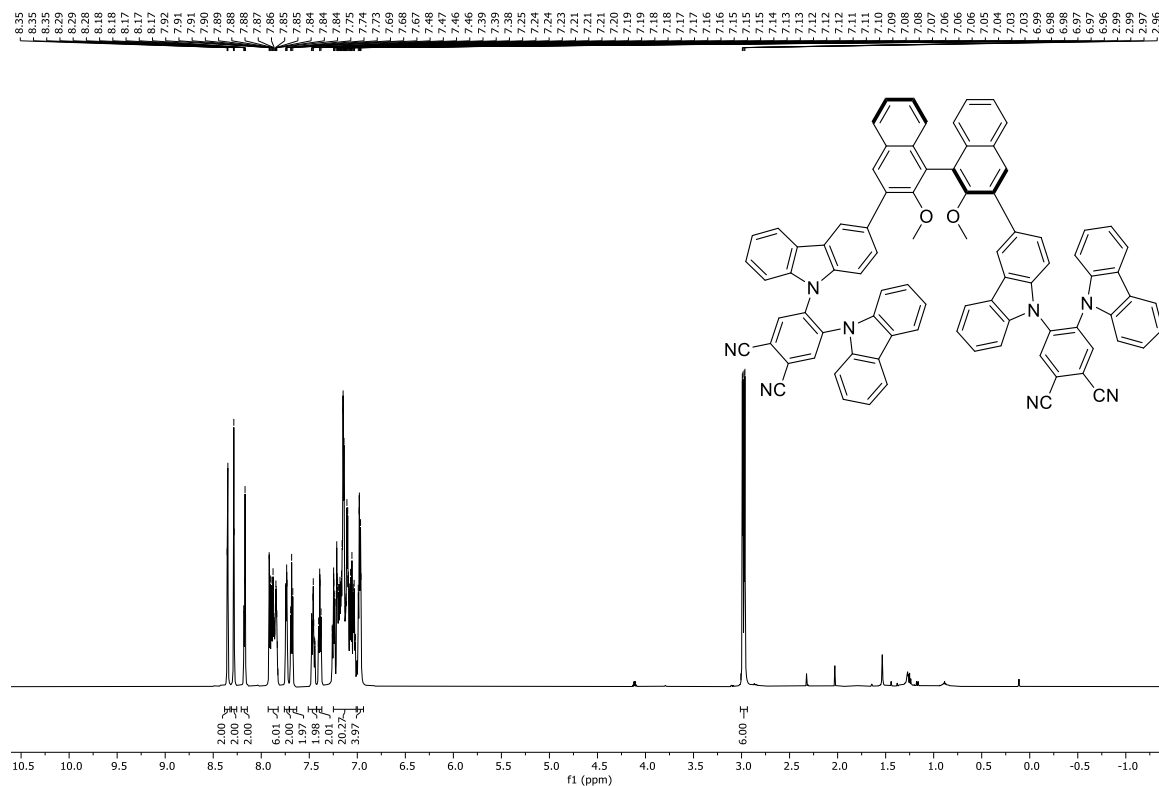


^{31}P NMR (243 MHz, $\text{DMSO-}d_6$) of 5,5'-((((11*bR*)-4-Hydroxy-4-oxidodiphthalazine[2,1-*d*:1',2'-*f*][1,3,2]dioxaphosphepine-2,6-diyl)bis(4,1-phenylene))bis(methylene))bis(2,3,4,6-tetra(9*H*-carbazol-9-yl)benzonitrile) (PCI)

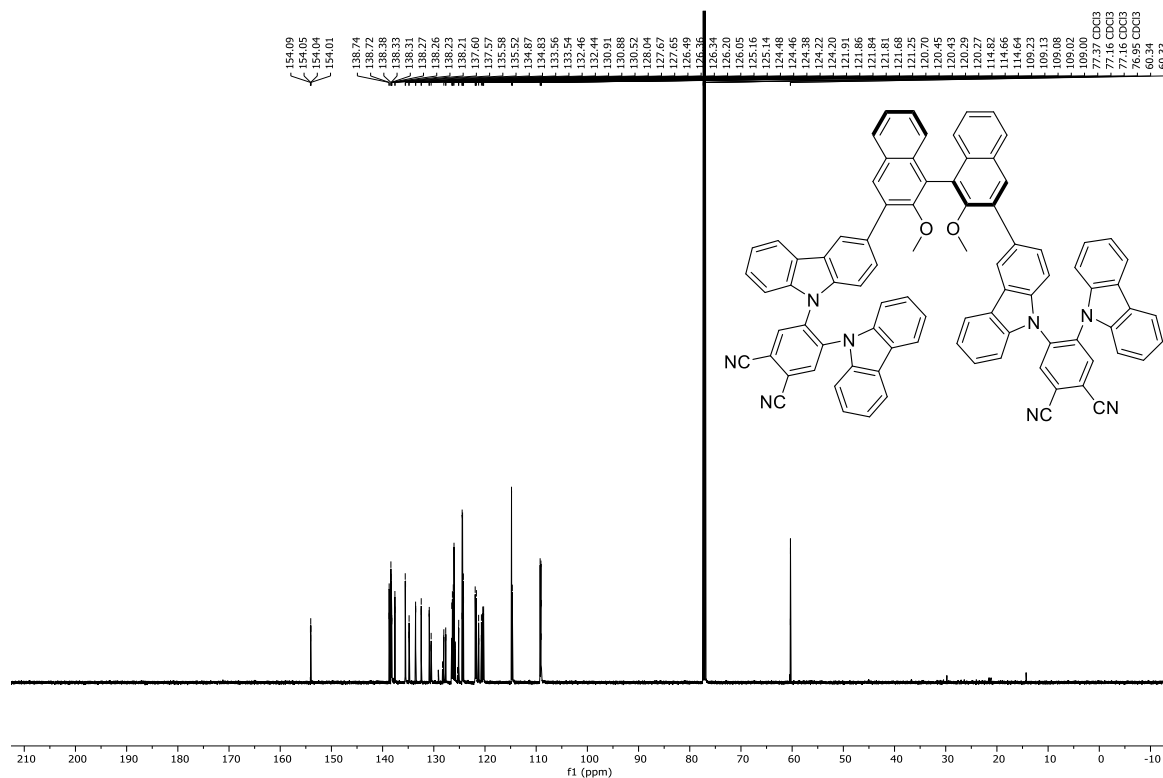


^1H NMR (500 MHz, CDCl_3) of (*R*)-3,3'-(2,2'-Dimethoxy-[1,1'-binaphthalene]-3,3'-diyl)bis(9*H*-carbazole) (11) **^{13}C NMR (126 MHz, CDCl_3) of (*R*)-3,3'-(2,2'-Dimethoxy-[1,1'-binaphthalene]-3,3'-diyl)bis(9*H*-carbazole) (11)**

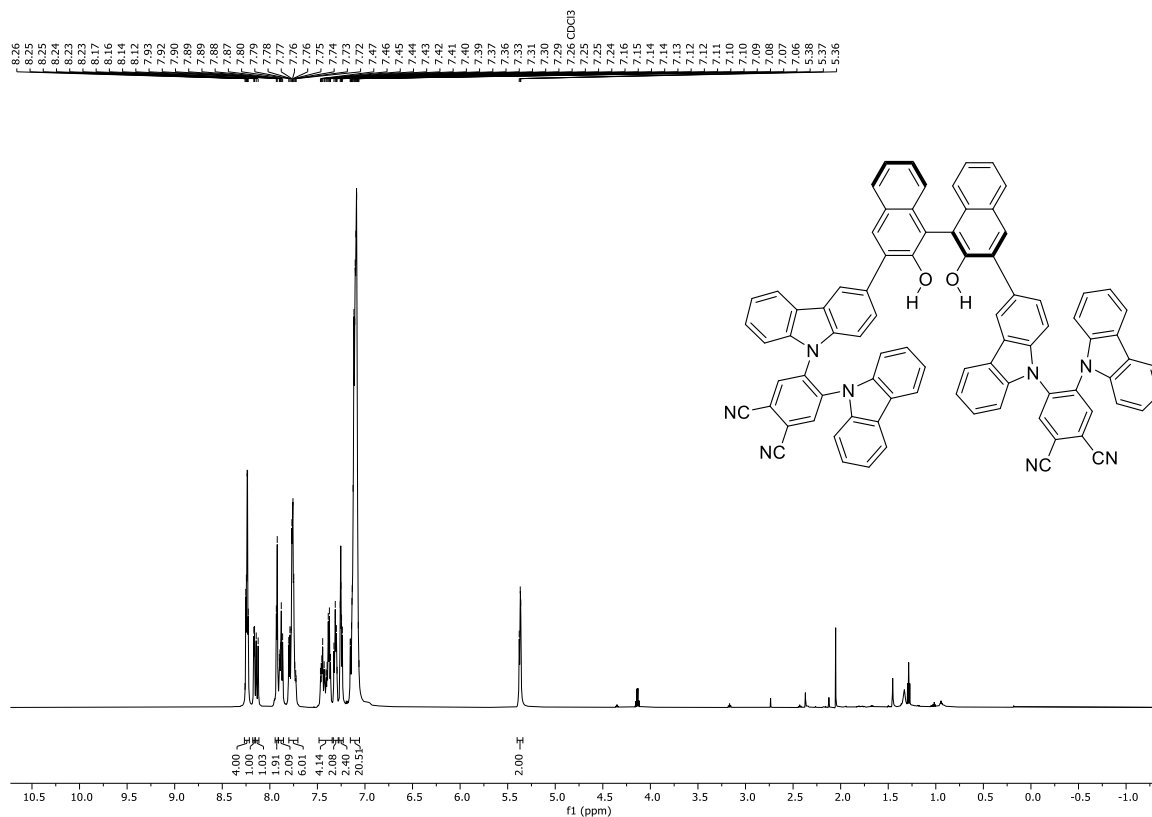
^1H NMR (600 MHz, CDCl_3) of (*R*)-5,5'-((2,2'-Dimethoxy-[1,1'-binaphthalene]-3,3'-diyl)bis(9*H*-carbazole-3,9-diyl))bis(4-(9*H*-carbazol-9-yl)phthalonitrile) (10)



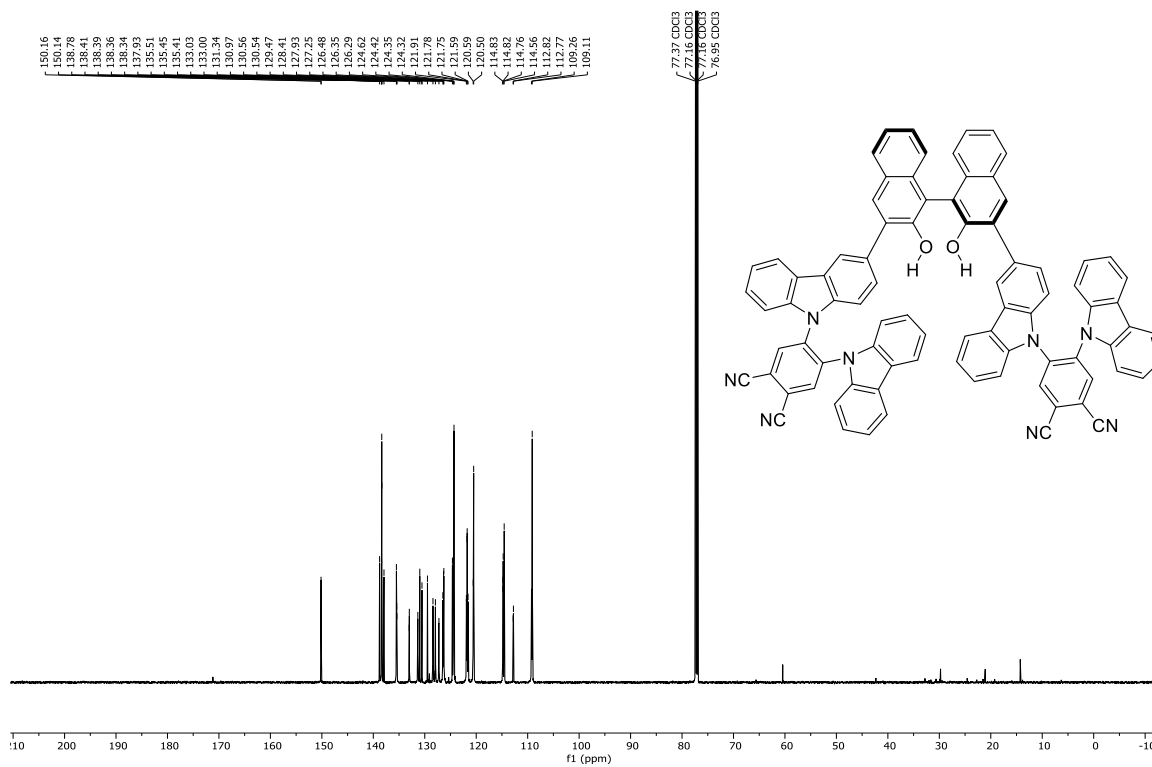
^{13}C NMR (151 MHz, CDCl_3) of (*R*)-5,5'-((2,2'-Dimethoxy-[1,1'-binaphthalene]-3,3'-diyl)bis(9*H*-carbazole-3,9-diyl))bis(4-(9*H*-carbazol-9-yl)phthalonitrile) (10)



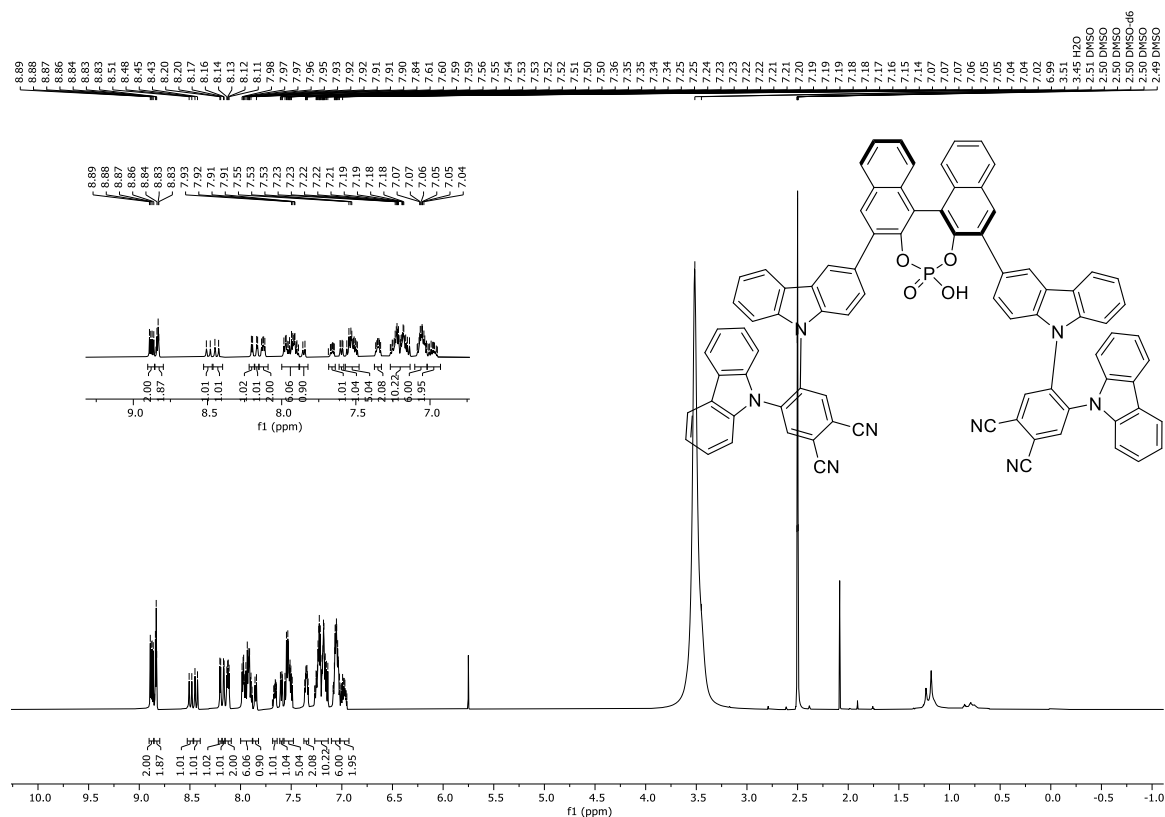
^1H NMR (600 MHz, CDCl_3) of (*R*)-5,5'-((2,2'-Dihydroxy-[1,1'-binaphthalene]-3,3'-diyl)bis(9H-carbazole-3,9-diyl))bis(4-(9H-carbazol-9-yl)phthalonitrile) (12)



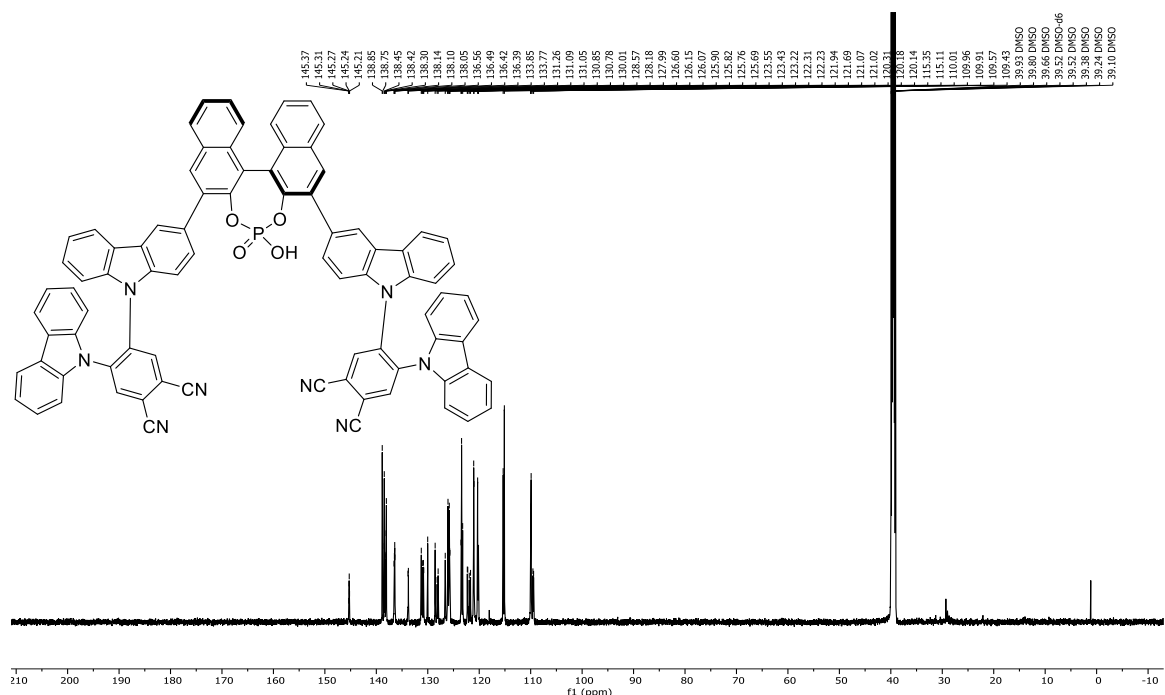
^{13}C NMR (151 MHz, CDCl_3) of (*R*)-5,5'-((2,2'-Dihydroxy-[1,1'-binaphthalene]-3,3'-diyl)bis(9H-carbazole-3,9-diyl))bis(4-(9H-carbazol-9-yl)phthalonitrile) (12)



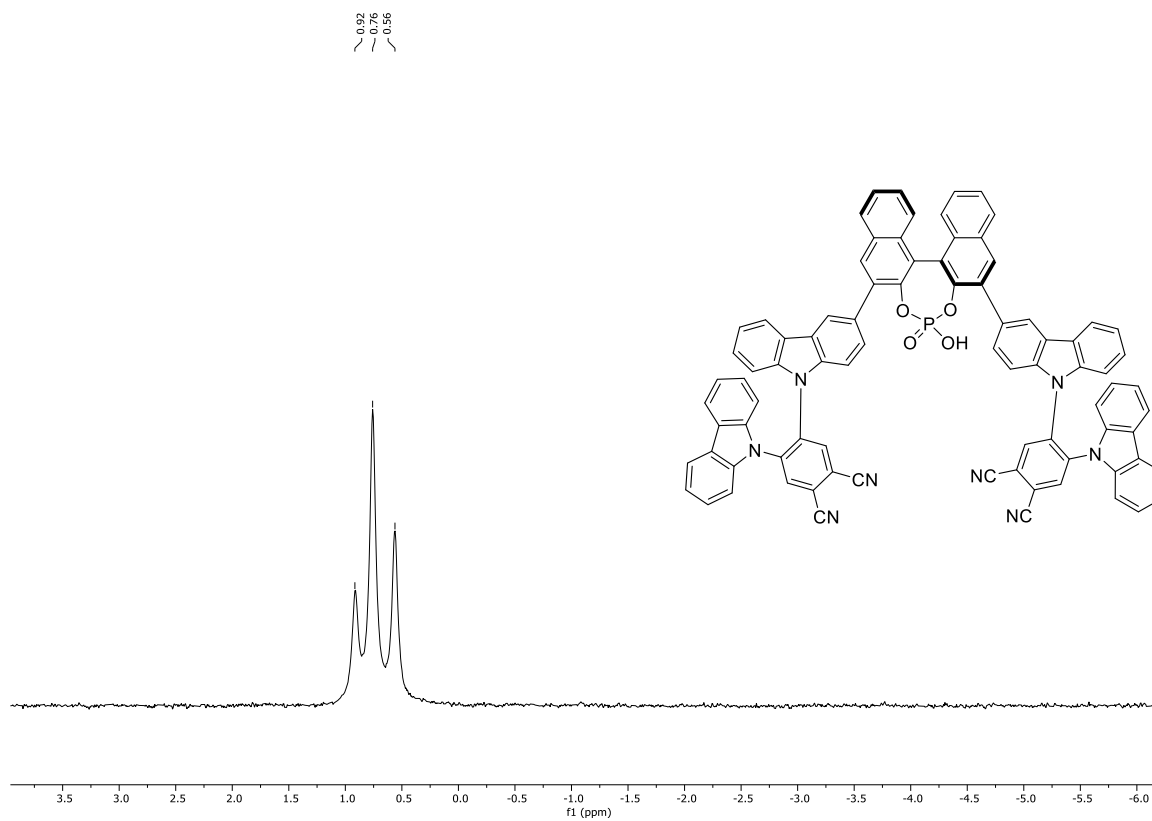
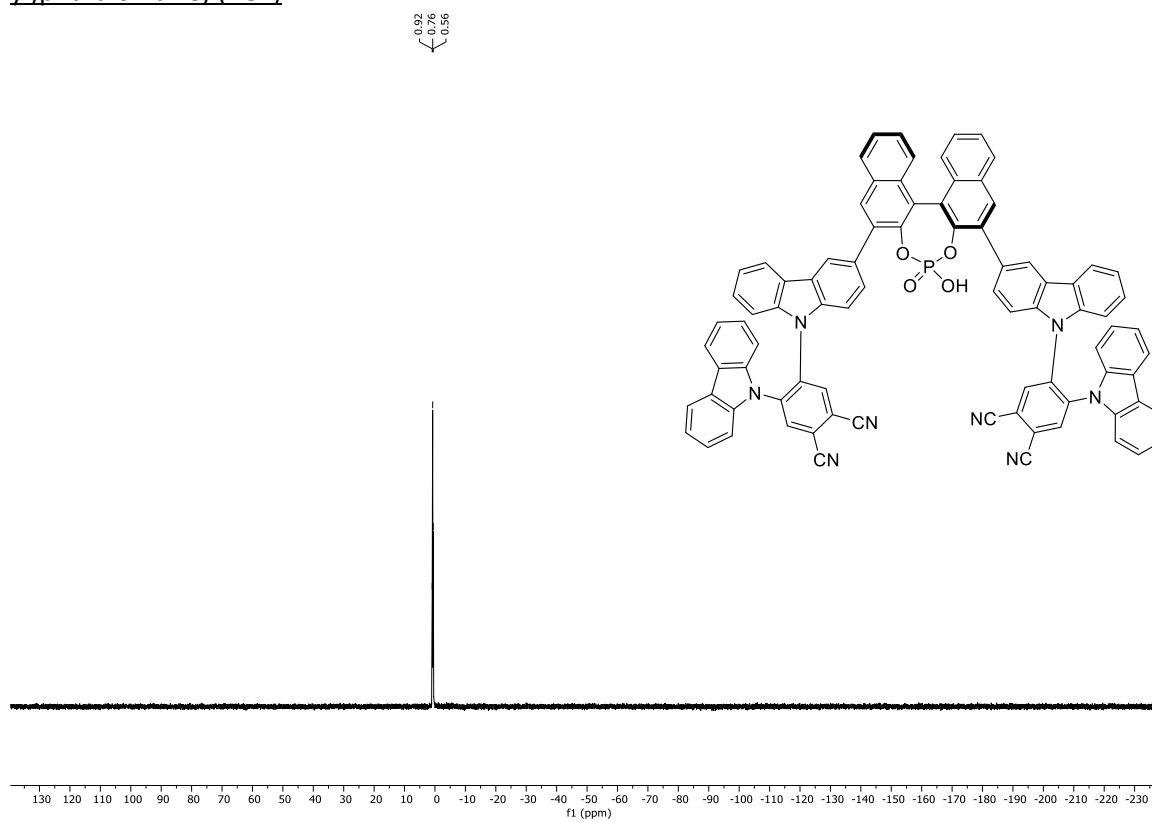
¹H NMR (600 MHz, DMSO-*d*₆) of (4*r*,4'*r*)-5,5'-(((11*b*s)-4-Hydroxy-4-oxidodiphtho[2,1-*d*:1',2'-*f*][1,3,2]dioxaphosphepine-2,6-diyl)bis(9*H*-carbazole-3,9-diyl))bis(4-(9*H*-carbazol-9-yl)phthalonitrile) (PCII)



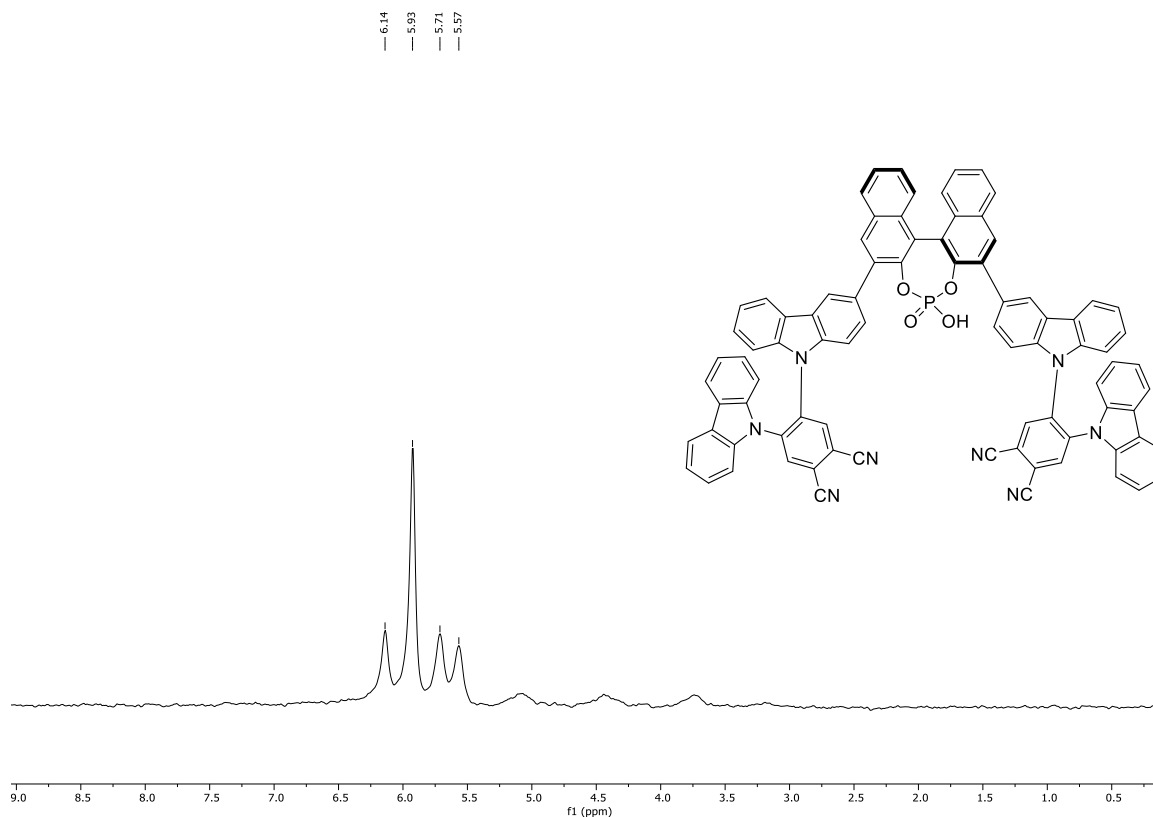
¹³C NMR (151 MHz, DMSO-*d*₆) of (4*r*,4'*r*)-5,5'-(((11*b*s)-4-Hydroxy-4-oxidodiphtho[2,1-*d*:1',2'-*f*][1,3,2]dioxaphosphepine-2,6-diyl)bis(9*H*-carbazole-3,9-diyl))bis(4-(9*H*-carbazol-9-yl)phthalonitrile) (PCII)



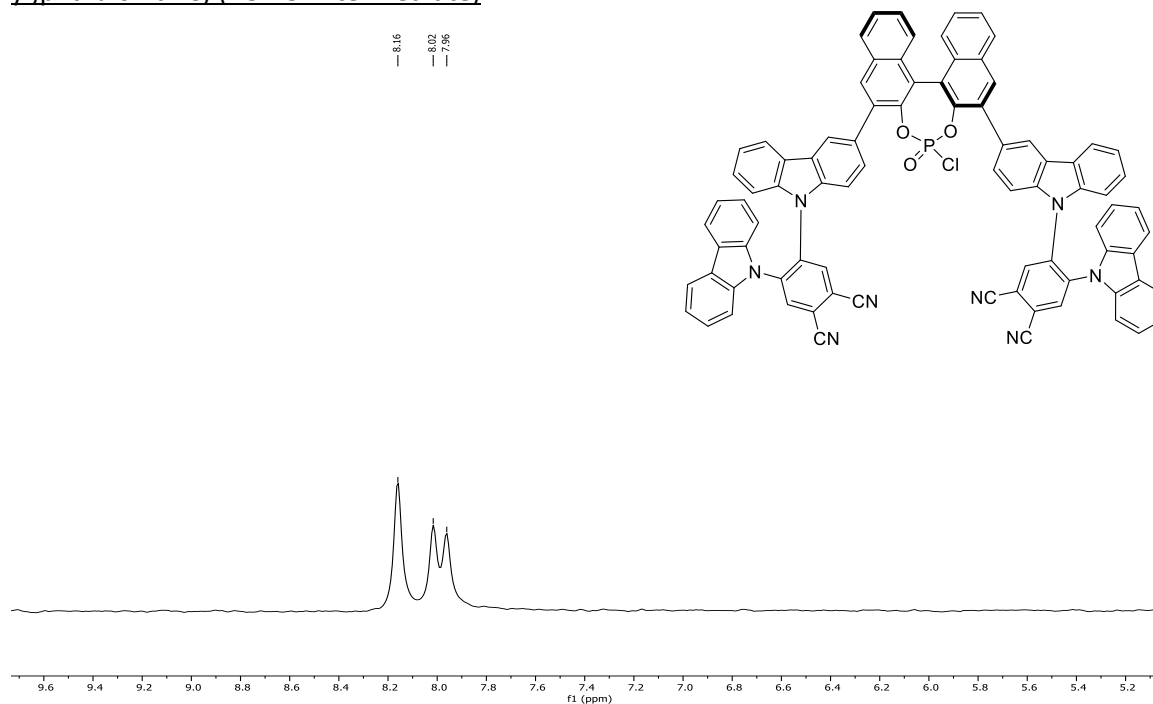
^{31}P NMR (243 MHz, $\text{DMSO-}d_6$) of (4*r*,4'*r*)-5,5'-(((11*b*S)-4-Hydroxy-4-oxidodinaphtho[2,1-*d*:1',2'-*f*][1,3,2]dioxaphosphepine-2,6-diyl)bis(9*H*-carbazole-3,9-diyl))bis(4-(9*H*-carbazol-9-yl)phthalonitrile) (PCI)



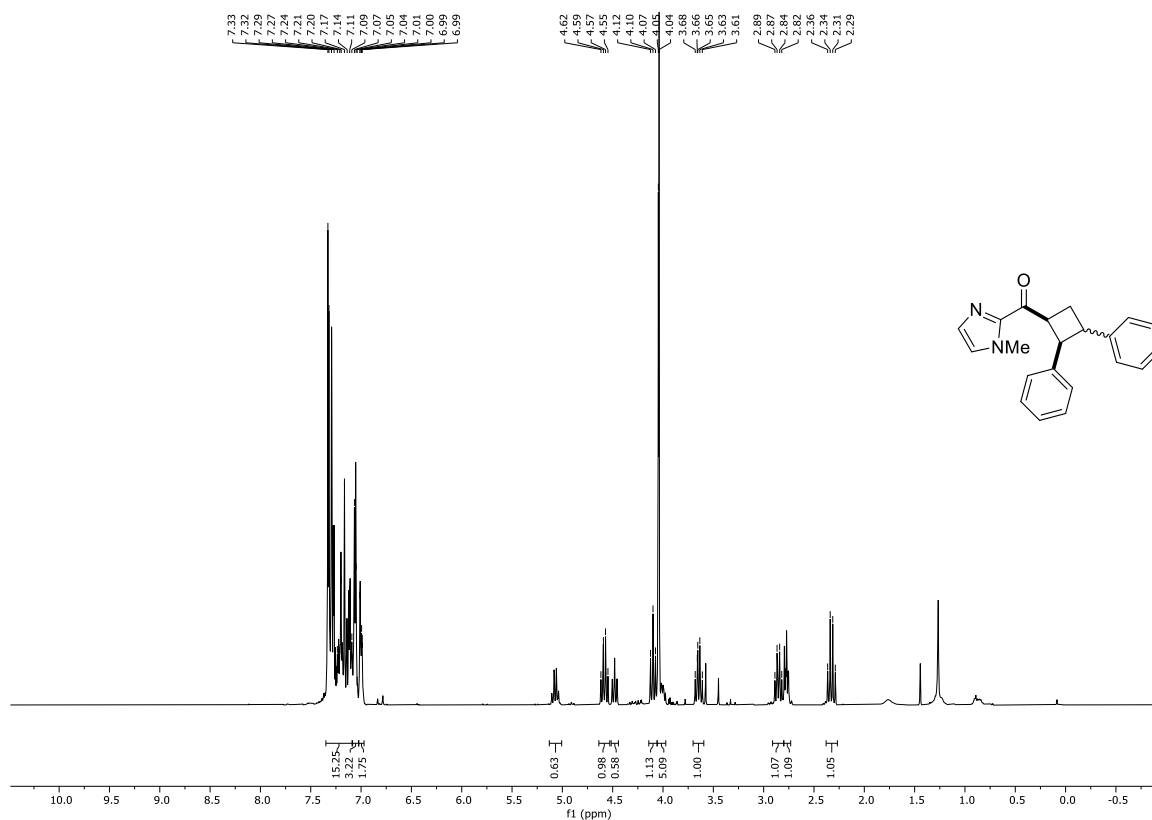
^{31}P NMR (202 MHz, CDCl_3) of (4*r*,4'*r*)-5,5'-(((11*bS*)-4-Hydroxy-4-oxidodina[2,1-*d*:1',2'-*f*][1,3,2]dioxaphosphepine-2,6-diyl)bis(9*H*-carbazole-3,9-diyl))bis(4-(9*H*-carbazol-9-yl)phthalonitrile) (PCII)**



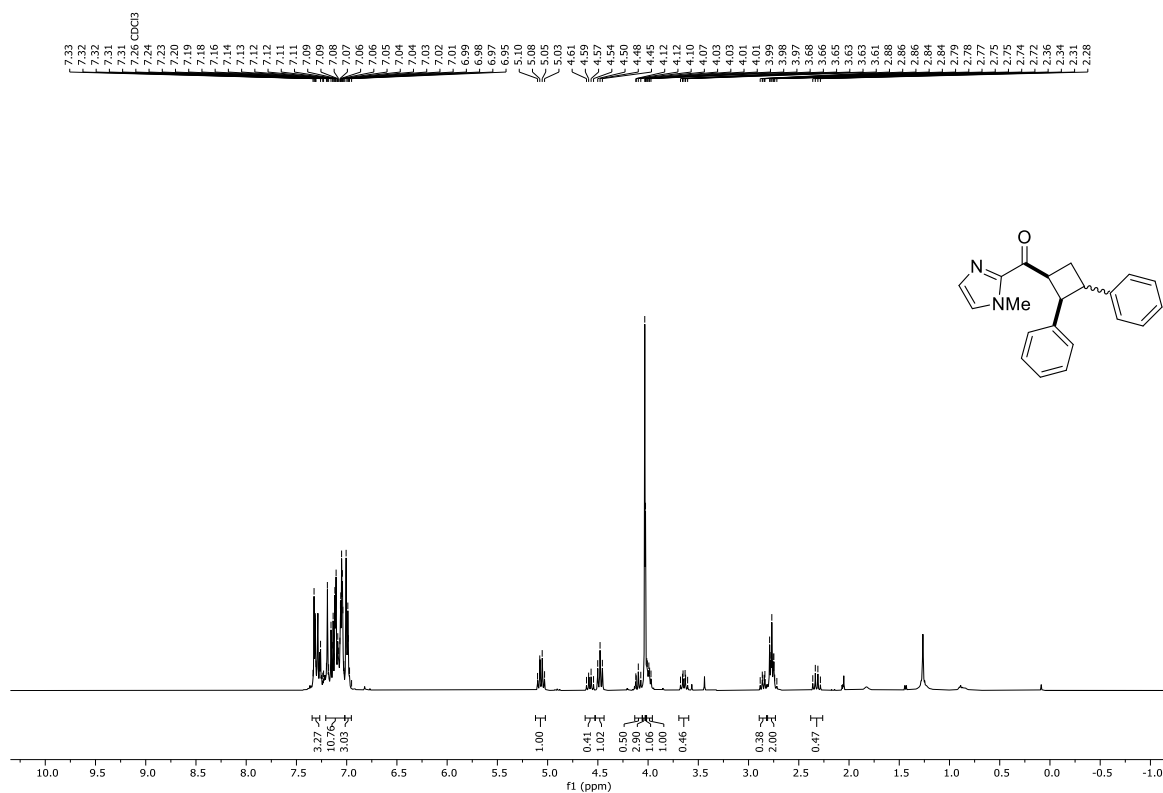
^{31}P NMR (202 MHz, CDCl_3) of (4*r*,4'*r*)-5,5'-(((11*bS*)-4-Chloro-4-oxidodina[2,1-*d*:1',2'-*f*][1,3,2]dioxaphosphepine-2,6-diyl)bis(9*H*-carbazole-3,9-diyl))bis(4-(9*H*-carbazol-9-yl)phthalonitrile) (PCII-Cl Intermediate)**



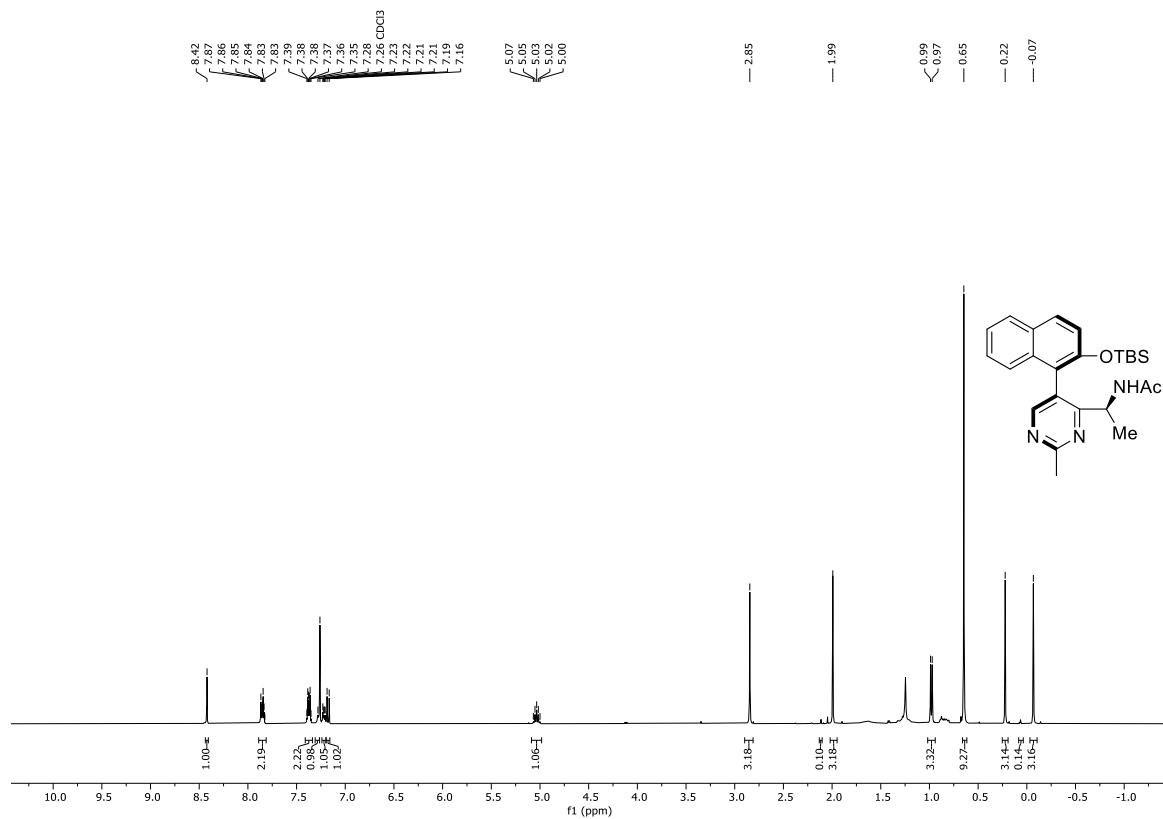
^1H NMR (400 MHz, CDCl_3) of (2,3-Diphenylcyclobutyl)(1-methyl-1H-imidazol-2-yl)methanone (14) with PCI at r.t.



^1H NMR (400 MHz, CDCl_3) of (2,3-Diphenylcyclobutyl)(1-methyl-1H-imidazol-2-yl)methanone (14) with PCI at -78°C



^1H NMR (400 MHz, CDCl_3) of *N*-((1*S*)-1-(5-(2-((*tert*-Butyldimethylsilyloxy)naphthalen-1-yl)-2-methylpyrimidin-4-yl)ethyl)acetamide (**17**)



4.6 References

- [1] For reviews covering enantioselective photocatalysis see: (a) Großkopf, J.; Kratz, T.; Rigotti, T.; Bach, T. Enantioselective Photochemical Reactions Enabled by Triplet Energy Transfer. *Chem. Rev.* **2022**, *122*, 1626-1653. (b) Prentice, C.; Morrisson, J.; Smith, A. D.; Zysman-Colman, E. Recent developments in enantioselective photocatalysis. *Beilstein J. Org. Chem.* **2020**, *16*, 2363-2441. (c) Saha, D. Catalytic Enantioselective Radical Transformations Enabled by Visible Light. *Chem. Asian J.* **2020**, *15*, 2129-215. (d) Silvi, M.; Melchiorre, P. Enhancing the potential of enantioselective organocatalysis with light. *Nature* **2018**, *554*, 41-49. (e) Zou, Y.-Q.; Hörmann, F. M.; Bach, T. Iminium and enamine catalysis in enantioselective photochemical reactions. *Chem. Soc. Rev.* **2018**, *47*, 278-290. (f) Brimioulle, R.; Lenhart, D.; Maturi, M. M.; Bach, T. Enantioselective Catalysis of Photochemical Reactions. *Angew. Chem. Int. Ed.* **2015**, *54*, 3872-3890.
- [2] Brenninger, C.; Jolliffe, J. D.; Bach, T. Chromophore Activation of α,β -Unsaturated Carbonyl Compounds and Its Application to Enantioselective Photochemical Reactions. *Angew. Chem. Int. Ed.* **2018**, *57*, 14338-14349.
- [3] Burg, F.; Bach, T. Lactam Hydrogen Bonds as Control Elements in Enantioselective Transition-Metal-Catalyzed and Photochemical Reactions. *J. Org. Chem.* **2019**, *84*, 8815-8836.
- [4] (a) Leverenz, M.; Merten, C.; Dreuw, A.; Bach, T. Lewis Acid Catalyzed Enantioselective Photochemical Rearrangements on the Singlet Potential Energy Surface. *J. Am. Chem. Soc.* **2019**, *141*, 20053-20057. (b) Stegbauer, S.; Jandl, C.; Bach, T. Enantioselective Lewis Acid Catalyzed ortho Photocycloaddition of Olefins to Phenanthrene-9-carboxaldehydes. *Angew. Chem. Int. Ed.* **2018**, *57*, 14593-14596. (c) Poplata, S.; Bach, T. Enantioselective Intermolecular [2+2] Photocycloaddition Reaction of Cyclic Enones and Its Application in a Synthesis of (-)-Grandisol. *J. Am. Chem. Soc.* **2018**, *140*, 3228-3231. (d) Brimioulle, R.; Bauer, A.; Bach, T. Enantioselective Lewis Acid Catalysis in Intramolecular [2+2] Photocycloaddition Reactions: A Mechanistic Comparison between Representative Coumarin and Enone Substrates. *J. Am. Chem. Soc.* **2015**, *137*, 5170-5176. (e) Brimioulle, R.; Bach, T. Enantioselective Lewis Acid Catalysis of Intramolecular Enone [2+2] Photocycloaddition Reactions. *Science* **2013**, *342*, 840-843. (f) Guo, H.; Herdtweck, E.; Bach, T. Enantioselective Lewis Acid Catalysis in Intramolecular [2+2] Photocycloaddition Reactions of Coumarins. *Angew. Chem. Int. Ed.* **2010**, *49*, 7782-7785.

- [5] (a) Daub, M. E.; Jung, H.; Lee, B. J.; Won, J.; Baik, M.-H.; Yoon, T. P. Enantioselective [2+2] Cycloadditions of Cinnamate Esters: Generalizing Lewis Acid Catalysis of Triplet Energy Transfer. *J. Am. Chem. Soc.* **2019**, *141*, 9543-9547. (b) Miller, Z. D.; Lee, B. J.; Yoon, T. P. Enantioselective Crossed Photocycloadditions of Styrenic Olefins by Lewis Acid Catalyzed Triplet Sensitization. *Angew. Chem. Int. Ed.* **2017**, *56*, 11891-11895. (c) Blum, T. R.; Miller, Z. D.; Bates, D. M.; Guzei, I. A.; Yoon, T. P. Enantioselective photochemistry through Lewis acid-catalyzed triplet energy transfer. *Science* **2016**, *354*, 1391-1395. (d) Amador, A. G.; Sherbrook, E. M.; Yoon, T.P. Enantioselective Photocatalytic [3+2] Cycloadditions of Aryl Cyclopropyl Ketones. *J. Am. Chem. Soc.* **2016**, *138*, 4722-4725. (e) Espelt, L. R.; McPherson, I. S.; Wiensch, E. M.; Yoon, T. P. Enantioselective Conjugate Additions of α -Amino Radicals via Cooperative Photoredox and Lewis Acid Catalysis. *J. Am. Chem. Soc.* **2015**, *137*, 2452-2455. (f) Du, J.; Skubi, K. L.; Schultz, D. M.; Yoon, T. P. A Dual-Catalysis Approach to Enantioselective [2+2] Photocycloadditions Using Visible Light. *Science* **2014**, *344*, 392-396.
- [6] (a) Huang, X.; Meggers, E. Asymmetric Photocatalysis with Bis-cyclometalated Rhodium Complexes. *Acc. Chem. Res.* **2019**, *52*, 833-847. (b) Steinlandt, P. S.; Zuo, W.; Harms, K.; Meggers, E. Bis-Cyclometalated Indazole Chiral-at-Rhodium Catalyst for Asymmetric Photoredox Cyanoalkylations. *Chem. Eur. J.* **2019**, *25*, 15333-15340. (c) Kuang, Y.; Wang, K.; Shi, X.; Huang, X.; Meggers, E.; Wu, J. Asymmetric Synthesis of 1,4-Dicarbonyl Compounds from Aldehydes by Hydrogen Atom Transfer Photocatalysis and Chiral Lewis Acid Catalysis. *Angew. Chem. Int. Ed.* **2019**, *58*, 16859-16863. (d) Huang, X.; Lin, J.; Shen, T.; Harms, K.; Marchini, M.; Ceroni, P.; Meggers, E. Asymmetric [3+2] Photocycloadditions of Cyclopropanes with Alkenes or Alkynes through Visible-Light Excitation of Catalyst-Bound Substrates. *Angew. Chem. Int. Ed.* **2018**, *57*, 5454-5458. (e) Huang, X.; Quinn, T. R.; Harms, K.; Webster, R. D.; Zhang, L.; Wiest, O.; Meggers, E. Direct Visible-Light-Excited Asymmetric Lewis Acid Catalysis of Intermolecular [2+2] Photocycloadditions. *J. Am. Chem. Soc.* **2017**, *139*, 9120-9123. (f) Huo, H.; Harms, K.; Meggers, E. Catalytic, Enantioselective Addition of Alkyl Radicals to Alkenes via Visible-Light-Activated Photoredox Catalysis with a Chiral Rhodium Complex. *J. Am. Chem. Soc.* **2016**, *138*, 6936-6939. (g) Huang, X.; Webster, R. D.; Harms, K.; Meggers, E. Asymmetric Catalysis with Organic Azides and Diazo Compounds Initiated by Photoinduced Electron Transfer. *J. Am. Chem. Soc.* **2016**, *138*, 12636-12642. (h) Huo, H.; Wang, C.; Harms, K.; Meggers, E. Enantioselective, Catalytic Trichloromethylation through Visible-Light-Activated

- Photoredox Catalysis with a Chiral Iridium Complex. *J. Am. Chem. Soc.* **2015**, *137*, 9551-9554.
- [7] Cauble, D. F.; Lynch, V.; Krische, M. J. Studies on the Enantioselective Catalysis of Photochemically Promoted Transformations: "Sensitizing Receptors" as Chiral Catalysts. *J. Org. Chem.* **2003**, *68*, 15-21.
- [8] (a) Maturi, M. M.; Bach, T. Enantioselective Catalysis of the Intermolecular [2+2] Photocycloaddition between 2-Pyridones and Acetylenedicarboxylates. *Angew. Chem. Int. Ed.* **2014**, *53*, 7661-7664. (b) Müller, C.; Bauer, A.; Maturi, M. M.; Cuquerella, M. C.; Miranda, M. A.; Bach, T. Enantioselective Intramolecular [2+2]-Photocycloaddition Reactions of 4-Substituted Quinolones Catalyzed by a Chiral Sensitizer with a Hydrogen-Bonding Motif. *J. Am. Chem. Soc.* **2011**, *133*, 16689-16697. (c) Müller, C.; Bauer, A.; Bach, T. Light-Driven Enantioselective Organocatalysis. *Angew. Chem. Int. Ed.* **2009**, *48*, 6640-6642. (d) Bauer, A.; Westkämper, F.; Grimme, S.; Bach, T. Catalytic enantioselective reactions driven by photoinduced electron transfer. *Nature* **2005**, *436*, 1139-1140.
- [9] Alonso, R.; Bach, T. A Chiral Thioxanthone as an Organocatalyst for Enantioselective [2+2] Photocycloaddition Reactions Induced by Visible Light. *Angew. Chem. Int. Ed.* **2014**, *53*, 4368-4371.
- [10] Pecho, F.; Zou, Y.-Q.; Gramüller, J.; Mori, T.; Huber, S. M.; Bauer, A.; Gschwind, R. M.; Bach, T. A Thioxanthone Sensitizer with a Chiral Phosphoric Acid Binding Site: Properties and Applications in Visible Light-Mediated Cycloadditions. *Chem. Eur. J.* **2020**, *26*, 5190-5194.
- [11] (a) Kratz, T.; Steinbach, P.; Breitenlechner, S.; Storch, G.; Bannwarth, C.; Bach, T. Photochemical Deracemization of Chiral Alkenes via Triplet Energy Transfer. *J. Am. Chem. Soc.* **2022**, *144*, 10133-10138. (b) Takagi, R.; Tanimoto, T. Enantioselective [2+2] photocycloaddition of quinolone using a C₁-symmetric chiral phosphoric acid as a visible-light photocatalyst. *Org. Biomol. Chem.* **2022**, *20*, 3940-3947. (c) Lyu, J.; Leone, M.; Claraz, A.; Allain, C.; Neuville, L.; Masson, G. Syntheses of new chiral chimeric photoorganocatalysts. *RSC Adv.* **2021**, *11*, 36663-36669. (d) Pecho, F.; Sempere, Y.; Gramüller, J.; Hörmann, F. M.; Gschwind, R. M.; Bach, T. Enantioselective [2+2] Photocycloaddition via Iminium Ions: Catalysis by a Sensitizing Chiral Brønsted Acid. *J. Am. Chem. Soc.* **2021**, *143*, 9350-9354. (e) Nikitas, N. F.; Gkizis, P. L.; Kokotos, C. G. Thioxanthone: a powerful photocatalyst for organic reactions. *Org. Biomol. Chem.* **2021**, *19*, 5237-5253. (f) Li, X.; Großkopf, J.; Jandl, C.; Bach, T. Enantioselective, Visible Light Mediated Aza Paternò-Büchi Reactions of Quinoxalinones. *Angew. Chem.* **2021**, *133*,

- 2716-2720. (g) Li, X.; Christian, J.; Bach, T. Visible-Light-Mediated Enantioselective Photoreactions of 3-Alkylquinolones with 4-O-Tethered Alkenes and Allenes. *Org. Lett.* **2020**, *22*, 3618-3622. (h) Lyu, J.; Claraz, A.; Vitale, M. R.; Allain, C.; Masson, G. Preparation of Chiral Photosensitive Organocatalysts and Their Application for the Enantioselective Synthesis of 1,2-Diamines. *J. Org. Chem.* **2020**, *85*, 12843-12855. (i) Rigotti, T.; Casado-Sánchez, A.; Cabrera, S.; Pérez-Ruiz, R.; Liras, M.; de la Peña O'Shea, V. A.; Alemán, J. A Bifunctional Photoaminocatalyst for the Alkylation of Aldehydes: Design, Analysis, and Mechanistic Studies. *ACS Catal.* **2018**, *8*, 5928-5940. (j) Mayr, F.; Mohr, L.-M.; Rodriguez, E.; Bach, T. Synthesis of Chiral Thiourea-Thioxanthone Hybrids. *Synthesis*, **2017**, *49*, 5238-5250. (k) Ding, W.; Lu, L.-Q.; Zhou, Q.-Q.; Wei, Y.; Chen, J.-R.; Xiao, W.-J. Bifunctional Photocatalysts for Enantioselective Aerobic Oxidation of β -Ketoesters. *J. Am. Chem. Soc.* **2017**, *139*, 63-66. (l) Tröster, A.; Alonso, R.; Bauer, A.; Bach, T. Enantioselective Intermolecular [2+2] Photocycloaddition Reactions of 2(1*H*)-Quinolones Induced by Visible Light Irradiation. *J. Am. Chem. Soc.* **2016**, *138*, 7808-7811.
- [12] (a) Some recent initial work has been done on modifying the photochemical properties of non-chiral thioxanthone-based triplet sensitizers: Elliott, L. D.; Kayal, S.; George, M. W.; Booker-Milburn, K. Rational Design of Triplet Sensitizers for the Transfer of Excited State Photochemistry from UV to Visible. *J. Am. Chem. Soc.* **2020**, *142*, 14947-14956. (b) For tuning of the absorption spectra see: Iyer, A.; Clay, A.; Jockusch, S.; Sivaguru, J. Evaluating brominated thioxanthenes as organo-photocatalysts. *Phys. Org. Chem.* **2017**, *30*, e3738.
- [13] (a) Speckmeier, E.; Fischer, T. G.; Zeitler, K. A Toolbox Approach To Construct Broadly Applicable Metal-Free Catalysts for Photoredox Chemistry: Deliberate Tuning of Redox Potentials and Importance of Halogens in Donor-Acceptor Cyanoarenes. *J. Am. Chem. Soc.* **2018**, *140*, 15353-15365. (b) Luo, J.; Zhang, J. Donor– Acceptor Fluorophores for Visible-Light-Promoted Organic Synthesis: Photoredox/Ni Dual Catalytic C(sp³)-C(sp²) Cross-Coupling. *ACS Catal.* **2016**, *6*, 873-87.
- [14] Shang, T.-Y.; Lu, L.-H.; Cao, Z.; Liu, Y.; He, W.-M.; Yu, B. Recent advances of 1,2,3,5-tetrakis(carbazol-9-yl)-4,6-dicyanobenzene (4CzIPN) in photocatalytic transformations. *Chem. Commun.* **2019**, *55*, 5408-5419.
- [15] Uoyama, H.; Goushi, K.; Shizu, K.; Nomura, H.; Adachi, C. Highly efficient organic light-emitting diodes from delayed fluorescence. *Nature* **2012**, *492*, 234-238.
- [16] Bryden, M. A.; Zysman-Colman, E. Organic thermally activated delayed fluorescence (TADF) compounds used in photocatalysis. *Chem. Soc. Rev.* **2021**, *50*, 7587-7680.

- [17] TADF-Molecules in Energy-Transfer-Catalysis: (a) Hojo, R.; Polgar, A. M.; Hudson, Z. M.; Thermally Activated Delayed Fluorescence Sensitizers As Organic and Green Alternatives in Energy-Transfer Photocatalysis. *ACS Sustainable Chem. Eng.* **2022**, *10*, 9665-9678. (b) Lu, J.; Pattengale, B.; Liu, Q.; Yang, S.; Shi, W.; Li, S.; Huang, J.; Zhang, J. Donor-Acceptor Fluorophores for Energy-Transfer-Mediated Photocatalysis. *J. Am. Chem. Soc.* **2018**, *140*, 13719-13725.
- [18] Lingenfelter, D. S.; Helgeson, R. C.; Cram, D. J. Host-guest complexation. 23. High chiral recognition of amino acid and ester guests by hosts containing one chiral element *J. Org. Chem.* **1981**, *46*, 393-406.
- [19] Simonsen, K. B.; Gothelf, K. V.; Jørgensen, K. A. A Simple Synthetic Approach to 3,3'-Diaryl BINOLs. *J. Org. Chem.* **1998**, *63*, 7536-7538.
- [20] (a) Grotjahn, S.; König, B. Photosubstitution in Dicyanobenzene-based Photocatalysts. *Org. Lett.* **2021**, *23*, 3146-3150. (b) Donabauer, K.; Maity, M.; Berger, A. L.; Huff, G. S.; Crespi, S.; König, B. Photocatalytic carbanion generation – benzylation of aliphatic aldehydes to secondary alcohols. *Chem. Sci.* **2019**, *10*, 5162-5166.
- [21] (a) Uraguchi, D.; Terada, M.; Chiral Brønsted Acid-Catalyzed Direct Mannich Reactions via Electrophilic Activation. *J. Am. Chem. Soc.* **2004**, *126*, 5356-5357. (b) Uraguchi, D.; Sorimachi K.; Terada, M. Enantioselective Mannich-Type Reaction Catalyzed by a Chiral Brønsted Acid. *J. Am. Chem. Soc.* **2004**, *126*, 11804-11805.
- [22] Rolka, A. B.; König, B. Dearomative Cycloadditions Utilizing an Organic Photosensitizer: An Alternative to Iridium Catalysis. *Org. Lett.* **2020**, *22*, 5035-5040.
- [23] Gan, S.; Hu, S.; Li, X.-L.; Zeng, J.; Zhang, D.; Huang, T.; Luo, W.; Zhao, Z.; Duan, L.; Su, S.-J.; Tang, B. Z. Heavy Atom Effect of Bromine Significantly Enhances Exciton Utilization of Delayed Fluorescence Luminogens. *ACS Appl. Mater. Interfaces* **2018**, *10*, 17327-17334.
- [24] Bhalodi, E. H.; Shah, V. R.; Butcher, R. J.; Bedekar, A. V.; Synthesis and Study of Photophysical Properties of 6,12-Dicyano-9-oxa[7]helicene. *ChemistrySelect* **2021**, *6*, 13514-13519.
- [25] Kulkarni, P. P.; Kadam, A. J.; Mane, R. B.; Desai, U. V. Wadgaonkar, P. P. Demethylation of Methyl Aryl Ethers using Pyridine Hydrochloride in Solvent-free Conditions under Microwave Irradiation. *J. Chem. Res. (S)*, **1999**, 394-395.
- [26] Jung, M. E.; Lyster, M. A. Quantitative dealkylation of alkyl ethers via treatment with trimethylsilyl iodide. A new method for ether hydrolysis. *J. Org. Chem.* **1977**, *42*, 3761-3764.

-
- [27] Romanov-Michailidis, F.; Romanova-Michaelides, M.; Pupier, M.; Alexakis, A. Enantioselective Halogenative Semi-Pinacol Rearrangement: Extension of Substrate Scope and Mechanistic Investigations. *Chem. Eur. J.* **2015**, *21*, 5561-5583.
- [28] Sherbrook, E. M.; Jung, H.; Cho, D.; Baik, M.-H.; Yoon, T. P. Brønsted acid catalysis of photosensitized cycloadditions. *Chem. Sci.* **2020**, *11*, 856-861.
- [29] Sherbrook, E. M.; Genzink, M. J.; Park, B.; Guzei, I. A.; Baik, M.-H.; Yoon, T. P. Chiral Brønsted acid-controlled intermolecular asymmetric [2+2] photocycloadditions. *Nat. Commun.* **2021**, *12*, 5735.
- [30] The shown example is based on: (a) Liang, D.; Chen, J.-R.; Tan, L.-P.; He, Z.-W.; Xiao, W.-J. Catalytic Asymmetric Construction of Axially and Centrally Chiral Heterobiaryls by Minisci Reaction. *J. Am. Chem. Soc.* **2022**, *144*, 6040-6049. (b) For previous and pioneering work on this topic see: Proctor, R. S. J.; Davis, H. J.; Phipps, R. J. Catalytic enantioselective Minisci-type addition to heteroarenes. *Science* **2018**, *360*, 419-422.
- [31] Nakashima, D.; Yamamoto, H. Design of Chiral *N*-Triflyl Phosphoramidate as a Strong Chiral Brønsted Acid and Its Application to Asymmetric Diels–Alder Reaction. *J. Am. Chem. Soc.* **2006**, *128*, 9626-9627.
- [32] Jin, L.-M.; Li, Y.; Ma, J.; Li, Q. Synthesis of Novel Thermally Reversible Photochromic Axially Chiral Spirooxazines. *Org. Lett.* **2010**, *12*, 3552-3555.

SUMMARY

5 Summary

The introduction of photocatalysis to the field of organic chemistry has resulted in significant advances in the development of novel and creative synthesis routes. By utilizing light in combination with a suitable photocatalyst, challenging transformations have been realized. Central to this progress has been the synthesis of new classes of photocatalysts whose properties are matched to the desired transformation. Selection and/or development of the appropriate photocatalyst for a reaction is especially important in the context of achieving asymmetric induction via a photocatalytic protocol as highlighted by the introductory **Chapter 1**. In this review chapter, existing chiral bifunctional organic photocatalysts that utilize visible-light for activation are summarized along with their applications in enantioselective photocatalysis. A special focus has been placed on the comparison of the bifunctional catalysts to related dual catalytic systems to evaluate possible benefits of bifunctional systems. The remaining three chapters of this thesis describe the identification of photocatalysts for dearomative cycloaddition and trifluoromethylthiolation reactions, as well as the development of novel photocatalysts for enantioselective photocatalysis.

Chapter 2 demonstrates that 1,2-bis(carbazol-9-yl)-4,5-dicyanobenzene (**2CzPN**) is an exceptional organic energy transfer catalyst for dearomative [2+2] cycloadditions and is capable of replacing the previously required rare-earth iridium complex $(\text{Ir}[\text{dF}(\text{CF}_3)\text{ppy}]_2(\text{dtbpy}))\text{PF}_6$ (**[Ir-F]**). This organic alternative, which was first reported in 2012 in the context of OLED research, effectively dearomatized naphthol and indole-derivatives in a process that occurs via triplet energy transfer to the aromatic rings through the **2CzPN** catalyst. Subsequent trapping of the excited aromatic compounds with tethered alkene or allene moieties yield complex, polycyclic molecules. It was further shown that **2CzPN** can be used on a larger reaction scale (7.0 mmol), is recyclable by means of column chromatography, and exhibits improved solubility in less polar solvents like toluene when compared to the iridium catalyst.

Chapter 3 explores the utilization of the decatungstate anion for the selective trifluoromethylthiolation of methylene $\text{C}(\text{sp}^3)\text{-H}$, methine $\text{C}(\text{sp}^3)\text{-H}$, α -oxygen $\text{C}(\text{sp}^3)\text{-H}$ and formyl $\text{C}(\text{sp}^2)\text{-H}$ bonds. Whereas previous protocols often relied upon dual catalytic systems consisting of a photocatalyst and a separate hydrogen atom transfer catalyst, the decatungstate anion was shown to act as a sole catalyst for these two processes. This methodology proved to be highly efficient and was applied to the late-stage derivatization of natural products. Additionally, it was demonstrated that the resulting trifluoromethylthiolated substrates can be used as building

blocks for drug synthesis, which is especially intriguing for medicinal chemistry, as the $-SCF_3$ group exhibits high lipophilicity.

Finally, the synthesis of two novel chiral and bifunctional photocatalysts is presented in **Chapter 4**. The two hybrid structures were accessed in seven steps each and link a chiral phosphoric acid backbone to donor-acceptor cyanoarene-based photocatalysts. Their utility in asymmetric energy transfer and photoredox catalysis was established in preliminary proof-of-concept reactions.

ZUSAMMENFASSUNG

6 Zusammenfassung

Mit der Einführung der Photokatalyse auf dem Gebiet der organischen Chemie wurden bedeutende Fortschritte bei der Entwicklung neuer und kreativer Synthesewege erzielt. Durch die Nutzung von Licht in Kombination mit einem geeigneten Photokatalysator konnten anspruchsvolle Umwandlungen realisiert werden. Entscheidend für diesen Fortschritt war die Synthese neuer Klassen von Photokatalysatoren, deren Eigenschaften auf die gewünschte Umwandlung abgestimmt sind. Die Auswahl und/oder Entwicklung eines geeigneten Photokatalysators für eine Reaktion ist besonders wichtig, wenn eine asymmetrische Induktion durch ein photokatalytisches Protokoll erreicht werden soll, wie im einleitenden **Kapitel 1** hervorgehoben wurde. In diesem Übersichtskapitel werden bekannte chirale, bifunktionale, organische Photokatalysatoren, die sichtbares Licht zur Aktivierung nutzen, zusammen mit ihren Anwendungen in der enantioselektiven Photokatalyse diskutiert. Ein besonderes Augenmerk wurde auf den Vergleich der bifunktionalen Katalysatoren mit verwandten, dualen katalytischen Systemen gelegt, um mögliche Vorteile bifunktionaler Systeme zu untersuchen. Die übrigen drei Kapitel dieser Arbeit beschreiben die Identifizierung von Photokatalysatoren für die dearomatisierende Cycloaddition und die Trifluormethylthiolierung, sowie die Entwicklung neuartiger Photokatalysatoren für die enantioselektive Photokatalyse.

In **Kapitel 2** wird gezeigt, dass 1,2-Bis(carbazol-9-yl)-4,5-dicyanobenzol (**2CzPN**) ein außergewöhnlicher organischer Energieübertragungskatalysator für dearomatisierende [2+2]-Cycloadditionen ist und den bisher benötigten Seltenen Erden Iridium-Komplex $(\text{Ir}[\text{dF}(\text{CF}_3)\text{ppy}]_2(\text{dtbpy}))\text{PF}_6$ (**[Ir-F]**) ersetzen kann. Diese organische Alternative, über die erstmals 2012 im Rahmen der OLED-Forschung berichtet wurde, dearomatisiert effektiv Naphthol- und Indol-Derivate in einem Prozess, der durch Triplett-Energieübertragung auf die aromatischen Ringe durch den **2CzPN**-Katalysator erfolgt. Durch anschließendes Abfangen der angeregten aromatischen Verbindungen mit angehängten Alken- oder Alleneinheiten werden komplexe, polyzyklische Moleküle erhalten. Es wurde ferner gezeigt, dass **2CzPN** in einem größeren Reaktionsmaßstab (7.0 mmol) eingesetzt werden kann, mittels Säulenchromatographie recycelbar ist und im Vergleich zum Iridiumkatalysator eine bessere Löslichkeit in weniger polaren Lösungsmitteln wie Toluol aufweist.

In **Kapitel 3** wird die Verwendung des Dekawolfram-Anions für die selektive Trifluormethylthiolierung von Methylen $\text{C}(\text{sp}^3)\text{-H}$, Methin $\text{C}(\text{sp}^3)\text{-H}$, α -Oxygen $\text{C}(\text{sp}^3)\text{-H}$ und

Formyl C(sp²)-H Bindungen beschrieben. Während frühere Protokolle häufig auf duale katalytische Systeme zurückgriffen, die aus einem Photokatalysator und einem separaten Katalysator für die Übertragung von Wasserstoffatomen bestanden, konnte gezeigt werden, dass das Dekawolframat-Anion als alleiniger Katalysator für diese beiden Prozesse fungiert. Diese Methode erwies sich als äußerst effizient und wurde auf die Funktionalisierung von Naturstoffen angewandt. Darüber hinaus wurde gezeigt, dass die resultierenden trifluormethylthiolierten Substrate als Bausteine für die Arzneimittelsynthese verwendet werden können. Dies ist besonders für die medizinische Chemie interessant, da die -SCF₃-Gruppe eine hohe Lipophilie aufweist.

Schließlich wird in **Kapitel 4** die Synthese von zwei neuartigen chiralen und bifunktionalen Photokatalysatoren vorgestellt. Die beiden Hybridstrukturen wurden in jeweils sieben Schritten hergestellt und verbinden ein chirales Phosphorsäure-Grundgerüst mit Donor-Akzeptor-Photokatalysatoren auf Cyanoarenbasis. Ihr Nutzen für die asymmetrische Energietransfer- und die Photoredox-Katalyse wurde in ersten Proof-of-Concept-Reaktionen nachgewiesen.

APPENDIX

7 Appendix

7.1 Abbreviations

°C	degrees Celsius
Å	Ångström (10^{-10} m)
λ	wavelength
2CzPN	1,2-bis(carbazol-9-yl)-4,5-dicyanobenzene
3DPA2FBN	2,4,6-tris(diphenylamino)-3,5-difluorobenzonitrile
3DPAFIPN	2,4,6-tris(diphenylamino)-5-fluoroisophthalonitrile
4CzIPN	2,4,5,6-tetrakis(carbazol-9-yl)-4,6-dicyanobenzene
Ac	acetyl
acac	acetylacetonate
Ad	adamantly group
APCI	Atmospheric-pressure chemical ionization
Ar	aryl; arene group
atm	atmosphere
BINOL	1,1'-Bi-2-naphthol
Bn	benzyl
boc	<i>tert</i> -butyloxycarbonyl
BODIPY	dipyrrrometheneboron difluoride
BOX	bis(oxazoline)
bpy	2,2'-bipyridine
Bu	butyl
Bz	benzoyl
Cbz	carbazole
CFL	compact fluorescent lamp
cm	centimeter
CPA	chiral phosphoric acid
CV	cyclic voltammetry
DCE	dichloroethane
DCM	dichloromethane
DIAD	diisopropyl azodicarboxylate
DMA	dimethylacetamide

DMAP	4-dimethylaminopyridine
DMF	dimethylformamide
DMSO	dimethyl sulfoxide
dppf	1,1'-bis(diphenylphosphino)ferrocene
d.r.	diastereomeric ratio
DT	decatungstate anion
dtbpy	di- <i>tert</i> -butyl-2,2'-bipyridine
ee	enantiomeric excess
<i>e.g.</i>	for example (<i>lat. exempli gratia</i>)
EI	electron ionization
<i>ent</i>	enantiomer
eq.	equivalent
ESI	electrospray ionization
Et	ethyl
<i>et al.</i>	and others (<i>lat. et alii</i>)
EtOAc	ethyl acetate
EtOH	ethanol
eV	electron volt
FID	flame ionization detector
FT-IR	Fourier transform infrared
g	gram
GABA	gamma-aminobutyric acid
GC	gas chromatography
h	hour(s)
HAT	hydrogen atom transfer
HRMS	high resolution mass spectrometry
<i>hν</i>	incident photon energy
Hz	Hertz
<i>i</i> -Pr	isopropyl
i.r.	isomeric ratio
IR	infrared
[Ir-F]	$\text{Ir}[\text{dF}(\text{CF}_3)\text{ppy}]_2(\text{dtbpy})\text{PF}_6$
K	Kelvin

L	liter
LA	Lewis Acid
LED	light emitting diode
LUMO	Lowest Unoccupied Molecular Orbital
M	molar (mol/L)
Me	methyl
MeCN	acetonitrile
MeOH	methanol
mg	milligram
min	minute
mL	milliliter
mM	millimolar (mmol/L)
mmol	millimole
MS	mass spectrometry
MTBE	Methyl- <i>tert</i> -butylether
μL	microliter
μmol	micromole
μs	microsecond
N/A	not applicable
NaHMDS	Sodium bis(trimethylsilyl)amide
<i>n</i> -Bu	<i>n</i> -butyl
n.d.	not detected
nd	not determined
nm	nanometer
NMR	nuclear magnetic resonance
OLED	organic light-emitting diode
O/N	overnight
PC	photocatalyst
PE	petroleum ether
Ph	phenyl group
Phth	phthalimide, phthalimidyl
PL	photoluminescence
ppm	parts per million

ppy	2-phenylpyridinato
PTC	phase-transfer catalyst
Py	pyridine
quant.	quantitative
QY	quantum yield
R	alkyl-, aryl- or functional groups
<i>rac</i>	racemic
rpm	revolution per minute
r.r.	regioisomeric ratio
r.t.	room temperature
s	second
SCE	saturated calomel electrode
Subs.	substrate
τ	lifetime
^t Bu	<i>tert</i> -butyl
TBADT	tetra- <i>n</i> -butylammonium decatungstate
TBS	<i>tert</i> -butyldimethylsilyl
Tf	triflyl (trifluoromethanesulfonyl)
TFA	trifluoroacetic acid
THF	tetrahydrofuran
TLC	thin layer chromatography
TMEDA	tetramethylethylenediamine
TPP	tetraphenylporphyrin
Ts	toluene sulfonyl group
TX	thioxanthone
UV	ultraviolet
VIS	visible light
vs.	against (<i>lat.</i> versus)
X-Ray	Röntgen radiation

7.2 Curriculum Vitae

ALESSA BLANKA ROLKA

18.02.1994 | Soest, NRW, Germany | German

EDUCATION AND RESEARCH EXPERIENCE

- 01/19 – 04/23 **PhD in Organic Chemistry, University of Regensburg**
Doctoral Thesis: Identification and Development of Photocatalysts for Building Molecular Complexity
Supervisor: Prof. Dr. Burkhard König
-
- 08/21 – 07/22 **Visiting Student Researcher, University of California, Berkeley (USA)**
Research Group Prof. Dr. F. Dean Toste
-
- 10/16 – 09/18 **Master of Science, Advanced Synthesis and Catalysis, University of Regensburg**
Master's Thesis: Photocatalytic Generation of Carbenes
Supervisor: Prof. Dr. Burkhard König
- 09/17 – 10/17 **Visiting Researcher, Stanford University (USA)**
Research Group Prof. Dr. Barry M. Trost
Research Topic: Desymmetrization of Phosphinic Acids
- 09/16 – 12/16 **Erasmus Student, University of Aberdeen (Scotland)**
Research Group Prof. Dr. John Storey
Research Topic: New Methods of Synthesizing Heterocycles using Green Solvents
-
- 10/13 – 07/16 **Bachelor of Science, Chemistry, University of Regensburg**
Bachelor's Thesis: Plasmonic Enhancement in Raman Spectroscopy for the Detection of Bioactive Compounds in Forensic Samples
Supervisors: Prof. Dr. Antje Bäumner, Dr. Thomas Hirsch
-

AWARDS AND FELLOWSHIPS

- 02/20 – 07/22 **Fellowship of the German Academic Scholarship Foundation**
Promotionsförderung durch die Studienstiftung des deutschen Volkes
-
- 08/19 – 08/21 **Kekulé Fellowship**
Kekulé-Stipendium der Stiftung Stipendien-Fonds des Verbandes der Chemischen Industrie
-

06/2019	Studienabschlusspreis Master Universitätsstiftung Dr. Alfons Paulus
09/16 – 12/16	Erasmus+ Scholarship Grant partially covering the expenses of studying abroad (Aberdeen)

CONFERENCES

09/2022	Ischia Advanced School of Organic Chemistry (Ischia): Poster Presentation
09/2022	Weizmann Summer School: Advances in Drug Discovery (Prague): Poster Presentation
08/2022	Toste 20th Anniversary Symposium: Poster Presentation
12/2021	Pacificchem 2021: Poster Presentation
08/2020	ACS Virtual National Fall Meeting: Oral presentation with Q&A
06/2020	SCS Photochemistry Symposium: Oral presentation (elevator talk)

PUBLICATIONS

5. **“Hybrid Catalysts for Enantioselective Photo-Phosphoric Acid Catalysis”**
Alessa B. Rolka, Burkhard König, F. Dean Toste.
ChemRxiv **2023**, DOI: 10.26434/chemrxiv-2023-0v38p
 4. **“Oxidative con-PET Catalysis for Arene Functionalization”**
Bartosz Bieszczad, Tobias Karl, **Alessa B. Rolka**, Patrick Nürnberger, Roger Kutta, Burkhard König. *ChemRxiv* **2022**, DOI: 10.26434/chemrxiv-2022-39x5l
 3. **“Photocatalytic C–H Trifluoromethylthiolation by the Decatungstate Anion”**
Tobias E. Schirmer†, **Alessa B. Rolka**†, Tobias Karl, Ferdinand Holzhausen, Burkhard König. *Org. Lett.* **2021**, *23*, 5729-5733. (†Equal contributions)
 2. **“Dearomative Cycloadditions Utilizing an Organic Photosensitizer: An Alternative to Iridium Catalysis”**
Alessa B. Rolka, Burkhard König, *Org. Lett.* **2020**, *22*, 5035-5040.
 1. **“Desymmetrization of Phosphinic Acids via Pd-Catalyzed Asymmetric Allylic Alkylation: Rapid Access to P-Chiral Phosphinates”**
Barry M. Trost, Simon M. Spohr, **Alessa B. Rolka**, Christopher A. Kalnmals
J. Am. Chem. Soc. **2019**, *141*, 14098-14103.
-

DANKSAGUNG

8 Danksagung

Als erstes möchte ich mich bei Prof. Dr. Burkhard König für die Möglichkeit bedanken, meine Doktorarbeit in seiner Gruppe anfertigen zu dürfen. Besonders die Freiheit, unterschiedliche Themen nach meinem Interesse bearbeiten zu dürfen und die kreativen Inputs habe ich besonders geschätzt, genauso wie die Möglichkeit, meine Forschungsergebnisse virtuell oder im Ausland vorstellen zu dürfen.

I am also very grateful for the flexibility offered to do part of my thesis abroad. In this context, I would like to thank Prof. Dr. F. Dean Toste from the University of California, Berkeley (USA) for accepting me as a member of his research group from 01.08.2021 to 31.07.2022. In addition, I am grateful to him for being the second referee of my thesis.

Die Finanzierung meiner Doktorarbeit und insbesondere der Arbeit im Ausland wäre nicht möglich gewesen ohne die finanzielle Unterstützung durch das Kekulé-Stipendium des Fonds der chemischen Industrie und ohne die Promotionsförderung der Studienstiftung des deutschen Volkes. Daher an dieser Stelle herzlichen Dank an die beiden Stipendiengeber für die Ermöglichung meiner Doktorarbeit in dieser Form. Auch Prof. Dr. Burkhard König soll an dieser Stelle erneut gedankt werden: für die Finanzierung bis zum Einsetzen der Stipendien und für die Finanzierung nach Abschluss der Stipendien.

Ich danke Prof. Dr. Patrick Nürnberger dafür, dass er als Drittprüfer eintritt, sowie Prof. Dr. Arno Pfitzner für die Übernahme des Prüfungsvorsitzes.

Besonderer Dank gilt auch Tobias Emanuel Schirmer für die sehr harmonische und großartige Zusammenarbeit an dem Projekt zur Trifluorothiomethylierung. Auch Tobias Alwin Karl und Ferdinand Holzhausen möchte ich für die Mitarbeit bei diesem Projekt danken, sowie Anamitra Chatterjee für die Synthese eines Moleküls für die dearomatisierende Cycloaddition mittels 2CzPN.

Susanne Märkl gilt mein Dank nicht nur als Kollaborationspartnerin und Studienkollegin, sondern auch als treue Freundin und Reisegefährtin.

Ebenfalls möchte ich mich bei meinem Praktikanten Dominik Kreutzer und Bacheloranden Jakob Weinberger für die Mitarbeit bedanken, sowie bei Navid Rahman für die Zusammenarbeit im Rahmen seiner Masterarbeit.

Further I want to thank Tobias Emanuel Schirmer for helpful and stimulating discussions, his valuable inputs and practical advice. This thanks also goes to Karsten Donabauer, Matthias Schmalzbauer, Saikat Das, Tanguy Saget and Jacob Schreiber Tracy.

Große Dankbarkeit empfinde ich auch gegenüber den festangestellten Mitarbeitern des AK Königs. Besonders bei oftmals nicht trivialen bürokratischen Angelegenheiten konnte ich mich immer zuverlässig an Barbara Bauer und Katharina Nickl wenden. Auch bei Julia Zach möchte ich mich für die tolle technische Unterstützung bei sämtlichen Fragestellungen zu Geräten am Arbeitskreis bedanken. Ebenso bei Ernst Lautenschlager für die großartige Laborordnung, die sicherstellt, dass Chemikalien und Glasgeräte stets auffindbar und verwendbar sind. Weiter Dank gilt auch Regina Hoheisel für CV-Messungen, Rudolf Vasold für GC-Messungen sowie Britta Badziura und Simone Strauß für Chemikalienbestellungen und Petra Hilgers.

Bei den Mitarbeitern der Röntgenstrukturanalyse, insbesondere bei Birgit Hischa, möchte ich mich für die Messung meiner Kristalle bedanken. Auch den anderen Abteilungen der Zentralen Analytik der Universität Regensburg möchte ich für die zuverlässige und sorgfältige Bearbeitung meiner Aufträge danken. Johannes Gramüller danke ich für die hilfreiche Unterstützung bei NMR-Angelegenheiten. From the University of California, Berkeley, I would like to thank Hasan Celik for his relentless work at the College of Chemistry NMR facilities and the QB3/Chemistry Mass Spectrometry Facility for HRMS measurements.

Meiner Laborkollegin Ulrike Wirth gilt mein Dank in vielfacher Art und Weise. Für die lustige und sehr schöne Laboratmosphäre, für die unterhaltsamen gemeinsamen Abende, für die tolle Zeit bei Konferenzen und im Urlaub. Und nicht zuletzt, für die Gewährung von Zuflucht in ihrer Wohnung nach meiner Rückkehr aus Amerika.

Für seine Hilfe bei Alltagsfragen möchte ich meinem Laborkollegen Shun Wang danken.

Special Thanks an Pepper Sweet, das weltweit beliebteste Beerpong Team. Wir haben zwar nicht direkt gewonnen, aber waren die Gewinner der Herzen.

Auch an alle ehemaligen und aktuellen Mitglieder des AK Königs möchte ich ein Dankeschön richten. Die gemeinschaftlichen Aktivitäten in der Küche und an sonstigen Orten auch schon während meiner Masterarbeit waren immer sehr unterhaltsam und ich werde es vermissen.

I also want to thank all current and former members of the Toste Lab at UC Berkeley for a memorable time.

I would like to especially thank Jacob Schreiber Tracy for his incredible patience and his support, for always believing in me and the great hiking and camping trips together.

Zuletzt möchte ich mich von ganzem Herzen bei meinen Freunden und bei meiner Familie – insbesondere meinen Eltern, meinen Großeltern und meinen Schwestern bedanken.

Eidesstattliche Erklärung

- (1) Ich erkläre hiermit an Eides statt, dass ich die vorliegende Arbeit ohne unzulässige Hilfe Dritter und ohne Benutzung anderer als der angegebenen Hilfsmittel angefertigt habe; die aus anderen Quellen direkt oder indirekt übernommenen Daten und Konzepte sind unter Angabe des Literaturzitats gekennzeichnet.
- (2) Bei der Auswahl und Auswertung folgenden Materials haben mir die nachstehend aufgeführten Personen in der jeweils beschriebenen Weise unentgeltlich geholfen:
 1. Chapter 2: Die Synthese des Edukts für 5d wurde von Anamitra Chatterjee durchgeführt.
 2. Chapter 3: Gekennzeichnete Experimente wurden von Tobias E. Schirmer und Tobias A. Karl durchgeführt. Ferdinand Holzhausen unterstützte das Projekt als Praktikant von Tobias E. Schirmer. Das Manuskript wurde von den angegebenen Personen mitverfasst bzw. verbessert oder korrigiert.
- (3) Weitere Personen waren an der inhaltlich-materiellen Herstellung der vorliegenden Arbeit nicht beteiligt. Insbesondere habe ich hierfür nicht die entgeltliche Hilfe eines Promotionsberaters oder anderer Personen in Anspruch genommen. Niemand hat von mir weder unmittelbar noch mittelbar geldwerte Leistungen für Arbeiten erhalten, die im Zusammenhang mit dem Inhalt der vorgelegten Dissertation stehen.
- (4) Die Arbeit wurde bisher weder im In- noch im Ausland in gleicher oder ähnlicher Form einer anderen Prüfungsbehörde vorgelegt.

Regensburg, der 15.02.2023